BIOGEOCHEMICAL IMPLICATIONS OF CHANGING GROUNDWATER AND SURFACE WATER HYDROLOGY AT LAKE POWELL, UTAH AND ARIZONA, AND THE MERCED RIVER, CALIFORNIA, USA

Thesis by

Richard Alan Wildman, Jr.

In Partial Fulfillment of the Requirements

for the Degree of

Doctor of Philosophy

California Institute of Technology

Pasadena, California

2009

Acknowledgements

I must begin by acknowledging my wonderful adviser, Janet Hering. Over the past five years, she has guided my intellectual and professional development with her constant professionalism, outstanding editing, attention to detail, patience, and unrelenting insistence on high standards. While these have all been extremely important to me, perhaps I value her open-mindedness most, for I am extremely grateful for the opportunity to develop and pursue my own ideas at Lake Powell. She found ways to fund projects that were slow to mature, and, in so doing, let me do research that has truly mattered to me. My wish for other graduate students is that they may also wake up each day excited to find the answers to the questions that they have asked, and that they have an adviser as supportive as mine.

I am very grateful to the U.S. National Science Foundation Special Grants for Exploratory Research program, the Alice Tyler Foundation, a gift by William Davidow to Caltech, the U.S. Bureau of Reclamation, Eawag, and the Summer Undergraduate Research Fellowship program at Caltech for funding portions of my research.

If Janet's supervision has been the foundation upon which my development has been built, then Claire Farnsworth, Kate Campbell, and Megan Ferguson have been the main people who helped me grow. Since she arrived at Caltech, Claire has helped in every facet of my research with balanced, thoughtful comments indoors and outstanding field assistance outdoors. Moving to Zürich and understanding the research culture of Switzerland was so much easier because she was there. Kate has been my role model since the first day I met her, teaching me about laboratory measurements, helping me develop my leadership skills, and understanding my daily life as a Caltech graduate

student. Her willingness to pass on her knowledge about porewater sampling has been invaluable. To a young graduate student, wise, “old” Megan was knowledgeable and composed during every experiment she ran and every presentation she gave in group meeting. Years after Kate and Megan answered all my questions in the lab and heard about my latest excitement, I hope I have followed their terrific examples.

Research with Dianne Newman was an outstanding experience. Her patient enthusiasm for discovery was exemplary, and working in her research group was an enlivening, enriching experience. Chad Saltikov taught me microbiology, Jeff Gralnick kept me grounded, and Arash Komeili made sure I always understood my research approach.

Thanks also to my committee members, Jess Adkins, Alex Sessions, and George Rossman, who have helped me see beyond my project and challenged my fundamental assumptions at exactly the right times. They, along with their colleagues, notably Andy Ingersoll, Joe Kirschvink, Paul Wennberg, Jared Leadbetter, Tapio Schneider, John Eiler, Ken Farley, Victoria Orphan, and Michael Hoffmann, have built an Environmental Science and Engineering department at Caltech from which I will be very proud to graduate.

I have been lucky to have been surrounded by excellent non-scientists at Caltech. Fran Matzen is among the most conscientious and reliable people I know, and she taught me that professionalism matters outside of research. Linda Scott’s bubbly, positive attitude was fun on good days and life-saving on the dark ones. Cecilia Gamboa and Dian Buchness can be counted on to support my work well, even from afar. Mike Vondrus is

the epitome of competence and kindness. Humble to a fault, he did let a smile slide across his face when I complemented him on the cleanliness of his workshop.

I simply could not have worked at Eawag without the help of Caroline Stengel, Thomas Rüttimann, and Hermann Mönch. They, along with Michael Berg and Christoph Aeppli, assured me of a soft landing there, which was so important to me in my first extended international experience.

I am so fortunate to have competent collaborators in all of my projects. Joe Domagalski took me out to the Merced River and showed a great deal of patience with an ignorant first-year graduate student. Nathan Dalleska was one of the crucial first few to stoke my excitement for research at Lake Powell, and he followed this with both field assistance and expert advice about all things analytical. His friendship and always-available help have made a big difference in my research experience. Mark Anderson has supported my research at Lake Powell unconditionally. My SURF students, Nathan Chan and Mike Easler, were outstanding, keeping me on my toes and helping me develop my projects in ways that no one else could. The sedimentological and mineralogical expertise of Lincoln Praton and Dennis Eberl, respectively, allows my research to become more interdisciplinary. They both have been exceptionally kind to me, as well. Mike DeLeon and Aurelio LaRotta have gone well out of their way to make sure my XRF data, and consequently, that entire project, turn out as well as possible.

Although I have not written a paper with them (yet!), several other scientists have made sure that my enthusiasm for my work has undergone constant renewal by giving me intellectual support, encouragement, and the examples of their own great work. Bernhard Wehrli, Johny Wüest, René Gächter, and Sharon Walker have been excellent mentors,

and Beat Müller, Flavio Anselmetti, and Michael Brett have given me key pieces of advice at key times. At Lake Powell, Bill Vernieu, Jerry Miller, and Nick Williams have been outstanding in creating opportunities for me and giving me all the resources at their disposal. Perhaps most importantly, Emily Stanley hosted me on a pivotal, mind-broadening visit to the University of Wisconsin.

Although I have never met them, there are a few writers and journalists who have inspired me in important ways. Kirk Johnson and Dean Murray wrote a 2004 article in The New York Times that first ignited my interest in studying Lake Powell. Thomas Friedman of The New York Times has helped me understand the world outside my scope. Ayn Rand taught me that my mind is my greatest asset. While in graduate school, I have become addicted to National Public Radio, so I must acknowledge Steve Julian and Larry Mantle of KPCC and Renee Montagne and Steve Inskeep of Morning Edition on NPR for their companionship during long days collecting and processing data.

I am grateful for the many friends who have helped in so many ways throughout graduate school. Buck McDaniel was an early partner in crime at Lake Powell, and Erika Anderson provided important balance during my first years. I have been buoyed by Ann Marie Cody's boundless energy, inspired by Drew Keppel's intelligence, and humbled by Lisa Keppel's perspective. Magnus Eek and Natalia Deligne were always up for an adventure, and Mark and Nathalie Vriend have been a huge help as I have visited Caltech since moving away. The Avery class of 2009 was outstanding in so many ways, and Jenni Taylor and Amy Frame of the Environmental Charter High School gave me an important opportunity to reach out to the larger community and understand the challenges facing scientists as we try to communicate to the public.

My best friend, of course, has been my wonderful wife, Zena Harris. Since we met, she has been the best girlfriend and spouse a graduate student could ever hope for, supporting my excitement, demanding clear explanations of why my research matters (e.g., questioning the relevance of a seminal paper on porewater diagenesis, noting that the graphs are “just a bunch of dots”), giving me the time to invest myself in my work, and sharing in all kinds of adventures away from science. I am so excited that she will be there as my career advances!

Before coming to Caltech, my career was shaped in crucial ways. At Yale, Albert Colman taught me proper lab protocol, Lauren Kolowith took me through my first research project, and Carmela Cuomo taught me that I can be solely responsible for my own work. Bob Berner was an outstanding supervisor and mentor for multiple projects, holding me to high standards and giving me the freedom to pursue projects with my own ideas. I surely would not be the researcher I am without the confidence he gave me.

Before Bob, Janet, Zena, or any of the other many important people I have mentioned here, there was Andy Card, head coach of Yale Lightweight Crew. Andy taught me the value of hard work, perseverance, and single-minded dedication toward one’s goals. His professionalism and enthusiasm for his work left a lasting impression on me. He gave me my first clear example of a person who put everything he had into his chosen pursuit, and he showed me that this approach would pay handsomely. He may have thought that he was coaching me to row and compete well, but he ended up teaching me so much more. On so many days during graduate school, I have drawn on the lessons he preached, and it’s not an overstatement to say that I would not have enjoyed my research or come close to earning my Ph.D. without his coaching.

Abstract

This thesis examines some effects of surface water and groundwater hydrology on the mobility of trace elements and phosphorus in natural environments. Three separate field sites are studied: 1) the shoreline of Lake Powell, a large reservoir on the Colorado River in Utah and Arizona where the surface elevation fluctuates on yearly and multi-yearly timescales, 2) the Colorado River inflow region to Lake Powell, where the sediment delta has been exposed due to low water levels, and 3) the lower Merced River, which is located in the San Joaquin Valley, California, amidst extensive agricultural development.

On the shoreline of Lake Powell, depth profiles of manganese and uranium were used to estimate the redox state of sediment porewater. Samples were collected before and after a fluctuation in reservoir level exposed two sampling locations to air and then resubmerged them. Results indicate that reducing conditions are re-established at different rates in two nearby shoreline locations, and that manganese reduction occurs more rapidly than uranium reduction upon resubmergence.

In the Colorado River inflow region of Lake Powell, sediment samples were collected from the lakebed and shoreline. Measurements indicate that particle size anticorrelates with the concentrations of most elements and clay minerals and explains much, but not all, of the variation in trace elements. Spatial trends of particle size imply that low reservoir levels may induce resuspension of fine sediment, a process that may lead to increased primary productivity observed in monitoring data. Sequential extractions performed on these sediment samples suggest that phosphorus, the limiting nutrient in Lake Powell, is primarily associated with calcite and biogenic apatite.

Sorption experiments indicate that fine particles sorb much more phosphorus than coarse particles, and that only a small amount of the sediment-associated phosphorus is desorbed during sediment resuspension. When reservoir levels are low, measurements of dissolved phosphorus suggest that sediment resuspended by the Colorado River may supply phosphorus to the photic zone under specific hydrologic conditions.

Samples of groundwater collected from beneath the Merced River were analyzed for a suite of trace elements. Statistical analyses suggest that hydrologic processes generally influence the transport of trace solutes more than redox chemistry, and results vary between strontium, barium, uranium, and phosphorus.

Table of Contents

List of Figures

List of Tables

List of Co-Authors

Mark Anderson (Chapter 3)
Aquatic Ecologist, Glen Canyon National Recreation Area

Nathan C. Chan (Chapter 3)
Graduate Student, Columbia University School of International and Public Affairs

Nathan F. Dalleska (Chapter 3)
Director, California Institute of Technology Environmental Analysis Center

Mike DeLeon (Chapter 4)
Applications Specialist - XRF, Spectro Analytical Instruments, Inc., Ametek

Joseph L. Domagalski (Chapter 6)
Project Leader, United States Geological Survey

Michael B. Easler (Chapter 4)
Undergraduate, University of Minnesota Department of Landscape Architecture

Dennis D. Eberl (Chapter 4)
Senior Scientist, National Research Program, United States Geological Survey

Aurelio LaRotta (Chapter 4)
Applications Scientist - XRF, Spectro Analytical Instruments, Inc., Ametek

Lincoln F. Pratson (Chapter 4)
Associate Professor, Nicholas School for the Environment, Duke University

Chapter 1

INTRODUCTION

1.1. Motivation

Extensive manipulation of river systems is a hallmark of irrigation infrastructure in the American West. As nineteenth-century exploration of Western lands revealed substantial acreage rich in sunshine but poor in water, the United States government created several legislative incentives to spur agricultural development. The Reclamation of Act of 1902 provided interest-free loans and long payback periods to farmers with the intention of creating new, agriculturally-based communities, and financial incentives continued for the next several decades (Ingram et al. 1991). To support these new communities, extensive water projects brought water from rivers to deserts and moderated seasonal flow patterns so that crops could be irrigated consistently throughout the growing season. Development increased rapidly as water infrastructure grew, so that, for example, more than one-quarter of the land area in California is now used for agriculture (Gronberg and Kratzer 2007).

Manipulations of surface water hydrology involve several related infrastructure components. A major initial step is the damming of a river, which creates a reservoir that can be used to ensure a steady supply of water to irrigation systems. Dams are often built to satisfy several needs, such as irrigation water supply, moderation of downstream river flows, production of hydroelectricity, and recreation. To meet these needs, dam releases may be seasonally greater than or less than inflows to reservoirs, leading to an unnatural downstream hydrograph and yearly fluctuations in reservoir water level. Over several years, reservoir storage can be depleted or increased when yearly inflows differ

substantially from releases required to satisfy downstream obligations. With water stored in reservoirs, nearby agricultural land can be irrigated by canals; without it, large-scale irrigation usually depends on groundwater pumping. Either way, Western irrigation adds water to the land surface during dry seasons, inducing groundwater infiltration and runoff to rivers when their flow would otherwise be low.

The construction of reservoirs is known to affect biogeochemical processes in rivers. When a river enters a reservoir, it deposits an oxygenated sediment load by gravitational settling (Friedl and Wüest 2002), and this is a probable mechanism for the spatial distribution of chemicals, which tend to associate with fine particles (Horowitz and Elrick 1987). This also changes the water clarity; a turbid river can become a clear lake, altering the carbon cycle by allowing increased primary productivity. Decaying biomass is an important source of sediment to most lakes, and the sedimentation of nutrients can substantially decrease nutrient concentrations in the river downstream of the dam (Friedl and Wüest 2002). As organic carbon in the sediment is consumed by microbial respiration, early diagenesis begins, although diagenesis at sedimentation rates as high as those observed in reservoirs has been minimally studied. Diagenesis affects the chemistry of sediment porewater, which can diffuse into surface water, sometimes leading to the release of phosphorus (Gächter and Müller 2003), methane, or mercury (Friedl and Wüest 2002) into the water column. The changing water levels of a reservoir will expose and re-wet sediment along the shoreline, possibly destroying and re-establishing subsurface redox gradients. However, this topic, while examined in the fields of floodplain ecology and soil chemistry, has not been studied previously for reservoir sediment. The long-term drawdown of reservoirs can affect primary productivity by transporting nutrient-rich

bottom water to the photic zone (Baldwin et al. 2008), or perhaps by exposing the previously-submerged sediment delta to the inflowing river, which may lead to desorption of chemicals from resuspended sediment.

Releases of water from the middle of the water column of a reservoir may be lower in dissolved oxygen (Friedl and Wüest 2002), higher in methane (Guérin et al. 2006), or colder (Vernieu et al. 2005) than the pre-dam river. Both dam releases and altered surface runoff can change the flow characteristics of a river, and these can affect organic matter transport, algal growth, and nutrient transport and retention (Doyle et al. 2005). Changing flow can also perturb the exchange of surface water and groundwater across the sediment-water interface (Essaid et al. 2008). This, in turn, will alter the contact time between surface water and the sediment matrix, which is a key factor influencing biogeochemical reactions in the subsurface (Findlay 1995). However, the extent of groundwater-surface water exchange has not been quantitatively related to the resulting biogeochemical processes in a river with altered groundwater flow.

1.2. Research Topics and Brief Overview of Chapters

The research in this thesis connects two important hydrological processes that occur as a result of damming and water diversion, reservoir level fluctuation and perturbed groundwater-surface water exchange, with biogeochemical processes. The focus is on inorganic chemicals, specifically trace metals and phosphorus, and the implications of their sequestration and mobilization for water quality.

After background information is presented in Chapter 2, four research topics in three hydrologically-different field locations are considered. Chapter 3 begins a three-part

study at Lake Powell, a large reservoir on the Colorado River in Utah and Arizona, with field measurements of sediment porewater geochemistry. Two sets of porewater samples were collected from submerged sediment before and after a lake level fluctuation exposed the sampling locations to air and then re-submerged them. Analyses of trace metals in porewater provide insight to the perturbation of redox gradients during unsaturation and resaturation processes. Furthermore, two shoreline locations were sampled to compare the effect of varying particle size.

With the exception of its appendices, Chapter 3 has been submitted for publication in *Limnology and Oceanography* with coauthors Nathan Chan, Nathan Dalleska, Mark Anderson, and Janet Hering. I designed the study, led all sampling campaigns, measured 9 of 12 porewater sample sets, analyzed and interpreted data, and wrote the manuscript. Mr. Chan, a Caltech Summer Undergraduate Research Fellowship program (SURF) student whom I mentored in the summer of 2005, assisted with fieldwork, analyzed the remaining porewater sample sets, and did some preliminary sediment extractions. Dr. Dalleska fine-tuned my measurement protocols on the inductively-coupled plasma mass spectrometer, making it possible to measure many elements simultaneously. Mr. Anderson provided essential field support and expertise during an exploratory trip to Lake Powell. Dr. Hering secured funding, guided the experimental design and data interpretation, and made many important improvements to the manuscript.

The long, narrow shape of Lake Powell and the high sediment load of the Colorado River enabled an interesting study of the patterns of deposition of inorganic chemicals in the reservoir. This study, which was conducted at a second field location, the Colorado River inflow region of Lake Powell, is described in Chapter 4. Therein, spatial trends in

particle size, trace element composition, and bulk mineralogy by laser diffractometry, X-ray fluorescence (XRF), elemental analysis, and X-ray diffraction (XRD) were assessed in the sediment delta. Particle size was assessed as a predictor of the other parameters, and the implications of spatial trends in the delta sediment were evaluated for their connection to observed water quality trends.

Chapter 4 will be submitted to *Environmental Science and Technology* with co-authors Michael Easler, Dennis Eberl, Lincoln Pratson, Mike DeLeon, Aurelio LaRotta, and Janet Hering. I designed the study, led some of the field expeditions and participated in others, measured all samples for particle size and elemental composition, processed and analyzed data, and wrote the manuscript. Mr. Easler, a SURF student whom I mentored in 2006, joined me on two of the field trips, processed many samples, and made preliminary measurements of solid-phase carbon. Dr. Eberl made all XRD measurements and processed those data into mineralogical concentrations. Dr. Pratson helped me understand sedimentation processes in Lake Powell and will contribute side-scan sonar figures to the appendices of the manuscript. Dr. DeLeon and Dr. LaRotta helped me design a sample preparation protocol for XRF analysis and taught me how to interpret XRF data. Dr. Hering secured funding for the project, guided data collection, and evaluated the manuscript.

Since 2000, Lake Powell has been drawn down by a combination of a serious drought in the headwaters of the Colorado River and an obligation to release water to downstream users. This has led to exposure of ~50 km of sediment delta and subsequent resuspension as the river flows through the sediment to the smaller reservoir. A third project (Chapter 5) examines the release of phosphorus (P), the limiting nutrient in Lake

Powell, by this sediment resuspension. Field measurements of dissolved P and laboratory measurements of P in sediments were conducted. The probability that this new source of P supports increasing primary productivity is discussed on the basis of the results of this study. These data will also support a detailed reservoir circulation model of Lake Powell in development by the United States Bureau of Reclamation by improving the calibrations of the biomass growth and subsequent dissolved oxygen consumption.

Chapter 5 will be submitted for publication in *Water Research* with co-author Janet Hering. The same sediment samples as mentioned in Chapter 4 were used. I designed the study, collected water samples, made all dissolved P measurements, and did all laboratory work for the sediment measurements. Dr. Hering secured funding for the project, guided data collection, and evaluated the manuscript.

At a third field location, the Merced River in the Central Valley of California, the effect of irrigation on the transport of solutes in groundwater was examined. In this setting, water is moved via canal to an almond orchard that is irrigated with the equivalent of a 7.5-cm rainstorm every two weeks. As a result, the local water table rises during the growing season (summer) and groundwater is generally discharged to the Merced River; little river water infiltrates into the riverbed. In this setting, groundwater samples beneath the Merced River were collected and analyzed for a suite of trace solutes, allowing for a statistical assessment of the relative importance of hydrologic processes and biogeochemistry for the transport and sequestration of trace solutes. This research, presented in Chapter 6, was done in conjunction with a detailed study on the transport of agricultural chemicals at this site conducted by the United States Geological Survey as part of its National Water Quality Assessment program, Phase II.

Chapter 6 has been accepted for publication in *Journal of Environmental Quality* after being written with co-authors Joseph Domagalski and Janet Hering. In this study, I collected most samples, analyzed all samples for trace solutes, statistically analyzed data, and wrote the manuscript. Dr. Domagalski enabled and guided sample collection, collected some samples, and provided supporting data sets of field parameters and dissolved organic carbon. Dr. Hering secured funding for the project, assisted with data interpretation, and made many important improvements to the manuscript.

Finally, in Chapter 7, the major results of this research are summarized and wider implications are discussed.

1.3. References

Baldwin, D. S., H. Gigney, J. S. Wilson, G. Wilson, and A. N. Boulding. (2008) Drivers of water quality in a large water storage reservoir during a period of extreme drawdown. *Water Research* 42: 4711-4724.

Doyle, M. W., E. H. Stanley, D. L. Strayer, R. B. Jacobson, and J. C. Schmidt. (2005) Effective discharge analysis of ecological processes in streams. *Water Resources Research* 41: W11411, doi:10.1029/2005WR004222.

Essaid, H. I., C. M. Zamora, K. A. McCarthy, J. R. Vogel, and J. T. Wilson. (2008) Using heat to characterize streambed water flux variability in four stream reaches. *Journal of Environmental Quality* 37: 1010-1023.

Findlay, S. (1995) Importance of surface-subsurface exchange in stream ecosystems: The hyporheic zone. *Limnology and Oceanography* 40(1): 159-164.

Friedl, G. and A. Wüest. (2002) Disrupting biogeochemical cycles – Consequences of damming. *Aquatic Science* 64: 55-65.

Gächter, R. and B. Müller. (2003) Why the phosphorus retention of lakes does not necessarily depend on the oxygen supply to their sediment surface. *Limnology and Oceanography* 48(2): 929-933.

Gronberg, J. A. M. and C. R. Kratzer. (2007) Environmental setting of the Lower Merced River Basin, California. *United States Geological Survey* Scientific Investigations Report 2006-5152.

Guérin, F., G. Abril, S. Richard, B. Burban, C. Reynouard, P. Seyler, and R. Delmas. (2006) Methane and carbon dioxide emissions from tropical reservoirs: Significance o f downstream rivers. *Geophysical Research Letters* 33: L21407, doi:10.1029/2006GL027929.

Horowitz, A. J. and K. A. Elrick. (1987) The relation of stream sediment surface area, grain size and composition to trace element chemistry. *Applied Geochemistry* 2: 437-451.

Ingram, H., A. D. Tarlock, and C. R. Oggins. The law and politics of the operation of Glen Canyon Dam. In *Colorado River Ecology and Dam Management: Proceedings of a Symposium May 24-25, 1990 Santa Fe, New Mexico.* Committee to Review the Glen Canyon Environmental Studies, Water Science and Technology Board, National Research Council: Washington, D.C., 1991.

Vernieu, W. S., S. J. Hueftle, and S. P. Gloss. Water quality in Lake Powell and the Colorado River. In *State of the Colorado River Ecosystem in Grand Canyon* (S. P. Gloss, J. E. Lovich, and T. S. Melis, eds.). Reston, Virginia: U.S. Geological Survey, 2005.

Chapter 2

BACKGROUND

2.1. Hydrology and Water Quality of the Colorado River

The Colorado River flows 2,317 km from its headwaters in the Southern Rocky Mountains to the Gulf of California (Figure 1). Together with its major tributary the Green River and their minor tributaries the Yampa, San Rafael, Gunnison, Dirty Devil, San Juan, Little Colorado, Virgin, and Gila Rivers, it drains ~632,000 km^2 of the American West and provides water for 24 million people and ~8,100 km^2 of farmland (Anderson 2002). The Colorado River Compact of 1922 divided the Colorado River Basin politically into Upper and Lower Basins at Lee's Ferry, a point in northern Arizona between Glen Canyon and Grand Canyon (Ingram et al. 1991). This division between the two basins has

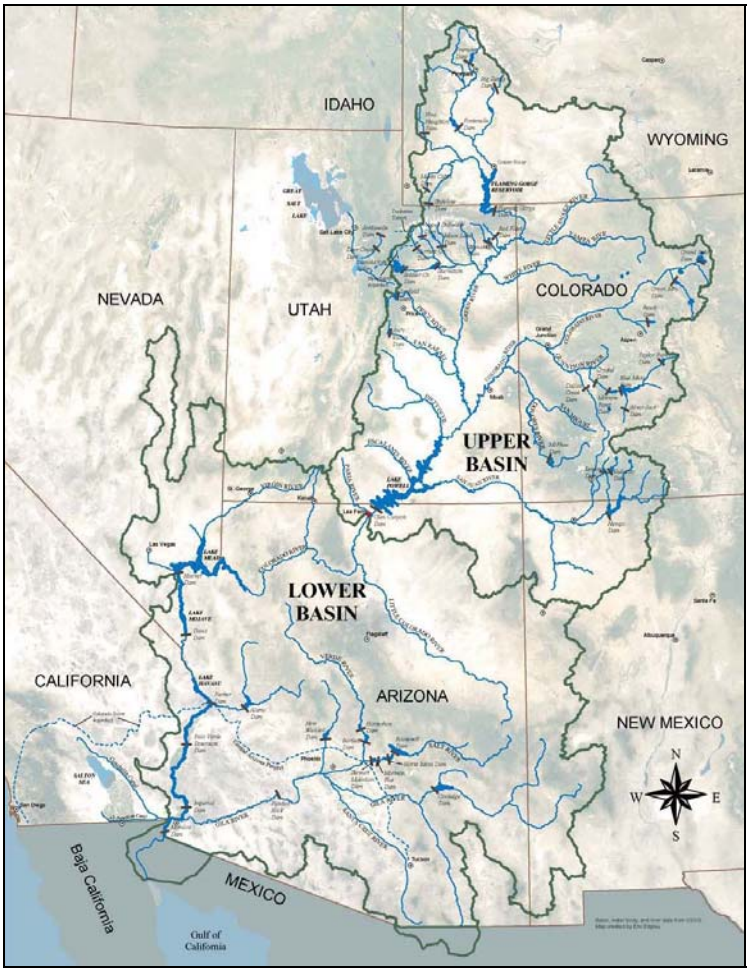

Figure 1. The Colorado River Basin (Anderson 2002).

shaped scientific investigations into the water resources of the region.

Precipitation falls mostly as winter snow in the Upper Colorado Basin (Spahr et al. 2000), whereas the North American monsoon brings the majority of the precipitation in the Lower Basin (Webb et al. 2004). However, these contributions are quite unequal; most of the flow in the Colorado River comes from snowmelt in the Upper Basin, 60% of which lies above 2,000 m above sea level (asl) as compared to 16% of the Lower Basin (Bales et al. 2008). Precipitation is highly variable on multi-year time scales, leading to corresponding variability in Colorado River flows. Climate change is adding to this variability, leading to more precipitation as rain and earlier snowmelt (Barnett et al. 2008).

Flows past Lee's Ferry have historically been used to judge the amount of water in the river. Since the 1963 creation of Lake Powell, a reservoir just upstream from Lee's Ferry (see section 2.2), the estimated inflow to the reservoir has been used as the theoretical unregulated flow at Lee's Ferry. Thus, flow on the Colorado River as measured by the historical record at Lee's Ferry (dating to 1895) ranges from 4.7 $km^3\ yr^{-1}$ (3.8 million acre-feet (MAF) yr^{-1}) to 27.4 $km^3\ yr^{-1}$ (22.2 MAF yr^{-1}). The estimated mean is 15.3 $km^3\ yr^{-1}$ (12.4 MAF yr^{-1}), although if consumptive use in the Upper Basin were excluded, the flow would be about 18.5 $km^3\ yr^{-1}$ (15 MAF yr^{-1}; Webb et al. 2004).

While the effect of the Pacific Decadal Oscillation and the El Niño Southern Oscillation are incompletely understood, these climate patterns commonly influence precipitation and river flow across the entire Colorado River Basin (Webb et al. 2004, Kurtzman and Scanlon 2007). Extended droughts (i.e., > 10 years) are a realistic possibility (Meko and Woodhouse 2005). From 1999 to the present, the Colorado River

Basin has experienced a severe drought, with only 2 years of slightly above-average flow during this period and all other years markedly below average. Dendrochronologic reconstructions of streamflow at Lee's Ferry since 1490 indicate that this is the most severe, extended dry period since 1850, although three periods were identified during which there is a ≥ 25% probability of lower flow than in the current drought (Woodhouse et al. 2006).

Estimated flow of the Colorado River at Lee's Ferry from 1895 to the present shows a decreasing trend (Webb et al. 2004) that can be attributed to several factors. First, the highest flows in the last 500 years occurred in the initial three decades of this time series (Woodhouse et al. 2006). Second, consumptive water use in the Upper Basin has steadily increased since the mid-1900s (Webb et al. 2004). Third, climate change appears to be shifting arid subtropical climatic patterns toward higher latitudes, leading to drier conditions on the Colorado Plateau (Seager et al. 2007). Together, these three phenomena may severely limit the water available for consumptive use, possibly leading to the draining of both major reservoirs on the Colorado River (Lake Powell and Lake Mead) in the coming decades (Barnett and Pierce 2008).

Water quality in the Colorado River can be impaired by high salinity, which results from evaporation, diversion of high-quality water, irrigation return flows, and dissolution of minerals from sedimentary rocks (Gloss et al. 1981). Salinity increases dramatically when the Colorado River leaves the Southern Rocky Mountains and enters the Colorado Plateau (Spahr et al. 2000), and it generally increases downstream, except when affected by flow through reservoirs (USBR 2008b). Mining in the Rocky Mountains contributes trace metals like copper, lead, zinc, and cadmium (Spahr et al. 2000), and these elements

are transported downstream in association with suspended sediment (Horowitz et al. 2001). Selenium, which can be leached out of the Mancos Shale formation of the Colorado Plateau and transported to the river by agricultural return flows, has warranted special attention (Engberg 1999, Naftz et al. 2005).

2.2. Hydrology and Water Quality of Lake Powell

Lake Powell (Figure 2) is the second-largest reservoir in the United States and the second reservoir constructed on the mainstem of the Colorado River, after Lake Mead which is further downstream. Located 24 km upriver from Lee's Ferry and 17 km downstream from the confluence of the Green and Colorado Rivers, it fills Glen Canyon and lies between Canyonlands National Park and Grand Canyon National Park. It was formed by the completion of Glen Canyon Dam (GCD) in 1963 to generate hydroelectric power and to ensure that the Upper Basin could reliably deliver water to the Lower Basin as required by the Colorado River Compact (Farmer 1999). When full, its surface elevation is 1128 m asl, its length is 299 km, and its depth is 178 m. The tortuous shape of Glen Canyon gave rise to a long, narrow reservoir with > 95 "side canyons" that extend off the original channel of the Colorado River. The reservoir is a major recreation destination, welcoming ~2 million visitors per year for camping, fishing, and a variety of water sports (Granet and Anderson 2005; Potter and Drake 1989).

Releases from GCD do not match inflows to Lake Powell on either a yearly or multi-year time scale. In order to maximize hydropower revenue, releases from GCD are highest during the summer months, when demand for electricity is greatest. In the fall and

winter, inflows are low due to precipitation falling as snowmelt. As a result, the surface elevation of the reservoir decreases from July until March. Dam releases are substantially

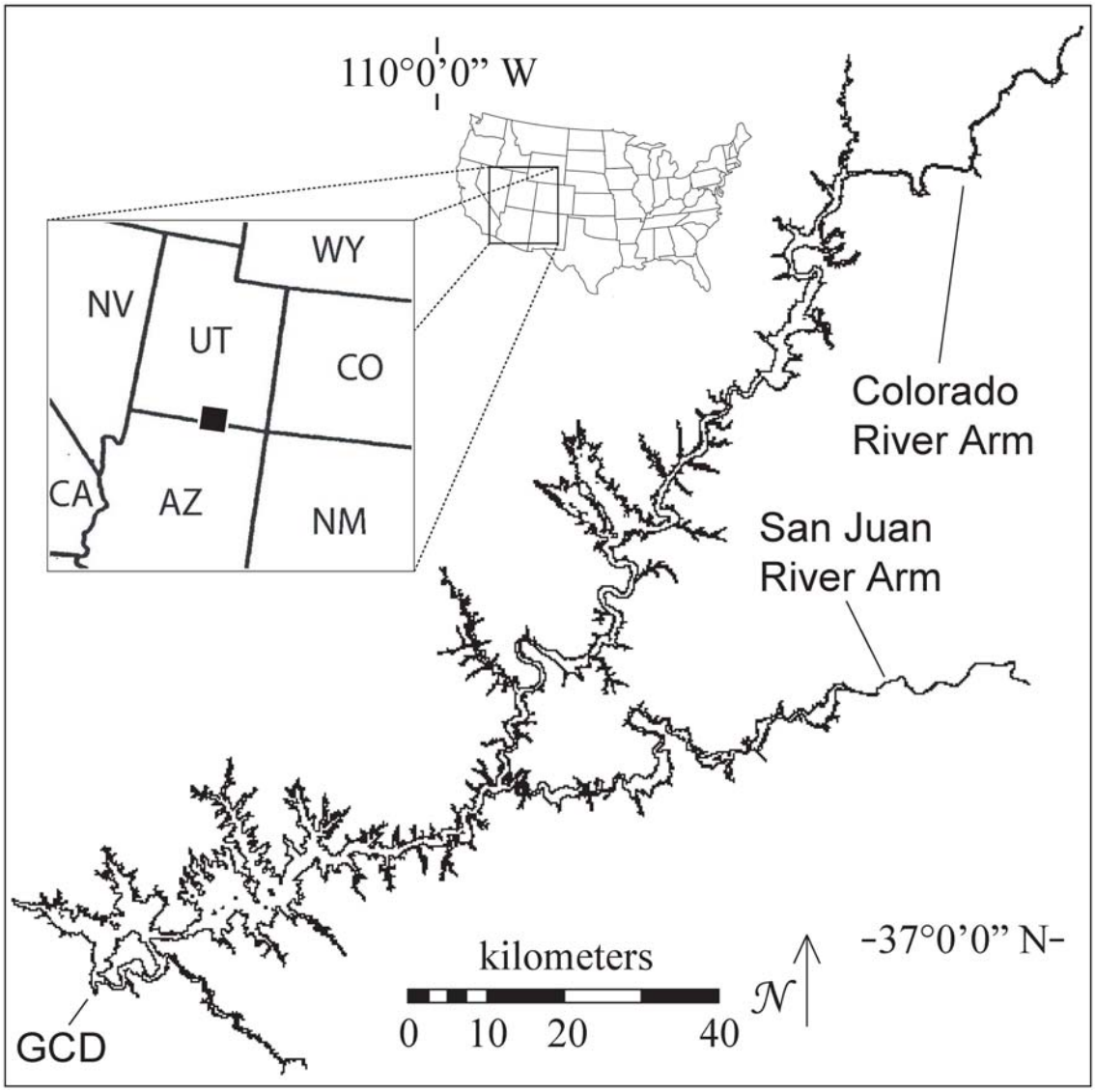

Figure 2. Lake Powell, impounded by Glen Canyon Dam (GCD) and located on the Utah-Arizona border, as denoted by the black rectangle on the inset map of the United States.

less than the spring inflows to the reservoir, which lead to a rapid increase of surface elevation from April to June (Figure 3). Regardless of total inflows in a given year, GCD must release 10.15 km^3 yr^{-1} (8.23 MAF yr^{-1}) to fulfill the legal obligations of the Upper Basin states; frequently volumes in excess of this are released to balance storage between Lake Powell and Lake Mead, which is downstream. As a result, Lake Powell experiences

multi-year periods when it is nearly full as well as extended periods of low water surface elevation, or “drawdown” (Figure 3).

The recent drawdown has resulted in a substantial amount of sediment transport within the reservoir. In the Colorado River inflow region, sandy sediment eroded from the uppermost region of the delta (the topset) was deposited on the region of maximum slope (the forset), and, in the San Juan River arm, topset and forset sediment was transported down the reservoir to Glen Canyon Dam (Pratson et al. 2008). The water quality implications of fluctuating water levels are explored in later chapters of this thesis.

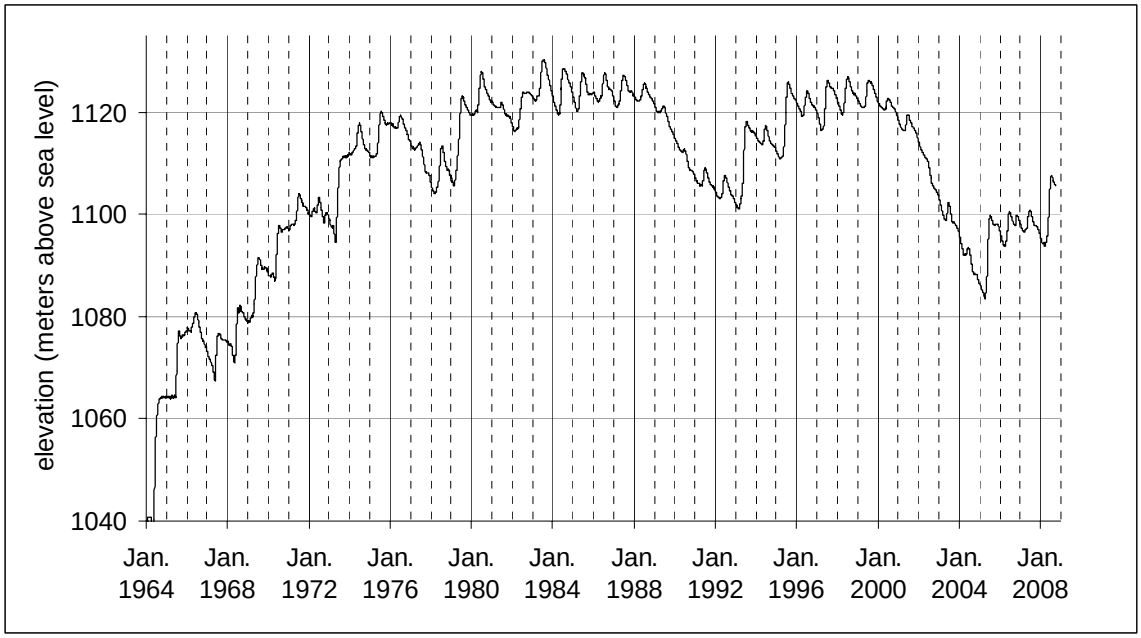

Figure 3. Surface elevation of Lake Powell (USBR 2008a).

Circulation in Lake Powell varies seasonally due to changing density of reservoir and river water. During late winter (January-March), the inflow of the Colorado River is cold and high in total dissolved solids (TDS), whereas the reservoir is still losing heat from the previous summer. The denser river water enters the reservoir as an underflow density current and either hugs the bottom for the entire length of the reservoir or

becomes an interflow current when it reaches a depth of similar density. Deep water in the path of the underflow current is pushed upward when it reaches the dam, and it then exits in the withdrawal current that passes through the dam. As a result, stagnant, deep water in Lake Powell is freshened and oxygenated not by convective mixing with surface water, but by advective transport of inflow water (Johnson and Merritt 1979, Potter and Drake 1989).

The spring snowmelt, which is warmer and more dilute than the wintertime river, and low summer inflows, which warm in response to summertime temperature increases more rapidly than the reservoir water, enter the reservoir as overflow density currents. These, coupled with intense summertime stratification characterized by a distinct thermocline ~20 m below the water surface, lead to several months of flow across the surface of the reservoir and stagnation at depth (Johnson and Merritt 1979). In the late autumn and early winter (November-December), convective circulation overturns the water column to a depth of ~60 m (Gloss et al. 1980) and the cooler river enters the reservoir as an interflow current (Johnson and Merritt 1979).

Nearly all water enters GCD through a combination of eight penstocks, located at 1058 m asl (70 m below the water surface when the reservoir is full), and exits through hydroelectric turbines (Hueftle and Stevens 2001). This depth is usually below the depth of summertime convective mixing, and, during fall overturn, the withdrawal current prevents overturn near the dam below a depth of 1020 m asl (Johnson and Merritt 1979). Epilimnetic and hypolimnetic water can be discharged through the spillway intakes (1114 m asl) and river outlet works (1029 m asl), respectively. While rarely used, releases from

the spillway and river outlet works can accelerate overflow and underflow circulation patterns (Hueftle and Stevens 2001).

Water in Lake Powell is generally very low in trace metals and anthropogenic organic chemicals (Hart et al. 2004). Concentration gradients may exist between the head and the mouth of a side canyon, although the basis for these has not been rigorously investigated. Gradients persist because side canyons are generally quiescent (Hart et al. 2004). Precipitation of calcite is an important summertime process that is more likely to occur in the lower region of the reservoir due to inhibition by organic compounds that are present in the inflow region (Reynolds 1978). In the inflow region of Lake Powell, sorption reactions between water and sediment limit the range of dissolved phosphorus (P) concentrations, yet silica varies in a range outside that predicted by laboratory sorption experiments (Mayer and Gloss 1980). The circulation patterns described above are very important for the dynamics of P, the limiting nutrient in the reservoir. When P enters in an underflow current, it bypasses the photic zone and does not contribute to primary productivity, but when it enters as an overflow current, it contributes to summer phytoplankton blooms (Gloss et al. 1980). Sediment resuspension during drawdown can double suspended sediment concentrations and may release additional nutrients into the water column (Vernieu 1997).

Storing water in Lake Powell affects water quality downstream. Precipitation of calcite offsets the increase of TDS that occurs due to evaporation such that there is no net change in TDS concentration (Gloss et al. 1981). An important additional consequence of storage in Lake Powell is the moderation of annual variability in TDS (USBR 2008b), which facilitates management of salinity downstream. Furthermore, Lake Powell retains

> 90% of total P, > 70% of dissolved P, > 20% of total nitrogen, and > 10% of total silica that enters from all sources (Gloss et al. 1981). Releases from Glen Canyon Dam, which draws water from the middle of the water column, are clear and cold, and this significant difference from historical conditions has damaged sensitive ecological habitat immediately downstream in Grand Canyon. Additionally, reservoir processes that are not completely understood can lead to seasonal plumes of anoxic water within Lake Powell (Vernieu et al. 2005), and, under certain hydrologic conditions, these can pass through the dam and impair water quality in the Colorado River (Williams 2007).

2.3. Early Diagenesis and its Implications for Inorganic Contaminants

Early diagenesis, the quantitative description of chemical changes during sediment deposition before lithification occurs, is characterized by chemical reactions that are generally a result of microbial metabolism of organic matter. During aerobic respiration, organic matter acts as an electron donor and is oxidized to carbon dioxide. Oxygen is the most thermodynamically favorable electron acceptor for this process. In most sediment, deposition of organic matter is such that diffusion of oxygen from surface water into porewater is insufficient to support microbial respiration. In this case, the concentration of dissolved oxygen in sediment porewater decreases with depth below the sediment-water interface, and, where it approaches zero, microbial respiration uses other electron acceptors in a sequence determined by their reduction potential. Reduction of nitrate (NO_3^-) to N_2 is the most favorable anaerobic process and an important means of reducing NO_3^- contamination in groundwater (e.g., Domagalski et al. 2008). When NO_3^- is depleted, manganese (Mn), iron (Fe), and sulfate (SO_4^{2-}) are reduced (Berner 1980,

Stumm and Morgan 1996, Froelich et al. 1979). Importantly, a single microbial species does not carry out each reaction. Rather, different species dominate the microbial population as the geochemical conditions change with depth. Furthermore, environmental conditions may change the relative availability or energetic yield of different electron acceptors, and thus the sequence of reduction described here may not always be clearly observed due to overlap of electron acceptor utilization (McGuire et al. 2002).

Redox reactions can control partitioning between the solid and the dissolved phase. The environmentally-important reduced species Mn(II) and Fe(II) can occur in solution as Mn^{2+} and Fe^{2+} ions, whereas their oxidized forms, Mn(III/IV) and Fe(III), generally occur in solids with very low solubilities (Morel and Hering 1993). Thus, the absence of oxygen and NO_3^- in sediment porewater leads to the reductive dissolution of Mn and Fe (Froelich et al. 1979, Kneebone et al. 2002). These elements can be removed from porewater by oxygenation, which leads to the precipitation of Mn(III/IV)-oxide and Fe(III)-oxide minerals, or by precipitation of reduced carbonate (e.g., siderite ($FeCO_3$) or rhodocrocite ($MnCo_3$)), sulfide (e.g., pyrite (FeS) or albandite (MnS)), or phosphate (e.g., vivianite ($Fe_3(PO_4)_2$)) solids. Sulfide (S^{2-}) produced during sulfate reduction can lead to precipitation of pyrite, which is more likely than that of albandite, since S^{2-} and Fe^{2+} react preferentially (Canfield 1989, Báez-Cazull et al. 2007) and undersaturation of albandite is generally observed in sulfidic porewater (Naylor et al. 2006). Isomorphic substitution of Mn^{2+} during vivianite ($Fe_3(PO_4)_2$) precipitation can reduce dissolved Mn^{2+} concomitantly with PO_4^{3-} (Taylor and Boult 2007).

Trace elements and P commonly sorb to the surfaces of Fe- and Mn-oxide minerals (Belzile et al. 2000, Dixit and Hering 2003, Lee et al. 2002, Tonkin et al. 2004, Gächter

and Müller 2003). Thus, reductive dissolution of these minerals can also release trace elements into sediment porewater (Kneebone et al. 2002, Campbell et al. 2008). Furthermore, some trace elements, such as arsenic and uranium, are redox active and will thus respond to the redox state of sediment porewater determined by the major redox species of a system (Campbell et al. 2006, Finneran et al. 2002).

2.4. Reservoir Sedimentation and Transport of Sediment-Bound Elements

Globally, sedimentation in reservoirs traps 20% of sediment transported by rivers; Lake Powell, which traps > 99% of the sediment that enters it, far exceeds global averages for its continent, ocean basin, climate, and elevation (Syvitski et al. 2005, Potter and Drake 1989). The ability of flowing water to entrain and transport particles depends principally on fluid density, fluid viscosity, and flow velocity. The first two of these remain approximately constant when a river is impounded; a decrease in flow velocity decreases particle transport (Prothero and Schwab 2004). As sediment particles in a river enter a reservoir, they will settle according to Stokes's law, which implies that, as the river flow slows, coarse particles will settle before fine ones. Specifically,

$$v_p = \frac{\Delta\rho}{\rho} \cdot \frac{g}{18\nu} \cdot D_p{}^2$$

where v_p is the sinking velocity (in m s^{-1}), $\Delta\rho$ is the density difference between particles and water (in kg m^{-3}), ρ is the density of water (≈ 1000 kg m^3), g is the gravitational acceleration (= 9.81 m s^{-2}), ν is the viscosity of water (≈ 1-1.5 · 10^{-6} m^2 s^{-1}), and D_p is the particle diameter (in m) (Friedl and Wüest 2002). As the energy of a river decreases upon reaching the flat surface of a lake, its turbulent upwelling will decrease in velocity and will fail to counteract the higher sinking velocity of large particles. The slowing river will

carry fine particles further into the reservoir and deposit them as it continues to slow. Thus, sediment deltas are usually deposited in gradients of particle size, with coarse particles closest to the river and fine particles deepest into a lake (Prothero and Schwab 2004). In a narrow lake, such as a reservoir that has filled a narrow valley, the shape of the sediment delta can lead to a clear gradient in sediment particle size. Sedimentation in the inflow region of a reservoir is derived from allochthonous sources, whereas, in the part of a reservoir that resembles a lake, sedimentation is autochthonous as in natural lakes (Friedl and Wüest 2002). Only deposition of river sediment will be reviewed briefly here.

Gradients of particle size in sediment deltas have been observed in several reservoirs most clearly when sediment deltas do not reach the dam (e.g., Riggsbee et al. 2007, Cheng and Granata 2007). Large deltas will be strongly influenced over time by changes in reservoir level, with decreases in water level allowing the river to mobilize coarse sediment from the upper region of the delta further into the reservoir, and subsequent increases in water level depositing fine sediment on top of coarse sediment (Snyder et al. 2006). Thus, vertical variations in sediment particle size will be closely tied to the management history of a reservoir.

Trace elements are generally enriched in particles < 0.125 mm in size. Small particles are high in both organic carbon and clay minerals, so it is not clear which of these phases contributes most to trace element sorption (Horowitz and Elrick 1987). Reservoirs have been observed to retain both inorganic contaminants, especially when downstream from mines (Castelle et al. 2007, Lee et al. 2008), and nutrients (Teodoru and Wehrli 2005) in their sediment. While the concentration of chemicals in reservoir

sediment is a means of purifying downstream river water, this sedimentation is an important sink for organic carbon (Downing et al. 2008). Both the rapid sedimentation of organic matter and the submergence of riparian biomass lead to greenhouse gas emissions (i.e., nitrous oxide and methane) from reservoirs that are much higher than those from lakes or undammed rivers (Guérin et al. 2008, 2006, Kemenes et al. 2007).

2.5. Phosphorus in Lakes

The bioavailability of P has long been understood to limit primary productivity in freshwater ecosystems, an assertion most recently stated by Schindler et al. (2008). The amount of P in the water column of a lake is dependent on input from land, rivers, and sediment diagenesis, loss to sedimentation and outflow, and consumption by primary productivity (Müller et al. 2007). The quantity of dissolved P in a lake has generally been thought to depend on lake depth and flushing rate, but recent research suggests that P input and water residence time may be more important (Brett and Benjamin 2008).

In unpolluted rivers, the vast majority of P is transported in particulate form (Meybeck 1982, Horowitz et al. 2001), and, once in a lake, several processes can move the remaining dissolved P into the solid phase as well. Phosphorus sorbs abiotically to Fe-oxide minerals, aluminum-oxide minerals, and carbon (Arias et al. 2006, Novak et al. 2006). Sorption characteristics change with salinity; increasing the salinity of freshwater to a range of 5-12 salinity units induces P desorption (Spiteri et al. 2008). Apatite precipitation or scavenging during calcite precipitation may be important in some lakes (Kleiner and Stabel 1989). Most importantly, uptake by biomass decreases dissolved P concentrations. If this biomass dies and degrades in surface water, then P re-enters the

dissolved pool. However, settling of dead biomass to sediment retains it in the solid phase for a much longer time (Kalff 2002).

To contribute to primary productivity, P must be in the photic zone of a lake. Bioavailable P that reaches the photic zone is generally taken up by biomass growth rapidly, and thus concentrations of P are often higher in bottom water than in surface waters. P can reach bottom waters by transport by underflow density currents (Gloss et al. 1980), diffusion from sediment porewater (Gächter and Müller 2003), or decay of sinking particulate organic matter (Kalff 2002). In this case, convective overturn of the water column is an important step that leads to primary productivity in surface waters, and the depth of overturn determines the extent to which hypolimnetic P reaches surface water (e.g., Baldwin et al. 2008, Kalff 2002). The importance of overturn events is magnified in reservoirs that release water from the middle or bottom of the water column, since advective circulation allows hypolimnetic P to exit the reservoir without entering the photic zone when overturn does not bring it to surface waters (Matzinger et al. 2007).

Once in sediment, chemical processes enrich P concentrations in porewater so that it diffuses back into bottom waters. Dissolution of Fe-oxides is generally cited as the main mechanism for this process. When water near the sediment-water interface is anoxic, Fe reduction can occur in surface sediment, liberating both Fe^{2+} and P to the dissolved phase. If these reach an oxic region of the water column, Fe will precipitate and scavenge P. However, if S^{2-} is present, it can sequester Fe^{2+} as FeS and allow P to accumulate in the water column (Baldwin and Mitchell 2000, Berner and Rao 1994, Jordan et al. 2008). Internal loading of a water body in this manner can maintain high dissolved P concentrations even if external loading is decreased (Ahlgren et al. 2006). Microbial

decomposition of organic matter in sediment can also contribute P to sediment porewater, where it will either sorb to particles or diffuse into overlying water. Sediment-associated calcite may be less likely to release P to the water column, but the implications of this have not been adequately determined.

2.6. Water Resources and Water Use in the Lower Merced River Basin, California

The Central Valley of California is a large, northwest-trending structural trough filled with alluvial and marine sediment, the southern half of which is the San Joaquin Valley (Figure 4). The valley floor is a productive agricultural region that receives water primarily from rivers that flow southwest from the Sierra Nevada range (Gronberg and Kratzer 2007). About 80% of the annual precipitation to the Valley falls between November and March, yet only 40-50% of the streamflow occurs at this time, as the remainder of precipitation is stored in the snowpack and reservoirs (Dubrovsky et al. 1998). This water is delivered to row crops and orchards throughout the

Figure 4. The San Joaquin Valley, from Dubrovsky et al. (1998).

summer growing season by an extensive network of irrigation canals (Gronberg and Kratzer 2007).

The Lower Merced River (Figure 5), a major tributary of the San Joaquin River, has been a focus of the United States Geological Survey Agricultural Chemicals Transport Study, which is part of the ongoing National Water Quality Assessment program. The semi-arid climate of the San Joaquin Valley leads to a mean annual precipitation of 31 cm with mean temperatures of 25°C and 8°C in July and January, respectively. The annual average flow of the Merced River at its confluence with the San Joaquin River is 19.4 $m^3 s^{-1}$ (Capel et al. 2008). This is modified both by releases from the McSwain Dam,

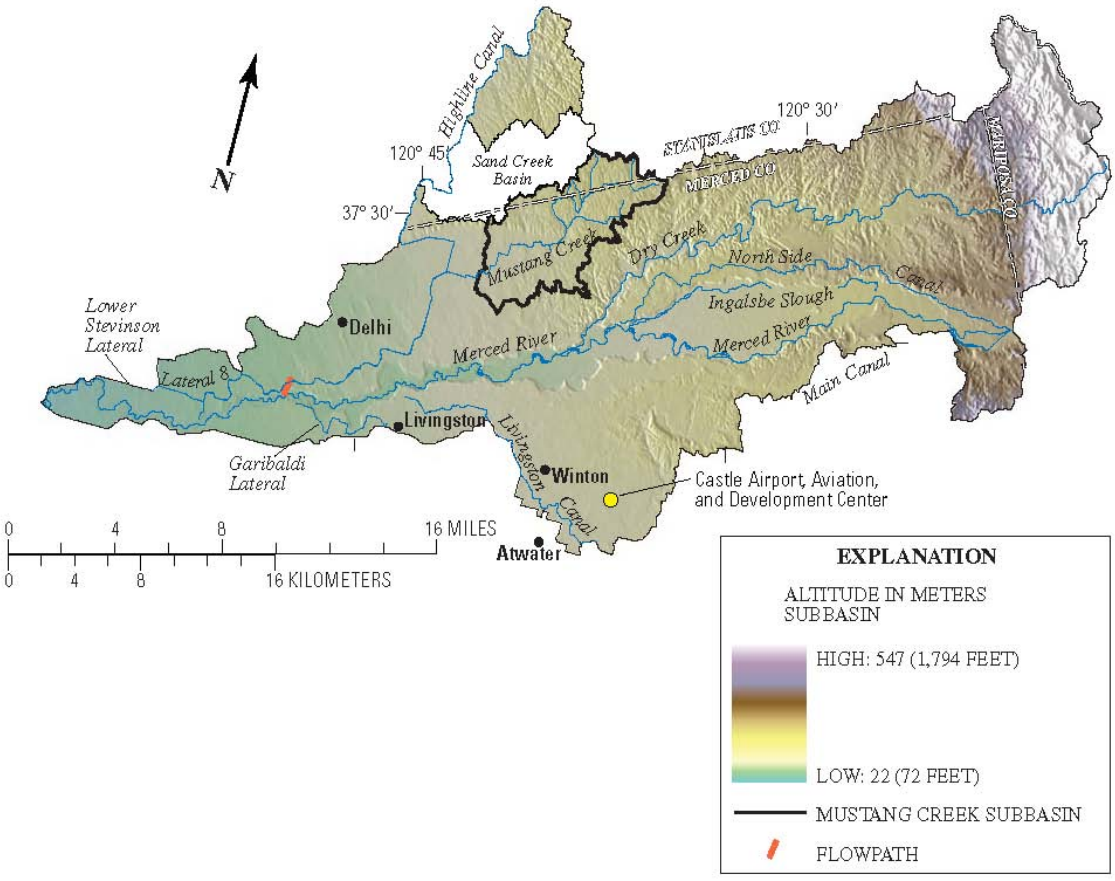

Figure 5. The Lower Merced River Basin, from Gronberg and Kratzer (2007). Water flow is from east to west. The location of the field site described in Chapter 6 is approximately where the Merced River intersects the flowpath labeled on the map.

which is just upstream of the boundary that defines the Lower Merced River basin, and five major irrigation and drainage canals that discharge to the river (Gronberg and Kratzer 2007). In this reach, the river is underlain by an unconfined aquifer that is bounded beneath by the Corcoran Clay formation, which is 28-85 m below ground surface (Capel et al. 2008).

More than half (55%) of the Lower Merced River Basin is used for agriculture, mostly almond orchards, with some corn and grain fields and vineyards (Capel et al. 2008). Irrigation seasonally raises the water table, inducing a gradual flow to the Merced River (Phillips et al. 2007). As a result, in the reach studied in Chapter 6, the Merced River usually gains water from the local aquifers, except when high river stage pushes water into the subsurface (Essaid et al. 2008). Groundwater-surface water exchange is minor, however, due to small differences in hydraulic head across the sediment-water interface, which may be due to the location of the study reach just downstream from a transition from a losing stream to a gaining stream, to negligible surface water slope, and to a wide channel for groundwater discharge (Essaid et al. 2008, Puckett et al. 2008). Furthermore, the residence time of groundwater in the streambed between the sediment-water interface and a depth of 3 m is on the order of 2 months (Puckett et al. 2008).

In addition to irrigation water, 1 million kg of pesticides, 7.3 million kg of nitrogen, and 1.3 million kg of phosphorus were applied to crops in 2003 in the Lower Merced River Basin (Capel et al. 2008). Pesticides generally degrade in soil and aquifer material, with atrazine and metolachlor occurring in lower concentrations in groundwater than their degradates (Steele et al. 2008). Denitrification removes most fertilizer-derived nitrate as groundwater flows through the riparian zones into the river subsurface, most

likely due to substantially more reducing conditions in the riverbed subsurface than in the nearby aquifer (Domagalski et al. 2008, Puckett et al. 2008).

2.7. Subsurface Hydrologic and Biogeochemical Processes in Rivers and Streams

Exchange between stream water and groundwater can affect surface water chemistry due to reactions in the river subsurface. The region of the riverbed groundwater that is hydrologically linked to surface water such that exchange occurs on short length and time scales is known as the hyporheic zone (Figure 6, Findlay 1995). Particle size is a particularly important parameter determining the amount of infiltration to the hyporheic zone; contact time with riverbed sediment can limit chemical reactions in sandy streambeds, whereas cobble streambeds provide a lesser physical barrier (Jackman and

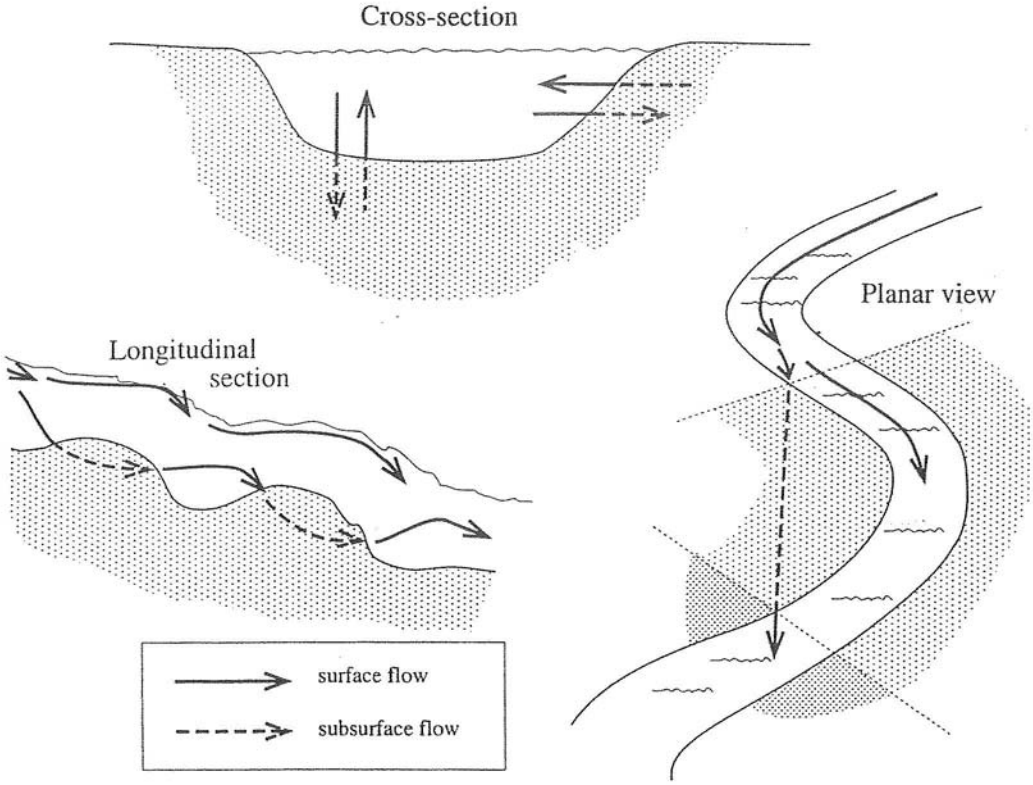

Figure 6. Schematic representations of hyporheic zone flowpaths (Findlay 1995).

Ng 1986). A coarse "armor" layer on top of finer sediment has been observed to have no effect on the advection of water into the river subsurface (Marion et al. 2008), yet streamflow does, with more surface-subsurface exchange occurring at lower streamflow than at higher streamflow (Harvey et al. 1996). The extent of infiltration is a master variable that controls the residence time of water in a river reach, which, in turn, is often the best explanation for observed differences in biogeochemical activity (Findlay 1995, Valett et al. 1996).

Interaction of solutes within the hyporheic zone depends on both the contact time of river water with the riverbed matrix and the type of solute. The mechanism of retention is generally believed to be chemical, often ion exchange or sorption, as injection experiments demonstrate that the downstream advection of inorganic solutes (Kennedy et al. 1984) or nutrients (Valett et al. 1996, Haggard et al. 2005) is retarded relative to a conservative tracer. Due to infiltration by stream water, the hyporheic zone is generally oxic, although pockets of reducing zones can exist where sediment is less permeable (Salehin et al. 2004). Thus, organic matter degradation is common, and this acts as a source of nutrients to surface water (Findlay 1995). Contact with sediment surfaces can also promote redox reactions: loads of dissolved Mn in a contaminated stream have been observed to decrease due to subsurface oxidation (Harvey and Fuller 1998).

2.8. References

Ahlgren, J., K. Reitzel, L. Tranvik, A. Gogll, and E. Rydin. (2006) Degradation of organic phosphorus compounds in anoxic Baltic Sea sediments: A ^{31}P nuclear magnetic resonance study. *Limnology and Oceanography* 51(5): 2341-2348.

Anderson, D.L. *Utah's Perspective: The Colorado River.* Utah Department of Natural Resources: Salt Lake City, 2002.

Arias, M., J. Da Silva-Carballal, L. Garcia-Rio, J. Mejuto, and A. Nunez. (2006) Retention of phosphorus by iron and aluminum-oxides-coated quartz particles. *Journal of Colloid and Interface Science* 295: 65-70.

Báez-Cazull, S, J. T. McGuire, I. M. Cozzarelli, A. Raymond, and L. Welsh. (2007) Centimeter-scale characterization of biogeochemical gradients at a wetland-aquifer interface using capillary electrophoresis. *Applied Geochemistry* 22: 2664-2683.

Baldwin, D. S., H. Gigney, J. S. Wilson, G. Watson, and A. N. Boulding. (2008) Drivers of water quality in a large water storage reservoir during a period of extreme drawdown. *Water Research* 42: 4711-4724.

Baldwin, D. S. and A. M. Mitchell. (2000) The effects of drying and re-flooding on the sediment and soil nutrient dynamics of lowland river-floodplain systems: A synthesis. *Regulated Rivers: Research and Management* 16: 457-467.

Bales, R. C., K. A. Dressler, B. Imam, S. R. Fassnacht, and D. Lampkin. (2008) Fractional snow cover in the Colorado and Rio Grande basins, 1995-2002. *Water Resources Research* 44: W01425, doi:10.1029/2006WR005377.

Barnett, T. P. and D. W. Pierce. (2008) When will Lake Mead go dry? *Water Resources Research* 44: W03201, doi:10.1029/2007WR006704.

Barnett, T. P., D. W. Pierce, H. G. Hidalgo, C. Bonfils, B. D. Santer, T. Das, B. Govindasamy, A. W. Wood, T. Nozawa, A. A. Mirin, D. R. Cayan, and M. D. Dettinger. (2008) Human-induced changes in the hydrology of the Western United States. *Science* 319: 1080-1084.

Belzile, N., Y.-W. Chen, and R. Xu. (2000) Early diagenetic behaviour of selenium in freshwater sediments. *Applied Geochemistry* 15: 1439-1454.

Berner, R. A. *Early Diagenesis: A Theoretical Approach*. Princeton University Press: Princeton, NJ, 1980.

Berner, R. A. and J.-L. Rao. (1994) Phosphorus in sediments of the Amazon River and estuary: Implications for the global flux of phosphorus to the sea. *Geochimica et Cosmochimica Acta* 58(10): 2333-2339.

Brett, M. T. and M. M. Benjamin. (2008) A review and reassessment of lake phosphorus retention and the nutrient loading concept. *Freshwater Biology* 53: 194-211.

Campbell, K. M., D. Malasarn, C. W. Saltikov, D. K. Newman, and J. G. Hering. (2006) Simultaneous microbial reduction of Iron(III) and Arsenic(V) in suspensions of hydrous ferric oxide. *Environmental Science and Technology* 40: 5950-5955.

Campbell, K. M., R. Root, P. A. O'Day, and J. G. Hering. (2008) A gel probe equilibrium sampler for measuring arsenic porewater profiles and sorption gradients in sediments: II. Field application to Haiwee Reservoir sediment. *Environmental Science and Technology* 42: 504-510.

Canfield, D. E. (1989). Reactive iron in marine sediments. *Geochimica et Cosmochimica Acta* 53: 619-632.

Capel, P. D., K. A. McCarthy, and J. E. Barbash. (2008) National, holistic, watershed-scale approach to understand the sources, transport, and fate of agricultural chemicals. *Journal of Environmental Quality* 37: 983-993.

Castelle, S., J. Schäfer, G. Blanc, S. Audry, H. Etcheber, J.-P. Lissalde. (2007) 50-year record and solid state speciation of mercury in natural and contaminated reservoir sediment. *Applied Geochemistry* 22: 1359-1370.

Cheng, F. and T. Granata. (2007) Sediment transport and channel adjustments associated with dam removal: Field observations. *Water Resources Research* 43: W03444, doi: 10.1029/2005WR004271.

Dixit, S. and J. G. Hering. (2003) Comparison of Arsenic(V) and Arsenic(III) sorption onto iron oxide minerals: Implications for arsenic mobility. *Environmental Science and Technology* 37: 4182-4189.

Domagalski, J. L., S. P. Phillips, E. R. Bayless, C. Zamora, C. Kendall, R. A. Wildman, Jr., and J. G. Hering. (2008) Influences of the unsaturated, saturated, and riparian zones on the transport of nitrate near the Merced River, California, USA. *Hydrogeology Journal* 16: 675-690.

Downing, J. A., J. J. Cole, J. J. Middelbury, R. G. Striegl, C. M. Duarte, P. Kortelainen, Y. T. Prairie, and K. A. Laube. (2008) Sediment organic carbon burial in agriculturally eutrophic impoundments over the last century. *Global Biogeochemical Cycles* 22: GB1018, doi:10.1029/2006GB002854.

Dubrovsky, N. M., C. R. Kratzer, L. R. Brown, J. M. Gronberg, and K. R. Burow. (1998) Water quality in the San Joaquin-Tulare Basins, California, 1992-95. *United States Geological Survey* Circular 1159.

Engberg, R. A. (1999). Selenium budgets for Lake Powell and the Upper Colorado River Basin. *Journal of the American Water Resources Association* 35(4): 771-786.

Essaid, H. I., C. M. Zamora, K. A. McCarthy, J. R. Vogel, and J. T. Wilson. (2008) Using heat to characterize streambed water flux variability in four stream reaches. *Journal of Environmental Quality* 37: 1010-1023.

Farmer, J. *Glen Canyon Dammed: Inventing Lake Powell and the Canyon Country.* Tucson: The University of Arizona Press, 1999.

Findlay, S. (1995). Importance of surface-subsurface exchange in stream ecosystems: The hyporheic zone. *Limnology and Oceanography* 40(1): 159-164.

Finneran, K. T., R. T. Anderson, K. P. Nevin, and D. R. Lovley. (2002) Potential for bioremediation of uranium-contaminated aquifers with microbial U(VI) reduction. *Soil and Sediment Contamination* 11(3): 339-357.

Friedl, G. and A. Wüest. (2002) Disrupting biogeochemical cycles – Consequences of damming. *Aquatic Science* 64: 55-65.

Froelich, P. N., G. P. Klinkhammer, M. L. Bender, N. A. Luedtke, G. R. Heath, D. Cullen, P. Dauphin, D. Hammond, B. Hartman, and V. Maynard. (1979) Early oxidation of organic matter in pelagic sediments of the eastern equatorial Atlantic: suboxic diagenesis. *Geochimica et Cosmochimica Acta* 43: 1075-1090.

Gächter, R. and B. Müller. (2003) Why the phosphorus retention of lakes does not necessarily depend on the oxygen supply to their sediment surface. *Limnology and Oceanography* 48(2): 929-933.

Gloss, S. P., L. M. Mayer, and D. E. Kidd. (1980) Advective control of nutrient dynamics in the epilimnion of a large reservoir. *Limnology and Oceanography* 15(4): 873-884.

Gloss, S. P., R. C. Reynolds, L. M. Mayer, and D. E. Kidd. (1981) "Reservoir influences on salinity and nutrient fluxes in the arid Colorado River Basin", p. 1618-1629. *In:* H.G. Stefan (ed.), *Proceedings of the Symposium on Surface Water Impoundments*. American Society of Civil Engineers, New York.

Granet, J. and M. Anderson. (2005) *2003 Lake Powell Beach Monitoring Report*. Glen Canyon National Recreation Area: Page, Arizona, 2005.

Gronberg, J. A. M. and C. R. Kratzer. (2007) Environmental setting of the Lower Merced River Basin, California. *United States Geological Survey* Scientific Investigations Report 2006-5152.

Guérin, F., G. Abril, S. Richard, B. Burban, C. Reynouard, P. Seyler, and R. Delmas. (2006) Methane and carbon dioxide emissions from tropical reservoirs: Significance of downstream rivers. *Geophysical Research Letters* 33: L21407, doi:10.1029/2006GL027929.

Guérin, F., G. Abril, A. Tremblay, and R. Delmas. (2008) Nitrous oxide emissions from tropical hydroelectric reservoirs. *Geophysical Research Letters* 35: L06404, doi:10.1029/2007GL033057.

Haggard, B. E., E. H. Stanley, and D. E. Storm. (2005) Nutrient retention in a point-source-enriched stream. *Journal of the North American Benthological Society* 24(1): 29-47.

Hart, R. J., H. E. Taylor, R. C. Antweiler, G. G. Fisk, G. M. Anderson, D. A. Roth, M. E. Flynn, D. B. Pearl, M. Truini, and L. B. Barber. (2004) Physical and chemical characteristics of Knowles, Forgotten, and Moqui Canyons, and effects of recreational use on Water Quality, Lake Powell, Arizona and Utah. *United States Geological Survey* Scientific Investigations Report 2004-5120.

Harvey, J. W. and C. C. Fuller. (1998) Effect of enhanced manganese oxidation in the hyporheic zone on basin-scale geochemical mass balance. *Water Resources Research* 34(4): 623-636.

Harvey, J. W., B. J. Wagner, and K. E. Bencala. (1996) Evaluating the reliability of the stream tracer approach to characterize stream-subsurface water exchange. *Water Resources Research* 32(8): 2441-2451.

Horowitz, A. J. and K.A. Elrick. (1987) The relation of stream sediment surface area, grain size and composition to trace element chemistry. *Applied Geochemistry* 2: 437-451.

Horowitz, A. J., K. A. Elrick, and J. J. Smith. (2001) Annual suspended sediment and trace element fluxes in the Mississippi, Columbia, Colorado, and Rio Grande drainage basins. *Hydrological Processes* 15: 1169-1207.

Hueftle, S. J. and L. E. Stevens. (2001) Experimental flood effects on the limnology of Lake Powell reservoir, Southwestern USA. *Ecological Applications* 11(3): 644-656.

Ingram, H., A. D. Tarlock, and C. R. Oggins. "The law and politics of the operation of Glen Canyon Dam", in *Colorado River Ecology and Dam Management: Proceedings of a Symposium May 24-25, 1990 Santa Fe, New Mexico.* Committee to Review the Glen Canyon Environmental Studies, Water Science and Technology Board, National Research Council: Washington, D.C., 1991.

Jackman, A. P. and K. T. Ng. (1986) The kinetics of ion exchange on natural sediments. *Water Resources Research* 22(12): 1664-1674.

Johnson, N. M. and D. H. Merritt. (1979) Convective and advective circulation of Lake Powell, Utah-Arizona, during 1972-1975. *Water Resources Research* 15(4): 873-884.

Jordan, T. E., J. C. Cornwell, W. R. Boynton, and J. T. Anderson. (2008) Changes in phosphorus biogeochemistry along an estuarine salinity gradient: The iron conveyor belt. *Limnology and Oceanography* 53(1): 172-184.

Kalff, J. *Limnology.* Upper Saddle River, New Jersey: Pretence Hall, Inc., 2002.

Kemenes, A., B. R. Forsberg, and J. M. Melack. (2007) Methane release below a tropical hydroelectric dam. *Geophysical Research Letters* 34: L12809, doi:10.1029/2007GL029479.

Kennedy, V. C., A. P. Jackman, S. M. Zand, G. W. Zellweger, and R. J. Avanzino. (1984) Transport and concentration controls for chloride, strontium, potassium and lead in Uvas Creek, a small cobble-bed stream in Santa Clara County, California, U.S.A. *Journal of Hydrology* 75: 67-110.

Kleiner, J. and H.-H. Stabel. (1989) Phosphorous transport to the bottom of Lake Constance. *Aquatic Sciences* 51(3): 181-191.

Kneebone, P. E., P. A. O'Day, N. Jones, and J. G. Hering. (2002) Deposition and fate of arsenic in iron- and arsenic-enriched reservoir sediments. *Environmental Science and Technology* 36: 381-386.

Kurtzman, D. and B. R. Scanlon. (2007) El Niño-Southern Oscillation and Pacific Decadal Oscillation impacts on precipitation in the southern and central United States: Evaluation of spatial distribution and predictions. *Water Resources Research* 43: W10427, doi:10.1029/2007WR005863.

Lee, G., J. M. Bigham, and G. Faure. (2002) Removal of trace metals by coprecipitation with Fe, Al and Mn from natural waters contaminated with acid mine drainage in the Ducktown Mining District, Tennessee. *Applied Geochemistry* 17: 569-581.

Lee, G., G. Faure, J. M. Bigham, and D. J. Williams. (2008) Metal release from bottom sediments of Ocoee Lake No. 3, a primary catchment area for the Ducktown mining district. *Journal of Environmental Quality* 37:344-352.

Marion, A., A. I. Packman, M. Zaramella, and A. Bottacin-Busolin. (2008) Hyporheic flows in stratified beds. *Water Resources Research* 44: W09433, doi:10.1029/2007WR006079.

Matzinger, A., R. Pieters, K. I. Ashley, G. A. Lawrence, A. Wüest. (2007) Effects of impoundment on nutrient availability and productivity in lakes. *Limnology and Oceanography* 52(6): 2629-2640.

Mayer, L.M. and S. P. Gloss. (1980) Buffering of silica and phosphate in a turbid river. *Limnology and Oceanography* 25(1): 12-22.

McGuire, J. T., D. T. Long, M. J. Klug, S. K. Haack, and D. W. Hyndman. (2002) Evaluating behavior of oxygen, nitrate, and sulfate during recharge and quantifying reduction rates in a contaminated aquifer. *Environmental Science and Technology* 36: 2693-2700.

Meko, D. M. and C. A. Woodhouse. (2005) Tree-ring footprint of joint hydrologic drought in Sacramento and Upper Colorado river basins, western USA. *Journal of Hydrology* 308: 196-213.

Meybeck, M. (1982) Carbon, nitrogen, and phosphorus transport by world rivers. *American Journal of Science* 282: 401-450.

Morel, F. M. M. and J. G. Hering. *Principles and Applications of Aquatic Chemistry*. John Wiley and Sons, Inc.: New York, 1993.

Müller, B., D. Finger, M. Sturm, V. Prasuhn, T. Haltmeier, P. Bossard, C. Hoyle, and A. Wüest. (2007) Present and past bio-available phosphorus budget in the ultra-oligotrophic Lake Brienz. *Aquatic Science* 69: 227-239.

Naftz, D. L., J. Yahnke, J. Miller, and S. Noyes. (2005) Selenium mobilization during a flood experiment in a contaminated wetland: Stewart Lake Waterfowl Management Area, Utah. *Applied Geochemistry* 20: 569-585.

Naylor, C., W. Davison, M. Motelica-Heino, G. A. van Den Berg, L. M. van Der Heijdt. (2006) Potential kinetic availability of metals in sulphidic freshwater sediments. *Science of the Total Environment* 357: 208-220.

Novak, J. M. and D. W. Watts. (2006) Phosphorus sorption by sediments in a Southeastern coastal plain in-stream wetland. *Journal of Environmental Quality* 35: 1975-1982.

Phillips, S. P., C. T. Green, K. R. Burow, J. L. Shelton, and D. L. Rewis. (2007) Simulation of multiscale ground-water flow in part of the Northeastern San Joaquin Valley, California. U.S. Geological Survey Scientific Investigations Report 2007-5009.

Potter, L. D. and C. L. Drake. *Lake Powell: Virgin Flow to Dynamo.* University of New Mexico Press, Albuquerque, 1989.

Pratson, L., J. Hughes-Clarke, M. Anderson, T. Gerber, D. Twichell, R. Ferrari, C. Nittrouer, J. Beaudoin, J. Granet, and J. Crockett. (2008) Timing and patterns of basin infilling as documented in Lake Powell during a drought. *Geology* 36(11): 843-846.

Prothero, D. R. and F. Schwab. *Sedimentary Geology, second edition.* New York: W.H. Freeman and Company, 2004.

Puckett, L. J., C. Zamora, H. Essaid, J. T. Wilson, H. M. Johnson, M. J. Brayton, and J. R. Vogel. (2008) Transport and fate of nitrate at the ground-water/surface-water interface. *Journal of Environmental Quality* 37: 1034-1050.

Reynolds, Jr., R. C. (1978) Polyphenol inhibition of calcite precipitation in Lake Powell. *Limnology and Oceanography* 23(4): 585-597.

Riggsbee, J. A., J. P. Julian, M. W. Doyle, and R. G. Wetzel. (2007) Suspended sediment, dissolved organic carbon, and dissolved nitrogen export during the dam removal process. *Water Resources Research* 43: W09414, doi: 10.1029/2006/WR005318.

Salehin, M., A. I. Packman, and M. Paradis. (2004) Hyporheic exchange with heterogeneous streambeds: Laboratory experiments and modeling. *Water Resources Research* 40: W11504, doi: 10.1029/2003WR002567.

Schindler, D. W., R. E. Hecky, D. L. Findlay, M. P. Stainton, B. R. Parker, M. J. Paterson, K. G. Beaty, M. Lyng, and S. E. M. Kasian. (2008) Eutrophication of lakes cannot be controlled by reducing nitrogen input: Results of a 37-year whole-ecosystem experiment. *Proceedings of the National Academy of Sciences of the USA* 105(32): 11254-11258.

Seager, R., M. Ting, I. Held, Y. Kushnir, J. Lu, G. Vecchi, H.-P. Huang, N. Harnik, A. Leetmaa, N.-C. Lau, C. Li, J. Velez, and N. Naik. (2007) Model profjections of an imminent transition to a more arid climate in Southwestern North America. *Science* 316: 1181-1184.

Snyder, N. P., S. A. Wright, C. N. Alpers, L. E. Flint, C. W. Holmes, and D. M. Rubin. (2006) Reconstructing depositional processes and history from reservoir stratigraphy: Englebright Lake, Yuba River, northern California. *Journal of Geophysical Research* 111: F04003, doi:10.1029/2005JF000451.

Spahr, N. E., L. E. Apodaca, J. R. Deacon, J. B. Bails, N. J. Bauch, C. M. Smith, and N. E. Driver. (2000) Water quality in the Upper Colorado River Basin, Colorado, 1996-98. *U.S. Geological Survey* Circular 1214.

Spiteri, C., P. van Cappellen, and P. Regnier. (2008) Surface complexation effects on phosphate adsorption to ferric iron oxyhydroxides along pH and salinity gradients in estuaries and coastal aquifers. *Geochimica et Cosmochimica Acta* 72: 3431-3445.

Steele, G. V., H. M. Johnson, M. W. Sandstrom, P. D. Capel, and J. E. Barbash. (2008) Occurrence and fate of pesticides in four contrasting agricultural settings in the Untied States. *Journal of Environmental Quality* 37: 1116-1132.

Stumm, W. and J. J. Morgan. *Aquatic Chemistry, 3rd edition.* New York: John Wiley and Sons, Inc., 1996.

Syvitski, J. P. M., C. J. Vörösmarty, A. J. Kettner, and P. Green. (2005) Impact of humans on the flux of terrestrial sediment to the global coastal ocean. *Science* 308: 376-380.

Taylor, K. G. and S. Boult. (2007) The role of grain dissolution and diagenetic mineral precipitation in the cycling of metals and phosphorus: A study of a contaminated urban freshwater sediment. *Applied Geochemistry* 22: 1344-1358.

Teodoru, C. and B. Wehrli. (2005) Retention of sediments and nutrients in the Iron Gate I Reservoir on the Danube River. *Biogeochemistry* 76: 539-565.

Tonkin, J. W., L. S. Balistrieri, and J. W. Murray. (2004) Modeling sorption of divalent metal cations on hydrous manganese oxide using the diffuse double layer model. *Applied Geochemistry* 19: 29-53.

United States Bureau of Reclamation. (2008a) *Bureau of Reclamation: Upper Colorado Region Historic Data*. Webpage viewed at http://www.usbr.gov/uc/crsp/GetSiteInfo on 21 December 2008.

United States Bureau of Reclamation. (2008b) *Untitled Document*. Webpage viewed at http://www.usbr.gov/uc/progact/salinity/pdfs/CRBannual_salinity_data.pdf on 6 January 2009.

Valett, H. M., J. A. Morrice, C. N. Dahm, and M. E. Campana. (1996) Parent lithology, surface-groundwater exchange, and nitrate retention in headwater streams. *Limnology and Oceanography* 41(2): 333-345.

Vernieu, W. S. (1997). Effects of reservoir drawdown on resuspension of deltaic sediments in Lake Powell. *Journal of Lake and Reservoir Management* 13(1): 67-78.

Vernieu, W. S., S. J. Hueftle, and S. P. Gloss. (2005) Water quality in Lake Powell and the Colorado River. In *State of the Colorado River Ecosystem in Grand Canyon* (S. P. Gloss, J. E. Lovich, and T. S. Melis, eds.). Reston, Virginia: United States Geological Survey, 2005.

Webb, R. H., G. H. McCabe, R. Hereford, and C. Wilkowske. (2004) Climate fluctuations, drought, and flow in the Colorado River Basin. *U.S. Geological Survey Fact Sheet* 2004-3062.

Williams, N. T. (2007) Modeling dissolved oxygen in Lake Powell using CE-QUAL-W2. Masters Thesis, Brigham Young University.

Woodhouse, C. A., S. T. Gray, and D. M. Meko. (2006) Updated streamflow reconstructions for the Upper Colorado River Basin. *Water Resources Research* 42: W05415, doi:10.1029/2005WR004455.

Chapter 3

POREWATER REDOX GEOCHEMISTRY BEFORE AND AFTER EXPOSURE AND RE-SUBMERGENCE OF SEDIMENT AT A RESERVOIR SHORELINE

Richard A. Wildman, Jr., Nathan C. Chan,

Nathan F. Dalleska, Mark Anderson, and Janet G. Hering

(submitted to *Limnology and Oceanography*)

Acknowledgements

The authors thank K.M. Campbell, M.A. Ferguson, A.A. Jones (each Caltech), and Z.E. Harris for laboratory assistance; C.E. Farnsworth, M. Vondrus, A.P. Kositsky, A.M. Cody (each Caltech), J.B. Miller (USBR), T. McDaniel, and Z.E. Harris for field assistance; and L.E. Bryant (Virginia Tech), C.E. Farnsworth (Caltech), L. Roberts, B. Wehrli, M. Schirmer (each Eawag), A. Voegelin (ETHZ), and M. Krom (Leeds University) for key thoughts during data interpretation. This work was funded by NSF SGER grants EAR-0408329 and EAR-0621371, the Alice Tyler Foundation, USBR grant 06PG400222, and the Carolyn Ash Summer Undergraduate Research Fellowship awarded to Nathan Chan at Caltech. Some sampling resources were provided by Glen Canyon National Recreation Area. The use of trade names is for identification purposes only and does not imply endorsement by the United States National Park Service.

Abstract –

At Lake Powell (a large reservoir in Utah and Arizona, United States of America), we collected high-resolution porewater samples before and after shoreline sediment was exposed to air and subsequently resubmerged by changing water levels. Using porewater manganese as a redox indicator, we observed subsurface reduction conditions in two separate locations before sediment was exposed to air. Non-zero dissolved manganese concentrations existed in samples collected after exposure to air and resubmergence by rising water level, despite our expectation that manganese-oxide precipitation would occur during low water levels due to microbially-mediated oxidation. Thus, the two locations appear to re-establish reducing conditions at different rates, with one location showing high dissolved manganese concentrations just below the surface only 3.5 days after resubmergence, whereas another location showed only moderately increased dissolved manganese after 11.5 days. The difference between the two sites may be explained by differences in local topography, with the former sampling location possibly receiving greater groundwater flow from a nearby hill than the latter location. Uranium data correspond to redox trends with depth in one sampling location. This suggests that this element can be a viable *in situ* redox indicator under certain conditions and that it responds more slowly to the onset of reducing conditions than manganese. Correlations between porewater manganese, arsenic, and lead were observed, indicating that redox conditions may influence the solubility of other trace elements at Lake Powell.

Introduction

The redox geochemistry of trace metals in sediment porewater has been extensively examined in studies both of early diagenesis (e.g., Froelich et al. 1979, Hyacinthe et al. 2001, Katsev et al. 2007) and of the behavior of trace contaminants in shallow groundwater and the hyporheic zone (e.g., Campbell et al. 2008a, Merritt and Amirbahman 2007). Reducing conditions in sediment porewater result from the microbial mineralization of organic carbon and the concomitant respiration of terminal electron acceptors (TEAs). The sequence in which TEAs are utilized generally corresponds to their standard reduction potentials such that the most energetically favorable TEAs, oxygen and nitrate, are reduced first, followed by the reductive dissolution of manganese (Mn) and iron (Fe) oxide minerals, then the reduction of sulfate (SO_4^{2-}) to sulfide (S^{2-}), and finally fermentation reactions (Stumm and Morgan 1996, Hyacinthe et al. 2001). This leads to characteristic depth profiles of the reduced species in porewaters.

Because Mn and Fe oxides often serve as carrier phases for inorganic contaminants such as arsenic (As) and lead (Pb), their reductive dissolution can result in contaminant mobilization and, conversely, their oxidative precipitation in contaminant sequestration (e.g., Campbell et al. 2008b). In addition, the solubility of inorganic contaminants themselves may be controlled by redox conditions. For example, uranium (U) is highly insoluble under reducing conditions, but can be mobile under oxidizing conditions (Wu et al. 2007).

Previous studies of the geochemistry of sediment porewater have focused primarily on lakes and marine basins. In these environments, undisturbed depositional sequences of sediments can be identified, sediments are always fully water-saturated, and advection of

porewater is usually negligible. Redox conditions in lake and marine sediments can change over time in response to changes in the composition of overlying water or the rate and composition of sediment deposition, but the resulting changes in porewater tend to be gradual (Granina et al. 2004, Katsev et al. 2007).

In contrast, shoreline-, tidal flat-, floodplain-, and hyporheic-zone sediments can be exposed to transient conditions associated with changes in water elevation, and they are potentially subject to advective transport (e.g., Baldwin 1996; Beck et al. 2008). In some cases, declining water levels result in exposure of sediments to atmospheric oxygen and the development of unsaturated conditions in the surficial sediments. Drying and rewetting of sediments disturbs ambient redox conditions and may result in changes in porewater redox chemistry (Campbell et al. 2008b), yet the effects of this process have not been extensively examined in field studies.

In this research, depth profiles of TEAs were examined in shoreline sediments subject to changing water levels and exposure to air. Observations before and after sediment exposure and resubmergence are interpreted to provide insight into the *in situ* rate of re-establishment of reducing conditions in porewater, and the effects of changing redox conditions in the sediments on contaminant mobility are examined. These sediments also reflect km-scale heterogeneity associated with spatially varying geology. Samples were collected from locations along the shoreline of Lake Powell, a large reservoir on the Colorado River in Utah and Arizona, where changes in water elevation can be anticipated based on consistent patterns of inflows and outflows. Preliminary surveys of porewater composition indicated that reducing conditions are prevalent in the

surficial shoreline sediments, suggesting that transient exposure to atmospheric oxygen might result in observable changes in porewater geochemistry.

Sampling and Methods

Field site—Lake Powell, a large reservoir on the Colorado River in southeastern Utah and northernmost Arizona, was created in 1963 by the closure of Glen Canyon Dam (Figure 1). Flooding of a dendritic canyon created a reservoir with a long, narrow thalweg and > 90 side canyons that comprise most of the shoreline. Away from the inflows of the Colorado and San Juan Rivers, the shoreline and near-shore lakebed are characterized by sandy sediment deposited by small, intermittent tributaries.

Water releases from Glen Canyon Dam are timed to optimize hydropower production and to fulfill obligations to downstream populations and ecosystems rather than to match inflow to Lake Powell; this reservoir moderates the variable flow of the Colorado River. There is a net loss of reservoir storage between early July and March, followed by a more rapid increase between March and late June, when snowmelt from the Rocky Mountains increases inflows. When yearly inflows and releases are similar in magnitude, this pattern leads to a fluctuation in the water surface elevation of ≤ 8 m. In some years, the increase in storage due to spring runoff does not match the yearly water release, leading to multi-year trends in lake level superimposed on the yearly pattern (Figure 2). All reservoir surface elevations used in this paper are collected by the United States Bureau of Reclamation (http://www.usbr.gov/uc/crsp/GetSiteInfo) at Glen Canyon Dam.

Sample collection—All sampling locations in this study were sandy shorelines that were surrounded by rock. Vegetation was generally very sparse and absent in the areas immediately surrounding the sampling locations. In June 2005, an initial survey of sediment porewater was conducted in White Canyon (WC), Moqui Canyon (MC), the bank of the San Juan River near its inflow (SJ), and Navajo Canyon (NC, Figure 1). Results from the initial survey guided a subsequent field experiment in WC and Farley Canyon (FC). These two side canyons derive most of their sediment from individual rock formations; the Cedar Mesa Sandstone surrounds WC, and the Organ Rock Formation, a shale, surrounds FC (Anderson et al. 2003).

Porewater samples (see below) were collected from FC and WC on 27 January and 28 March 2007 in sediment submerged beneath 10-25 cm of water and located 40-100 cm from the shoreline (Figures 2 and 3). The March sampling location in FC was < 5 m from the January sampling location; in WC, the distance was < 1 m. Multiple samplers were deployed in FC in January (FC-Jan) and March (FC-Mar) and in WC in March (WC-Mar). Sampler FC-Jan-A was located 44 cm from samplers FC-Jan-B and FC-Jan-C, which were 4 cm apart. In January, a single sampler, WC-Jan, was deployed in WC. Samplers FC-Mar-A and FC-Mar-B were separated by 32 cm; samplers WC-Mar-A and WC-Mar-B by 29 cm. The water depth above replicate samplers varied by < 10 cm. In March, > 32 cm-deep sediment cores were collected within 10 cm of each porewater sampler. The FC sampling location was at the base of a small hill (highest point ~8 m above the water level), whereas the WC sampling location was at the end of a flat stretch of sand (highest point ~1 m above the water level).

Sampling and analytical methods—Porewater samples were collected with a constrained "diffusive equilibrium in thin-films" sampler, and gel synthesis followed recently revised methods (Davison et al. 1994, Harper et al. 1997). A 0.45 μm filter membrane separated gel slabs from sediment during deployment, which lasted 20-28 hours according to established sampling methods (Campbell et al. 2008a). Upon removal of the sampler from the sediment, gels were removed from the sampler, transported to the laboratory in polypropylene microcentrifuge tubes, and re-equilibrated in 1% nitric acid (Campbell et al. 2008a). Solutions were diluted and analyzed for Mn, As, U, and Pb on an Agilent 4500 inductively-coupled plasma mass spectrometer (ICP-MS). ICP-MS data were calibrated with multi-element calibration solutions prepared from ICP-grade single element standards for each element (EMD Chemicals, Gibbstown, NJ). Analytical detection limits (μM) were: 0.04 for Mn, 0.008 for U, 0.001 for Pb, and 0.03 for As; relative standard deviations were < 5%.

Sediment cores were collected in 2.5-cm diameter butyrate tubes that were kept cool during transport to the laboratory, frozen ≤ 3 d after collection, and sectioned anoxically at 8 cm intervals. Particle size and chemical analyses of these cores are described elsewhere (Chapter 4). Porosity was measured in the laboratory by adding a known volume of freeze-dried sediment to a known volume of water, measuring the overlying water, and solving

$$\varphi = \frac{V_{w,tot} - V_{w,over}}{(V_{w,tot} - V_{w,over}) + V_{sed}} \qquad (1)$$

where $V_{w,tot}$ is the total volume of water, $V_{w,over}$ is the volume of overlying water after the sediment settles, and V_{sed} is the volume of sediment added. Replicate porosity measurements were made in homogenized sediment core sections 0-4 cm and 8-12 cm

below the SWI in both FC and WC. Any effect of freeze-drying on porosity should be negligible in this sediment because of its large particle size (i.e., the amount of clays that can adsorb water is negligible) and low carbon content (Chapter 4; M. Huettel, Florida State University, personal communication).

Porewater Flux Calculations—When a diffusional gradient of a chemical exists across the sediment-water interface (SWI), the flux from porewater to overlying water can be estimated using

$$J = -\varphi \cdot D_s \cdot \frac{dC}{dz} \qquad (2)$$

where J is flux in μmol L^{-1} cm^{-2} d^{-1}, φ is porosity, D_s is the diffusivity of Mn^{2+} in sediment, expressed in cm^2 s^{-1}, and dC/dz is the vertical concentration gradient, in μmol L^{-1} cm^{-1}. D_s is calculated following Boudreau (1996)

$$D_s = \frac{D_0}{1 - \ln(\varphi^2)} \qquad (3)$$

where D_0, the diffusivity of Mn^{2+} in solution, is adjusted for temperature with the Stokes-Einstein equation,

$$\left(\frac{D\eta}{T}\right)_{T1} = \left(\frac{D\eta}{T}\right)_{T2} \qquad (4)$$

Results

Observations Related to Sediment Transport—The visual appearance of the sediments at each sampling location, observed during repeated field trips, indicated lateral homogeneity on the scale of meters, probably due to isolated sediment-transport events. For example, in WC, a sediment embankment observed on 19 June 2005 was apparently washed away before a return visit on 4-5 December 2005 (Figure 4). The

location of the shoreline in this side canyon was also pushed *downstream* between June and December despite the water elevation being ~49 cm *higher* in December (lake surface elevations = 1097.38 and 1097.87 m above sea level on 19 June and 4 December, respectively), which would be consistent with deposition of the displaced sediment in the streambed. Furthermore, in December 2005, the dry streambed showed evidence of rapid water flow, debris piled on the upstream side of obstructions, and depressions representative of eddies immediately downstream of large rocks. Between the sampling events in January and March 2007, however, there was no evidence of large-scale sediment disturbance in either canyon.

Reservoir Level Fluctuations and Environmental Variables—The surface elevation of Lake Powell varied during this field experiment as a result of different inflows and dam releases. During the 27 January sampling, the reservoir level was at its lowest since the preceding spring, 1097.21 m above sea level (asl), and was falling at ~3.4 cm d^{-1} (Figure 2). By 16 March, continued water level decline led to the yearly minimum, 1096.48 m asl. At the time of the 28 March sampling, 11.5 d later (all times are rounded to 0.5 d), the water surface had risen 34 cm to an elevation of 1096.82 m asl at a rate of ~3.0 cm d^{-1}.

Sediment depths sampled in January had been below the lake surface elevation since May 2006 (Figure 2). After the January sampling, the falling lake level led to similar amounts of time above the water level for the sediment where each sampler was deployed in March: ~26.5 and ~29.0 days for FC-Mar-A and FC-Mar-B, respectively, and ~29.0 and ~20.5 days for WC Mar-A and WC Mar-B, respectively. Upon sampling, the SWI at the locations FC-Mar-A and FC-Mar-B had been resubmerged for 4.0 and 3.5

d, respectively, and the SWI at the locations of WC-Mar-A and WC-Mar-B had been re-submerged for 2.0 and 5.0 d, respectively. The deepest samples of samplers FC-Mar-A, WC-Mar-A, and WC-Mar B were below the minimum reservoir surface elevation in 2007 (henceforth, "low-water line"); these depths had been continuously below the water line since May 2006. The deepest depth sampled by FC-Mar-B was 3.2 cm above the low-water line, so it was above the reservoir water level for 5.0 d and then resubmerged for 10.0 d before sampling.

Daily high air temperature during both sampling events was ~9°C. In January, porewater temperature (T) was 7°C in FC and 5°C in WC. March sampling coincided with a cold front; air T was > 19°C for 3 weeks before dropping the day before sampling. Porewater T was not measured in March, but rapid changes in T are not expected to be translated deep into groundwater (Schmidt et al. 2007). Thus, porewater T can be estimated at 5°C near the SWI and 15°C at depth. Windy conditions during deployment led to overnight accumulation of 5 cm of sediment at the top of samplers WC-Mar-A and WC-Mar-B. However, conditions were calm at the time of sampler retrieval.

At time of sampling, the shoreline near the FC sites were moist even 1-2 m above the water line, whereas the shoreline near the WC sites was mostly dry and disaggregated sand.

Porewater chemistry: overview—Most porewater samples obtained from shoreline sediment at Lake Powell contained Mn and As in concentrations above U.S. Environmental Protection Agency drinking water standards (U.S. EPA 2008). Some samples exceeded the drinking water standard for U, and almost none exceeded the standard for Pb (Table 1).

Porewater chemistry: manganese—Porewater profiles measured from all FC samples and WC-Jan showed approximately similar trends in Mn: concentrations were low in surface water and increased across the SWI to a plateau at depth (Figure 5). WC-Mar samples differed, increasing in Mn concentration below the SWI with no obvious plateau at depth. Maximum Mn concentrations reached 23.8 μmol L^{-1} and 18.6 μmol L^{-1} in FC and WC, respectively. At both sites, small-scale variability with depth was observed in the subsurface. Consistent, low Mn concentrations with depth in the surface water indicated minimal analytical variability.

Profiles from replicate samplers deployed at FC in January and March showed similar variability within consistent ranges. Major trends with depth were similar; fine scale variations with depth did not correspond in the replicate samplers. Porewater profiles at FC and WC differed distinctly between January and March samples with different patterns observed in FC and WC. In FC, maximum concentrations at depth were higher in March than in January, leading to a higher concentration at the sediment-water interface (5.3 μmol L^{-1} versus 1.1 μmol L^{-1} in January) and a steeper gradient (i.e., 1.79 μmol L^{-1} cm^{-1} in FC-Mar-A versus 1.08 μmol L^{-1} cm^{-1} in FC-Jan-A). The opposite was true in WC, where the January profile showed higher values at depth and a steeper gradient than in March (i.e., 2.32 μmol L^{-1} cm^{-1} in WC-Jan versus 0.89 μmol L^{-1} cm^{-1} in WC-Mar-B).

A porosity of 0.45 was measured for all samples. We assume that this value reasonably represents porosity at the sediment surface because 1) the rapid and intermittent sediment deposition at these sites should lead to uniform porosity at depth, and 2) dewatering after sedimentation should remove depth variation due to compaction

by compacting all depths equally on the scale of our porewater measurements. Thus, this value is adequate for use in equation 2. Using the D_0 value of Li and Gregory (1974) and adjusting for temperatures measured in January and estimated in March, $D_s = 1.43 \times 10^{-6}$ $cm^2\ s^{-1}$ in FC and 1.42×10^{-6} $cm^2\ s^{-1}$ in WC in January and 1.42×10^{-6} $cm^2\ s^{-1}$ near the SWI in March. Together with the observed Mn gradients, these values implied fluxes to overlying water of 6.00×10^{-5} μmol Mn^{2+} cm^{-2} d^{-1} in the FC-Jan-A profile, 9.88×10^{-5} µmol Mn^{2+} cm^{-2} d^{-1} in FC-Mar-A, and 1.28×10^{-4} μmol Mn^{2+} cm^{-2} d^{-1} in WC-Jan. In March in WC, gradients across the SWI were negligible, leading to no flux to the overlying water.

Porewater chemistry: uranium—In FC, U concentrations ranged from undetectable to 0.017 μmol L^{-1} in January and 0.005 to 0.025 μmol L^{-1} in March (Figure 6). No samples exceed the drinking water standard of 0.126 µmol L^{-1} (30 μg L^{-1}). Observations of vertical cm-scale variability and replicate profiles resembled those for Mn (described above), though surface water values varied more, suggesting higher analytical variability. Below the SWI, all profiles decreased in concentration from surface maxima, though the January and March profiles changed slope at different depths. In January, concentrations decreased across the SWI to a depth of 5 cm, below which they were constant. However, March concentrations decreased until the low-water line (21 cm), below which they were constant.

Surface water concentrations in WC resembled those of FC, but porewater concentrations were higher (Figure 6). January WC concentrations ranged from 0.003 to 0.065 µM; WC-Mar concentrations were much higher than all other profiles, ranging from 0.015 to 0.13 µmol L^{-1} and exceeding the US EPA standard near the SWI. Unlike

all other profiles, concentrations increased with depth in WC-Jan. Below the SWI, WC-Mar profiles resembled FC-Mar profiles, with concentrations decreasing with depth until the depths of the low-water line at each sampler. Above the SWI, U concentrations in WC-Mar-B decreased sharply over ~4 cm, above which they are constant. A similar trend exists at WC-Mar-A, though the sharp decrease occurs across the SWI, not above it.

Porewater chemistry: lead and arsenic—No trend with depth was observed for Pb or As in January porewater data, and concentration ranges were similar in FC and WC (data not shown). Concentrations of Pb were generally < 0.02 μmol L^{-1}, and As ranged from 0.10 to 0.31 μmol L^{-1}.

In March, Pb concentrations were again < 0.02 μmol L^{-1}, and As concentrations ranged from 0.20 to 0.37 μmol L^{-1} (Figure 7). In FC-Mar-A and FC-Mar-B, concentrations increased across the SWI until a depth of ~11 cm and ~14 cm, respectively, below which they were steady. Trends in WC were small relative to the variability of the data. The trend with depth observed in FC was also observed for As in profile WC-Mar-B, but not in WC-Mar-A.

Discussion

Sediment chemistry—Organic carbon was low (0.03-0.11%), total carbon ranged from 1.0-2.4% and increased with depth, and mineralogical data suggest that the total carbon (C) was mostly carbonate (Chapter 4). Neither parameter showed a statistical difference between FC and WC (t-test, $p < 0.05$), so C was not expected to explain differences in redox chemistry between side canyons. Sediment in FC contained significantly higher Mn, Fe, and Pb than that of WC (t-test, $p < 0.05$); As follows a

similar trend. Concentrations of Mn and Fe in sediment were much higher than those in porewater (Chapter 4) and thus the sedimentary reservoir of these elements was not expected to be depleted.

Scale of sediment deposition and homogeneity—In small, arid washes, sediment is generally transported through brief, intense, "flash" flooding events (Malmon et al. 2004; Prothero and Schwab 2004), which are common on the Colorado Plateau (Dick et al. 1997). Observations during repeated scouting trips to WC in 2005 strongly suggest that a flash flood occurred there in late 2005, moving a substantial amount of sediment downstream such that the shoreline was displaced 1 km down the canyon at a lake level of ~1097 m asl. No such events were observed in FC, yet the close proximity of FC to WC implies that flash floods should also be an important mechanism of sediment transport in that intermittent streambed. Flash flood events are expected to occur energetically and turbulently, leading to spatial homogenization of sediment on the scale of meters, yet not necessarily at the centimeter scale (Prothero and Schwab 2004). This implies that major trends in porewater chemistry measured in replicate samplers should be comparable. However, minor, random, cm-scale variations in both the horizontal and vertical directions could be expected in all sampling locations.

Groundwater advection—During low reservoir levels at Lake Powell, groundwater stored in sediment and rock formations along its banks flows into the reservoir (Potter and Drake 1989). Although we have no data that directly pertain to groundwater advection, estimations are possible based on the slope of the shoreline and the sediment particle size. Sediment from side canyons of Lake Powell consists mostly of sand. The mean values of mean particle sizes measured in multiple samples were 142 and 106 μm

in WC and FC, respectively (samples WC E, 0-8 and 16-24 cm and FC B, 0-8 and 16-24 cm reported in Chapter 4). Since this sediment is well-sorted, the intrinsic permeability (k) can be estimated following an empirical relationship presented by Bear (1972):

$$k = 0.617 \times 10^{-11} \cdot s_{mean} \quad (5)$$

where s_{mean} is the mean particle size of the sediment. From the values reported in Chapter 4, intrinsic permeabilities are estimated at 8.75×10^{-10} cm^2 and 6.52×10^{-10} cm^2 for WC and FC, respectively. These values can be used to calculate hydraulic conductivity (K) using

$$K = k \cdot \frac{\rho \cdot g}{\mu} \quad (6)$$

where ρ is the density of water (in g cm^{-3}), g is gravitational acceleration (980 cm s^{-1}), and μ is the viscosity of water (in g cm^{-1} s^{-1}; Bear 1972). Both the density and viscosity of water were calculated for temperatures of 5°C for WC in January, 7°C for FC in January, and 15°C for both canyons in March. Thus, hydraulic conductivities are estimated to be 5.7×10^{-5} cm s^{-1} and 7.5×10^{-5} cm s^{-1} for WC in January and March, respectively, and 4.5×10^{-5} cm s^{-1} and 5.6×10^{-5} cm s^{-1} for FC in January and March, respectively.

We can estimate the maximum groundwater advection (ω) from the banks of the side canyons into the reservoir by using the slope of the ground surface as the slope of the water table in the equation

$$\omega = K \cdot \frac{dh}{dl} \quad (7)$$

where dh is the difference in groundwater elevations and dl is the length of flow along the groundwater flowpath (Santos et al. 2009). Using the slope of the land at each porewater sampling location and the values of hydraulic conductivity calculated for each sampling

location and time, groundwater advection is estimated to be 3.5×10^{-5} cm s^{-1} and 1.2×10^{-5} cm s^{-1} for WC in January and March, respectively, and 1.4×10^{-5} cm s^{-1} and 1.3×10^{-5} cm s^{-1} for FC in January and March, respectively.

Although these values are slightly more than one order of magnitude larger than the diffusivities calculated for dissolved Mn, they are not directly comparable because advection rates were calculated for groundwater flow in the banks of the reservoir, not at the sampling locations. On one hand, it is possible that this advection may influence the porewater sampling locations, and this influence could not only vary with depth due to cm-scale variations in hydraulic conductivity (thus leading to some of the small-scale variability in the porewater profiles) but also influence the shape of the major trends in the porewater profiles. Conversely, while the above calculation results from the maximum possible hydraulic head that could have existed in the exposed shoreline, the porewater samplers were located in submerged sediment, where we assume no variations in hydraulic head exist. Furthermore, porewater samplers were located > 40 cm from the shoreline, and it is unclear to what extent groundwater flow in the banks of the reservoir could have decreased by groundwater discharge out the sediment surface both above the water level and between the shoreline and the sampling locations. It is also possible that groundwater flow could be less than calculated because of decreased permeability above the water level due to clogging of pore spaces by small particles transported shortly after the decrease in reservoir level. Since the maximum estimated groundwater flow is both not very much greater than the diffusivity of manganese and likely to be much higher than the groundwater flow at the location of the porewater samplers, we tentatively

assume that sediment geochemistry and diffusion, not groundwater advection, are the dominant processes influencing porewater profiles.

Manganese redox chemistry—Concentrations of Mn are used as a porewater redox indicator in this study. Its fast reduction kinetics (Davies and Morgan 1989) make it a good indicator of redox processes on short time scales. Measurements of Mn by ICP-MS are assumed to represent Mn^{2+} due to the low solubility of Mn(III/IV)-oxide compounds.

The similarity of major trends and apparently random, minor, cm-scale variation in porewater Mn observed in replicate samplers is consistent with sediment transport by flash floods. Major trends, such as increases in Mn concentration with depth followed by steadily elevated concentrations, indicate complete consumption of O_2 and reducing conditions just below the SWI. Lateral advection through porewater sampling locations, which could create horizontal redox gradients and confound interpretation of porewater data (Beck et al. 2008), is assumed to be negligible here because side canyon water at Lake Powell is quiescent (Hart et al. 2004), there was no evidence of flow in the FC and WC creeks during this experiment, and the sampling was timed such that the daily lake level change was small.

Variation of $\geq$ 2-5 μmol L^{-1} at the cm-scale has been observed previously due to random, localized sources of solid, reactive organic matter (Shuttleworth et al. 1999; Fones et al. 2001). In this depositional setting, localizations of organic material probably come from decomposing plant debris. Furthermore, cm-scale variation at these sites indicates no physical disruption of sediment. Minor variation with depth may also be due to precipitation of Mn(II) solid minerals, but albandite (MnS) is generally undersaturated in porewater that contains sulfide (Naylor et al. 2006). Rhodocrocite ($MnCO_3$)

precipitation can affect multi-cm trends in Mn and may also vary at the scale of ≤ 1 cm if porewater CO_2 varies at this scale. In this setting, high calcite concentrations are expected to buffer changes in pH that may occur as reducing conditions develop (Masscheleyn et al. 1991).

Similar shapes of Mn profiles collected in both January and March in FC suggest re-establishment of subsurface redox conditions in ≤ 3.5 d after re-flooding. Notably higher concentrations at depth in March are probably attributable to enhanced microbial respiration at higher temperatures. In WC, Mn porewater profiles measured in March samples have lower concentrations than those measured in January samples, and they increase in concentration for several cm below the SWI. These observations indicate that, unlike FC, reducing conditions were not fully re-established in the sediment porewater of WC. These rates of re-establishment are comparable to another study that shows steady-state porewater Mn^{2+} after 3 d in laboratory column experiments (Masscheleyn et al. 1991).

A key assumption underlying this interpretation is that Mn^{2+} was oxidized during sediment exposure. In between the sampling events, the sediment sampled in March is expected to receive oxygen by exposure to air during unsaturation at times of low reservoir level and by reflooding of oxygenated surface water from a rising reservoir. Thermodynamic calculations show that oxidative precipitation of dissolved Mn is highly favorable in the presence of small concentrations of oxygen (Stumm and Morgan 1996), and microbially-mediated oxidation of Mn^{2+} has been observed to occur on a time scale of hours in an air-equilibrated solution (Bargar et al. 2000). Furthermore, U data (discussed below) suggest that oxidizing conditions occurred when the sediment was

above the water line. Thus, we expect that substantial oxidiation of Mn^{2+} would have occurred in unsaturated sediment exposed by the minimum reservoir levels experienced during the study period.

The difference in the rates of *in situ* Mn(III/IV) reduction between FC and WC may be explained by the varying topography at the sampling locations. The wet sediment surface above the water line in FC suggests that groundwater flow from the hill discharged to the sediment surface, keeping it wet several weeks after exposure to air. However, the dry sediment in WC indicates that this did not occur there. This difference may have led to more complete unsaturation and aeration of the sediment matrix in WC during low water levels and better infiltration of oxygenated surface water after re-flooding. This enhanced supply of oxygen would support microbial respiration in sediment porewater, slowing the development of reducing conditions and the subsequent release of Mn^{2+} to the dissolved phase. This difference between side canyons may be augmented by the slightly higher hydraulic conductivity in WC as compared to FC. The larger particle size in WC, which leads to the larger hydraulic conductivity, may result from the different rock formations surrounding the two canyons, implying that local geology may influence the response of porewater chemistry to changing reservoir levels. Other variables, such as sediment chemistry and limnological trends, do not explain the difference between FC and WC: solid-phase C concentrations are similar, solid-phase Mn concentrations far exceed those in porewater, and these side canyons enter the main channel of Lake Powell 0.5 km apart, so they should experience similar trends in lake level and water chemistry. We did not characterize the microbial populations, which might be different in the two canyons. Variations in iron and manganese mineralogy,

which may affect the respiration of chemoautotrophic bacteria, may also contribute to differences in porewater chemistry between FC and WC.

The accumulation of sediment on the samplers deployed in March in WC does not seem to have affected porewater profiles of Mn. These samplers require < 1 h to equilibrate with the sediment porewater (Davison et al. 1994), so this observation implies that a few hours is too short a time for porewater chemistry to change after a rapid sedimentation event.

Our porewater trends differ from those reported from marine basins. In other settings, Mn^{2+} gradients are steeper (e.g., Froelich et al. 1979; Fones et al. 2001; Hyacinthe et al. 2001), resulting in diffusive fluxes an order of magnitude higher than those reported here, which are on par with another shoreline study (Table 2). This difference may result from the rapid, intermittent sedimentation at our field location and the rapid sedimentation at the site of Campbell et al. (2008b). In our Mn profiles, concentrations increase sharply across the SWI, whereas Mn concentration gradients reported by studies of marine basins and that of Campbell et al. (2008b) occur below the SWI. The shallow placement of our Mn gradients may result from high sedimentation rate (Granina et al. 2004) or more reactive organic C in our sediment.

Uranium chemistry—Profiles of porewater U can add to an interpretation of redox geochemistry based on Mn. In oxidizing conditions, carbonate generally complexes UO_2^{2+} in the dissolved phase; upon reduction, solid uraninite (UO_2) precipitates (Wu et al. 2007). Porewater U measured in January in FC suggest that U reduction appears to occur concomitantly with Mn reduction, since the concentrations of these elements anticorrelate with depth. This is consistent with groundwater bioremediation and laboratory studies,

which show that low levels of Mn(III/IV)- and Fe(III)-oxide minerals oxidize U(IV) and thus frequently control its mobility in groundwater (Tokunaga et al. 2008; Fredrickson et al. 2008). In March, however, the steady decrease of U concentrations from the SWI to near the low-water line and constant concentration below this depth imply that U was oxidized when the sediment was unsaturated in between the sampling times. This agrees with a groundwater biostimulation study in which the onset of reducing conditions led to nearly complete reduction and precipitation of U(IV) and subsequent introduction of dissolved oxygen promptly oxidized and dissolved U solids (Wu et al. 2007). In FC, the higher concentrations of porewater U above the low-water line in March relative to January suggest that further U reduction may have been possible after the March sampling event, which may have captured an ongoing process. This differs from the porewater Mn observations and suggests that, after exposure to oxygen and re-flooding, reduction of U(VI) may occur at a slower rate than that of Mn(IV).

In WC in January, an increase of porewater U with depth, despite reducing conditions indicated by Mn, may imply that U is complexed in solution, perhaps by dissolved organic carbon (Wan et al. 2008), or (bi)carbonate (Ginder-Vogel et al. 2006). Such complexation would depend on pH and the type and amount of Fe(III)-oxides present (Stewart et al. 2007), yet quantification of this reaction is not possible since porewater pH, dissolved carbonate, and detailed iron mineralogy data were not collected as part of this study. While our data do not allow conclusions about the mechanism causing the observed depth profiles of U, they show that, whereas U and Mn reduction occur in concert in FC, these reactions are controlled by separate processes in WC.

Despite the slow onset of reducing conditions in WC after sediment exposure and re-flooding, U concentrations decrease with depth below the SWI, suggesting that the onset of reducing conditions after resubmergence may affect both Mn and U. High subsurface concentrations suggest that, as in FC, sediment exposure oxidized and mobilized U. Higher concentrations in WC than in FC may be a result of the legacy of U mining in the WC catchment from 1948-1954 (Farmer 1999).

Lead and arsenic—In sediment porewater, Pb and As are known to correspond to trends in redox chemistry. In FC and WC, variations with depth are nonexistent or small (i.e., in FC in March) and only generally correspond to Mn trends, suggesting that Mn-oxide minerals may not be dominant sorbents of As and Pb in this setting. Instead, As and Pb are probably sorbed to Fe minerals, which occur at this site and commonly sorb trace elements. In samples collected across Lake Powell in an initial survey of porewater conditions, correlations are most consistent between porewater Mn and Pb (Table 3). When considered along with the detailed results collected in FC and WC, this preliminary finding suggests that porewater redox chemistry plays a role in trace contaminant mobility in different regions of the Lake Powell shoreline.

Implications—The yearly rise and fall of the surface elevation at Lake Powell is a result of the snowmelt-dominated runoff of the Colorado River and dam operation that prioritizes hydropower production and downstream water supply. When the surface elevation of Lake Powell is steady or falling slightly, Mn diffuses out of shoreline sediment submerged under < 30 cm of water. This observation, which is not common among studies of porewater diagenesis, may be attributed to sporadic deposition of organic C associated with sedimentation that occurs due to flash floods. This process

could impair water quality as concentrations of Mn and As in porewater frequently exceed drinking water standards, although elevated Mn concentrations in the overlying water occur only just above the SWI. This is unlikely to pose a public health threat, since water in Lake Powell side canyons is extremely low in trace metals due to dilution (Hart et al. 2004) and most recreational visitors to shorelines at Lake Powell are expected to be exposed to porewater only through dermal contact. Porewater U may be enhanced in White Canyon due to the mining legacy of that catchment.

We know of no other study that reports high-resolution, *in situ*, porewater profiles of redox-active elements during non-equilibrium conditions such as the ones imposed at the shoreline of Lake Powell during yearly variation in lake level. Upon re-flooding, redox gradients are re-established at rates that may differ based on sediment permeability, which may relate to the local geology in specific regions of the shoreline. During a slow rise in lake level, it appears unlikely that Mn diffusion out of sediment will occur at all shoreline locations.

Our data also suggest that, under certain conditions, uranium may be a useful redox indicator in shallow porewater and that the comparisons of manganese and uranium profiles may provide insight into the response of a system to changing redox conditions. Our results suggest that reduction of Mn(IV/III) is more facile than that of U(VI), which is consistent both with the thermodynamics of the reactions and the results of laboratory and groundwater biostimulation studies.

References

Anderson, P. B., T. C. Chidsey, D. A. Sprinkel, and G. C. Willis. Geology of Glen Canyon National Recreation Area, Utah-Arizona. 2003. *In* D. A. Sprinkel, T. C.

Chidsey, and P. B. Anderson [eds.], Geology of Utah's Parks and Monuments, 2nd ed. Utah Geological Association.

Baldwin, D. S. 1996. Effects of exposure to air and subsequent drying on the phosphate sorption characteristics of sediments from a eutrophic reservoir. Limnol. Oceanogr. 41: 1725-1732.

Bargar, J. R., B. M. Tebo, and J. E. Villinski. 2000. In situ characterization of Mn(II) oxidation by spores of the marine *Bacillus* sp. strain SG-1. Geochim. Cosmochim. Acta 64: 2775-2778.

Bear, J. *Dynamics of fluids in porous media.* Dover Publications, Inc.: Mineola, NY, 1972.

Beck, M., O. Dellwig, B. Schnetger, and H.-J. Brumsack. 2008. Cycling of trace metals (Mn, Fe, Mo, U, V, Cr) in deep pore waters of intertidal flat sediments. Geochim. Cosmochim. Acta 72: 2822-2840.

Berner, R. A. 1980. Early Diagenesis: A Theoretical Approach. Princeton University Press.

Boudreau, B. P. 1996. The diffusive tortuosity of fine-grained unlithified sediments. Geochim. Cosmochim. Acta 60: 3139-3142.

Campbell, K. M., R. Root, P. A. O'Day, and J. G. Hering. 2008a. A gel probe equilibrium sampler for measuring arsenic porewater profiles and sorption gradients in sediments: 1. Laboratory development. Environ. Sci. Technol. 42: 497-503.

Campbell, K. M., R. Root, P. A. O'Day, and J. G. Hering. 2008b. A gel probe equilibrium sampler for measuring arsenic porewater profiles and sorption gradients in sediments: II. Field application to Haiwee Reservoir sediment. Environ. Sci. Technol. 42: 504-510.

Davies, S. H. R. and J. J. Morgan. 1989. Manganese(II) oxidation kinetics on metal oxide surfaces. J. Col. Int. Sci. 129: 63-77.

Davison, W., H. Zhang, and G. W. Grime. 1994. Performance characteristics of gel probes used for measuring the chemistry of pore waters. Environ. Sci. Technol. 28: 1623-1632.

Dick, G. S., R. S. Anderson, and D. E. Sampson. 1997. Controls on flash flood magnitude and hydrograph shape, Upper Blue Hills badlands, Utah. Geology 25: 45-48.

Farmer, J. 1999. Glen Canyon Dammed: Inventing Lake Powell and the Canyon Country. The University of Arizona Press.

Fones, G. R., W. Davison, O. Holby, B. B. Jorgensen, and B. Thamdrup. 2001. High-resolution metal gradients measured by *in situ* DGT/DET deployment in Black Sea sediments using an autonomous benthic lander. Limnol. Oceanogr. 46: 982-988.

Fredrickson, J. K., J. M. Zachara, D. W. Kennedy, C. Liu, M. C. Duff, D. B. Hunter, and A. Dohnalkova. 2008. Influence of Mn oxides on the reduction of uranium(VI) by the metal-reducing bacterium Shewanella putrefaciens. Geochim. Cosmochim. Acta 66: 3247-3262.

Froelich, P. N., G. P. Klinkhammer, M. L. Bender, N. A. Luedtke, G. R. Heath, D. Cullen, P. Dauphin, D. Hammond, B. Hartman, and V. Maynard. 1979. Early oxidation of organic matter in pelagic sediments of the eastern equatorial Atlantic: suboxic diagenesis. Geochim. Cosmochim. Acta 43: 1075-1090.

Ginder-Vogel, M., C. S. Criddle, and S. Fendorf. 2006. Thermodynamic constraints on the oxidation of biogenic UO_2 by Fe(III) (Hydr)oxides. Environ. Sci. Technol. 40: 3544-3550.

Granina, L., B. Muller, and B. Wehrli. 2004. Origin and dynamics of Fe and Mn sedimentary layers in Lake Baikal. Chem. Geol. 205: 55-72.

Harper, M. P., W. Davison, and W. Tych. 1997. Temporal, spatial, and resolution constraints for *in situ* sampling devices using diffusional equilibrium: dialysis and DET. Environ. Sci. Technol. 31: 3110-3119.

Hart, R. J., H. E. Taylor, R. C. Antweiler, G. G. Fisk, G. M. Anderson, D. A. Roth, M. E. Flynn, D. B. Pearl, M. Truini, and L. B. Barber. 2004. Physical and chemical characteristics of Knowles, Forgotten, and Moqui Canyons, and effects of recreational use on Water Quality, Lake Powell, Arizona and Utah. United States Geol. Surv. Sci. Inv. Rep. 2004-5120.

Hyacinthe, C., P. Anschutz, P. Carbonel, J.-M. Jouanneau, and F. J. Jorissen. 2001. Early diagenetic processes in the muddy sediments of the Bay of Biscay. Mar. Geol. 177: 111-128.

Katsev, S., G. Chaillou, B. Sundby, and A. Mucci. 2007. Effects of progressive oxygen depletion on sediment diagenesis and fluxes: A model for the lower St. Lawrence River Estuary. Limnol. Oceanogr. 52: 2555-2568.

Kneebone, P. E. 2000. Arsenic geochemistry in a geothermally impacted system: The Los Angeles Aqueduct. Ph.D. thesis. Calif. Inst. of Tech.

Li, Y.-H. S. Gregory. 1974. Diffusion of ions in sea water and in deep-sea sediments. Geochim. Cosmochim. Acta 38: 703-714.

Malmon, D. V., S. L. Reneau, and T. Dunne. 2004. Sediment sorting and transport by floods. J. Geophys. Res. 109: F02005, doi:10.1029/2003JF000067.

Masch, F. D. and K. J. Denny. 1966. Grain size distribution and its effect on the permeability of unconsolidated soils. Wat. Resour. Res. 2: 665-677.

Masscheleyn, P. H., R. D. Delaune, and W. H. Patrick, Jr. 1991. Effect of redox potential and pH on arsenic speciation and solubility in a contaminated soil. Environ. Sci. Technol. 25: 1414-1419.

Merritt, K. A. and A. Amirbahman. 2007. Mercury dynamics in sulfide-rich sediments: Geochemical influence on contaminant mobilization within the Penobscot River estuary, Maine, USA. Geochim. Cosmochim. Acta 71: 929-941.

Naylor, C., W. Davison, M. Motelica-Heino, G. A. van den Berg, L. M. van der Heijdt. 2006. Potential kinetic availability of metals in sulphidic freshwater sediments. Sci. Tot. Environ. 357: 208-220.

Potter, L. D. and C. L. Drake. *Lake Powell: Virgin Flow to Dynamo.* University of New Mexico Press, Albuquerque, 1989.

Prothero, D.R. and F. Schwab. 2004. Sedimentary Geology, 2nd ed. Freeman.

Schmidt, C., B. Conant, Jr., M. Bayer-Raich, and M. Schirmer. 2007. Evaluation and field-scale application of an analytical method to quantify groundwater discharge using mapped streambed temperatures. J. Hydrol. 357: 292-307.

Shuttleworth, S. M., W. Davison, and J. Hamilton-Taylor. 1999. Two-dimensional and fine structure in the concentrations of iron and manganese in sediment pore-waters. Environ. Sci. Technol. 33: 4169-4175.

Stewart, B. D., J. Neiss, and S. Fendorf. 2007. Quantifying constraints imposed by calcium and iron on bacterial reduction of uranium(VI). J. Environ. Qual. 36: 363-372.

Stumm, W. and J. J. Morgan. 1996. Aquatic Chemistry, 3rd ed. Wiley.

Tokunaga, T. K, J. Wan, Y. Kim, S. R. Sutton, M. Newville, A. Lanzirotti, and W. Rao. 2008. Real-time x-ray absoption spectroscopy of uranium, iron, and manganese in contaminated sediments during bioreduction. Environ. Sci. Technol. 42: 2839-2844.

United States Environmental Protection Agency. 2008. Drinking Water Contaminants. Webpage viewed on 14 December 2008 at http://www.epa.gov/safewater/contaminants/index.html#listmcl.

Wan, J., T. K. Tokunaga, Y. Kim, E. Brodie, R. Daly, T. C. Hazen, and M. K. Firestone. 2008. Effects of organic carbon supply rates on uranium mobility in a previously bioreduced contaminated sediment. Environ. Sci. Technol. 42: 7573-7579.

Wu, W.-M., J. Carley, J. Luo, M. A. Ginder-Vogel, E. Cardenas, M. B. Leigh, C. Hwang, S. D. Kelly, C. Ruan, L. Wu, J. van Nostrand, T. Gentry, K. Lowe, T. Mehlhorn, S. Carroll, W. Luo, M. W. Fields, B. Gu, D. Watson, K. M. Kemner, T. Marsh, J. Tiedje, J. Zhou, S. Fendorf, P. K. Kitanidis, P. M. Jardine, and C. S. Criddle. 2007. In situ bioreduction of uranium (VI) to submicromolar levels and reoxidation by dissolved oxygen. Environ. Sci. Technol. 41: 5716-5723.

Tables

Table 1. Trace elements in sediment porewater sampled at the Lake Powell shoreline

element	Mn	U	Pb	As
EPA standard[a,b]	0.91	0.13	0.072	0.13
Farley Canyon				
median[a]	7.0	0.005	0.009	0.22
standard deviation[a]	4.2	0.005	0.009	0.32
number of samples	207	207	203	203
% above standard	100	0	1	100
White Canyon				
median[a]	8.3	0.048	0.012	0.22
standard deviation[a]	5.5	0.030	0.016	0.28
number of samples	197	198	198	120
% above standard	97	0	1	98
Moqui Canyon				
median[a]	1.8	0.006	0	
standard deviation[a]	5.6	0.006	0.03	
number of samples	53	53	53	
% above standard	91	0	6	
San Juan River				
median[a]	0	0.03	0.04	
standard deviation[a]	14	0.003	0.06	
number of samples	53	53	53	
% above standard	45	0	17	
Navajo Canyon				
median[a]	3.7	0.08	0.03	
standard deviation[a]	3.3	0.001	0.02	
number of samples	53	53	53	
% above standard	87	0	6	97

[a] Concentrations in μM.

[b] Primary drinking water standards for U, Pb, As; secondary drinking water standard for Mn (US EPA 2008)

Table 2. Porewater Mn^{2+} flux across the sediment-water interface[a]

porosity	T (K)	dC/dz	flux[b]	source[c]
0.45	278	-2.3	0.047	(1)
0.45	278	-1.6	0.012	(2)
0.45	278	-1.8	0.036	(3)
0.61[d]	298	-4.8	0.19	(4)
?[e]	280	-10.5	0.50	(5)
			0.2	(6)
			2.6	(6)
?[f]	?[f]		4.5	(6)
			5.6	(6)
			6.2	(6)

[a] Fluxes for Cambell et al. (2008b) and Fones et al. (2001) calculated from ideal Mn2+ diffusivity and porewater profiles in their figures.

[b] in μmol cm^{-2} d^{-1} or μmol cm^{-2} yr^{-1}

[c] References: 1: WC-Jan-A (this study), 2: FC-Jan-A (this study), 3: FC-Mar-A (this study), 4: Campbell et al. 2008b, 5: Fones et al. 2001, 6: Hyacinthe et al. 2001

[d] Porosity from Kneebone (2000).

[e] Porosity not reported, estimated at 0.7.

[f] Porosity and temperature not reported for all fluxes reported by Hyacinthe et al. (2001).

Table 3. Correlations[a] of solutes with Mn

location	month	U	Pb	As	n
FC	01/07		0.087	**0.211**	161
FC	03/07	**-0.705**	**0.482**	**0.855**	121
WC	01/07		0.070	-0.087	46
WC	03/07	**0.282**	0.059	**0.388**	101
WC	06/05	0.176	**0.842**		79
NC	06/05	-0.001	**0.946**		43
SJ	06/05	0.085	**0.972**		54
MC	06/05	0.028	**0.946**		53

[a] Bold text indicates $p < 0.05$, underline indicates $p < 0.0001$.

Figure Captions

Figure 1. Map of Lake Powell. Water flows through the reservoir from the northeast to the southwest, where it passes through Glen Canyon Dam (GCD). The Colorado River arm is north of the San Juan River arm. Other abbreviations indicate sampling locations as described in the text. The black box in the inset represents the area covered by the map.

Figure 2. Lake Powell water surface elevation above sea level. *Left panel*: 1997-2007; the box highlights the time range in the right panel. *Right panel*: 1 December 2006 to 1 December 2007; the box shows the sampling period for this study.

Figure 3. Sample deployment in White Canyon. Vertical rectangles indicate locations of samplers WC-Jan, WC-Mar-A, and WC-Mar-B from left to right. The intersection of the each sampler with the sediment-water interface (SWI) is shown. Dashed horizontal lines represent reservoir levels, including the low-water line during the experiment (see text). Sample deployment in Farley Canyon was similar.

Figure 4. Qualitative evidence of sediment transport in WC. Above: Side view photograph taken 5 December 2005. The white dashed line shows the approximate extent of a sediment embankment observed on 19 June 2005. A person (1.8 m tall) is in the white oval for scale. Left: Map view. Arrows, located in the streambed, indicate direction of intermittent flow. Solid lines show approximate shoreline location in June (upstream) and December (downstream) at the same reservoir elevation. Crescent formed by dashed lines shows the estimated extent of sediment removal from the embankment in the side

view. Person in side view is standing at the June shoreline location. Upper image courtesy Andrew Kositsky, Caltech; lower image from Google Earth.

Figure 5. Porewater profiles of Mn concentrations in Farley Canyon (left panel) and White Canyon (right panel) as a function of depth in the sediment where zero depth corresponds to the sediment-water interface (SWI) and negative depths correspond to the height above the SWI. Samples were collected before (Jan) and after (Mar) exposure and re-submergence of shoreline sediment. Solid horizontal lines indicate the lowest water elevation between January and March relative to the SWI on the sampling date of samplers FC-Mar-A, WC-Mar-A (gray line), and WC-Mar-B (black line). These lines occur at different depths because replicate samplers were inserted into sloping sediment and these graphs are normalized to the SWI. In the left panel, running averages of replicate samplers are displayed. In the right panel, the dashed line above the SWI shows the depth of sedimentation that occurred during sampler deployment in March.

Figure 6. Porewater profiles of U concentrations in Farley Canyon (left panel) and White Canyon (right panel) as a function of depth in the sediments where zero depth corresponds to the sediment-water interface (SWI) and negative depths correspond to the height above the SWI. Note the difference in scale between the two panels. Samples were collected before (Jan) and after (Mar) exposure and re-submergence of shoreline sediment. Solid horizontal lines indicate the lowest water elevation between January and March relative to the SWI on the sampling date of samplers FC-Mar-A, WC-Mar-A (gray line), and WC-Mar-B (black line). These lines occur at different depths because replicate

samplers were inserted into sloping sediment and these graphs are normalized to the SWI. In the left panel, running averages of replicate samplers are displayed. In the right panel, the dashed line above the SWI shows the depth of sedimentation that occurred during sampler deployment in March.

Figure 7. Porewater profiles of Pb (triangles and diamonds) and As (circles and squares) concentrations in Farley Canyon (left panel) and White Canyon (right panel) as a function of depth in the sediments where zero depth corresponds to the sediment-water interface (SWI) and negative depths correspond to the height above the SWI. Note the difference in scale between the two panels. Samples were collected before (Jan) and after (Mar) exposure and re-submergence of shoreline sediment. Solid horizontal lines indicate the lowest water elevation between January and March relative to the SWI on the sampling date of samplers FC-Mar-A, WC-Mar-A (gray line), and WC-Mar-B (black line). These lines occur at different depths because replicate samplers were inserted into sloping sediment and these graphs are normalized to the SWI. In the right panel, the dashed line above the SWI shows the depth of sedimentation that occurred during sampler deployment in March.

Figure 1

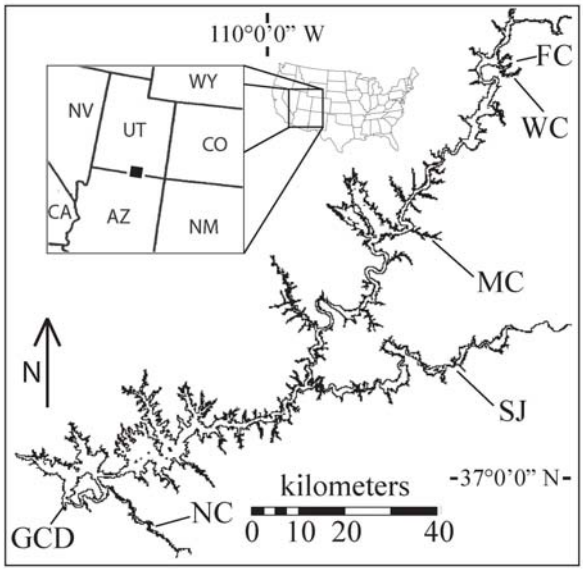
110°0'0" W
WY
NV
UT
CO
CA
AZ
NM
FC
WC
MC
N
SJ
kilometers
-37°0'0" N-
NC
GCD
0 10 20 40

Figure 2

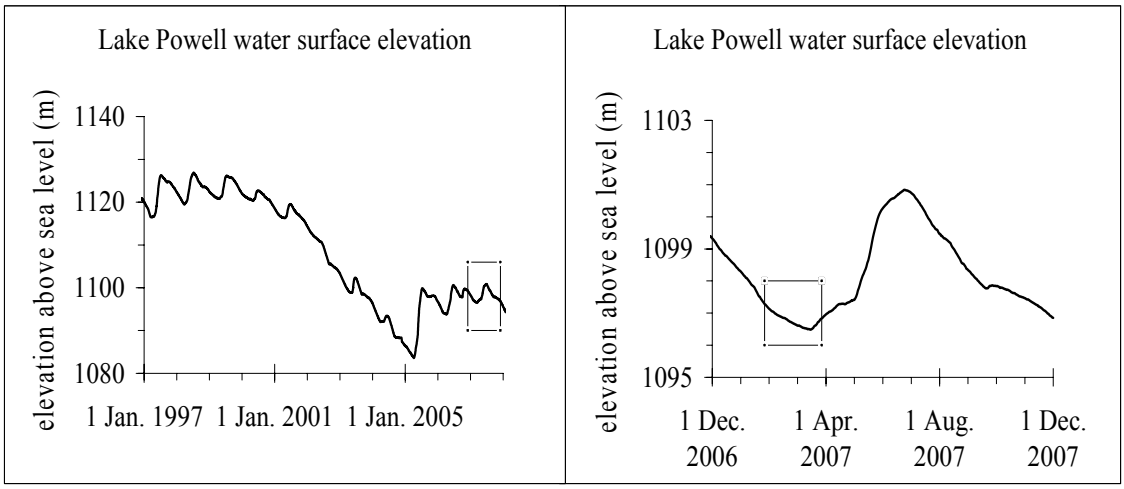
Lake Powell water surface elevation
elevation above sea level (m)
1140
1120
1100
1080
1 Jan. 1997
1 Jan. 2001
1 Jan. 2005
Lake Powell water surface elevation
elevation above sea level (m)
1103
1099
1095
1 Dec. 2006
1 Apr. 2007
1 Aug. 2007
1 Dec. 2007

Figure 3

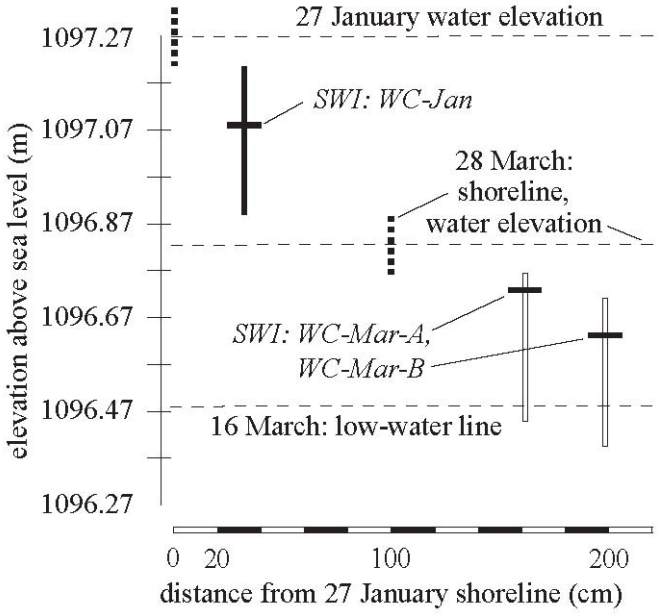
27 January water elevation
1097.27
1097.07
1096.87
1096.67
1096.47
1096.27
elevation above sea level (m)
SWI: WC-Jan
28 March:
shoreline,
water elevation
SWI: WC-Mar-A,
WC-Mar-B
16 March: low-water line
0
20
100
200
distance from 27 January shoreline (cm)

Figure 4

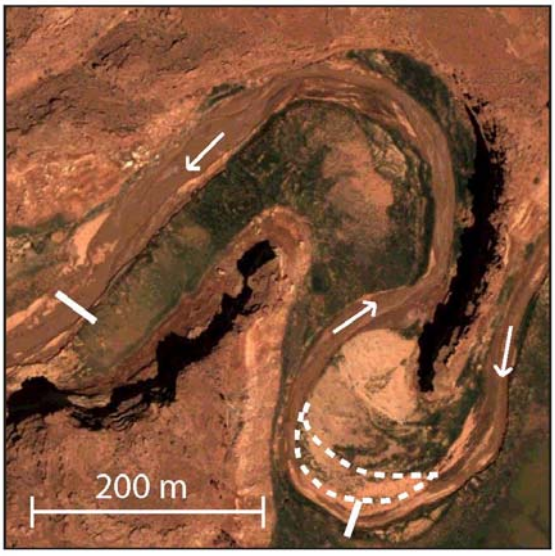

Figure 5

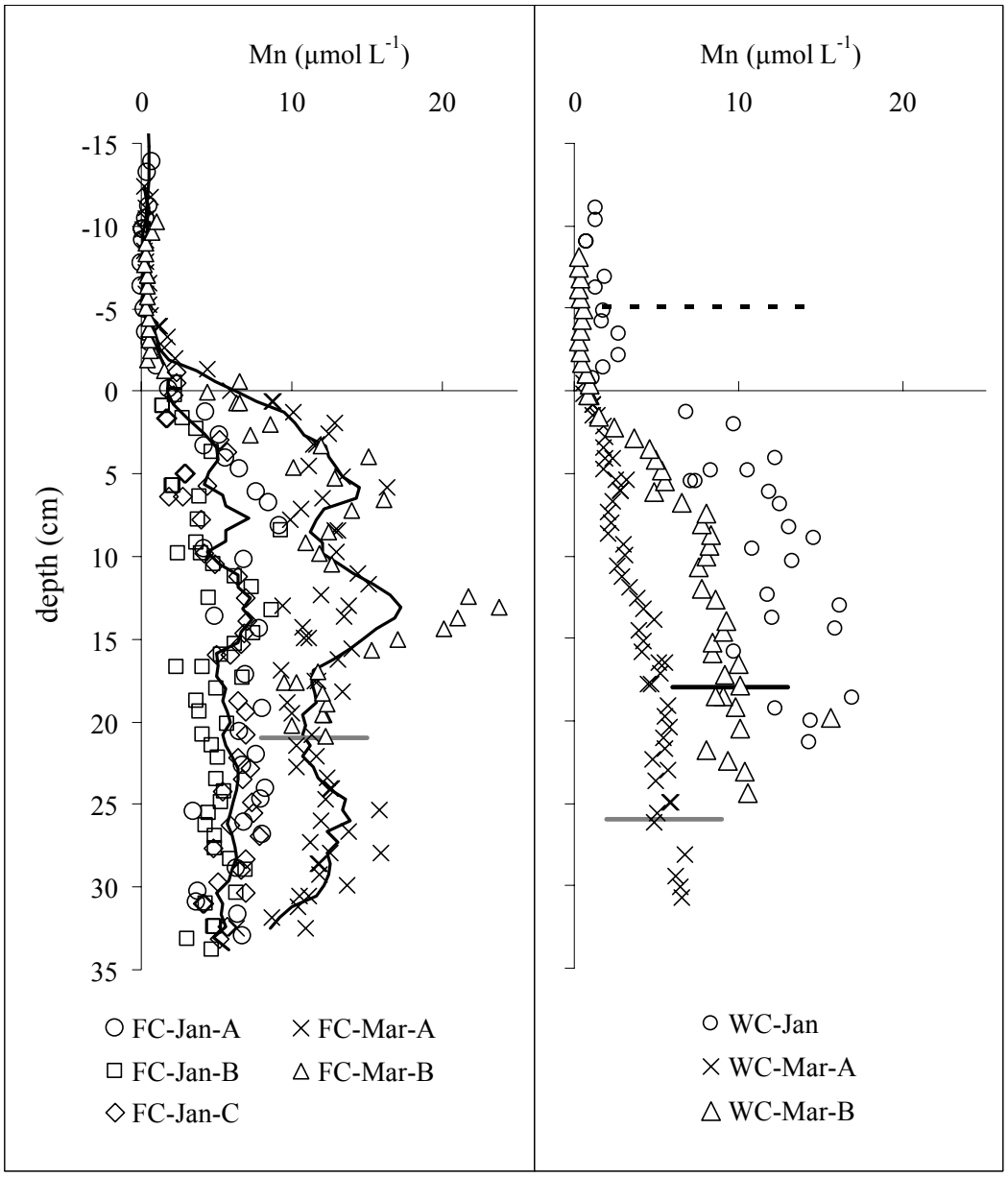
Mn (µmol L-1)
0
10
20
-15
-10
-5
0
5
10
15
20
25
30
35
depth (cm)
FC-Jan-A
FC-Jan-B
FC-Jan-C
FC-Mar-A
FC-Mar-B
Mn (µmol L-1)
0
10
20
WC-Jan
WC-Mar-A
WC-Mar-B

Figure 6

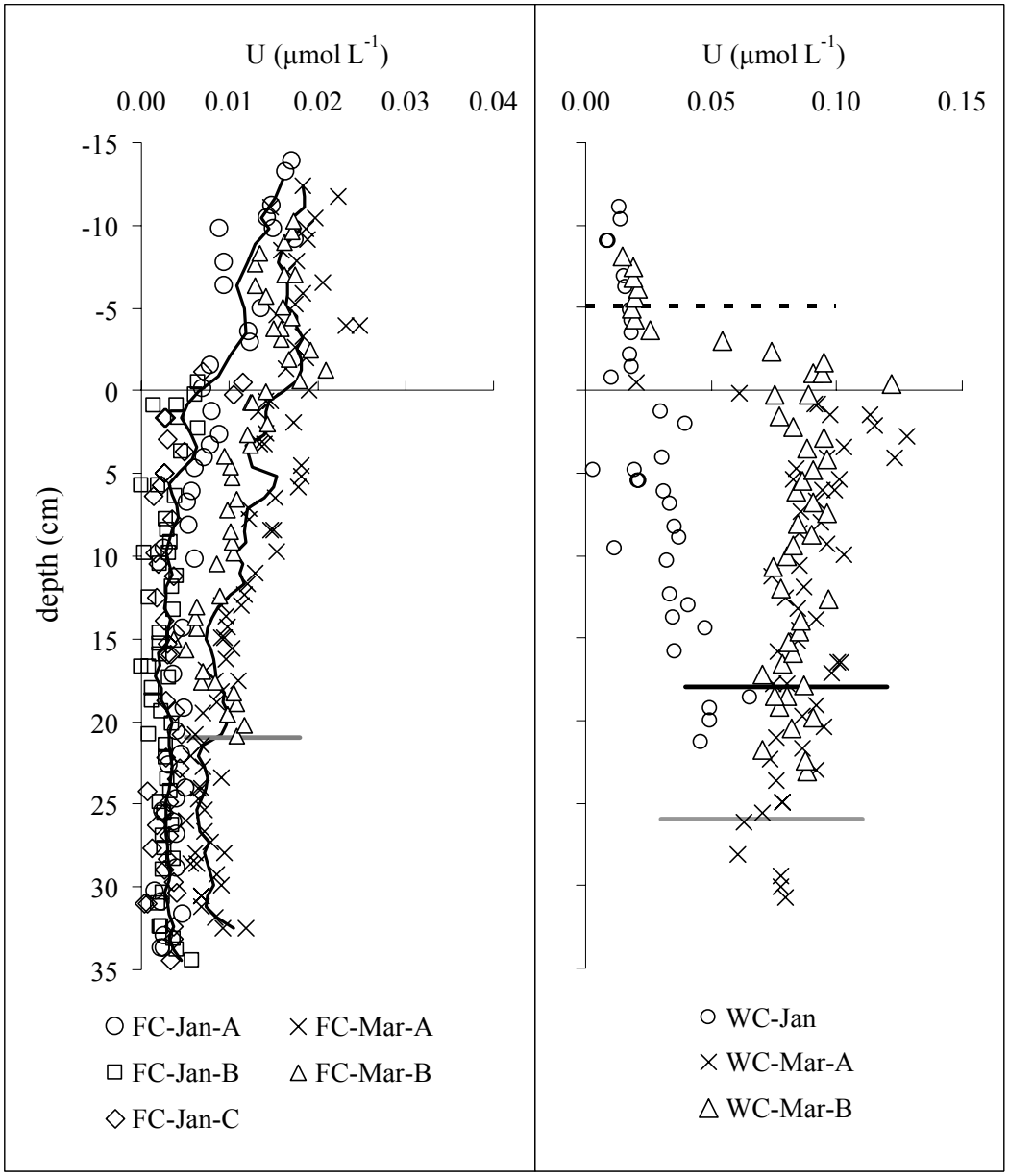
U (µmol L-1)
0.00
0.01
0.02
0.03
0.04
-15
-10
-5
0
5
10
15
20
25
30
35
depth (cm)
FC-Jan-A
FC-Jan-B
FC-Jan-C
FC-Mar-A
FC-Mar-B
U (µmol L-1)
0.00
0.05
0.10
0.15
WC-Jan
WC-Mar-A
WC-Mar-B

Figure 7

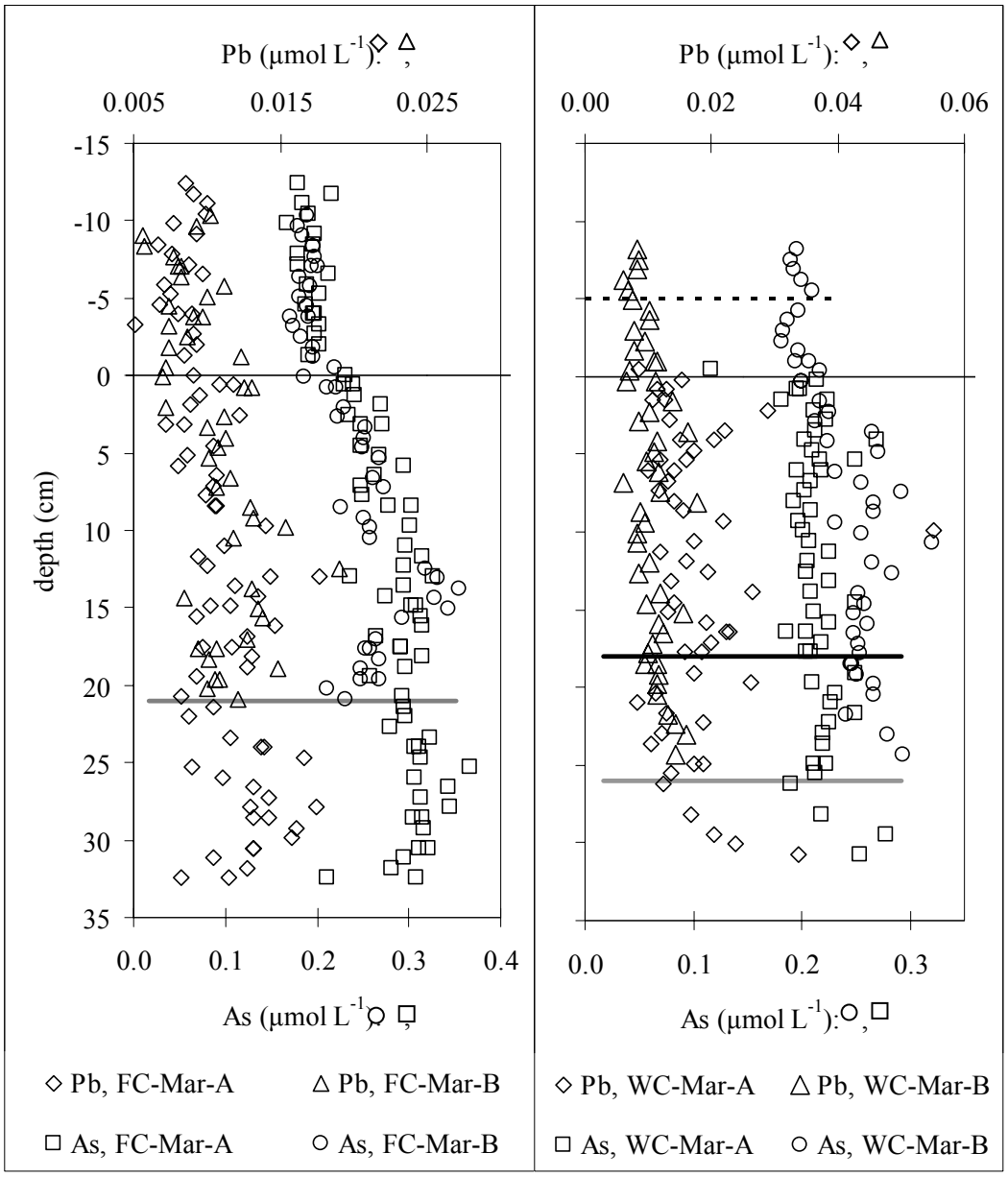
Pb (µmol L-1): ◇, △
0.005
0.015
0.025
-15
-10
-5
0
5
10
15
20
25
30
35
depth (cm)
0.0
0.1
0.2
0.3
0.4
As (µmol L-1): ○, □
◇ Pb, FC-Mar-A
△ Pb, FC-Mar-B
□ As, FC-Mar-A
○ As, FC-Mar-B
Pb (µmol L-1): ◇, △
0.00
0.02
0.04
0.06
0.0
0.1
0.2
0.3
As (µmol L-1): ○, □
◇ Pb, WC-Mar-A
△ Pb, WC-Mar-B
□ As, WC-Mar-A
○ As, WC-Mar-B

Appendix

Table A1. Concentrations (in μM) of manganese (Mn), uranium (U), and lead (Pb) measured during a June 2005 survey of porewater in side canyon sediment of Lake Powell; depth (in cm) of 0 is the sediment-water interface

depth	Mn	U	Pb	depth	Mn	U	Pb
White Canyon				*Moqui Canyon*			
-1.30	11.96	0.041	0.040	-0.65	2.12	0.006	0.039
-0.65	13.82	0.031	0.039	0.00	0.55	0.006	0.031
0.00	9.99	0.020	0.030	0.65	-0.18	0.006	0.030
0.65	10.16	0.021	0.040	1.30	-0.50	0.006	0.029
1.30	12.06	0.042	0.037	1.95	-0.60	0.006	0.029
1.95	13.85	0.023	0.050	2.60	0.13	0.006	0.035
2.60	11.66	0.023	0.041	3.25	-0.08	0.006	0.035
3.25	18.47	0.025	0.041	3.90	-0.18	0.006	0.038
3.90	14.92	0.025	0.049	4.55	0.65	0.006	0.058
4.55	11.72	0.018	0.041	5.20	0.44	0.006	0.056
5.20	12.98	0.020	0.041	5.85	-1.23	0.006	0.032
5.85	12.78	0.019	0.039	6.50	4.11	0.006	0.075
6.50	10.04	0.018	0.048	7.15	7.46	0.006	0.079
7.15	8.91	0.017	0.039	7.80	6.41	0.006	0.070
7.80	12.84	0.020	0.039	8.45	13.65	0.000	0.097
8.45	10.50	0.018	0.042	9.10	22.74	0.006	0.120
9.10	27.09	0.021	0.074	9.75	30.59	0.006	0.140
9.75	17.26	0.023	0.062	10.40	32.89	0.030	0.145
10.40	11.72	0.018	0.060	11.05	11.02	0.030	0.088
11.05	10.51	0.018	0.054	11.70	7.35	0.030	0.068
11.70	8.86	0.018	0.043	12.35	9.13	0.030	0.096
12.35	15.58	0.022	0.080	13.00	4.84	0.030	0.053
13.00	11.72	0.019	0.057	13.65	0.97	0.030	0.039
13.65	13.24	0.019	0.080	14.30	1.81	0.030	0.041
14.30	9.35	0.016	0.041	14.95	0.44	0.030	0.032
14.95	9.76	0.018	0.045	15.60	0.55	0.030	0.032
15.60	10.68	0.020	0.036	16.25	0.44	0.030	0.031
16.25	6.52	0.014	0.026	16.90	0.44	0.030	0.030
16.90	14.61	0.022	0.045	17.55	0.49	0.000	0.030
17.55	11.84	0.029	0.042	18.20	0.55	0.006	0.029
18.20	16.86	0.028	0.056	18.85	0.65	0.030	0.031
18.85	12.00	0.026	0.046	19.50	0.76	0.030	0.029
19.50	7.09	0.020	0.028	20.15	1.60	0.030	0.032
20.15	15.31	0.024	0.071	20.80	0.44	0.006	0.028

Table A1: Concentrations of Mn, U, and Pb in side canyon porewater, continued.

depth	Mn	U	Pb	depth	Mn	U	Pb
White Canyon, continued				*Moqui Canyon, continued*			
20.80	13.08	0.020	0.059	21.45	2.75	0.030	0.035
21.45	9.96	0.021	0.042	22.10	2.12	0.030	0.032
22.10	11.79	0.025	0.039	22.75	0.55	0.030	0.029
22.75	9.10	0.023	0.024	23.40	0.34	0.006	0.030
23.40	9.01	0.025	0.023	24.05	0.65	0.030	0.029
24.05	10.88	0.027	0.033	24.70	0.34	0.006	0.029
24.70	17.98	0.039	0.068	25.35	0.76	0.030	0.028
25.35	18.16	0.033	0.045	26.00	0.24	0.030	0.026
26.00	39.13	0.042	0.107	26.65	0.55	0.006	0.032
27.30	20.11	0.041	0.061	27.30	0.55	0.006	0.028
27.95	17.68	0.034	0.053	27.95	0.44	0.006	0.030
28.60	20.65	0.039	0.050	28.60	0.03	0.030	0.030
29.25	20.87	0.041	0.059	29.25	0.34	0.006	0.028
29.90	25.29	0.052	0.097	29.90	0.03	0.006	0.029
30.55	26.27	0.048	0.122	30.55	0.24	0.006	0.033
31.20	31.33	0.059	0.144	31.20	0.13	0.006	0.029
31.85	25.51	0.048	0.097	31.85	-0.08	0.006	0.030
32.50	17.59	0.038	0.066	32.50	0.34	0.030	0.035
33.15	15.78	0.036	0.076	33.15	1.70	0.030	0.046
33.80	11.40	0.034	0.047	*San Juan River*			
34.45	11.58	0.030	0.049	-0.65	52.68	0.030	0.201
35.10	13.03	0.033	0.051	0.00	66.50	0.030	0.284
35.75	11.52	0.031	0.034	0.65	66.70	0.030	0.340
36.40	10.23	0.028	0.041	1.30	40.95	0.030	0.201
37.05	11.05	0.034	0.043	1.95	29.75	0.030	0.201
37.70	8.01	0.030	0.027	2.60	22.32	0.030	0.146
38.35	10.30	0.039	0.027	3.25	13.11	0.030	0.090
39.00	8.78	0.033	0.034	3.90	7.25	0.030	0.062
39.65	9.32	0.035	0.037	4.55	4.21	0.030	0.062
40.30	10.04	0.036	0.044	5.20	6.52	0.030	0.035
40.95	9.01	0.028	0.044	5.85	3.27	0.030	0.035
41.60	8.55	0.036	0.032	6.50	4.00	0.030	0.062
42.25	7.77	0.034	0.036	7.15	2.64	0.030	0.062
42.90	8.20	0.041	0.025	7.80	1.70	0.030	0.035
43.55	6.83	0.041	0.024	8.45	1.18	0.030	0.035
44.20	8.18	0.040	0.022	9.10	3.59	0.030	0.035
44.85	7.14	0.032	0.031	9.75	1.49	0.030	0.035

Table A1. Concentrations of Mn, U, and Pb in side canyon porewater, continued

depth	Mn	U	Pb	depth	Mn	U	Pb
White Canyon, continued				*San Juan River, continued*			
45.50	10.21	0.062	0.041	10.40	0.65	0.030	0.035
46.15	10.45	0.049	0.026	11.05	2.96	0.030	0.035
46.80	8.88	0.061	0.022	11.70	0.55	0.030	0.035
Navajo Canyon				12.35	3.90	0.030	0.062
47.45	10.39	0.071	0.024	13.00	4.11	0.030	0.035
48.10	13.17	0.080	0.029	13.65	2.22	0.030	0.035
48.75	8.18	0.077	0.024	14.30	5.78	0.030	0.035
49.40	6.33	0.059	0.028	14.95	3.90	0.030	0.035
50.05	6.85	0.040	0.043	15.60	6.20	0.030	0.035
-0.65	2.12	0.006	0.039	16.25	2.22	0.030	0.035
0.00	0.55	0.006	0.031	16.90	1.60	0.030	0.035
0.65	-0.18	0.006	0.030	17.55	0.76	0.006	0.035
1.30	-0.50	0.006	0.029	18.20	3.27	0.030	0.035
1.95	-0.60	0.006	0.029	18.85	3.59	0.030	0.035
2.60	0.13	0.006	0.035	19.50	2.64	0.030	0.035
3.25	-0.08	0.006	0.035	20.15	6.10	0.030	0.035
3.90	-0.18	0.006	0.038	20.80	7.25	0.030	0.035
4.55	0.65	0.006	0.058	21.45	15.62	0.030	0.090
5.20	0.44	0.006	0.056	22.10	6.20	0.030	0.062
5.85	-1.23	0.006	0.032	22.75	4.95	0.030	0.035
6.50	4.11	0.006	0.075	23.40	7.46	0.030	0.062
7.15	7.46	0.006	0.079	24.05	11.02	0.030	0.062
7.80	6.41	0.006	0.070	24.70	20.33	0.030	0.090
8.45	13.65	0.000	0.097	25.35	28.92	0.030	0.146
9.10	22.74	0.006	0.120	26.00	12.59	0.030	0.062
9.75	30.59	0.006	0.140	26.65	8.71	0.030	0.062
10.40	32.89	0.030	0.145	27.30	4.53	0.030	0.035
11.05	11.02	0.030	0.088	27.95	3.38	0.030	0.035
11.70	7.35	0.030	0.068	28.60	4.53	0.030	0.035
12.35	9.13	0.030	0.096	29.25	2.01	0.030	0.035
13.00	4.84	0.030	0.053	29.90	3.17	0.030	0.035
13.65	0.97	0.030	0.039	30.55	3.90	0.030	0.035
14.30	1.81	0.030	0.041	31.20	4.00	0.030	0.035
14.95	0.44	0.030	0.032	31.85	2.22	0.030	0.035
15.60	0.55	0.030	0.032	32.50	4.53	0.030	0.035
16.25	0.44	0.030	0.031	33.15	3.27	0.030	0.035
16.90	0.44	0.030	0.030	33.80	4.00	0.030	0.035

Table A1. Concentrations of Mn, U, and Pb in side canyon porewater, continued

depth	Mn	U	Pb
Navajo Canyon			
17.55	0.49	0.000	0.030
18.20	0.55	0.006	0.029
18.85	0.65	0.030	0.031
19.50	0.76	0.030	0.029
20.15	1.60	0.030	0.032
20.80	0.44	0.006	0.028
21.45	2.75	0.030	0.035
22.10	2.12	0.030	0.032
22.75	0.55	0.030	0.029
23.40	0.34	0.006	0.030
24.05	0.65	0.030	0.029
24.70	0.34	0.006	0.029
25.35	0.76	0.030	0.028
26.00	0.24	0.030	0.026
26.65	0.55	0.006	0.032

Table A2. Concentrations (in μM) of lead (Pb) and arsenic (As) measured during January 2007 in Farley Canyon and White Canyon, Lake Powell; depth (in cm) of 0 is the sediment-water interface

depth	Pb	As	depth	Pb	As
White Canyon, probe A			*Farley Canyon, probe A*		
-11.08	0.029	0.559	-13.24	0.014	0.262
-10.39	0.031	0.211	-12.55	0.013	0.219
-9.70	0.029	0.190	-12.55	0.009	0.237
-9.01	0.015	0.212	-11.86	0.016	0.211
-9.01	0.015	0.225	-11.17	0.022	0.193
-7.63	0.014	0.194	-10.48	0.014	0.171
-7.63	0.011	0.215	-10.48	0.004	0.000
-6.94	0.022	0.188	-9.79	0.014	0.235
-6.25	0.022	0.189	-9.79	-0.015	0.202
-5.56	0.023	0.174	-9.10	0.015	0.230
-4.87	0.023	0.192	-7.72	0.015	0.323
-4.18	0.025	0.197	-6.34	0.012	0.215
-3.49	0.029	0.220	-6.34	0.013	0.208
-2.80	0.028	0.194	-4.96	0.018	0.208
-2.11	0.030	0.214	-4.27	0.015	0.158
-1.42	0.073	0.207	-3.58	-0.007	0.128
-0.73	0.021	0.271	-2.89	0.018	0.198
-0.73	0.000	0.261	-1.51	0.016	0.172
-0.04	0.028	0.205	-0.13	0.017	0.209
0.65	0.035	0.188	1.25	0.018	0.202
1.34	0.024	0.228	1.94	0.016	0.195
2.03	0.026	0.243	2.63	0.017	0.211
2.72	0.025	0.222	3.32	0.021	0.227
4.10	0.025	0.237	4.01	0.017	0.197
4.79	0.018	0.237	4.70	0.053	0.193
4.79	-0.008	0.218	6.08	0.019	0.240
5.48	0.035	0.219	6.77	0.018	0.247
6.17	0.033	0.000	7.46	0.020	0.230
6.86	0.027	0.184	8.15	0.009	0.220
8.24	0.038	0.164	9.53	0.016	0.288
8.93	0.035	0.000	10.22	0.014	0.228
9.62	-0.001	0.172	10.91	0.023	0.244
10.31	0.025	0.209	12.98	0.016	0.237
11.00	0.015	0.246	13.67	0.012	0.245

Table A2. Concentrations lead and arsenic in side canyon porewater, continued

depth	Pb	As	depth	Pb	As
White Canyon, probe A, continued			*Farley Canyon, probe A, continued*		
11.00	0.012	0.275	14.36	-0.012	0.163
12.38	0.023	0.272	15.05	0.017	0.240
13.07	0.048	0.259	15.74	0.013	0.240
13.76	0.045	0.289	16.43	0.019	0.233
14.45	0.034	0.167	17.12	0.012	0.237
15.14	0.022	0.242	19.19	0.019	0.236
15.83	0.026	0.247	20.57	0.017	0.263
17.90	0.016	0.260	21.95	0.020	0.238
18.59	0.023	0.294	22.64	0.023	0.224
19.28	0.019	0.280	24.02	0.019	0.244
19.97	0.022	0.259	24.71	0.020	0.264
21.35	0.028	0.262	25.40	0.015	0.220
Farley Canyon, probe B			26.09	0.022	0.250
-1.15	0.085	0.212	26.78	0.017	0.228
-1.15	0.081	0.210	28.85	0.014	0.255
-0.47	0.018	0.186	30.23	0.013	0.207
0.22	0.024	0.190	30.92	0.019	0.214
0.91	0.019	0.119	31.61	0.020	0.275
0.91	0.019	0.121	32.99	0.018	0.219
1.59	0.022	0.152	*Farley Canyon, probe C*		
2.28	0.020	0.207	-1.15	0.042	0.227
3.65	0.017	0.203	-0.47	0.032	0.198
5.02	0.022	0.191	0.22	0.033	0.232
5.70	0.017	0.185	0.91	0.062	0.212
5.70	0.017	0.218	1.59	0.033	0.237
6.39	0.017	0.191	1.59	0.032	0.228
7.76	0.019	0.219	2.28	0.017	0.205
8.44	0.015	0.165	2.96	0.037	0.154
9.13	0.019	0.208	3.65	0.030	0.201
9.81	0.015	0.231	5.02	0.020	0.225
9.81	-0.011	0.230	5.02	0.020	0.223
10.50	0.016	0.195	5.70	0.027	0.208
11.18	0.021	0.230	6.39	0.030	0.230
11.87	0.024	0.191	6.39	0.011	0.198
12.55	0.012	0.218	7.07	0.026	0.188
13.24	0.017	0.215	7.76	0.027	0.166

Table A2. Concentrations lead and arsenic in side canyon porewater, continued

depth	Pb	As	depth	Pb	As
Farley Canyon, probe B, continued			*Farley Canyon, probe C, continued*		
13.92	0.026	0.253	8.44	0.037	0.213
14.61	0.025	0.180	9.81	0.030	
15.29	0.020	0.257	10.50	0.024	0.154
15.98	0.020	0.221	11.18	0.025	0.237
16.66	0.014	0.236	11.87	0.011	0.201
16.66	-0.010	0.238	12.55	0.026	
17.35	0.012	0.220	13.92	3.173	
18.03	0.020	0.179	14.61	0.018	0.221
18.72	0.025	0.000	15.29	0.021	0.139
19.40	0.013	0.210	15.98	0.015	0.207
20.09	0.013	0.226	15.98	0.013	0.191
20.77	0.020	0.000	16.66	0.015	0.235
21.46	0.015	0.227	17.35	0.014	0.221
22.14	0.015	0.198	18.03	0.012	0.242
22.83	0.012	0.202	18.72	0.127	0.215
23.51	0.014	0.208	19.40	0.015	0.212
24.20	0.012	0.232	20.09	0.017	0.238
24.88	0.017	0.237	20.77	0.090	0.198
25.57	0.021	0.250	21.46	0.017	0.201
26.25	0.010	0.200	22.14	0.021	0.218
26.94	0.015	0.181	22.83	0.017	0.209
27.62	0.016	0.214	23.51	0.016	0.207
28.31	0.018	0.142	24.20	0.018	0.191
28.99	0.013	0.211	24.88	0.017	0.216
30.36	0.021	0.155	25.57	0.017	0.133
31.05	0.023	0.223	26.25	0.017	0.334
31.73	0.015	0.232	26.94	0.017	0.215
32.42	0.012	0.239	27.62	0.024	0.243
32.42	0.011	0.237	28.31	0.021	0.185
33.10	0.019	0.275	28.99	0.018	0.259
33.79	0.070	0.395	29.68	0.015	0.197
			30.36	0.016	0.250
			31.05	0.016	0.174
			31.05	0.016	0.195
			31.73	0.009	0.229
			31.73	0.010	0.277
			32.42	0.017	0.261
			33.10	0.016	0.226

Chapter 4

PARTICLE SIZE CONTROLS SEDIMENTARY CHEMICAL DISTRIBUTION IN A LARGE RESERVOIR, LAKE POWELL, USA

Richard A. Wildman, Jr., Michael B. Easler, Dennis D. Eberl, Lincoln F. Pratson, Michael DeLeon, Aurelio LaRotta, and Janet G. Hering

(in preparation for *Environmental Science and Technology*)

Abstract

Trace elements are known to associate with small particles in the solid phase. In reservoirs, physical processes can separate sediment into geographical regions of varying particle size. We collected sediment cores from the lakebed and shoreline of Lake Powell, a large reservoir on the Colorado River, southwestern USA, and measured particle size, elemental abundance, total and organic carbon, and mineral composition in sediment samples. We observe a spatial trend in particle size in the delta sediment of Lake Powell, but no statistically significant trends along the shoreline. Organic carbon and most major and trace elements anticorrelate highly significantly with particle size. Thus, geographical location within the Lake Powell deltas predicts solid-phase chemical concentrations. This finding may have implications for water quality during reservoir drawdown, a process that leads to resuspension of delta sediment by the inflowing rivers.

Introduction

Sedimentation occurs in reservoirs as a consequence of damming. Physical studies of sedimentation have focused on the rate, texture, and spatial distribution with applications to watershed erosion (Bennett et al. 2005) and river restoration (Cheng and Granata 2007; Snyder et al. 2004). This process also has chemical implications because reservoirs can be long-term sinks for sediment enriched in inorganic contaminants (Kneebone et al. 2002; Castelle et al. 2007; Lee et al. 2008) or nutrients (Orr et al. 2006; Riggsbee et al. 2007; Downing et al. 2008). Furthermore, chemical analyses of reservoir sediment can answer questions about long-term contaminant transport in watersheds (Bennett and Rhoton 2007) and influent stream quality of urban reservoirs (Van Metre and Mahler 2004).

Solid-phase trace element concentrations increase with decreasing particle size in reservoirs (Bennett and Rhoton 2007) and river suspended sediment (e.g., Horowitz and Elrick 1987). Mechanistic determinations of this phenomenon are problematic; particle size (and, by extension, surface area) and geochemical phase (i.e., organic carbon (org-C) content) are so interrelated that it is unclear which dominates metal transport (Horowitz and Elrick 1987). In separate, controlled experiments, vermiculite, a clay mineral, and lignite, a C-rich solid, have shown similarly high sorption of metals (Maladrino et al. 2006, Mohan and Chandler 2006).

If particle size predicts trace elements concentrations, then sedimentation patterns should influence the geographic distribution of trace elements in a reservoir. Previous studies of chemicals in reservoir sediment have generally occurred in reservoirs where trends in physical sorting of sediment and spatial distribution of chemicals seem

unimportant. However, in a large reservoir, the sediment delta can extend over tens of km and physical sorting may lead to physically and chemically distinct regions of sedimentation. Furthermore, different tributaries may contribute distinct sediment loads, possibly leading to further heterogeneity.

This chapter examines sediment particle size and deposition as two factors that control of the fate of elements in Lake Powell, a large reservoir on the mainstem of the Colorado River in southeastern Utah and northern Arizona. This reservoir traps >99% of its sediment load (Topping et al. 2000), far more than similar reservoirs (Syvitski et al. 2005). Furthermore, its sediment may have a higher chemical load than other reservoirs, due to a history of mining in the Upper Colorado River Basin (Farmer 1999; Spahr et al. 2000). We hypothesize that 1) particle size, org-C, and chemical content of sediment will correlate here, 2) particle size is controlled by location within the Colorado River delta of Lake Powell, with downstream samples containing more fine particles and org-C, and 3) shoreline particle size is influenced by local geology.

Sampling and Analytical Methods

Sediment in Lake Powell. The closure of Glen Canyon Dam (GCD) in 1963 impounded the turbid Colorado River and created Lake Powell, which is 299 km long when full. It stores >30 km^3 of water for 25 million people and >6000 km^2 of farmland. Its sedimentation rate has been estimated at 21-52 Mt yr^{-1} (Ferrari 1988, Horowitz et al. 2001), implying a lifetime of 601-1488 years. Most sediment reaches Lake Powell via the Colorado and San Juan Rivers, which drain the southern Rocky Mountains, contribute 80% and 15% of the water to the lake, respectively, and build large deltas into the two

upper arms of the reservoir (Figure 1; Potter and Drake 1989). Additionally, 95 tributaries, each with its own "side canyon", flow into Lake Powell intermittently and deposit ~10% of the Lake Powell sediment load away from the thalweg and main deltas of the reservoir (Potter and Drake 1989). Many side canyons are <20 km long and are surrounded by only one type of rock formation (Anderson et al. 2003). Supporting information section S1 provides additional detail on sedimentation in Lake Powell. This study focuses on the Colorado River delta, which is assumed to be generally representative of processes in the San Juan River delta, and side canyon sediment.

Sediment collection. "Lakebed" sediment cores were collected from the thalweg of Lake Powell on 21-23 March 2006. Gravity cores were collected in plastic, 5 cm × 1 m core liners, at locations, identified by their distance in river km upstream from GCD (all rounded to the nearest 0.5 km), in a longitudinal transect through the upper region of Lake Powell. Samples were collected in (245.0, 241.2, 238.7, and 235.4 km) and below (168.0 km) the Colorado River sediment delta (Figure 1, see Table S1 for exact locations). Samples were kept cool after sampling, transported on ice to the laboratory, and frozen within 3 days of collection.

Sampling followed a 6-month period during which lake levels were steady for 3 months and slowly fell for the 3 months immediately before sampling (Figure S1). This should have minimized complications from changing lake levels, which influence the location of sediment deposition. To check this assumption, 4 cores (at 241.2 km, 238.7 km, and replicates at 178.0 km; Figure 1, Table S1) were collected on 16-18 May 2006, when the lake level had risen 2.6 m from the level of the March sampling. Colorado

River flow, taken as the sum of flow past United States Geological Survey (USGS) gages on the Green River at Green River, Utah and the Colorado River near Cisco, Utah, was ~192 $m^3 s^{-1}$ in March and ~668 $m^3 s^{-1}$ in May (USGS 2008).

Since the Colorado River delta aggrades ≤2-3 m yr^{-1} (Ferrari 1988), we assume that the top 20 cm of a delta sample represents accumulation from only the previous months. Our analyses focus on these "surface" (0-20 cm depth) samples, but they are presented along with some "deep" (25-80 cm depth) samples for comparison. Sediment accumulation rates in the middle of the lake are much less than in the delta. Cores collected at 168.0 km and 178.0 km were sampled as close to their surfaces as possible and these may contain sediment deposited over a longer period of time. No effort was made to date sediment.

We also collected "delta shoreline" samples from shore locations 247.5 and 249.5 river km above the dam, respectively, that were above the water line (Figure 1, Table S1). For these samples and those in side canyons (described below), repeat sampling or different sites at the same general location are denoted by a letter following the distance from GCD or side canyon abbreviation. Samples were collected 12 April 2005 (sample 247.5 A), 18 June 2005 (247.5 B), 5 December 2005 (247.5 C). At the 249.5 km location, 1.5 vertical m of sediment were collected in a set of stacked cores on 21 March 2006.

Fourteen sites were sampled in 7 side canyons: Navajo Canyon (NC), Moqui Canyon (MC), Trachyte Canyon (TC), White Canyon (WC), Farley Canyon (FC), the Dirty Devil River (DD). Also, a sample collected from a bank of the San Juan River (SJ) is included in this set (Figure 1, Table S1). Sampling occurred on 7 February 2005 (WC A), 12-13 April 2005 (WC B), 19-23 June 2005 (NC A, NC B, SJ, MC, and WC C), 4-5

December 2005 (WC D), 22 March 2006 (TC A), 17-19 May 2006 (TC B, FC B, and DD), and 27-28 March 2007 (WC E and FC B). All samples were collected <2 m from the edge of the lake except for NC B. This sample came from sediment submerged in a pool of water beneath a small waterfall ~100 m from the lakeshore. Cores were kept cool during transport to the laboratory and frozen <6 (usually <3) days later. All shoreline cores were collected in butyrate core liners (diameter = 2.5 or 5 cm) pushed into the sediment by hand.

Laboratory Processing and Analyses. Lakebed sediment cores were inspected visually and sampled anoxically based on distinct differences in color and particle size between sedimentary layers. Where no visual changes with depth were observed in delta shoreline or lakebed cores for >20 cm, two samples were often selected for analyses; otherwise, one sample represents a single section. No obvious layers existed in side canyon samples, so cores collected in 2005 were sectioned at 2 cm intervals under a low-oxygen atmosphere and later combined to provide sufficient mass for analyses. Cores collected in 2007 were sectioned anoxically at 4- or 8-cm intervals.

Each sample was thawed, homogenized, and freeze-dried. Most samples from lakebed and delta shoreline cores were analyzed for most parameters. Usually, only the top 10 cm of side canyon cores were analyzed, but additional depths of some cores were measured for some parameters. In total, 113 samples were analyzed for at least one parameter. Overlapping depth ranges from the same location originate from replicate cores.

Particle size was measured with a Mastersizer 2000 laser diffractometer (Malvern Instruments Ltd., Worcestershire, UK) following Sperazza et al. (2004). Elemental abundance of most elements from Na to U was measured with a XEPOS energy dispersive X-ray fluorescence (XRF) spectrometer (Spectro Analytical Instruments, Inc., Mahwah, NJ). Carbonate minerals were extracted from sediment samples with hydrochloric acid. These and untreated sediment samples were analyzed on a 2010 Elemental Combustion System (Costech Analytical Instruments, Valencia, CA). Mineralogical composition was measured on a D500 X-ray diffractometer (Siemens AG, Berlin), and the X-ray intensities were analyzed using RockJock software following Eberl (2003). Supporting Information sections S2, S3, S4, and S5 contain details of particle size, elemental abundance, carbon, and mineralogical measurements, respectively.

Data Analyses. Data sets in this study were collected as mass percentages and subsequently expressed as molar ratios with elements and minerals normalized to silicon and silica, respectively. Molar ratios of minerals were calculated using molar masses presented by Klein and Hurlbut (1999). Data were compared by creating a matrix of correlation estimates ("correlations") using the software packages R 2.1.1 and R 2.8.0 (R Development Core Team 2005, 2008). Two separate arithmetic tests for the influence of particle size were carried out in which data for 17 samples that included all parameters were either divided or multiplied (one operation in each test) by the mean particle size of each sample. Relative standard deviations were computed for this data set. A linear regression model was created using mean particle size as the predictor variable and all elemental and mineralogical molar ratios as response variables. The residuals from this

model were then correlated with all other parameters as another test of the influence of particle size. Errors of correlations are assumed to have a normal distribution, which implies that the standard deviation (σ) of these errors is $1/\sqrt{n}$, where n is the number of samples. Correlations 2σ and 4σ from zero are considered significant and highly significant, respectively. Where carbon concentrations or elemental abundances were below detection limits (BDL), values of 0.01% or 0.00005% were used.

Results

Thirteen sediment cores collected from 5 lakebed locations varied in length from <30 cm to >60 cm. No significant variability was observed during visual inspection of these cores, so the top and bottom of each core were usually sampled. Visual differences were obvious in delta shoreline samples, especially in the cores collected 249.5 km from GCD. A total of 8 samples were collected from clayey layers at depth ranges -132 to -109 cm (negative values indicate depths above the sediment-water interface), -47 to 14 cm and 14 to 20 cm and sandy layers at -109 to -77 cm and -77 to -47 cm (see Figure S2 for photographs). Additionally, a sandy layer that was not sampled overlaid the top clayey layer. These sediment layers almost certainly represent sediment deposited during very different lake levels at this location, in contrast to the lakebed samples, which were collected at different locations and two very similar lake levels. Side canyon cores showed no visible variation with depth and were sandy, brown, and odorless except for NC B, which was black and smelled of hydrogen sulfide, and TC A and TC B, which contained visible layers of small plant debris. Core 247.5 C also contained plant debris.

Particle Size. Sediment in Lake Powell is a mixture of silt (mean <2 μm), clay (2-63 μm), and sand (>63 μm) with sample means ranging from 5-445 μm, an overall mean of 86 μm, and an overall standard deviation (σ) of 93 μm (Table S2). The lakebed samples (mean = 10.4 μm, σ = 6 μm) were significantly finer (t-test, $p < 0.01$) than both the shoreline delta samples (mean = 135 μm, σ = 127 μm) and the side canyon samples (mean = 112 μm, σ = 77 μm), which were not significantly differently from each other.

The mean particle size of lakebed surface samples collected in March 2006 correlates with distance from Glen Canyon Dam (Figures 2, S3). This trend also occurs in the two samples collected in May 2006, which are notably coarser than the corresponding locations in March (Figures 2, S4). Deep samples are coarser than surface samples at all locations analyzed (Figure 2, Table S2).

The apparent similarity of the delta shoreline and side canyon samples is somewhat misleading. Whereas the set of all side canyon samples has an apparently random distribution, the delta samples have a trimodal distribution, with 3 samples near 130 μm, 6 samples <45 μm, and 4 samples near 300 μm (Table S2). This reflects the distinct sediment layers, one of which is much coarser than most side canyon samples (and all lakebed samples) and one of which is much finer than the side canyon samples.

Mean particle sizes of samples from side canyons surrounded by sandstone rock formations, NC, WC, and MC, are 168, 147, and 120 μm, respectively. Canyons surrounded by shale formation, TC and FC, have mean particle sizes of 104 μm and 80 μm. Thus, the type of rock surrounding a side canyon may predict the particle size of the sediment therein. However, these differences are not statistically significant (t-test, $p < 0.05$) and greater numbers of samples would be required to validate this trend.

Elemental Abundance. Inorganic elements were measured in 71 lakebed, delta, and side canyon samples (Tables S3A, S3B). Lake Powell sediment is mostly composed of Na, Mg, Al, Si, K, Ca, and Fe (concentrations generally >0.5%) with minor amounts of P, S, Ti, and Mn (concentrations >0.01%). At trace levels (<0.01%), Rb, Sr, Ba, Ce, Cl, and Zn were usually present and V, Cr, Ni, Cu, Ga, As, Br, Y, La, Pb, Th, and U were occasionally found. When Zr was measured, it was >0.01%, but, in many samples were BDL. The many samples BDL imply that, if contamination by the ZrO milling balls occurred, it is less than the XRF detection limit. Thus, Zr will be included in this analysis. Concentrations of Se were usually BDL.

Results are not consistent across the three groups of samples. A majority of elements (Mg, Al, P, K, Ca, Ti, Mn, Fe, Ni, Zn, Ga, As, Br, Rb, Sr, Y, Pb, Th, U) are significantly higher (t-test, $p < 0.05$) in lakebed samples than in side canyon samples; the opposite is true for Si and Zr. In all samples, Cl, S, and K are approximately near median crustal abundance (MCA) values, and Ba exceeds this value (Lide 2007). In the lakebed samples, Ca, Zn, Br, Rb, Pb, Th, and U exceed MCA values, and Si and Zr exceed them in most side canyon samples. Comparison of delta shoreline samples to lakebed and side canyon samples was not considered useful because, as with the particle size results, specific depths sampled at the delta shoreline resembled either the lakebed or side canyon sample sets.

Org-C was analyzed in 15 lakebed, 11 delta shoreline, and 58 side canyon samples; total C was analyzed in 13 lakebed, 13 delta shoreline, and 67 side canyon samples (Tables S3A, S3B). Generally, org-C is very low, except in the three cores that contained plant debris (249.5 C, TC A, TC B). When these samples are removed from the

analysis, lakebed samples contain significantly more (t-test, $p < 0.01$) organic (mean = 1.00%, $\sigma = 0.28\%$) and total (mean = 3.15%, $\sigma = 1.52\%$) C than side canyon samples, which average 0.15% ($\sigma = 0.19\%$) organic and 1.61% ($\sigma = 0.71\%$) total C. Notably, one total C value (8.55%) from the 178 km lakebed location is a high outlier, perhaps due to high precipitation of calcite, which is unlikely, but possible, in this region of Lake Powell (Reynolds 1978). However, a duplicate core collected at this location contained only 3.50% total C.

Mineralogy. Mineral composition was measured in 8 lakebed samples, 8 shoreline delta samples, and 6 side canyon samples collected from Lake Powell. Lakebed samples contain slightly more clay minerals (mean = 51.7%, $\sigma = 6.3\%$) than non-clay minerals (mean = 45.5%, $\sigma = 7.6\%$; Tables S4A, S4B). This is significantly different (t-test, $p < 0.01$) than side canyon samples, which average 94.5% non-clay minerals ($\sigma = 1.5\%$) and 10.7% clay minerals ($\sigma = 1.6\%$). Of the non-clay minerals, quartz dominates, followed by calcite, dolomite, multiple feldspars, iron-oxide minerals, and apatite. Calcite, dolomite, apatite, and maghemite are higher in the lakebed than in the side canyons, whereas the opposite is true for quartz. Of the clay minerals in the lakebed samples, illites dominate, followed by muscovite, smectites, and kaolinite.

Correlation between particle size, elements, and minerals. Due to varying numbers of samples in each analysis, separate significance thresholds were created for each pairing of data sets (Table S5A). Correlation analysis was completed after samples with visible plant debris (247.5 C, TC A, and TC B) were removed from the data set.

All particle size parameters analyzed (mean, median, mode, and the logarithms of these) correlate positively and highly significantly with each other. Henceforth, only the mean particle size (MEAN) and the logarithm of the mean particle size (log(MEAN)) will be discussed, but all correlations are presented in Tables S5B and S5C, which correspond to the mass percent and molar ratio data, respectively. Trends between correlations based on mass percentage and molar ratios are similar; only the latter will be explicitly reported and discussed for all elements and minerals here except silicon and silica. Both MEAN and log(MEAN) anticorrelate highly significantly (-0.672 and -0.887) with org-C. Anticorrelations of total C with MEAN and log(MEAN) are significant (-0.537) and highly significant (0.732), respectively (Table S5C, Figure S5). These observations are consistent with published results (e.g., Horowitz and Elrick 1987), and the stronger correlation between carbon and the logarithm of particle size parameters suggests a nonlinear dependence of C concentration on particle size that has not been previously described.

Both log(MEAN) and org-C anticorrelate and correlate highly significantly (i.e., $r < -0.556$ for particle size and >0.539 for org-C), respectively, with most metals analyzed, i.e., Mg, Al, P, K, Ca, Ti, V, Mn, Fe, Ni, Zn, Ga, As, Br, Rb, Sr, Y, Pb, Th, and U. This trend is reversed for Si and Zr. Thus, the influence of particle size and organic carbon on metal concentrations in sediment is closely linked: with the exception of Si and Zr, major and trace elements associate with small particles that are high in org-C.

Molar ratios of non-clay minerals correlate highly significantly (i.e., $r >0.853$) with log(MEAN) and anticorrelate significantly with org-C (i.e., $r < -0.459$), whereas the opposite is true for total clay minerals (Table S5C, Figure S6). Within these categories,

most individual clay minerals anticorrelate significantly with log(MEAN), yet the same is not true for non-clays. Some feldspars, Goethite, and quartz correlate significantly with log(MEAN), whereas calcite, dolomite, and maghemite anticorrelate significantly with this parameter. Furthermore, elements that associate with smaller particles generally correlate and anticorrelate with clay minerals and non-clay minerals, respectively. This both agrees with previous work showing that clay minerals are known to sorb metals very effectively (Malandrino et al. 2006) and suggests that trace elements may be scavenged during precipitation of carbonate minerals (i.e., calcite and dolomite) or, in the case of certain metals (e.g., manganese and iron) incorporated into the mineral structure (Friedl et al. 1997; Prothero and Schwab 2004).

Effects of Particle Size. The two separate arithmetic tests in which the values of elemental or mineralogical molar ratios of 17 samples were either divided or multiplied by MEAN led to relative standard deviations that were always larger than 50% and often larger than 100% (analysis not shown). The residuals of a linear regression model using MEAN as a predictor variable and all other parameters as response variables correlated positively and significantly (i.e., $r > 0.485$) with total C, Al, P, S, Ca, V, Cr, Mn, Fe, Cu, Zn, Ga, As, Br, Rb, Sr, Ba, Pb, Th, U, orthoclase feldspar, albite feldspar, oligoclase feldspar, calcite, maghemite, apatite, disordered kaolinite, ferruginous smectite, 1Md illite, 1M illite, Fe-chlorite, muscovite, total non-clays, and total clays.

Discussion

Particle size and location in the Colorado River delta. Particle size trends created by the deposition of the Colorado River delta exist over several kilometers and can be observed in surface sediment during periods of relatively steady lake level (Figure 2). This agrees with other studies in which reservoir sediment deltas do not reach dams (e.g., Snyder et al. 2006, Riggsbee et al. 2007). Although particle size may influence spatial distribution of elements and minerals in this system, the large variations in data normalized to particle size and the significant correlations of some elements and minerals with the residuals of a linear model based on particle size imply that it is not the exclusive driver of elemental and mineralogical abundance in Lake Powell sediment. When the influence of particle size is removed, other factors like the abundance of clay and non-clay minerals or the concentration of organic carbon may play an important role.

The coarser mean particle sizes of deeper samples probably result from movement of the depositional region due to changes in lake level. Before the steady lake levels of late 2005 and early 2006, the surface elevation of Lake Powell had risen ~17 meters in spring/summer of 2005 after >1 year below the elevation of March 2006, when sampling occurred (Figure S1). At a lower lake level, the region of sediment deposition would have been closer to GCD, leading to coarser particles underlying finer particles at our sampling locations. Variations in reservoir level exert a complicated influence on particle size (Snyder et al. 2006). While the details of this relationship are beyond the scope of this study, broad differences observed between our samples are consistent with the recent surface elevation changes in Lake Powell.

The distinct sediment layers sampled at the delta shoreline locations provide further indication that different lake levels lead to deposition of different particle sizes in a given location. The alternating coarse and fine layers from the 249.5 km location indicate that the Colorado River deposits sediment that ranges from <10 to >300 μm, a much wider range of particle size than we observed in our lakebed samples. Since particle size decreases away from the river inflow in a long, narrow delta, this implies that our lakebed locations sampled only the downstream end of the sediment delta and that the upstream portion of the delta is probably composed of sand. This fraction may be very large; we recently observed sediment banks >10 m high 271.5 km from GCD. Thus, our data imply that small trends in particle size (i.e., a change in mean of a few μm over <10 km) can be observed after months of steady sedimentation and major trends may be robust over tens of km.

Sedimentation in Lake Powell is an active process, and several physical processes can complicate the trend of particle size increasing with distance from the dam. Our samples collected in May 2006 are notably coarser than those collected in the same or similar locations <2 months earlier, suggesting that the increased river flow in May moved coarse sediment from exposed sections of the sediment delta into the sampling region. Underflow density currents are common in Lake Powell (Johnson and Merritt 1979), and these may transport sediment along the lakebed after deposition. Subaqueous, ≤40-cm thick gravity flows can also move sediment along the reservoir floor, especially in the delta region (Pratson et al. 2008).

Implications. Particle size trends in Lake Powell are important because our data show that they correspond to significant variations in sediment mineralogy and chemistry. Thus, the substantial chemical load associated with suspended sediment in the Colorado and San Juan Rivers (Horowitz et al. 2001) is deposited in the lower regions of their respective deltas, an observation consistent with previous data collected at Lake Powell (Hart et al. 2005). Conversely, the upper regions of the deltas (and the side canyons) are comparatively lower in trace elements.

Since 2000, the Colorado River Basin has experienced a drought that has drawn Lake Powell down ≤44 m (USBR 2008). This process exposes delta sediment, which is then resuspended by the rivers and deposited further into the smaller lake (Vernieu 1997, Pratson et al. 2008). Sediment resuspension can release contaminants into ecosystems (Castelle et al. 2007), and the recent removal of a 4-m dam in North Carolina, USA led to release of carbon and nitrogen from resuspended reservoir sediment (Riggsbee et al. 2007).

In Lake Powell, quarterly water quality monitoring data show an abrupt increase in summertime total chlorophyll concentration during hydrologic year 2003 in surface water collected 193.3, 208.5, and 225.5 km from GCD (Figure 3; Vernieu, in preparation). Primary productivity in Lake Powell is limited by P (Gloss et al. 1980), so an increase in chlorophyll implies that an additional source of P entered the upper region of Lake Powell. Our data show that P is highly significantly correlated with particle size, organic carbon, and calcite, significantly correlated with several clay minerals, and highly significantly anticorrelated with quartz and feldspar, in agreement with previous work relating P to particle size (Blecker et al. 2006) and clays (Borgnino et al. 2006). Therefore,

elevated chlorophyll may have been caused by P release during resuspension of fine sediment. The data presented here do not prove this connection; ongoing research will quantify the release of P during resuspension of Lake Powell sediment.

Importantly, chlorophyll does not increase when reservoir drawdown begins; rather, it occurs ~3 years later. Since the current drought followed a period of steady and high reservoir levels during the late 1990s, the initial drawdown should have led to resuspension of sandy sediment in the upper regions of the deltas, which our findings show are low in carbon and inorganic chemicals. The resuspension of fine particles would not have occurred until the lake was low enough to expose the lower portions of the deltas. This may explain the delay in the response of chlorophyll concentrations. If correct, it suggests that a slight drawdown has little effect on nutrient release from sediments, but a lake level threshold exists below which the resuspension of fine sediments begins and water quality can be affected. This is particularly important at Lake Powell, where the decay of this additional biomass may have contributed to a parcel of water low in dissolved oxygen (DO) that persisted below the thermocline in summer 2005 and passed through GCD that autumn. The subsequent DO concentrations of 3-4 mg L^{-1} in dam releases impaired a fishery near Lees Ferry, Arizona, ~25 km below GCD (Vernieu, in preparation).

Climate change may lead to substantial changes and variations to the hydrographs of Western United States rivers (Barnett et al. 2008), which may lead to the extreme drawdown of Lake Powell (Barnett and Pierce 2008). Our results link the concentration of chemicals in the sediment of this reservoir to sediment particle size and show that spatial trends of particle size exist in the long, narrow Colorado River delta. A similar

trend probably exists in the San Juan River delta, also, and these trends raise the possibility that extreme reservoir drawdown can impair reservoir and downstream water quality. This possibility suggests that reservoir managers should consider water quality in addition to hydropower production, downstream needs, and recreation when optimizing yearly dam release plans.

Future Work. This study can serve as the start of many distinct and interesting avenues of future research; three examples will be discussed here. First, a detailed mineralogical investigation using electron microscopy would allow quantification of the shape of small particles, which would give insight into their surface area and their ability to sorb water or chemicals. Also, electron microscopy would allow a better determination of the ratio of oxide minerals to calcite, which form in different environmental conditions. This would enable a statement regarding which of these is the primary sorbent of elements like P.

The varying concentrations of carbon in the Colorado River Delta of Lake Powell could lead to a study of carbon degradation in delta settings. Lake Powell would be a particularly useful setting because of the long, narrow shape of the delta and the reliable measurements of river inflow. Such a study could include careful dating and reconstruction of depositional patterns in the delta. Samples would be collected, extracted with organic solvents, and analyzed by gas chromatography-mass spectrometry to determine variations in the concentrations of individual carbon compounds as functions of depth and spatial distribution in the delta.

Finally, the association of trace elements with sediment particles of varying size may reflect the composition of the source rocks upstream, or it may be the result of sorption of dissolved trace elements to particles during riverine transport. These two influences could be separated by determining the composition of representative source rocks in the Southern Rocky Mountains and the Colorado Plateau and calculating an average weighted to the erosion of these rocks in the watershed. This average would be compared to the molar ratios presented in this study. This comparison could be bolstered by sampling suspended sediment in the catchments of the various source rock types to verify that the composition of eroded sediment matches that of rocks in formations. This final step may be an operational way of accounting for *in situ* chemical weathering and should be compared to theoretical calculations.

Acknowledgements

The authors are grateful to Jerry Miller, Robert Radkte, Nick Williams, Rafael Lopez (USBR), Andrew Kositsky, Nathan Chan, Claire Farnsworth (Caltech), and Mark Anderson (Glen Canyon NRA) for assistance with sample collection; Nathan Dalleska, Kate Campbell, Megan Ferguson (Caltech), Andreas Papritz, René Saladin, Andreas Müller (ETHZ), Jo Raber (Ametek), Alex Blum (USGS), Manuel Kunz, Matteo Bonalumi (Eawag), and Zena Harris for assistance with data collection; and Susan Hueftle (GRMRC) for helpful discussions. This work was funded by NSF SGER grant EAR-0621371, the Alice Tyler Foundation, USBR grant 06PG400222, and a Summer Undergraduate Research Fellowship awarded to Mike Easler at Caltech. The U.S. Bureau of Reclamation, Upper Colorado Region, and Glen Canyon National Recreation Area

provided essential sampling support. The use of trade names is for identification purposes only and does not imply endorsement by the U.S. Geological Survey or Bureau of Reclamation.

References

Anderson, P. B., T. C. Chidsey, D. A. Sprinkel, and G. C. Willis. (2003) Geology of Glen Canyon National Recreation Area, Utah-Arizona. In *Geology of Utah's Parks and Monuments, second edition* (Sprinkel, D.A., T. C. Chidsey, and P. B. Anderson, eds.), Utah Geological Association Publication 28: Salt Lake City, 2003.

Barnett, T. P. and D. W. Pierce. (2008) When will Lake Mead go dry? *Water Resources Research* 44: W03201, doi:10.1029/2007WR006704.

Barnett, T. P., D. W. Pierce, H. G. Hidalgo, C. Bonfils, B. D. Santer, T. Das, B. Govindasamy, A. W. Wood, T. Nozawa, A. A. Mirin, D. R. Cayan, and M. D. Dettinger. (2008) Human-induced changes in the hydrology of the Western United States. *Science* 319: 1080-1084.

Bennett, S. J. and F. E. Rhoton. (2007) Reservoir sedimentation and environmental degradation: Assessing trends in sediment-associated trace elements in Grenada Lake, Mississippi. *Journal of Environmental Quality* 36: 815-825.

Bennett, S. J., F. E. Rhoton, and J. A. Dunbar. (2005) Texture, spatial distribution, and rate of reservoir sedimentation within a highly erosive, cultivated watershed: Grenada Lake, Mississippi. *Water Resources Research* 41: W01005.

Blecker, S. W., J. A. Ippolito, J. E. Barrett, D. H. Wall, R. A. Virginia, and K. L. Norvell. (2006) Phosphorus fractions in soils of Taylor Valley, Antarctica. *Soil Science Society of America Journal* 70: 806-815.

Borgnino, L., C. Orona, M. Avena, M. A. Maine, A. Rodriguez, and C. P. de Pauli. (2006) Phosphate concentration and association as revealed by sequential extraction and microprobe analysis: The case of sediments in two Argentinean reservoirs. *Water Resources Research* 42: W01414.

Castelle, S., J. Schäfer, G. Blanc, S. Audry, H. Etcheber, J.-P. Lissalde. (2007) 50-year record and solid state speciation of mercury in natural and contaminated reservoir sediment. *Applied Geochemistry* 22: 1359-1370.

Cheng, F. and Granata, T. (2007). Sediment transport and channel adjustments associated with dam removal: Field observations. *Water Resources Research* 43: W03444, doi: 10.1029/2005WR004271.

Downing, J. A., J. J. Cole, J. J. Middelbury, R. G. Striegl, C. M. Duarte, P. Kortelainen, Y. T. Prairie, and K. A. Laube. (2008) Sediment organic carbon burial in agriculturally eutrophic impoundments over the last century. *Global Biogeochemical Cycles* 22: GB1018, doi:10.1029/2006GB002854.

Eberl, D. D. (2003) User guide to RockJock – A program for determining quantitative mineralogy from X-ray diffraction data. *United States Geological Survey* Open File Report OF 03-78.

Farmer, J. *Glen Canyon Dammed: Inventing Lake Powell and the Canyon Country.* Tucson: The University of Arizona Press, 1999.

Ferrari, R. (1988) *1986 Lake Powell Survey.* U.S. Bureau of Reclamation Technical Report REC-ERC-88-6: Denver, CO, 67 pp.

Friedl, G., B. Wehrli, and A. Manceau. (1997) Solid phases in the cycling of manganese in eutrophic lakes: New insights from EXAFS spectroscopy. *Geochimica et Cosmochimica Acta* 61(2): 275-290.

Gloss, S. P., L. M. Mayer, and D. E. Kidd. (1980) Advective control of nutrient dynamics in the epilimnion of a large reservoir. *Limnology and Oceanography* 15(4): 873-884.

Hart, R. J., H. E. Taylor, R. C. Antweiler, D. D. Graham, G. G. Fisk, S. G. Riggins, and M. E. Flynn. (2005) *Sediment chemistry of the Colorado River delta of Lake Powell, Utah, 2001*. U.S. Geological Survey open-file report 2005-1178.

Horowitz, A. J. and K. A. Elrick. (1987) The relation of stream sediment surface area, grain size and composition to trace element chemistry. *Applied Geochemistry* 2: 437-451.

Horowitz, A. J., K. A. Elrick, and J. J. Smith. (2001) Annual suspended sediment and trace element fluxes in the Mississippi, Columbia, Colorado, and Rio Grande drainage basins. *Hydrological Processes* 15: 1169-1207.

Johnson, N. M. and D. H. Merritt. (1979) Convective and advective circulation of Lake Powell, Utah-Arizona, during 1972-1975. *Water Resources Research* 15(4): 873-884.

Klein, C. and C. S. Hurlbut, Jr. Manual of Mineralogy, 21st edition. John Wiley and sons, Inc.: New York, 1999.

Kneebone, P. E., P. A. O'Day, N. Jones, and J. G. Hering. (2002) Deposition and fate of arsenic in iron- and arsenic-enriched reservoir sediments. *Environmental Science and Technology* 36: 381-386.

Lee, G., G. Faure, J. M. Bigham, and D. J. Williams. (2008) Metal release from bottom sediments of Ocoee Lake No. 3, a primary catchment area for the Ducktown mining district. *Journal of Environmental Quality* 37:344-352.

Lide, D. R. *CRC Handbook of Chemistry and Physics, 87th edition*. CRC Press: Boca Raton, FL, 2007.

Malandrino, M., O. Abollino, A. Giacomino, M. Aceto, and E. Mentasti. (2006) Adsorption of heavy meatls on vermiculite: Influence of pH and organic ligands. *Journal of Colloid and Interface Science* 299: 537-546.

Mohan, D. and S. Chander. (2006) Single, binary, and multicomponent sorption of iron and manganese on lignite. *Journal of Colloid and Interface Science* 299: 76-87.

Orr, C. H., K. L. Rogers, and E. H. Stanley. (2006) Channel morphology and P uptake following removal of a small dam. *Journal of the North American Benthological Society* 25(3): 556-568.

Potter, L. D. and C. L. Drake. *Lake Powell: Virgin Flow to Dynamo*. University of New Mexico Press, Albuquerque, 1989.

Pratson, L., J. Hughes-Clarke, M. Anderson, T. Gerber, D. Twichell, R. Ferrari, C. Nittrouer, J. Beaudoin, J. Granet, J. Crockett. (2008) Timing and patterns of basin infilling as documented in Lake Powell during a drought. *Geology* 36(11): 843-846.

Prothero, D. R. and F. Schwab. *Sedimentary Geology, second edition.* New York: W. H. Freeman and Company, 2004.

R Development Core Team (2005) R: A language and environment for statistical computing. R Foundation for Statistical Computing, Vienna, Austria. ISBN 3-900051-07-0, URL http://www.R-project.org.

R Development Core Team (2008) R: A language and environment for statistical computing. R Foundation for Statistical Computing, Vienna, Austria. ISBN 3-900051-07-0, URL http://www.R-project.org.

Reynolds, Jr., R. C. (1978) Polyphenol inhibition of calcite precipitation in Lake Powell. *Limnology and Oceanography* 23(4): 585-597.

Riggsbee, J. A., J. P. Julian, M. W. Doyle, and R. G. Wetzel. (2007) Suspended sediment, dissolved organic carbon, and dissolved nitrogen export during the dam removal process. *Water Resources Research* 43: W09414, doi:10.1029/2006WR005318.

Snyder, N. P., D. M. Rubin, C. N. Alpers, J. R. Childs, J. A. Curtis, L. E. Flint, and S. A. Wright. (2004) Estimating accumulation rates and physical properties of sediment behind a dam: Englebright Lake, Yuba River, northern California. *Water Resources Research* 40: W11301.

Snyder, N. P., S. A. Wright, C. N. Alpers, L. E. Flint, C. W. Holmes, and D. M. Rubin. (2006) Reconstructing depositional processes and history from reservoir stratigraphy: Englebright Lake, Yuba River, northern California. *Journal of Geophysical Research* 111: F04003, doi:10.1029/2005JF000451.

Spahr, N. E., L. E. Apodaca, J. R. Deacon, J. B. Bails, N. J. Bauch, C. M. Smith, and N. .E. Driver. (2000) Water quality in the Upper Colorado River Basin, Colorado, 1996-98. *U.S. Geological Survey* Circular 1214.

Sperazza, M., J. N. Moore, and M. S. Hendrix. (2004) High-resolution particle size analysis of naturally occurring very fine-grained sediment through laser diffractometry. *Journal of Sedimentary Research* 74(5): 736-743.

Syvitski, J. P. M., C. J. Vörösmarty, A. J. Kettner, and P. Green, P. (2005) Impact of humans on the flux of terrestrial sediment to the global coastal ocean. *Science* 308: 376-380.

Topping, D. J., D. M. Rubin, and L. E. Vierra Jr. (2000) Colorado River sediment transport 1. Natural sediment supply limitation and the influence of Glen Canyon Dam. *Water Resources Research* 36(2): 515-542.

United States Bureau of Reclamation. *Upper Colorado Region Reservoir Operations: Lake Powell*. Viewed online at http://www.usbr.gov/uc/crsp/GetDateInfo?d0=1719&d1=1792&d2=1862&d3=1872&d4=1928&idCount=5&l=LAKE+POWELL on 16 October 2008.

United States Geological Survey. (2008) *USGS Real-Time Data for Utah – Streamflow*. Webpage viewed at http://waterdata.usgs.gov/ut/nwis/current/?type=flow on 21 December 2008.

Van Metre, P. C. and B. J. Mahler. (2004) Contaminant trends in reservoir sediment cores as records of influent stream quality. *Environmental Science and Technology* 38: 2978-2986.

Vernieu, W. S. (1997) Effects of reservoir drawdown on resuspension of deltaic sediments in Lake Powell. *Journal of Lake and Reservoir Management* 13(1): 67-78.

Figure 1

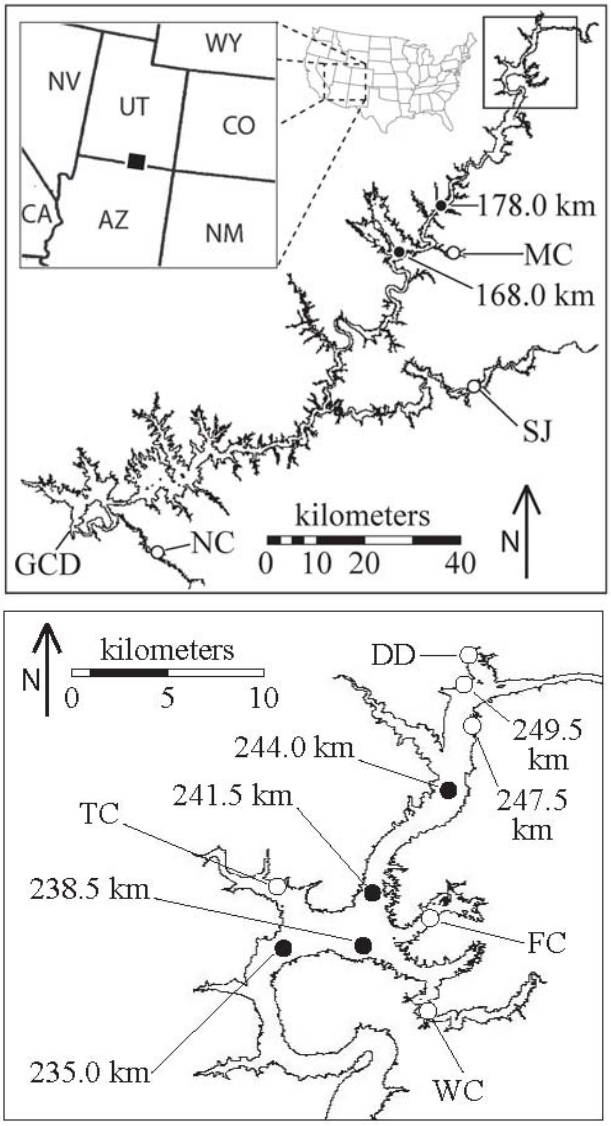

Figure 1. Sampling locations at Lake Powell. White and black circles represent shoreline and lakebed sampling sites, respectively. *Upper panel:* Side canyon sampling sites Navajo Canyon (NC), Moqui Canyon (MC), and the San Juan River (SJ) and lakebed sampling sites 168.0 and 178.0 river km from Glen Canyon Dam (GCD). The box in the northern portion of the lake delineates the inflow region. *Lower panel:* Side canyon sampling sites White Canyon (WC), Farley Canyon (FC), the Dirty Devil River (DD), delta shoreline sites 249.5 and 247.5 km from GCD, and lakebed sampling sites 235.0, 238.5, 241.5, and 245.0 km from GCD.

Figure 2

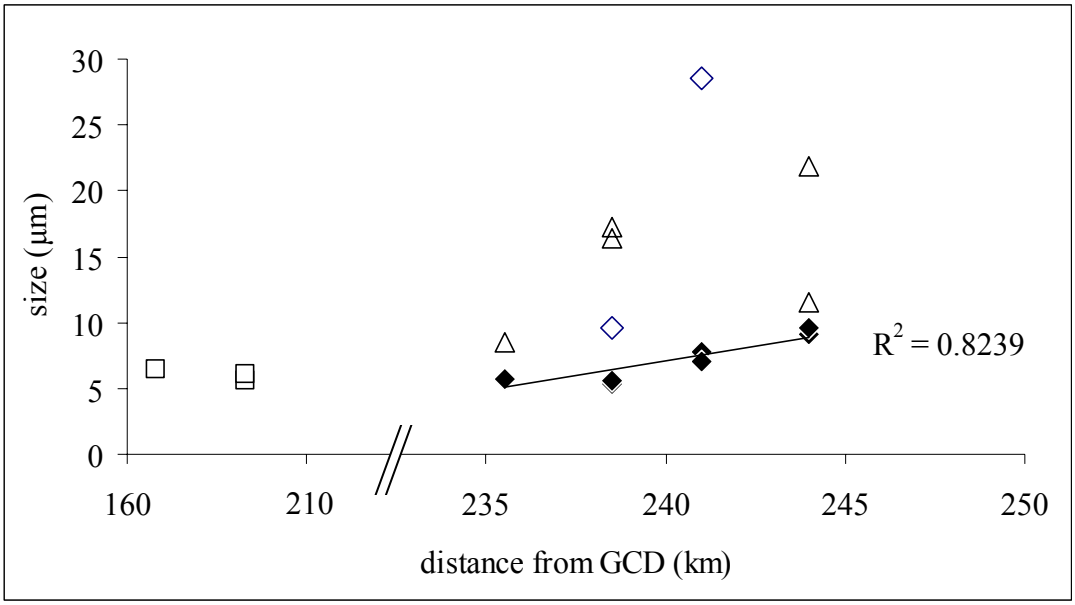

Figure 2. Particle size of lakebed sediment in Lake Powell: delta surface samples, March (♦), delta surface samples, May (◇), mid-lake surface samples (□), and delta deep samples, March (△). The trendline and the R^2 value apply only to the delta surface samples from March.

Figure 3

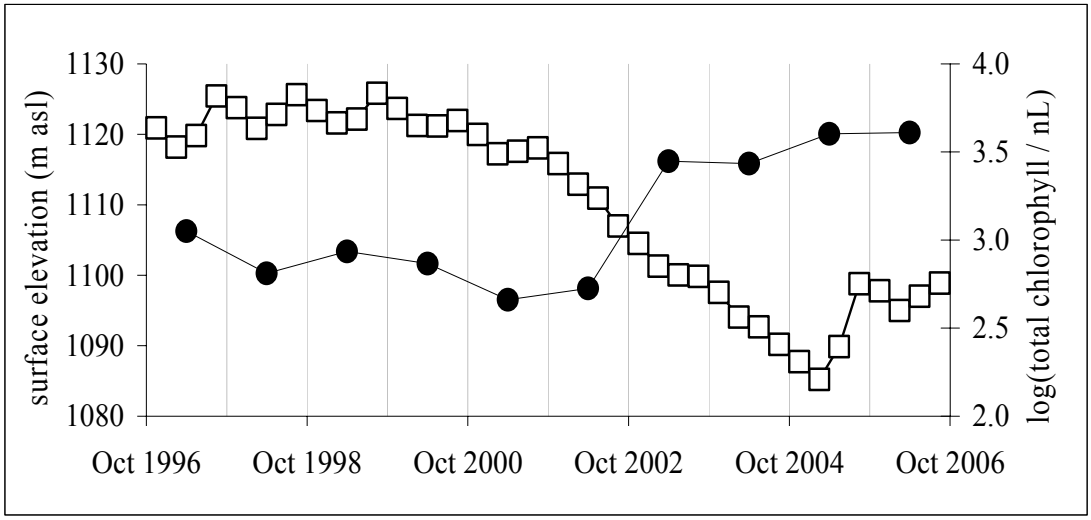

Figure 3. Possible impact of drawdown on water quality, hydrologic years 1997-2006: lake surface elevation (□), logarithm of average summertime chlorophyll (●). The surface elevation parameter is a quarterly average of daily lake elevation measurements (USBR 2008). The chlorophyll parameter is an average of 6 data points, two summertime sampling times (typically May and August or June and October) at 193.3, 208.5, and 225.5 km from Glen Canyon Dam (from Vernieu, in preparation).

Supporting Information for

Particle size controls sedimentary chemical distribution in a large reservoir, Lake Powell, USA.

Richard A. Wildman, Jr., Michael B. Easler, Dennis D. Eberl, Lincoln F. Pratson, Michael DeLeon, Aurelio LaRotta, and Janet G. Hering

(In preparation for *Environmental Science and Technology*)

Section S1: Sedimentation in Lake Powell. Lake Powell receives most of its sediment from its two main tributaries, the Colorado and San Juan Rivers. The Colorado River drains consists of a mixture of sediment from the Colorado and Green Rivers (and their many tributaries), which together flow well over 1500 km before reaching Lake Powell. These drain the southern Rocky Mountains, which are formed by a variety of limestones, igneous, and metamorphic formations, and the northeastern Colorado Plateau, which is mostly sandstones and mudstones with some basalt (Spahr et al. 2000; Anderson et al. 2003). Land use upstream from Lake Powell includes agriculture, mining, ranching, logging, recreational uses, and limited urban activity (Spahr et al. 2000). Conversely, the side canyons of Lake Powell drain sedimentary rock almost exclusively and a single formation often. Lake Powell is contained within Glen Canyon National Recreation Area and surrounded by remote desert, so there is exceedingly sparse human presence in the side canyon drainages away from the lake.

In the Colorado River inflow region of the reservoir, the river brings an uninterrupted, yet seasonally variable, sediment supply. At a given lake level, sediment is thought to settle out over ~25 km (S. B. Hueftle, Grand Canyon Monitoring and Research Center, personal communication, 2005), yet our monitoring observations suggest that the

Colorado River sediment delta is spread out as much as 100 km due to varying lake level and bedload transport. After sediment is deposited, it is reasonable to expect that preferential re-entrainment of small particles (i.e., winnowing) may occur near the river inflow when energetic flows reach the sediment, though we are not aware of any studies on this process in Lake Powell. This process should transport small particles further into the reservoir than large particles, exaggerating sediment sorting that we expect during initial sedimentation in the inflow region. Although we can not discount the possibility of winnowing, we expect it to be a minor effect in the upper area of the inflow region, which is dominated by the deposition of riverine suspended sediment.

As opposed to the main river deltas, intermittent desert creeks feed the side canyons. In this setting, nearly all of fine sediment and the majority of coarse sediment can be expected to be transported in short-duration, high-energy, "flash" floods (Malmon et al. 2004, Dick et al. 1997, US NWS 2008). We have observed this firsthand in the study area (Chapter 3). The sediment loads deposited in the side canyons are spatially distinct from one another because they are confined to separate creekbeds. While they occasionally spill into the thalweg of the reservoir, their sediment load is much smaller and intermittent than that of the Colorado River, whose sediment delta is not expected to contain meaningful amounts of side canyon sediment.

Section S2: Particle size analysis. Before particle size analysis, 0.04-0.5 g of dry sediment was shaken in 5.5 g L^{-1} sodium hexametaphosphate for ≥4 h. Samples were allowed to settle until analysis, and then shaken vigorously by hand to resuspend particles. Particle size was analyzed with a Mastersizer 2000 laser diffractometer (Malvern

Instruments Ltd., Worcestershire, UK). The sample-solution ratio was adjusted so that most samples were analyzed with an obscuration of 20 ± 4% (Sperazza et al. 2004). Samples were stirred at a rate of 1750 rotations per minute and ultrasonicated while in the sample introduction chamber (~2.5 min). To collect each particle size distribution, 1000 readings per second were collected for 10 seconds, and data were compiled with the Mastersizer 2000 computer program (version 5.22, Malvern Instruments Ltd., Worcestershire, UK) using a particle absorbance index of 1.0 and a refractive index of 1.52 (Sperazza et al. 2004). Five analytical replicates of each subsample were analyzed and averaged. Most sediment samples were subsampled in triplicate to compensate for any inhomogeneities due to the small sample mass. Variation between triplicate samples was small, so sample replicates were averaged.

Section S3: Elemental abundance measurements. Elemental abundances of a suite of elements were measured in samples with a XEPOS energy dispersive X-ray fluorescence (XRF) spectrometer (Spectro Analytical Instruments, Inc., Mahwah, NJ). Before analysis, samples were milled to a median particle size of < 100 μm in polypropylene tubes with zirconium oxide milling balls. Milled sample was mixed with binder wax (Licowax C Micropowder PM, APC Solutions SA) at a ratio of 4 g sample to 1.1 g wax and pressed into a pellet at a pressure of 15 tons for 2 min. Samples were analyzed on the XEPOS using a 50 W Pd tube and several polarizing/secondary targets for optimized excitation (see below). The measurement was carried out under vacuum (pressure <60 Pa) to prevent absorption of the characteristic radiation of the light elements (Na - Ti) in air. The fluorescent radiation was recorded using a high count rate Silicon Drift Detector and

analyzed via a general purpose standardless calibration package (TurboQuant Pellets) based on fundamental parameters and matrix-correction via Compton-peak analysis (provided by Spectro Analytical Instruments, Inc., Mahwah, NJ).

For optimized excitation and detection limits, each sample was irradiated for 5 minutes from each of the following targets: a curved highly oriented pyrolithic graphite target (HOPG), producing polarized quasi-monochromatic Pd-L X-rays for the excitation of 22 (Na) to 51 (V), a molybdenum secondary target for optimized excitation of the K-lines of 52-91 (Cr-Zr) and the L-lines of 141-238 (Pr-U), and an Al2O3 Barkla scatterer target, providing polarized Bremsstrahlung (deceleration radiation in a continuous spectrum) for the elements 89-140 (Y-Ce). To judge the accuracy of this measurement, certified standards NIST 2709 (National Institute of Standards and Technology) and TILL-1 (Canadian Certified Reference Materials Project) were analyzed. These standards were selected because the Compton scatter peaks (an indication of the average atomic number in the sample) matched those of the Lake Powell samples most closely, implying that matrix effects would be similar between these standards and the unknowns. Errors were below 20% for Mg, Al, Si, K, Ca, Ti, Mn, Fe, Ni, Cu, Zn, Ga, As, Br, Sr, Y, Ba, Pb, and Th. Errors exceeded 20% for P, V, Ce. The inaccuracies for the latter list of elements are, however, expected to be a systematic variation (a matrix-dependent constant scaling factor) rather than random variation, thus consistent comparison between samples is possible for these elements. Detection limits of the XEPOS vary by element and are ≤0.0001% (1 ppm) for most elements (as specified by the manufacturer for similar matrices). Concentrations of Ge, Nb, Mo, Ag, Cd, In, Sn, Sb, Te, I, Hf, Ta, W, Hg, and Tl, were consistently below detection limits, so these elements are not included in this study.

Cobalt data were rejected due to overlap of its spectroscopic peak with that of Fe, which occurred in much larger concentrations. Analytical precision was excellent; relative standard deviations were <5% for elements with concentrations consistently above the detection limit.

Eight to ten analytical replicates were measured for 17 samples, and the detection limit for each element was set at 3 times the average standard deviation of these replicate analyses

Section S4: Carbon measurements. Carbonate minerals were extracted from sediment samples by treating 0.5 g of each sample with two washes of 15 mL 1 N hydrochloric acid followed by a water wash and freeze-drying (Hedges and Stern 1984, White et al. 2005, Longworth et al. 2007, ASTM 2008). These samples and untreated sediment samples were analyzed on the elemental analyzer using an 8-point acetanilide calibration and a detection limit of 0.02%.

Section S5: Mineralogical measurements. Samples were prepared for mineralogical analyses by grinding 1 g of sample and 4 g methanol with corundum (Al_2O_3) milling weights. After drying overnight at 90°C, ground samples were mixed with 0.111 g zincite (ZnO), which was used as an internal standard. Samples were analyzed on the X-ray diffractometer using Cu Kα radiation over a 2θ range of 5-65°, a step interval of 0.02°, and duration of 2 s $step^{-1}$. Mineral concentrations in each sample were created from linear

combinations of several previously-analyzed standards as described by Eberl (2003). Deviation of the sum of mineral concentrations from 100% gives an indication of error in the measurement.

References for Supporting Information

American Society for Testing and Materials. *Annual Book of ASTM Standards,* volume 04.08. ASTM International: West Conshohocken, Pennsylvania, 2008.

Anderson, P. B., T. C. Chidsey, D. A. Sprinkel, and G. C. Willis. (2003) Geology of Glen Canyon National Recreation Area, Utah-Arizona. In *Geology of Utah's Parks and Monuments, second edition* (Sprinkel, D.A., T. C. Chidsey, and P. B. Anderson, eds.), Utah Geological Association Publication 28: Salt Lake City, 2003.

Dick, G. S., R. S. Anderson, and D. E. Sampson. (1997) Controls on flash flood magnitude and hydrograph shape, Upper Blue Hills badlands, Utah. *Geology* 25(1): 45-48.

Eberl, D. D. (2003) User guide to RockJock – A program for determining quantitative mineralogy from X-ray diffraction data. *United States Geological Survey* Open File Report OF 03-78.

Hedges, J. I. and J. H. Stern. (1984) Carbon and nitrogen determinations of carbonate-containing solids. *Limnology and Oceanography* 29(3): 657-663.

Longworth, B. E., S. T. Petsch, P. A. Raymond, and J. E. Bauer. (2007) Linking lithology and land use to sources of dissolved and particulate organic matter in headwaters of a temperature, passive-margin river system. *Geochimica et Cosmochimica Acta* 71: 4233-4250.

Malmon, D. V., S. L. Reneau, and T. Dunne. (2004) Sediment sorting and transport by floods. *Journal of Geophysical Research* 109: F02005, doi:10.1029/2003JF000067.

Pratson, L., J. Hughes-Clarke, M. Anderson, T. Gerber, D. Twichell, R. Ferrari, C. Nittrouer, J. Beaudoin, J. Granet, and J. Crockett. (2008) Timing and patterns of basin infilling as documented in Lake Powell during a drought. *Geology* 36(11): 843-846.

Spahr, N. E., L. E. Apodaca, J. R. Deacon, J. B. Bails, N. J. Bauch, C. M. Smith, and N. E. Driver. (2000) Water quality in the Upper Colorado River Basin, Colorado, 1996-98. *U.S. Geological Survey* Circular 1214.

Sperazza, M., J. N. Moore, and M. S. Hendrix. (2004) High-resolution particle size analysis of naturally occurring very fine-grained sediment through laser diffractometry. *Journal of Sedimentary Research* 74(5): 736-743.

United States Geological Survey. (2008) *USGS Real-Time Data for Utah – Streamflow*. Webpage viewed at http://waterdata.usgs.gov/ut/nwis/current/?type=flow on 21 December 2008.

United States National Weather Service. *Flash Floods*. Viewed online at http://www.wrh.noaa.gov/fgz/science/flashfld.php?wfo=fgz on 1 May, 2008.

White, H. K., C. M. Reddy, and T. I. Eglinton. (2005) Isotopic constraints on the fate of petroleum residues sequestered in salt marsh sediments. *Environmental Science and Technology* 39: 2545-2551.

Tables

Table S1: Sampling locations.

location[a]	number of cores	latitude	longitude	water depth (m)	collection date
Lakebed Samples, March 2006					
244.0	2	37.8455	-110.4236	1.2	21-23 March 2006
241.0	2	37.8244	-110.4363	6.7	21-23 March 2006
238.5	2	37.8067	-110.4334	19.1	21-23 March 2006
235.5	2	37.8106	-110.4674	27.7	21-23 March 2006
168.0	1	37.4580	-110.7277	72.5	21-23 March 2006
Lakebed Samples, May 2006					
241.0	1	37.8151	-110.4324	22.1	16-18 May 2006
238.5	1	37.8099	-110.4676	30.2	16-18 May 2006
193.0	2	37.5807	-100.5984	68.8	16-18 May 2006
Delta Shoreline Samples					
249.5	1	37.8873	-110.4003		21 March 2006
247.5 A	1	37.8734	-110.4050		12 April 2005
247.5 B	2	37.8734	-110.4050		18 June 2005
247.5 C	2	37.8734	-110.4050		05 December 2005
Side Canyon Samples					
DD	1	37.9029	-110.3973		16-18 May 2006
FC A	1	37.8193	-110.4120		16-18 May 2006
FC B	3	37.8188	-110.4122		27 March 2007
WC A	4	37.7926	-110.4136		07 February 2005
WC B	2	37.7947	-110.4133		13 April 2005
WC C	3	37.7839	-110.4044		19 June 2005
WC D	3	37.7867	-110.4065		05 December 2005
WC E	3	37.7853	-110.4083		27 March 2007
TC A	1	37.8276	-110.4738		21-23 March 2006
TC B	1	37.8276	-110.4738		16-18 May 2006
MC	1	37.4732	-110.6162		22 June 2005
SJ	3	37.2640	-110.4623		21 June 2005
NC A	1	36.8780	-111.2389		20 June 2005
NC B	2	36.8756	-111.2382		20 June 2005

[a] Numbers indicate distance from Glen Canyon Dam rounded to nearest 0.5 km. Letters indicate abbreviations of side canyons for Dirty Devil River (DD), Farley Canyon (FC), White Canyon (WC), Trachyte Canyon (TC), Moqui Canyon (MC), San Juan River (SJ), and Navajo Canyon (NC).

Table S2: Particle size statistics.

location[a]	depth (cm)	median (μm)	mean (μm)	mode (μm)
Lakebed Samples, March 2006				
244.0	0-5	6.09	9.07	9.77
244.0	0-16	6.39	9.54	10.20
244.0	15-30	7.56	11.59	12.69
244.0	60-75	6.90	21.84	44.60
241.2	0-5	4.67	7.03	4.96
241.2	0-12.5	5.15	7.80	6.57
238.7	0-12.5	3.80	5.38	3.69
238.7	0-15	3.97	5.56	4.11
238.7	25-40	11.00	16.45	17.81
238.7	40-50	12.66	17.27	19.23
235.4	0-15	3.90	5.69	3.68
235.4	0-15	3.93	5.73	3.73
235.4	25-40	5.74	8.48	7.36
168.0	5-15	3.78	6.38	2.67
Lakebed Samples, May 2006				
241.2	5-15	21.10	28.55	40.52
238.7	0-5	6.47	9.55	8.84
193.3	0-15	3.79	5.54	3.49
193.3	0-15	4.11	6.11	3.86
Delta Shoreline Samples				
247.5 A	0-8	133.53	141.32	154.55
247.5 B	0-10	119.19	122.30	135.67
247.5 B	0-8	131.42	135.54	146.49
247.5 C	0-8	30.92	41.93	45.60
247.5 C	0-16	18.29	20.32	26.36
249.5	-132 to -122	15.14	21.49	33.47
249.5	-102 to -94	264.12	291.87	272.47
249.5	-94 to -87	276.10	304.77	283.90
249.5	-77 to -67	290.96	297.94	327.74
249.5	-57 to -47	308.36	322.28	319.83
249.5	-47 to -37	6.41	10.30	8.17
249.5	-12 to -2	6.15	10.35	7.69
249.5	14 to 20	7.64	27.61	73.11
Side Canyon Samples				
FC A	0-12	49.97	51.95	57.23
FC A	17.5-27.5	59.99	62.20	66.89
FC A	42.5-52.5	53.61	55.20	63.78
FC A	57.5-67.5	66.82	69.06	74.75

Table S2: Particle size statistics, continued.

location[a]	depth (cm)	median (μm)	mean (μm)	mode (μm)
FC B	0-4	53.16	55.03	61.55
FC B	0-8	84.94	95.01	92.85
FC B	0-8	84.98	95.28	92.20
FC B	16-24	97.16	110.08	110.10
FC B	16-24	106.79	122.63	123.17
WC A	0-12	78.24	81.94	90.84
WC B	0-8	80.67	92.65	88.26
WC B	0-8	62.35	68.89	71.96
WC C	0-8	18.67	70.44	188.56
WC D	30-44	402.01	444.50	408.34
WC E	0-4	140.54	148.20	159.70
WC E	0-8	178.36	186.60	198.00
WC E	16-24	106.58	114.71	118.10
WC E	16-24	112.68	117.73	126.24
TC A	10-20	40.76	43.92	58.27
TC A	35-45	36.69	46.92	50.41
TC A	80-90	141.62	150.08	149.54
TC A	123-133	35.46	39.04	45.22
TC A	165-175	135.80	143.65	145.47
TC A	187.5-197.5	184.95	198.32	244.31
MC	0-8	115.60	120.04	123.49
SJ	0-8	96.32	100.96	110.10
SJ	0-6	77.38	81.80	106.62
NC A	0-12	157.99	167.92	163.01
NC B	0-8	107.27	115.14	128.50

[a] "Location" refers to distance from Glen Canyon Dam (in river km) for delta samples and to side canyon location.

Table S3A: Elemental abundances (%) in sediment samples.

sample description				*element*								
location[a]	depth (cm)	org C	tot C	Mg	Al	Si	P	S	Cl	K	Ca	Ti
Lakebed Samples, March 2006												
245.0	0-5	1.03	2.59	1.747	6.301	22.030	0.057	0.042	0.008	1.942	5.782	0.359
245.0	0-16	1.19	2.67	1.822	6.657	22.640	0.059	0.055	0.018	2.041	6.029	0.374
245.0	15-30	1.42	2.94	1.969	7.323	24.950	0.069	0.061	0.017	2.154	6.322	0.381
245.0	60-75	0.96	2.85	1.787	6.538	22.760	0.060	0.047	0.012	2.026	5.921	0.362
241.0	0-5	1.03	2.53	1.688	7.200	23.010	0.058	0.048	0.015	2.032	5.109	0.369
241.0	0-12.5	0.97	2.72	1.872	7.552	24.510	0.065	0.049	0.022	2.200	5.674	0.392
238.5	0-12.5	0.87		1.719	7.677	23.860	0.062	0.045	0.007	2.288	4.777	0.378
238.5	0-15			1.623	7.217	22.640	0.057	0.043	0.008	2.197	4.719	0.365
238.5	25-40	1.18	3.14	1.863	6.752	25.030	0.072	0.070	0.009	1.968	6.737	0.364
238.5	40-50	1.10	3.15	1.833	6.440	25.300	0.074	0.073	0.011	1.958	6.903	0.369
235.5	0-15	0.86	2.31	1.859	8.134	26.503	0.064	0.041	0.011	2.476	5.380	0.433
235.5	0-15	0.94	2.37	1.590	6.935	22.563	0.056	0.035	0.009	2.069	4.754	0.368
235.5	25-40	0.97	2.65	1.802	7.717	25.661	0.070	0.056	0.012	2.224	5.585	0.397
168.0	5-15	1.07	2.66	1.661	7.960	24.943	0.074	0.079	0.011	2.018	5.398	0.374
Lakebed Samples, May 2006												
241.0	5-15	1.23		1.396	4.695	24.290	0.062	0.070	0.008	1.694	5.584	0.277
238.5	0-5	1.27	2.89	1.664	6.650	22.980	0.063	0.070	0.014	1.996	5.639	0.372
193.0	0-15	0.90	8.55	1.576	6.883	22.790	0.057	0.034	0.008	2.036	4.855	0.360
Delta Shoreline Samples												
249.5	-132 to -122		2.49	1.697	6.291	25.597	0.061	0.053	0.009	2.046	6.083	0.357
249.5	-102 to -94	0.05	1.25	0.678	2.716	34.360	0.025	0.007	0.007	1.481	3.320	0.119
249.5	-94 to -87	0.03	1.34	0.833	3.087	31.950	0.037	0.019	0.006	1.535	3.997	0.144
249.5	-77 to -67	0.06	0.71	0.819	2.992	31.900	0.032	0.033	0.009	1.467	3.737	0.131
249.5	-57 to -47	0.07	0.68	0.716	2.910	31.260	0.028	0.015	0.008	1.493	3.929	0.123
249.5	-47 to -37	1.01	2.70	1.508	6.327	22.535	0.059	0.051	0.007	1.958	5.306	0.358
249.5	-12 to -2	1.01	2.58	1.426	6.033	21.325	0.056	0.045	0.008	1.867	5.251	0.336
249.5	14 to 20			1.533	6.602	23.240	0.062	0.048	0.006	1.977	5.313	0.340

Table S3A (continued): Elemental abundances (%) in sediment samples.

sample description				*element*								
location[a]	depth (cm)	org C	tot C	Mg	Al	Si	P	S	Cl	K	Ca	Ti
247.5 A	0-8	0.06	1.02	0.796	2.929	34.070	0.033	0.013	0.019	1.567	3.665	0.159
247.5 B	0-8	0.16	1.30	0.908	3.408	32.190	0.041	0.014	0.015	1.692	3.997	0.162
247.5 B	0-10	0.12	1.02	0.901	3.331	33.440	0.038	0.009	0.007	1.662	3.810	0.150
247.5 C	0-8	3.70	4.50	1.542	5.800	24.540	0.069	0.180	0.015	1.893	5.728	0.310
247.5 C	0-16	5.26	5.59	1.482	5.492	25.540	0.079	0.144	0.011	1.883	5.622	0.296
247.5 C	14-24	1.31	2.64	1.335	4.835	26.677	0.059	0.097	0.011	1.878	5.485	0.251
Side Canyon Samples												
DD[c]	0-10		1.44	0.972	2.487	22.720	0.038	0.056	0.019	1.335	5.012	0.178
DD	20-30		2.17	1.124	3.285	22.730	0.046	0.101	0.014	1.493	6.093	0.210
DD	47-57		3.44	0.563	1.376	19.100	0.015	0.026	0.013	0.997	3.185	0.104
DD	57-67		1.90	1.209	3.154	22.150	0.055	0.078	0.063	1.460	6.148	0.213
DD	77-87	0.78		1.499	4.485	21.310	0.052	0.075	0.016	1.721	7.580	0.293
DD	102-122	0.22	1.89	1.358	4.327	21.630	0.047	0.073	0.014	1.587	5.578	0.227
DD	130-140		1.72									
DD	167.5-177.5		3.13									
DD	180-190	0.84	2.68	1.402	5.060	20.140	0.051	0.059	0.007	1.630	6.087	0.305
DD	195-205		3.31									
FC A	0-12	0.23	1.37	1.337	4.875	23.730	0.027	0.205	0.021	2.215	3.650	0.303
FC A	12-17			0.991	4.172	24.000	0.025	0.019	0.009	1.994	2.916	0.270
FC A	17.5-27.5	0.09	1.14									
FC A	42.5-52.5	0.15	1.28	1.343	5.835	22.360	0.033	0.038	0.013	2.328	3.548	0.310
FC A	57.5-67.5	0.08	1.09	1.237	4.324	31.640	0.013	0.013	0.015	2.404	3.124	0.255

Table S3A (continued): Elemental abundances (%) in sediment samples.

sample description				*element*								
location[a]	depth (cm)	org C	tot C	Mg	Al	Si	P	S	Cl	K	Ca	Ti
FC B	0-4	0.23	1.59	1.462	4.618	31.110	0.023	0.024	0.014	2.443	3.697	0.309
FC B	0-8	0.07	1.30	1.305	3.398	31.995	0.020	BDL	0.008	2.021	4.118	0.231
FC B	0-8	0.06	1.28	1.257	3.331	32.564	0.025	0.006	0.009	2.018	4.033	0.232
FC B	4-8	0.06	1.27									
FC B	8-12	0.08	1.31									
FC B	8-16	0.06	1.46									
FC B	8-16	0.05	1.38									
FC B	12-16	0.08	1.50									
FC B	16-20	BDL	1.28									
FC B	16-24	0.05	1.35	1.276	3.200	32.200	0.014	0.00020	0.014	1.933	4.362	0.211
FC B	16-24	0.05	1.62	1.308	3.392	31.280	0.019	0.00020	0.019	1.980	4.571	0.220
FC B	20-24	0.08	1.75									
FC B	24-28	0.05	1.51									
FC B	24-32	0.05	1.79									
FC B	24-32	0.04	2.41									
FC B	28-32	0.04	1.45									
FC B	32-36	0.04	1.41									
WC A	0-10		3.79									
WC A	0-10			1.610	4.124	28.120	0.026	0.036	0.011	2.037	5.502	0.237
WC A	0-12	0.31	2.57	1.504	3.299	30.750	0.034	0.004	0.007	1.870	4.843	0.208
WC A	0-14	0.38	2.14	1.371	2.814	30.940	0.030	0.015	0.009	1.630	4.767	0.187
WC B	0-8	0.12	1.78	1.488	3.111	31.850	0.023	0.007	0.006	1.765	4.780	0.207
WC B	0-8	0.19	1.86	1.567	3.557	31.020	0.028	0.004	0.006	1.921	4.966	0.247
WC C	0-8	0.64	2.21	1.813	8.229	23.604	0.041	0.119	0.032	2.758	5.552	0.405
WC C	0-10	0.56	2.64	1.739	7.962	24.090	0.039	0.055	0.023	2.759	5.207	0.418
WC C	4-6			1.545	7.632	20.160	0.031	0.079	0.010	2.796	4.377	0.402
WC C	10-12			1.428	7.042	19.320	0.036	0.113	0.012	2.514	4.429	0.373
WC C	20-22			0.736	2.020	19.300	0.013	0.077	0.017	1.065	3.353	0.122

Table S3A (continued): Elemental abundances (%) in sediment samples.

sample description				*element*								
location[a]	depth (cm)	org C	tot C	Mg	Al	Si	P	S	Cl	K	Ca	Ti
WC D	0-10	0.08	1.16									
WC D	0-10	0.12	1.56	1.342	2.782	31.490	0.031	0.008	0.010	1.398	4.391	0.199
WC D	0-11	0.12	2.01	1.314	2.560	32.630	0.006	0.001	0.005	1.346	4.373	0.176
WC D	30-44	0.03	1.14	0.971	1.110	32.860	0.014	0.006	0.008	0.871	4.665	0.103
WC E	0-4	BDL	1.28	1.241	1.973	33.960	0.00062	0.003	0.018	1.351	3.919	0.129
WC E	0-8			1.146	1.619	34.090	0.00067	0.004	0.009	1.179	3.748	0.118
WC E	0-8	0.05	1.18	1.217	1.898	33.790	0.001	0.003	0.008	1.281	3.953	0.131
WC E	4-8	0.05	0.99									
WC E	8-12	0.03	1.01									
WC E	8-16	0.10	1.41									
WC E	12-16	0.04	0.97									
WC E	16-20	0.03	1.34									
WC E	16-24			1.296	2.531	32.620	0.016	0.003	0.011	1.603	4.062	0.170
WC E	16-24	0.11	1.47	1.289	2.416	32.590	0.010	0.005	0.011	1.569	4.020	0.141
WC E	20-24	0.07	1.18									
WC E	24-28	0.03	1.31									
WC E	28-32	0.11	1.51									
TC A[c]	10-20	4.63	6.19	0.966	5.014	24.819	0.083	0.053	0.008	1.805	4.034	0.273
TC A	35-45	12.82	16.85	0.934	3.795	17.028	0.096	0.126	0.007	1.323	4.962	0.208
TC A	80-90	0.05	1.01	0.644	1.962	26.520	0.011	BDL	0.006	1.186	2.706	0.102
TC A	123-133	7.16	16.65	1.062	4.811	22.510	0.099	0.120	0.007	1.702	4.644	0.288
TC A	165-175	0.04	0.85	0.683	2.027	23.900	0.011	0.004	0.007	1.242	2.886	0.092
TC A	187.5-197.5	0.57	1.23	0.664	2.241	19.510	0.026	0.072	0.008	1.073	2.953	0.094
TC A	205-215		0.77									
TC B[c]	7.5-17.5	0.24	0.90	0.770	2.640	22.020	0.030	0.017	0.006	1.362	3.574	0.131
TC B	33-43		0.78	0.612	1.816	36.660	0.011	BDL	0.006	1.173	2.626	0.099
TC B	50-58		6.06	0.845	4.590	18.880	0.102	0.129	0.010	1.429	4.024	0.244
MC	0-8	0.60	0.29	0.706	2.191	37.160	BDL	0.036	0.009	1.848	1.150	0.107

Table S3A (continued): Elemental abundances (%) in sediment samples.

sample description				*element*								
location[a]	depth (cm)	org C	tot C	Mg	Al	Si	P	S	Cl	K	Ca	Ti
SJ	0-5			1.035	5.099	30.680	0.023	0.027	0.004	1.801	3.609	0.290
SJ	0-6	0.26		0.867	4.288	33.130	0.018	0.026	0.007	1.809	3.160	0.244
SJ	0-8	0.04	0.63	0.743	3.310	34.360	0.008	0.048	0.030	1.775	2.769	0.216
SJ	10-15			0.972	4.446	31.580	0.021	0.015	0.006	1.869	3.555	0.255
SJ	20-25			0.723	3.570	32.130	0.007	0.011	0.003	1.790	2.869	0.195
SJ	30-35			0.679	3.269	33.260	0.014	0.004	0.004	1.731	2.521	0.194
NC A	0-12	BDL	0.19	0.470	1.364	37.920	0.013	BDL	0.010	1.511	0.986	0.090
NC B	0-8	0.16	0.61	0.905	2.904	36.090	0.004	0.015	0.010	1.963	2.150	0.160
NC B	0-12	0.31	0.89	1.206	3.689	31.970	0.033	0.074	0.005	2.055	2.719	0.175
median crustal abundance[b]				2.33	8.23	28.2	0.105	0.0350	0.0145	2.09	4.1500	0.565

sample description		*element*										
location[a]	depth (cm)	V	Cr	Mn	Fe	Ni	Cu	Zn	Ga	As	Se	Br
Lakebed Samples, March 2006												
245.0	0-5	0.017	0.006	0.057	2.973	0.002	0.003	0.009	0.0016	0.0010	BDL	0.0004
245.0	0-16	0.014	0.007	0.062	3.085	0.002	0.003	0.009	0.0016	0.0010	0.0001	0.0005
245.0	15-30	0.012	0.007	0.059	2.934	0.002	0.002	0.009	0.0015	0.0010	0.0001	0.0005
245.0	60-75	0.014	0.007	0.053	2.898	0.002	0.003	0.009	0.0016	0.0010	0.0001	0.0003
241.0	0-5	0.016	0.007	0.051	3.214	0.002	0.003	0.010	0.0020	0.0011	0.0001	0.0005
241.0	0-12.5	0.015	0.009	0.056	3.286	0.002	0.003	0.010	0.0019	0.0010	0.0002	0.0005
238.5	0-12.5	0.018	0.006	0.051	3.364	0.002	0.003	0.010	0.0020	0.0011	0.0001	0.0003
238.5	0-15	0.017	0.006	0.051	3.299	0.002	0.003	0.010	0.0019	0.0010	0.0001	0.0003
238.5	25-40	0.016	0.006	0.063	2.749	0.002	0.002	0.009	0.0014	0.0008	0.0001	0.0003
238.5	40-50	0.014	0.004	0.064	2.610	0.002	0.002	0.008	0.0012	0.0009	0.0001	0.0003
235.5	0-15	0.022	0.006	0.054	3.352	0.002	0.003	0.010	0.0018	0.0008	0.0001	0.0003
235.5	0-15	0.018	0.006	0.053	3.249	0.002	0.003	0.010	0.0018	0.0009	0.0001	0.0003
235.5	25-40	0.018	0.007	0.059	3.216	0.002	0.003	0.011	0.0018	0.0010	0.0001	0.0004
168.0	5-15	0.018	0.007	0.040	2.884	0.003	0.002	0.010	0.0019	0.0007	0.0001	0.0003

Table S3A (continued): Elemental abundances (%) in sediment samples.

sample description		*element*										
location[a]	depth (cm)	V	Cr	Mn	Fe	Ni	Cu	Zn	Ga	As	Se	Br
Lakebed Samples, May 2006												
241.0	5-15	0.006	0.003	0.042	1.739	0.002	0.002	0.006	0.0009	0.0005	BDL	0.0003
238.5	0-5	0.016	0.007	0.060	3.075	0.002	0.003	0.010	0.0017	0.0009	0.0001	0.0005
193.0	0-15	0.017	0.006	0.053	3.224	0.002	0.003	0.010	0.0016	0.0010	0.0001	0.0003
Delta Shoreline Samples												
249.5	-132 to -122	0.011	0.006	0.048	2.319	0.002	0.002	0.007	0.0013	0.0008	0.0001	0.0002
249.5	-102 to -94	0.002	BDL	0.022	0.732	0.000	0.001	0.002	0.0006	0.0003	BDL	0.0001
249.5	-94 to -87	0.004	BDL	0.027	0.980	0.000	0.000	0.003	0.0005	0.0003	BDL	0.0001
249.5	-77 to -67	0.003	0.013	0.027	0.969	0.000	0.001	0.003	0.0005	0.0005	0.0001	0.0001
249.5	-57 to -47	0.003	BDL	0.024	0.821	BDL	0.001	0.002	0.0006	0.0004	BDL	0.0001
249.5	-47 to -37	0.017	0.006	0.057	3.013	0.002	0.002	0.010	0.0017	0.0008	0.0001	0.0002
249.5	-12 to -2	0.015	0.007	0.051	2.826	0.002	0.003	0.009	0.0015	0.0007	0.0001	0.0003
249.5	14 to 20	0.015	0.005	0.050	2.767	0.002	0.003	0.009	0.0016	0.0008	0.0001	0.0003
247.5 A	0-8	BDL	BDL	0.025	0.800	0.000	0.001	0.002	0.0006	0.0003	BDL	0.0001
247.5 B	0-8	0.002	BDL	0.026	0.854	0.000	0.001	0.003	0.0008	0.0003	BDL	0.0001
247.5 B	0-10	0.004	BDL	0.024	0.839	0.001	0.001	0.002	0.0006	0.0003	BDL	0.0001
247.5 C	0-8	0.014	0.005	0.046	2.340	0.002	0.018	0.014	0.0013	0.0011	0.0001	0.0005
247.5 C	0-16	0.012	BDL	0.048	2.120	0.002	0.003	0.008	0.0011	0.0008	0.0001	0.0005
247.5 C	14-24	0.007	0.003	0.037	1.639	0.002	0.024	0.014	0.0008	0.0005	0.0001	0.0003

Table S3A (continued): Elemental abundances (%) in sediment samples.

sample description		*element*										
location[a]	depth (cm)	V	Cr	Mn	Fe	Ni	Cu	Zn	Ga	As	Se	Br
Side Canyon Samples												
DD[c]	0-10	0.003	0.021	0.029	0.935	0.000	0.001	0.002	0.0006	0.0003	0.0001	0.0001
DD	20-30	0.005	0.004	0.034	1.182	0.001	0.001	0.003	0.0006	0.0004	BDL	0.0001
DD	47-57	0.003	0.047	0.019	0.720	0.001	0.001	0.001	0.0003	0.0003	BDL	0.0001
DD	57-67	0.004	0.037	0.032	1.301	0.001	0.001	0.003	0.0008	0.0004	0.0000	0.0002
DD	77-87	0.006	0.006	0.048	1.879	0.001	0.002	0.005	0.0009	0.0006	0.0001	0.0001
DD	102-122	0.008	0.009	0.032	1.423	0.001	0.001	0.003	0.0008	0.0003	BDL	0.0001
DD	180-190	0.011	0.007	0.040	2.597	0.002	0.002	0.007	0.0013	0.0006	0.0001	0.0001
FC A	0-12	0.004	0.015	0.027	1.438	0.001	0.001	0.002	0.0008	0.0002	0.0001	0.0001
FC A	12-17	BDL	0.016	0.025	1.194	0.001	0.001	0.002	0.0008	0.0003	0.0001	0.0001
FC A	42.5-52.5	0.005	0.038	0.032	1.764	0.002	0.001	0.003	0.0008	0.0004	BDL	0.0001
FC A	57.5-67.5	BDL	0.004	0.026	0.977	0.001	0.001	0.002	0.0005	0.0003	BDL	0.0001
FC B	0-4	0.003	0.007	0.031	1.216	0.001	0.001	0.002	0.0008	0.0005	BDL	0.0001
FC B	0-8	BDL	0.002	0.031	0.929	0.001	0.001	0.002	0.0005	0.0003	BDL	0.0001
FC B	0-8	0.003	0.002	0.030	0.919	0.001	0.001	0.002	0.0005	0.0003	0.0001	0.0001
FC B	16-24	BDL	0.004	0.032	0.914	0.001	0.001	0.001	0.0005	0.0002	BDL	0.0001
FC B	16-24	BDL	BDL	0.033	0.888	0.001	0.001	0.002	0.0005	0.0004	BDL	0.0001
WC A	0-10	0.005	0.004	0.037	1.157	0.001	0.013	0.008	0.0005	0.0005	BDL	0.0002
WC A	0-12	BDL	BDL	0.032	0.808	0.001	0.001	0.002	0.0004	0.0002	0.0001	0.0001
WC A	0-14	BDL	BDL	0.030	0.758	0.001	0.001	0.002	0.0005	0.0002	BDL	0.0001
WC B	0-8	BDL	BDL	0.031	0.808	0.001	0.001	0.002	0.0004	0.0002	BDL	0.0001
WC B	0-8	BDL	0.003	0.034	0.972	0.001	0.001	0.002	0.0007	0.0003	BDL	0.0001

Table S3A (continued): Elemental abundances (%) in sediment samples.

sample description		*element*										
location[a]	depth (cm)	V	Cr	Mn	Fe	Ni	Cu	Zn	Ga	As	Se	Br
WC C	0-8	0.009	0.006	0.052	2.905	0.003	0.003	0.006	0.0016	0.0010	0.0001	0.0003
WC C	0-10	0.010	0.009	0.052	2.803	0.002	0.003	0.005	0.0016	0.0007	0.0001	0.0002
WC C	4-6	0.009	0.007	0.056	3.385	0.002	0.003	0.006	0.0019	0.0009	BDL	0.0002
WC C	10-12	0.014	0.004	0.044	3.369	0.003	0.004	0.007	0.0017	0.0011	0.0001	0.0004
WC C	20-22	BDL	0.002	0.020	0.578	0.000	0.001	0.001	0.0001	0.0001	BDL	0.0001
WC D	0-10	0.002	0.003	0.029	0.814	0.000	0.007	0.004	0.0003	0.0002	0.0000	0.0001
WC D	0-11	BDL	BDL	0.031	0.716	0.000	0.001	0.001	0.0003	0.0003	BDL	0.0001
WC D	30-44	BDL	BDL	0.028	0.501	0.000	0.008	0.003	0.0002	0.0003	BDL	0.0001
WC E	0-4	BDL	BDL	0.027	0.534	0.000	0.001	0.001	0.0004	0.0003	0.0001	0.0001
WC E	0-8	BDL	BDL	0.025	0.475	0.000	0.001	0.001	0.0002	0.0001	BDL	0.0001
WC E	0-8	BDL	BDL	0.025	0.548	0.000	0.001	0.001	0.0003	0.0002	BDL	0.0001
WC E	16-24	BDL	BDL	0.026	0.678	0.000	0.001	0.001	0.0004	0.0001	0.0000	0.0001
WC E	16-24	BDL	BDL	0.027	0.614	0.001	0.001	0.001	0.0004	0.0003	0.0000	0.0000
TC A[c]	10-20	0.007	0.003	0.053	1.582	0.001	0.002	0.005	0.0009	0.0005	0.0001	0.0002
TC A	35-45	0.007	0.003	0.070	1.456	0.001	0.002	0.005	0.0008	0.0005	0.0001	0.0008
TC A	80-90	0.002	0.012	0.017	0.504	0.000	0.001	0.001	0.0003	0.0001	BDL	0.0000
TC A	123-133	0.008	0.003	0.082	1.820	0.001	0.003	0.007	0.0010	0.0006	0.0001	0.0004
TC A	165-175	0.002	0.009	0.017	0.500	0.000	0.001	0.001	0.0002	0.0001	BDL	BDL
TC A	187.5-197.5	0.003	0.005	0.021	0.669	0.000	0.001	0.001	0.0004	0.0002	0.0001	0.0001
TC B[c]	7.5-17.5	0.002	0.003	0.022	0.654	0.000	0.001	0.001	0.0003	0.0001	0.0001	0.0001
TC B	33-43	BDL	BDL	0.020	0.428	BDL	0.001	0.001	0.0003	0.0001	0.0000	0.0001
TC B	50-58	0.009	0.002	0.082	1.791	0.001	0.003	0.007	0.0010	0.0005	0.0001	0.0007
MC	0-8	BDL	BDL	0.012	0.339	0.000	0.000	0.001	0.0003	BDL	BDL	0.0001

Table S3A (continued): Elemental abundances (%) in sediment samples.

sample description		*element*										
location[a]	depth (cm)	V	Cr	Mn	Fe	Ni	Cu	Zn	Ga	As	Se	Br
SJ	0-5	0.004	0.004	0.040	1.454	0.001	0.002	0.005	0.0009	0.0003	BDL	0.0001
SJ	0-6	0.004	BDL	0.034	1.094	0.001	0.001	0.004	0.0008	0.0001	BDL	0.0002
SJ	0-8	0.002	0.005	0.027	0.767	0.000	0.001	0.002	0.0005	0.0002	BDL	0.0001
SJ	10-15	0.004	0.007	0.033	1.135	0.000	0.001	0.003	0.0007	0.0003	BDL	0.0001
SJ	20-25	BDL	BDL	0.027	0.761	0.000	0.001	0.002	0.0005	0.0002	BDL	BDL
SJ	30-35	BDL	0.007	0.024	0.754	0.000	0.001	0.002	0.0006	0.0001	BDL	0.0000
NC A	0-12	BDL	BDL	0.012	0.199	BDL	0.000	0.001	0.0003	BDL	0.0001	BDL
NC B	0-8	BDL	BDL	0.019	0.510	0.000	0.001	0.001	0.0004	0.0001	BDL	0.0001
NC B	0-12	BDL	BDL	0.028	0.718	0.001	0.001	0.002	0.0005	0.0003	0.0000	0.0001
median crustal abundance[b]		0.0012	0.0010	0.0950	5.6300	0.0084	0.0060	0.0070	0.0019	0.0002	$5 \cdot 10^{-6}$	0.0002

sample description		*element*									
location[a]	depth (cm)	Rb	Sr	Y	Zr	Ba	La	Ce	Pb	Th	U
Lakebed Samples, March 2006											
245.0	0-5	0.0104	0.0252	0.0024	BDL	0.0445	0.0037	0.0086	0.0024	0.0014	0.0007
245.0	0-16	0.0107	0.0260	0.0024	BDL	0.0425	0.0045	0.0080	0.0025	0.0014	0.0004
245.0	15-30	0.0100	0.0256	0.0024	BDL	0.0473	0.0066	0.0084	0.0023	0.0011	0.0004
245.0	60-75	0.0105	0.0246	0.0025	BDL	0.0405	0.0049	0.0075	0.0022	0.0013	0.0004
241.0	0-5	0.0108	0.0241	0.0025	BDL	0.0447	0.0067	0.0115	0.0024	0.0014	0.0005
241.0	0-12.5	0.0112	0.0256	0.0027	BDL	0.0424	0.0036	0.0076	0.0028	0.0013	0.0006
238.5	0-15	0.0122	0.0244	0.0025	BDL	0.0438	0.0055	0.0139	0.0027	0.0016	0.0006
238.5	0-12.5	0.0119	0.0243	0.0024	BDL	0.0420	0.0057	0.0095	0.0027	0.0014	0.0005
238.5	25-40	0.0091	0.0268	0.0026	BDL	0.0534	0.0061	0.0131	0.0026	0.0013	0.0005
238.5	40-50	0.0089	0.0268	0.0025	BDL	0.0522	0.0071	0.0131	0.0025	0.0014	0.0007
235.5	0-15	0.0120	0.0239	0.0027	BDL	0.0415	0.0067	0.0113	0.0029	0.0015	0.0009
235.5	0-15	0.0114	0.0239	0.0025	BDL	0.0456	0.0052	0.0100	0.0026	0.0014	0.0006
235.5	25-40	0.0113	0.0254	0.0025	BDL	0.0485	0.0063	0.0115	0.0028	0.0015	0.0006
168.0	5-15	0.0118	0.0225	0.0026	BDL	0.0326	0.0053	0.0106	0.0023	0.0016	0.0006

Table S3A (continued): Elemental abundances (%) in sediment samples.

sample description		*element*									
location[a]	depth (cm)	Rb	Sr	Y	Zr	Ba	La	Ce	Pb	Th	U
Lakebed Samples, May 2006											
241.0	5-15	0.0072	0.0217	0.0019	BDL	0.0593	0.0067	0.0105	0.0020	0.0008	0.0003
238.5	0-5	0.0106	0.0253	0.0023	BDL	0.0437	BDL	0.0069	0.0025	0.0015	0.0004
193.0	0-15	0.0113	0.0241	0.0023	BDL	0.0448	0.0057	0.0103	0.0027	0.0015	0.0006
Delta Shoreline Samples											
249.5	-132 to -122	0.0087	0.0233	0.0024	BDL	0.0510	0.0067	0.0097	0.0019	0.0012	0.0005
249.5	-102 to -94	0.0044	0.0152	0.0016	0.0507	0.0546	0.0064	0.0095	0.0015	0.0005	BDL
249.5	-94 to -87	0.0048	0.0165	0.0015	0.0528	0.0561	0.0046	0.0064	0.0019	0.0004	0.0003
249.5	-77 to -67	0.0047	0.0160	0.0014	0.0505	0.0505	0.0056	0.0099	0.0017	0.0003	0.0003
249.5	-57 to -47	0.0045	0.0166	0.0011	0.0536	0.0545	0.0044	0.0097	0.0016	0.0004	BDL
249.5	-47 to -37	0.0108	0.0257	0.0025	BDL	0.0520	0.0078	0.0123	0.0027	0.0013	0.0006
249.5	-12 to -2	0.0103	0.0244	0.0025	BDL	0.0450	0.0054	0.0115	0.0026	0.0013	0.0007
249.5	14 to 20	0.0098	0.0241	0.0022	BDL	0.0459	0.0037	0.0086	0.0027	0.0012	0.0004
247.5 A	0-8	0.0049	0.0159	0.0017	0.0577	0.0525	0.0040	0.0096	0.0013	0.0005	BDL
247.5 B	0-8	0.0054	0.0177	0.0017	0.0536	0.0526	0.0045	0.0080	0.0013	0.0005	BDL
247.5 B	0-10	0.0054	0.0176	0.0020	0.0577	0.0559	0.0053	0.0072	0.0014	0.0004	0.0003
247.5 C	0-8	0.0084	0.0240	0.0023	BDL	0.0502	0.0047	0.0095	0.0034	0.0011	0.0003
247.5 C	0-16	0.0081	0.0233	0.0022	0.0479	0.0546	0.0050	0.0092	0.0023	0.0010	0.0003
247.5 C	14-24	0.0071	0.0222	0.0017	BDL	0.0600	0.0047	0.0083	0.0027	0.0007	0.0005

Table S3A (continued): Elemental abundances (%) in sediment samples.

sample description		*element*									
location[a]	depth (cm)	Rb	Sr	Y	Zr	Ba	La	Ce	Pb	Th	U
Side Canyon Samples											
DD[c]	0-10	0.0055	0.0162	0.0012	BDL	0.0525	0.0065	0.0099	0.0009	0.0004	0.0002
DD	20-30	0.0061	0.0196	0.0015	BDL	0.0478	0.0047	0.0062	0.0013	0.0005	0.0004
DD	47-57	0.0039	0.0101	0.0006	BDL	0.0393	0.0031	0.0069	0.0006	0.0004	0.0002
DD	57-67	0.0061	0.0188	0.0016	0.0493	0.0548	0.0077	0.0136	0.0013	0.0006	0.0004
DD	77-87	0.0074	0.0263	0.0021	BDL	0.0420	0.0050	0.0074	0.0017	0.0010	0.0004
DD	102-122	0.0068	0.0216	0.0015	0.0461	0.0459	0.0040	0.0063	0.0013	0.0006	0.0004
DD	180-190	0.0096	0.0267	0.0022	BDL	0.0347	0.0054	0.0142	0.0020	0.0012	0.0005
FC A	0-12	0.0065	0.0091	0.0019	0.0641	0.0392	0.0024	0.0068	0.0013	0.0006	0.0004
FC A	12-17	0.0059	0.0078	0.0017	0.0666	0.0449	0.0057	0.0120	0.0012	0.0006	0.0002
FC A	42.5-52.5	0.0069	0.0095	0.0017	0.0714	0.0425	0.0102	0.0135	0.0014	0.0007	BDL
FC A	57.5-67.5	0.0058	0.0072	0.0016	0.0542	0.0453	0.0090	0.0137	0.0013	0.0006	BDL
FC B	0-4	0.0061	0.0078	0.0022	0.0653	0.0410	0.0051	0.0112	0.0011	0.0006	BDL
FC B	0-8	0.0049	0.0067	0.0025	0.0683	0.0412	0.0035	0.0073	0.0012	0.0005	BDL
FC B	0-8	0.0048	0.0066	0.0022	0.0722	0.0435	0.0061	0.0101	0.0011	0.0005	0.0002
FC B	16-24	0.0046	0.0066	0.0018	BDL	0.0400	0.0071	0.0141	0.0013	0.0005	BDL
FC B	16-24	0.0048	0.0069	0.0018	0.0629	0.0383	0.0044	0.0077	0.0011	0.0006	BDL
WC A	0-10	0.0057	0.0118	0.0018	0.0515	0.0537	0.0106	0.0147	0.0032	0.0005	0.0003
WC A	0-12	0.0050	0.0093	0.0026	0.0672	0.0407	0.0038	BDL	0.0012	0.0004	BDL
WC A	0-14	0.0046	0.0086	0.0023	0.0698	0.0358	0.0040	0.0070	0.0010	0.0005	BDL
WC B	0-8	0.0047	0.0092	0.0019	0.0658	0.0413	0.0035	0.0071	0.0012	0.0005	BDL
WC B	0-8	0.0053	0.0101	0.0023	0.0694	0.0426	0.0061	0.0079	0.0012	0.0006	0.0003

Table S3A (continued): Elemental abundances (%) in sediment samples.

sample description		*element*									
location[a]	depth (cm)	Rb	Sr	Y	Zr	Ba	La	Ce	Pb	Th	U
WC C	0-8	0.0091	0.0207	0.0021	BDL	0.0402	0.0045	0.0086	0.0024	0.0011	0.0006
WC C	0-10	0.0089	0.0186	0.0024	BDL	0.0383	0.0035	0.0094	0.0022	0.0010	0.0006
WC C	4-6	0.0106	0.0203	0.0021	BDL	0.0402	0.0070	0.0082	0.0026	0.0012	0.0006
WC C	10-12	0.0109	0.0221	0.0021	BDL	0.0443	0.0050	0.0126	0.0028	0.0012	0.0005
WC C	20-22	0.0034	0.0064	0.0007	0.0467	0.0315	0.0068	0.0064	0.0008	0.0002	BDL
WC D	0-10	0.0037	0.0075	0.0024	0.0861	0.0357	0.0075	0.0111	0.0012	0.0006	BDL
WC D	0-11	0.0035	0.0074	0.0025	0.0580	0.0325	BDL	0.0061	0.0008	0.0005	BDL
WC D	30-44	0.0021	0.0068	0.0018	0.0638	0.0366	0.0074	0.0113	0.0008	0.0002	BDL
WC E	0-4	0.0034	0.0063	0.0012	0.0493	0.0344	0.0059	0.0086	0.0006	0.0003	BDL
WC E	0-8	0.0030	0.0059	0.0009	0.0505	0.0297	0.0032	0.0068	0.0007	0.0002	BDL
WC E	0-8	0.0032	0.0063	0.0010	0.0528	0.0291	0.0036	0.0059	0.0009	0.0003	BDL
WC E	16-24	0.0041	0.0074	0.0018	0.0687	0.0402	0.0058	0.0078	0.0011	0.0003	BDL
WC E	16-24	0.0042	0.0071	0.0015	0.0493	0.0381	0.0066	0.0097	0.0009	0.0005	BDL
TC A[c]	10-20	0.0075	0.0229	0.0018	BDL	0.0597	0.0049	0.0092	0.0023	0.0009	0.0005
TC A	35-45	0.0060	0.0230	0.0022	BDL	0.0512	0.0051	0.0093	0.0022	0.0007	0.0005
TC A	80-90	0.0042	0.0106	0.0007	BDL	0.0381	0.0042	0.0083	0.0010	0.0001	0.0002
TC A	123-133	0.0074	0.0228	0.0021	BDL	0.0578	0.0029	0.0099	0.0026	0.0010	0.0006
TC A	165-175	0.0044	0.0095	0.0006	0.0454	0.0413	0.0042	0.0059	0.0010	0.0003	BDL
TC A	187.5-197.5	0.0040	0.0135	0.0006	BDL	0.0443	0.0054	0.0078	0.0009	0.0003	0.0003
TC B[c]	7.5-17.5	0.0051	0.0116	0.0008	BDL	0.0447	0.0050	0.0081	0.0011	0.0003	0.0003
TC B	33-43	0.0030	0.0112	0.0012	0.0547	0.0385	0.0048	0.0061	0.0007	0.0002	BDL
TC B	50-58	0.0067	0.0268	0.0023	BDL	0.0565	0.0074	0.0101	0.0028	0.0010	0.0007
MC	0-8	0.0051	0.0058	0.0007	BDL	0.0388	0.0047	0.0065	0.0011	0.0003	BDL

Table S3A (continued): Elemental abundances (%) in sediment samples.

sample description		*element*									
location[a]	depth (cm)	Rb	Sr	Y	Zr	Ba	La	Ce	Pb	Th	U
SJ	0-5	0.0068	0.0186	0.0018	0.0458	0.0572	0.0064	0.0112	0.0020	0.0008	0.0002
SJ	0-6	0.0063	0.0160	0.0018	0.0582	0.0587	0.0050	0.0072	0.0019	0.0007	BDL
SJ	0-8	0.0058	0.0138	0.0016	0.0662	0.0631	0.0068	0.0114	0.0012	0.0006	0.0002
SJ	10-15	0.0067	0.0178	0.0018	0.0600	0.0598	0.0042	0.0109	0.0014	0.0008	0.0002
SJ	20-25	0.0059	0.0134	0.0013	0.0471	0.0557	0.0053	0.0093	0.0013	0.0005	BDL
SJ	30-35	0.0057	0.0127	0.0016	0.0731	0.0658	0.0072	0.0120	0.0013	0.0006	BDL
NC A	0-12	0.0043	0.0038	0.0021	0.0660	0.0333	0.0044	0.0087	0.0008	0.0001	BDL
NC B	0-8	0.0057	0.0060	0.0012	0.0546	0.0421	0.0047	0.0061	0.0012	0.0004	BDL
NC B	0-12	0.0062	0.0072	0.0018	0.0539	0.0448	0.0052	0.0069	0.0011	0.0004	BDL
median crustal abundance[b]		0.0090	0.0370	0.0033	0.0165	$1 \cdot 10^{-7}$	0.0003	0.0425	0.0014	0.0010	0.0003

[a] "Location" refers to distance from Glen Canyon Dam (in river km) for delta samples and to side canyon location.

[b] Median crustal abundance data from Lide (2007).

[c] For DD and TC side canyon samples only, depth refers to depth below the tops of sets of cores collected above the water line.

Table S3B: Elemental abundances (molar ratios, normalized to silicon) in sediment samples.

sample description				*element*								
location[a]	depth (cm)	org C	tot C	Mg	Al	Si	P	S	Cl	K	Ca	Ti
Lakebed Samples, March 2006												
245.0	0-5	0.11	0.28	0.092	0.298	1	0.0023	0.0017	2.8E-04	0.063	0.184	0.0096
245.0	0-16	0.12	0.28	0.093	0.306	1	0.0024	0.0021	6.2E-04	0.065	0.187	0.0097
245.0	15-30	0.13	0.28	0.091	0.306	1	0.0025	0.0021	5.5E-04	0.062	0.178	0.0090
245.0	60-75	0.10	0.29	0.091	0.299	1	0.0024	0.0018	4.3E-04	0.064	0.182	0.0093
241.0	0-5	0.10	0.26	0.085	0.326	1	0.0023	0.0018	5.3E-04	0.063	0.156	0.0094
241.0	0-12.5	0.09	0.26	0.088	0.321	1	0.0024	0.0017	6.9E-04	0.064	0.162	0.0094
238.5	0-12.5	0.09		0.083	0.335	1	0.0023	0.0016	2.4E-04	0.069	0.140	0.0093
238.5	0-15			0.083	0.332	1	0.0023	0.0016	3.0E-04	0.070	0.146	0.0095
238.5	25-40	0.11	0.29	0.086	0.281	1	0.0026	0.0025	2.9E-04	0.056	0.189	0.0085
238.5	40-50	0.10	0.29	0.084	0.265	1	0.0027	0.0025	3.3E-04	0.056	0.191	0.0086
235.5	0-15	0.08	0.20	0.081	0.319	1	0.0022	0.0013	3.2E-04	0.067	0.142	0.0096
235.5	0-15	0.10	0.25	0.081	0.320	1	0.0022	0.0014	3.2E-04	0.066	0.148	0.0096
235.5	25-40	0.09	0.24	0.081	0.313	1	0.0025	0.0019	3.6E-04	0.062	0.153	0.0091
168.0	5-15	0.10	0.25	0.077	0.332	1	0.0027	0.0028	3.4E-04	0.058	0.152	0.0088
Lakebed Samples, May 2006												
241.0	5-15	0.12		0.066	0.201	1	0.0023	0.0025	2.5E-04	0.050	0.161	0.0067
238.5	0-5	0.13	0.29	0.084	0.301	1	0.0025	0.0027	4.7E-04	0.062	0.172	0.0095
193.0	0-15	0.09	0.88	0.080	0.314	1	0.0023	0.0013	2.8E-04	0.064	0.149	0.0093
Delta Shoreline Samples												
249.5	-132 to -122		0.23	0.077	0.256	1	0.0022	0.0018	2.9E-04	0.057	0.167	0.0082
249.5	-102 to -94	0.00	0.09	0.023	0.082	1	0.0007	0.0002	1.6E-04	0.031	0.068	0.0020
249.5	-94 to -87	0.00	0.10	0.030	0.101	1	0.0010	0.0005	1.6E-04	0.035	0.088	0.0026
249.5	-77 to -67	0.00	0.05	0.030	0.098	1	0.0009	0.0009	2.2E-04	0.033	0.082	0.0024
249.5	-57 to -47	0.01	0.05	0.026	0.097	1	0.0008	0.0004	2.1E-04	0.034	0.088	0.0023
249.5	-47 to -37	0.10	0.28	0.077	0.292	1	0.0024	0.0020	2.6E-04	0.062	0.165	0.0093
249.5	-12 to -2	0.11	0.28	0.077	0.294	1	0.0024	0.0018	3.0E-04	0.063	0.173	0.0092
249.5	14 to 20			0.076	0.296	1	0.0024	0.0018	2.1E-04	0.061	0.160	0.0086

Table S3B (continued): Elemental abundances (molar ratios, normalized to silicon) in sediment samples.

sample description				*element*								
location[a]	depth (cm)	org C	tot C	Mg	Al	Si	P	S	Cl	K	Ca	Ti
247.5 A	0-8	0.00	0.07	0.027	0.089	1	0.0009	0.0003	4.5E-04	0.033	0.075	0.0027
247.5 B	0-8	0.01	0.09	0.033	0.110	1	0.0011	0.0004	3.8E-04	0.038	0.087	0.0030
247.5 B	0-10	0.01	0.07	0.031	0.104	1	0.0010	0.0002	1.6E-04	0.036	0.080	0.0026
247.5 C	0-8	0.35	0.43	0.073	0.246	1	0.0025	0.0064	4.9E-04	0.055	0.164	0.0074
247.5 C	0-16	0.48	0.51	0.067	0.224	1	0.0028	0.0049	3.3E-04	0.053	0.154	0.0068
247.5 C	14-24	0.11	0.23	0.058	0.189	1	0.0020	0.0032	3.2E-04	0.051	0.144	0.0055
Side Canyon Samples												
DD[c]	0-10		0.15	0.049	0.114	1	0.0015	0.0022	6.8E-04	0.042	0.155	0.0046
DD	20-30		0.22	0.057	0.150	1	0.0018	0.0039	4.8E-04	0.047	0.188	0.0054
DD	47-57		0.42	0.034	0.075	1	0.0007	0.0012	5.3E-04	0.037	0.117	0.0032
DD	57-67		0.20	0.063	0.148	1	0.0022	0.0031	2.2E-03	0.047	0.195	0.0056
DD	77-87	0.09		0.081	0.219	1	0.0022	0.0031	6.0E-04	0.058	0.249	0.0081
DD	102-122	0.02	0.20	0.073	0.208	1	0.0020	0.0030	5.2E-04	0.053	0.181	0.0061
DD	130-140		0.19									
DD	167.5-177.5		0.34									
DD	180-190	0.10	0.31	0.080	0.262	1	0.0023	0.0026	2.6E-04	0.058	0.212	0.0089
DD	195-205		0.36									
FC A	0-12	0.02	0.14	0.065	0.214	1	0.0010	0.0076	7.0E-04	0.067	0.108	0.0075
FC A	12-17			0.048	0.181	1	0.0009	0.0007	2.9E-04	0.060	0.085	0.0066
FC A	17.5-27.5	0.01	0.10									
FC A	42.5-52.5	0.02	0.13	0.069	0.272	1	0.0014	0.0015	4.5E-04	0.075	0.111	0.0081
FC A	57.5-67.5	0.01	0.08	0.045	0.142	1	0.0004	0.0004	3.7E-04	0.055	0.069	0.0047

Table S3B (continued): Elemental abundances (molar ratios, normalized to silicon) in sediment samples.

sample description				*element*								
location[a]	depth (cm)	org C	tot C	Mg	Al	Si	P	S	Cl	K	Ca	Ti
FC B	0-4	0.02	0.12	0.054	0.155	1	0.0007	0.0007	3.6E-04	0.056	0.083	0.0058
FC B	0-8	0.01	0.10	0.047	0.111	1	0.0006	BDL	1.9E-04	0.045	0.090	0.0042
FC B	0-8	0.00	0.09	0.045	0.106	1	0.0007	0.0002	2.3E-04	0.045	0.087	0.0042
FC B	4-8	0.00	0.09									
FC B	8-12	0.01	0.10									
FC B	8-16	0.00	0.11									
FC B	8-16	0.00	0.10									
FC B	12-16	0.01	0.11									
FC B	16-20	BDL	0.09									
FC B	16-24	0.00	0.10	0.046	0.103	1	0.0004	BDL	3.4E-04	0.043	0.095	0.0038
FC B	16-24	0.00	0.12	0.048	0.113	1	0.0005	BDL	4.7E-04	0.045	0.102	0.0041
FC B	20-24	0.01	0.13									
FC B	24-28	0.00	0.11									
FC B	24-32	0.00	0.13									
FC B	24-32	0.00	0.18									
FC B	28-32	0.00	0.11									
FC B	32-36	0.00	0.10									
WC A	0-10		0.30									
WC A	0-10			0.066	0.153	1	0.0008	0.0011	3.1E-04	0.052	0.137	0.0049
WC A	0-12	0.02	0.20	0.057	0.112	1	0.0010	0.0001	1.8E-04	0.044	0.110	0.0040
WC A	0-14	0.03	0.16	0.051	0.095	1	0.0009	0.0004	2.2E-04	0.038	0.108	0.0035
WC B	0-8	0.01	0.13	0.054	0.102	1	0.0007	0.0002	1.5E-04	0.040	0.105	0.0038
WC B	0-8	0.01	0.14	0.058	0.119	1	0.0008	0.0001	1.5E-04	0.044	0.112	0.0047
WC C	0-8	0.06	0.22	0.089	0.363	1	0.0016	0.0044	1.1E-03	0.084	0.165	0.0101
WC C	0-10	0.05	0.26	0.083	0.344	1	0.0015	0.0020	7.6E-04	0.082	0.151	0.0102
WC C	4-6			0.089	0.394	1	0.0014	0.0034	3.9E-04	0.100	0.152	0.0117
WC C	10-12			0.085	0.379	1	0.0017	0.0051	4.9E-04	0.093	0.161	0.0113
WC C	20-22			0.044	0.109	1	0.0006	0.0035	7.0E-04	0.040	0.122	0.0037

Table S3B (continued): Elemental abundances (molar ratios, normalized to silicon) in sediment samples.

sample description				*element*								
location[a]	depth (cm)	org C	tot C	Mg	Al	Si	P	S	Cl	K	Ca	Ti
WC D	0-10	0.01	0.08									
WC D	0-10	0.01	0.12	0.049	0.092	1	0.0009	0.0002	2.6E-04	0.032	0.098	0.0037
WC D	0-11	0.01	0.14	0.047	0.082	1	0.0002	0.0000	1.3E-04	0.030	0.094	0.0032
WC D	30-44	0.00	0.08	0.034	0.035	1	0.0004	0.0002	1.9E-04	0.019	0.099	0.0018
WC E	0-4	BDL	0.09	0.042	0.060	1	BDL	0.0001	4.2E-04	0.029	0.081	0.0022
WC E	0-8			0.039	0.049	1	BDL	0.0001	2.2E-04	0.025	0.077	0.0020
WC E	0-8	0.00	0.08	0.042	0.058	1	0.0000	0.0001	1.9E-04	0.027	0.082	0.0023
WC E	4-8	0.00	0.07									
WC E	8-12	0.00	0.07									
WC E	8-16	0.01	0.10									
WC E	12-16	0.00	0.07									
WC E	16-20	0.00	0.09									
WC E	16-24			0.046	0.081	1	0.0004	0.0001	2.8E-04	0.035	0.087	0.0031
WC E	16-24	0.01	0.11	0.046	0.077	1	0.0003	0.0001	2.7E-04	0.035	0.086	0.0025
WC E	20-24	0.00	0.08									
WC E	24-28	0.00	0.09									
WC E	28-32	0.01	0.11									
TC A[c]	10-20	0.44	0.58	0.045	0.210	1	0.0030	0.0019	2.7E-04	0.052	0.114	0.0064
TC A	35-45	1.76	2.32	0.063	0.232	1	0.0051	0.0065	3.2E-04	0.056	0.204	0.0072
TC A	80-90	0.00	0.09	0.028	0.077	1	0.0004	BDL	1.7E-04	0.032	0.072	0.0023
TC A	123-133	0.74	1.73	0.055	0.222	1	0.0040	0.0047	2.6E-04	0.054	0.145	0.0075
TC A	165-175	0.00	0.08	0.033	0.088	1	0.0004	0.0001	2.3E-04	0.037	0.085	0.0023
TC A	187.5-197.5	0.07	0.15	0.039	0.120	1	0.0012	0.0032	3.3E-04	0.040	0.106	0.0028
TC A	205-215		0.08									
TC B[c]	7.5-17.5	0.03	0.10	0.040	0.125	1	0.0013	0.0007	2.0E-04	0.044	0.114	0.0035
TC B	33-43		0.05	0.019	0.052	1	0.0003	BDL	1.2E-04	0.023	0.050	0.0016
TC B	50-58		0.75	0.052	0.253	1	0.0049	0.0060	4.1E-04	0.054	0.149	0.0076
MC	0-8	0.04	0.02	0.022	0.061	1	BDL	0.0008	1.8E-04	0.036	0.022	0.0017

Table S3B (continued): Elemental abundances (molar ratios, normalized to silicon) in sediment samples.

sample description												
							element					
location[a]	depth (cm)	org C	tot C	Mg	Al	Si	P	S	Cl	K	Ca	Ti
SJ	0-5			0.039	0.173	1	0.0007	0.0008	1.0E-04	0.042	0.082	0.0055
SJ	0-6	0.02		0.030	0.135	1	0.0005	0.0007	1.7E-04	0.039	0.067	0.0043
SJ	0-8	0.00	0.04	0.025	0.100	1	0.0002	0.0012	6.9E-04	0.037	0.056	0.0037
SJ	10-15			0.036	0.147	1	0.0006	0.0004	1.5E-04	0.043	0.079	0.0047
SJ	20-25			0.026	0.116	1	0.0002	0.0003	8.1E-05	0.040	0.063	0.0036
SJ	30-35			0.024	0.102	1	0.0004	0.0001	8.8E-05	0.037	0.053	0.0034
NC A	0-12	BDL	0.01	0.014	0.037	1	0.0003	BDL	2.0E-04	0.029	0.018	0.0014
NC B	0-8	0.01	0.04	0.029	0.084	1	0.0001	0.0004	2.1E-04	0.039	0.042	0.0026
NC B	0-12	0.02	0.07	0.044	0.120	1	0.0009	0.0020	1.2E-04	0.046	0.060	0.0032
median crustal abundance[b]				0.095	0.304	1	0.0034	0.0011	4.1E-04	0.053	0.103	0.0118

sample description												
							element					
location[a]	depth (cm)	V	Cr	Mn	Fe	Ni	Cu	Zn	Ga	As	Se	Br
Lakebed Samples, March 2006												
245.0	0-5	4.2E-04	1.6E-04	0.0013	0.068	4.5E-05	5.5E-05	1.7E-04	3.0E-05	1.6E-05	BDL	6.5E-06
245.0	0-16	3.5E-04	1.8E-04	0.0014	0.069	4.7E-05	5.5E-05	1.8E-04	2.8E-05	1.7E-05	1.4E-06	8.2E-06
245.0	15-30	2.7E-04	1.4E-04	0.0012	0.059	4.4E-05	4.2E-05	1.5E-04	2.5E-05	1.5E-05	1.7E-06	7.0E-06
245.0	60-75	3.4E-04	1.6E-04	0.0012	0.064	4.3E-05	5.1E-05	1.6E-04	2.8E-05	1.7E-05	1.6E-06	5.1E-06
241.0	0-5	3.8E-04	1.6E-04	0.0011	0.070	5.1E-05	5.4E-05	1.8E-04	3.4E-05	1.7E-05	1.0E-06	7.7E-06
241.0	0-12.5	3.4E-04	2.0E-04	0.0012	0.067	4.1E-05	5.7E-05	1.8E-04	3.1E-05	1.5E-05	2.2E-06	7.7E-06
238.5	0-12.5	4.2E-04	1.4E-04	0.0011	0.071	4.4E-05	5.8E-05	1.8E-04	3.4E-05	1.7E-05	8.9E-07	4.7E-06
238.5	0-15	4.1E-04	1.5E-04	0.0011	0.073	5.0E-05	5.3E-05	1.8E-04	3.4E-05	1.6E-05	9.4E-07	4.9E-06
238.5	25-40	3.4E-04	1.3E-04	0.0013	0.055	3.9E-05	4.3E-05	1.6E-04	2.3E-05	1.3E-05	1.7E-06	4.8E-06
238.5	40-50	2.9E-04	7.8E-05	0.0013	0.052	3.9E-05	3.7E-05	1.4E-04	2.0E-05	1.3E-05	1.1E-06	4.6E-06
235.5	0-15	4.5E-04	1.3E-04	0.0010	0.064	4.3E-05	4.5E-05	1.7E-04	2.8E-05	1.2E-05	1.4E-06	4.2E-06
235.5	0-15	4.3E-04	1.5E-04	0.0012	0.072	4.9E-05	5.0E-05	1.9E-04	3.2E-05	1.6E-05	1.3E-06	4.7E-06
235.5	25-40	3.8E-04	1.6E-04	0.0012	0.063	4.6E-05	4.6E-05	1.8E-04	2.9E-05	1.4E-05	1.6E-06	5.6E-06
168.0	5-15	4.1E-04	1.5E-04	0.0008	0.058	4.9E-05	4.1E-05	1.7E-04	3.1E-05	1.1E-05	1.9E-06	4.6E-06

Table S3B (continued): Elemental abundances (molar ratios, normalized to silicon) in sediment samples.

sample description		*element*										
location[a]	depth (cm)	V	Cr	Mn	Fe	Ni	Cu	Zn	Ga	As	Se	Br
Lakebed Samples, May 2006												
241.0	5-15	1.3E-04	6.7E-05	0.0009	0.036	3.3E-05	3.3E-05	9.8E-05	1.6E-05	8.0E-06	BDL	3.8E-06
238.5	0-5	3.9E-04	1.6E-04	0.0013	0.067	5.0E-05	5.7E-05	1.8E-04	3.0E-05	1.4E-05	9.3E-07	7.5E-06
193.0	0-15	4.1E-04	1.3E-04	0.0012	0.071	5.1E-05	5.1E-05	1.9E-04	2.9E-05	1.7E-05	9.4E-07	4.9E-06
Delta Shoreline Samples												
249.5	-132 to -122	2.4E-04	1.3E-04	0.0010	0.046	3.3E-05	3.9E-05	1.2E-04	2.1E-05	1.1E-05	1.1E-06	2.7E-06
249.5	-102 to -94	3.9E-05	BDL	0.0003	0.011	5.0E-06	8.0E-06	2.7E-05	7.4E-06	2.8E-06	BDL	9.2E-07
249.5	-94 to -87	7.3E-05	BDL	0.0004	0.015	6.1E-06	6.4E-06	4.0E-05	6.4E-06	3.4E-06	BDL	5.5E-07
249.5	-77 to -67	4.6E-05	2.3E-04	0.0004	0.015	6.0E-06	1.1E-05	3.5E-05	6.7E-06	5.8E-06	5.6E-07	1.3E-06
249.5	-57 to -47	5.6E-05	BDL	0.0004	0.013	BDL	8.5E-06	3.4E-05	7.3E-06	5.2E-06	BDL	5.6E-07
249.5	-47 to -37	4.0E-04	1.4E-04	0.0013	0.067	5.0E-05	4.6E-05	1.9E-04	3.0E-05	1.3E-05	1.9E-06	3.6E-06
249.5	-12 to -2	3.9E-04	1.7E-04	0.0012	0.067	4.7E-05	5.3E-05	1.9E-04	2.8E-05	1.3E-05	1.3E-06	4.3E-06
249.5	14 to 20	3.5E-04	1.2E-04	0.0011	0.060	4.2E-05	5.2E-05	1.6E-04	2.7E-05	1.3E-05	2.1E-06	3.8E-06
247.5 A	0-8	BDL	BDL	0.0004	0.012	6.6E-06	7.8E-06	3.0E-05	6.9E-06	3.2E-06	BDL	7.2E-07
247.5 B	0-8	3.0E-05	BDL	0.0004	0.013	7.1E-06	1.1E-05	3.5E-05	9.5E-06	4.0E-06	BDL	7.6E-07
247.5 B	0-10	6.3E-05	BDL	0.0004	0.013	1.1E-05	8.6E-06	3.0E-05	7.5E-06	2.9E-06	BDL	1.2E-06
247.5 C	0-8	3.1E-04	1.2E-04	0.0010	0.048	4.7E-05	3.3E-04	2.4E-04	2.1E-05	1.7E-05	1.9E-06	6.4E-06
247.5 C	0-16	2.5E-04	BDL	0.0010	0.042	3.3E-05	4.4E-05	1.3E-04	1.8E-05	1.1E-05	1.5E-06	7.4E-06
247.5 C	14-24	1.5E-04	5.4E-05	0.0007	0.031	2.8E-05	4.0E-04	2.3E-04	1.3E-05	6.5E-06	1.3E-06	3.6E-06

Table S3B (continued): Elemental abundances (molar ratios, normalized to silicon) in sediment samples.

sample description		*element*										
location[a]	depth (cm)	V	Cr	Mn	Fe	Ni	Cu	Zn	Ga	As	Se	Br
Side Canyon Samples												
DD[c]	0-10	6.5E-05	4.9E-04	0.0006	0.021	8.8E-06	2.1E-05	3.1E-05	1.0E-05	4.8E-06	9.4E-07	1.2E-06
DD	20-30	1.1E-04	9.3E-05	0.0008	0.026	1.7E-05	2.7E-05	5.5E-05	1.1E-05	6.3E-06	BDL	2.2E-06
DD	47-57	7.9E-05	1.3E-03	0.0005	0.019	1.4E-05	1.7E-05	2.2E-05	5.3E-06	5.1E-06	BDL	1.8E-06
DD	57-67	8.8E-05	8.9E-04	0.0007	0.030	2.1E-05	2.2E-05	5.3E-05	1.4E-05	6.4E-06	6.4E-07	2.5E-06
DD	77-87	1.5E-04	1.4E-04	0.0011	0.044	3.2E-05	3.3E-05	9.7E-05	1.8E-05	9.7E-06	1.0E-06	1.3E-06
DD	102-122	2.1E-04	2.3E-04	0.0008	0.033	1.5E-05	2.5E-05	6.5E-05	1.4E-05	5.9E-06	BDL	2.0E-06
DD	180-190	3.0E-04	2.0E-04	0.0010	0.065	3.8E-05	4.0E-05	1.6E-04	2.5E-05	1.1E-05	2.1E-06	2.4E-06
FC A	0-12	8.4E-05	3.4E-04	0.0006	0.030	2.0E-05	1.8E-05	4.1E-05	1.3E-05	3.8E-06	9.0E-07	1.3E-06
FC A	12-17	BDL	3.6E-04	0.0005	0.025	1.5E-05	1.6E-05	3.2E-05	1.3E-05	5.3E-06	7.4E-07	1.0E-06
FC A	42.5-52.5	1.2E-04	9.2E-04	0.0007	0.040	3.2E-05	2.4E-05	5.4E-05	1.4E-05	6.5E-06	BDL	1.7E-06
FC A	57.5-67.5	BDL	6.0E-05	0.0004	0.016	1.3E-05	9.5E-06	2.7E-05	6.6E-06	4.0E-06	BDL	7.8E-07
FC B	0-4	4.6E-05	1.2E-04	0.0005	0.020	1.8E-05	1.1E-05	2.9E-05	1.1E-05	6.0E-06	BDL	9.0E-07
FC B	0-8	BDL	4.1E-05	0.0005	0.015	1.1E-05	8.7E-06	2.1E-05	6.2E-06	3.4E-06	BDL	6.6E-07
FC B	0-8	4.3E-05	3.6E-05	0.0005	0.014	1.1E-05	9.2E-06	2.0E-05	6.1E-06	3.7E-06	6.6E-07	7.5E-07
FC B	16-24	BDL	6.4E-05	0.0005	0.014	9.8E-06	1.2E-05	1.9E-05	6.1E-06	2.7E-06	BDL	5.5E-07
FC B	16-24	BDL	BDL	0.0005	0.014	8.7E-06	1.1E-05	2.1E-05	6.3E-06	4.6E-06	BDL	6.7E-07
WC A	0-10	9.2E-05	6.9E-05	0.0007	0.021	1.7E-05	2.1E-04	1.1E-04	7.7E-06	6.0E-06	BDL	2.1E-06
WC A	0-12	BDL	BDL	0.0005	0.013	9.2E-06	1.9E-05	2.1E-05	5.8E-06	2.0E-06	5.8E-07	6.9E-07
WC A	0-14	BDL	BDL	0.0005	0.012	7.7E-06	1.9E-05	2.2E-05	6.1E-06	1.8E-06	BDL	1.6E-06
WC B	0-8	BDL	BDL	0.0005	0.013	9.2E-06	1.8E-05	2.1E-05	5.1E-06	2.4E-06	BDL	1.5E-06
WC B	0-8	BDL	5.9E-05	0.0006	0.016	1.5E-05	1.9E-05	2.5E-05	9.2E-06	3.6E-06	BDL	1.3E-06

Table S3B (continued): Elemental abundances (molar ratios, normalized to silicon) in sediment samples.

sample description		*element*										
location[a]	depth (cm)	V	Cr	Mn	Fe	Ni	Cu	Zn	Ga	As	Se	Br
WC C	0-8	2.0E-04	1.3E-04	0.0011	0.062	5.1E-05	6.4E-05	1.1E-04	2.7E-05	1.6E-05	8.1E-07	4.7E-06
WC C	0-10	2.2E-04	2.0E-04	0.0011	0.059	4.6E-05	5.9E-05	8.6E-05	2.6E-05	1.1E-05	1.0E-06	3.5E-06
WC C	4-6	2.5E-04	2.0E-04	0.0014	0.084	5.8E-05	7.3E-05	1.3E-04	3.8E-05	1.7E-05	BDL	2.8E-06
WC C	10-12	3.9E-04	1.2E-04	0.0012	0.088	7.0E-05	8.8E-05	1.6E-04	3.5E-05	2.1E-05	1.8E-06	6.5E-06
WC C	20-22	BDL	5.5E-05	0.0005	0.015	9.4E-06	2.1E-05	1.7E-05	2.9E-06	9.7E-07	BDL	1.1E-06
WC D	0-10	4.0E-05	4.6E-05	0.0005	0.013	5.6E-06	9.7E-05	4.8E-05	4.4E-06	2.8E-06	4.5E-07	1.3E-06
WC D	0-11	BDL	BDL	0.0005	0.011	5.9E-06	1.6E-05	1.6E-05	3.7E-06	2.9E-06	BDL	1.1E-06
WC D	30-44	BDL	BDL	0.0004	0.008	2.8E-06	1.1E-04	4.2E-05	2.9E-06	2.9E-06	BDL	1.3E-06
WC E	0-4	BDL	BDL	0.0004	0.008	2.8E-06	1.4E-05	1.4E-05	4.3E-06	3.3E-06	5.2E-07	1.0E-06
WC E	0-8	BDL	BDL	0.0004	0.007	3.1E-06	1.1E-05	1.2E-05	2.7E-06	1.5E-06	BDL	6.2E-07
WC E	0-8	BDL	BDL	0.0004	0.008	5.7E-06	1.1E-05	1.3E-05	3.3E-06	2.4E-06	BDL	6.2E-07
WC E	16-24	BDL	BDL	0.0004	0.010	6.0E-06	1.5E-05	1.5E-05	4.6E-06	1.3E-06	4.4E-07	6.5E-07
WC E	16-24	BDL	BDL	0.0004	0.009	9.8E-06	1.1E-05	1.5E-05	4.6E-06	2.9E-06	4.4E-07	4.3E-07
TC A[c]	10-20	1.5E-04	6.7E-05	0.0011	0.032	2.0E-05	3.3E-05	9.0E-05	1.5E-05	7.7E-06	8.8E-07	2.8E-06
TC A	35-45	2.3E-04	1.1E-04	0.0021	0.043	2.5E-05	6.1E-05	1.2E-04	1.8E-05	1.1E-05	1.4E-06	1.7E-05
TC A	80-90	3.7E-05	2.4E-04	0.0003	0.010	5.6E-06	1.0E-05	1.4E-05	5.0E-06	7.1E-07	BDL	5.3E-07
TC A	123-133	2.1E-04	8.0E-05	0.0019	0.041	2.8E-05	5.5E-05	1.3E-04	1.7E-05	1.0E-05	1.3E-06	6.1E-06
TC A	165-175	3.7E-05	2.0E-04	0.0004	0.011	4.6E-06	1.1E-05	1.7E-05	3.2E-06	1.3E-06	BDL	BDL
TC A	187.5-197.5	9.1E-05	1.5E-04	0.0005	0.017	8.4E-06	1.7E-05	3.0E-05	7.2E-06	3.3E-06	9.1E-07	1.2E-06
TC B[c]	7.5-17.5	5.0E-05	7.7E-05	0.0005	0.015	8.7E-06	1.0E-05	2.5E-05	5.9E-06	2.4E-06	8.1E-07	1.4E-06
TC B	33-43	BDL	BDL	0.0003	0.006	BDL	6.4E-06	1.1E-05	3.2E-06	1.0E-06	3.9E-07	4.8E-07
TC B	50-58	2.5E-04	7.0E-05	0.0022	0.048	3.1E-05	7.1E-05	1.7E-04	2.2E-05	1.1E-05	1.7E-06	1.3E-05
MC	0-8	BDL	BDL	0.0002	0.005	2.2E-06	4.4E-06	8.3E-06	3.1E-06	BDL	BDL	9.5E-07

Table S3B (continued): Elemental abundances (molar ratios, normalized to silicon) in sediment samples.

sample description		*element*										
location[a]	depth (cm)	V	Cr	Mn	Fe	Ni	Cu	Zn	Ga	As	Se	Br
SJ	0-5	6.8E-05	6.3E-05	0.0007	0.024	1.3E-05	2.3E-05	6.5E-05	1.2E-05	3.4E-06	BDL	1.5E-06
SJ	0-6	6.8E-05	BDL	0.0005	0.017	9.8E-06	1.8E-05	4.8E-05	1.0E-05	1.1E-06	BDL	1.7E-06
SJ	0-8	3.4E-05	7.6E-05	0.0004	0.011	6.7E-06	1.1E-05	2.4E-05	5.5E-06	2.6E-06	BDL	8.2E-07
SJ	10-15	6.6E-05	1.2E-04	0.0005	0.018	5.6E-06	1.8E-05	3.5E-05	9.3E-06	3.4E-06	BDL	1.2E-06
SJ	20-25	BDL	BDL	0.0004	0.012	5.2E-06	1.1E-05	2.8E-05	6.0E-06	2.3E-06	BDL	BDL
SJ	30-35	BDL	1.2E-04	0.0004	0.011	5.6E-06	7.0E-06	2.4E-05	6.7E-06	1.4E-06	BDL	4.2E-07
NC A	0-12	BDL	BDL	0.0002	0.003	BDL	4.9E-06	5.8E-06	3.2E-06	BDL	4.7E-07	BDL
NC B	0-8	BDL	BDL	0.0003	0.007	4.5E-06	1.0E-05	1.7E-05	4.8E-06	8.3E-07	BDL	9.7E-07
NC B	0-12	BDL	BDL	0.0004	0.011	8.4E-06	1.4E-05	2.4E-05	6.8E-06	3.2E-06	4.0E-05	8.8E-07
median crustal abundance[b]		2.3E-05	2.0E-05	0.0017	0.100	1.4E-04	9.4E-05	1.1E-04	2.7E-05	2.4E-06	6.3E-08	3.0E-06

sample description		*element*									
location[a]	depth (cm)	Rb	Sr	Y	Zr	Ba	La	Ce	Pb	Th	U
Lakebed Samples, March 2006											
245.0	0-5	1.5E-04	3.7E-04	3.4E-05	BDL	4.1E-04	3.4E-05	7.8E-05	1.5E-05	7.4E-06	3.6E-06
245.0	0-16	1.6E-04	3.7E-04	3.3E-05	BDL	3.8E-04	4.0E-05	7.1E-05	1.5E-05	7.4E-06	2.1E-06
245.0	15-30	1.3E-04	3.3E-04	3.0E-05	BDL	3.9E-04	5.3E-05	6.7E-05	1.3E-05	5.5E-06	2.1E-06
245.0	60-75	1.5E-04	3.5E-04	3.5E-05	BDL	3.6E-04	4.4E-05	6.6E-05	1.3E-05	6.9E-06	1.8E-06
241.0	0-5	1.5E-04	3.4E-04	3.4E-05	BDL	4.0E-04	5.8E-05	1.0E-04	1.4E-05	7.2E-06	2.6E-06
241.0	0-12.5	1.5E-04	3.3E-04	3.4E-05	BDL	3.5E-04	3.0E-05	6.2E-05	1.5E-05	6.2E-06	2.8E-06
238.5	0-15	1.7E-04	3.3E-04	3.3E-05	BDL	3.8E-04	4.7E-05	1.2E-04	1.5E-05	8.1E-06	2.8E-06
238.5	0-12.5	1.7E-04	3.4E-04	3.3E-05	BDL	3.8E-04	5.1E-05	8.4E-05	1.6E-05	7.5E-06	2.8E-06
238.5	25-40	1.2E-04	3.4E-04	3.2E-05	BDL	4.4E-04	4.9E-05	1.0E-04	1.4E-05	6.3E-06	2.2E-06
238.5	40-50	1.2E-04	3.4E-04	3.1E-05	BDL	4.2E-04	5.7E-05	1.0E-04	1.3E-05	6.6E-06	3.2E-06
235.5	0-15	1.5E-04	2.9E-04	3.3E-05	BDL	3.2E-04	5.1E-05	8.6E-05	1.5E-05	7.0E-06	4.0E-06
235.5	0-15	1.7E-04	3.4E-04	3.4E-05	BDL	4.1E-04	4.7E-05	8.8E-05	1.6E-05	7.7E-06	3.2E-06
235.5	25-40	1.4E-04	3.2E-04	3.1E-05	BDL	3.9E-04	4.9E-05	9.0E-05	1.5E-05	6.9E-06	2.7E-06
168.0	5-15	1.6E-04	2.9E-04	3.2E-05	BDL	2.7E-04	4.3E-05	8.5E-05	1.2E-05	7.7E-06	2.9E-06

Table S3B (continued): Elemental abundances (molar ratios, normalized to silicon) in sediment samples.

sample description		*element*									
location[a]	depth (cm)	Rb	Sr	Y	Zr	Ba	La	Ce	Pb	Th	U
Lakebed Samples, May 2006											
241.0	5-15	9.8E-05	2.9E-04	2.5E-05	BDL	5.0E-04	5.6E-05	8.7E-05	1.1E-05	4.2E-06	1.6E-06
238.5	0-5	1.5E-04	3.5E-04	3.1E-05	BDL	3.9E-04	BDL	6.0E-05	1.5E-05	7.6E-06	2.0E-06
193.0	0-15	1.6E-04	3.4E-04	3.2E-05	BDL	4.0E-04	5.1E-05	9.1E-05	1.6E-05	7.8E-06	2.9E-06
Delta Shoreline Samples											
249.5	-132 to -122	1.1E-04	2.9E-04	3.0E-05	BDL	4.1E-04	5.3E-05	7.6E-05	1.0E-05	5.8E-06	2.5E-06
249.5	-102 to -94	4.2E-05	1.4E-04	1.4E-05	4.5E-04	3.2E-04	3.8E-05	5.5E-05	5.8E-06	1.6E-06	BDL
249.5	-94 to -87	4.9E-05	1.7E-04	1.5E-05	5.1E-04	3.6E-04	2.9E-05	4.0E-05	7.9E-06	1.6E-06	9.6E-07
249.5	-77 to -67	4.9E-05	1.6E-04	1.4E-05	4.9E-04	3.2E-04	3.5E-05	6.2E-05	7.1E-06	1.3E-06	1.0E-06
249.5	-57 to -47	4.8E-05	1.7E-04	1.1E-05	5.3E-04	3.6E-04	2.8E-05	6.2E-05	6.8E-06	1.5E-06	BDL
249.5	-47 to -37	1.6E-04	3.7E-04	3.4E-05	BDL	4.7E-04	7.0E-05	1.1E-04	1.6E-05	7.2E-06	3.2E-06
249.5	-12 to -2	1.6E-04	3.7E-04	3.7E-05	BDL	4.3E-04	5.1E-05	1.1E-04	1.6E-05	7.3E-06	3.9E-06
249.5	14 to 20	1.4E-04	3.3E-04	3.0E-05	BDL	4.0E-04	3.2E-05	7.4E-05	1.6E-05	6.1E-06	2.0E-06
247.5 A	0-8	4.7E-05	1.5E-04	1.5E-05	5.2E-04	3.2E-04	2.4E-05	5.6E-05	5.2E-06	1.8E-06	BDL
247.5 B	0-8	5.5E-05	1.8E-04	1.7E-05	5.1E-04	3.3E-04	2.8E-05	5.0E-05	5.5E-06	1.8E-06	BDL
247.5 B	0-10	5.3E-05	1.7E-04	1.9E-05	5.3E-04	3.4E-04	3.2E-05	4.3E-05	5.8E-06	1.6E-06	1.1E-06
247.5 C	0-8	1.1E-04	3.1E-04	3.0E-05	BDL	4.2E-04	3.9E-05	7.8E-05	1.9E-05	5.2E-06	1.4E-06
247.5 C	0-16	1.0E-04	2.9E-04	2.7E-05	5.8E-04	4.4E-04	4.0E-05	7.2E-05	1.2E-05	4.6E-06	1.4E-06
247.5 C	14-24	8.8E-05	2.7E-04	2.1E-05	BDL	4.6E-04	3.5E-05	6.2E-05	1.4E-05	3.4E-06	2.3E-06

Table S3B (continued): Elemental abundances (molar ratios, normalized to silicon) in sediment samples.

sample description		*element*									
location[a]	depth (cm)	Rb	Sr	Y	Zr	Ba	La	Ce	Pb	Th	U
Side Canyon Samples											
DD[c]	0-10	7.9E-05	2.3E-04	1.7E-05	BDL	4.7E-04	5.8E-05	8.7E-05	5.3E-06	2.3E-06	1.0E-06
DD	20-30	8.9E-05	2.8E-04	2.0E-05	BDL	4.3E-04	4.2E-05	5.5E-05	7.6E-06	2.7E-06	2.2E-06
DD	47-57	6.7E-05	1.7E-04	9.1E-06	BDL	4.2E-04	3.3E-05	7.2E-05	4.4E-06	2.2E-06	1.5E-06
DD	57-67	9.1E-05	2.7E-04	2.3E-05	6.9E-04	5.1E-04	7.0E-05	1.2E-04	7.8E-06	3.1E-06	2.0E-06
DD	77-87	1.1E-04	4.0E-04	3.1E-05	BDL	4.0E-04	4.7E-05	7.0E-05	1.1E-05	5.6E-06	2.1E-06
DD	102-122	1.0E-04	3.2E-04	2.1E-05	6.6E-04	4.3E-04	3.7E-05	5.8E-05	8.1E-06	3.4E-06	2.3E-06
DD	180-190	1.6E-04	4.2E-04	3.4E-05	BDL	3.5E-04	5.4E-05	1.4E-04	1.3E-05	7.5E-06	3.0E-06
FC A	0-12	8.9E-05	1.2E-04	2.5E-05	8.3E-04	3.4E-04	2.0E-05	5.7E-05	7.5E-06	3.0E-06	1.9E-06
FC A	12-17	8.0E-05	1.0E-04	2.2E-05	8.5E-04	3.8E-04	4.8E-05	1.0E-04	6.9E-06	2.8E-06	1.1E-06
FC A	42.5-52.5	1.0E-04	1.4E-04	2.4E-05	9.8E-04	3.9E-04	9.2E-05	1.2E-04	8.7E-06	3.8E-06	BDL
FC A	57.5-67.5	6.0E-05	7.3E-05	1.5E-05	5.3E-04	2.9E-04	5.8E-05	8.7E-05	5.7E-06	2.2E-06	BDL
FC B	0-4	6.4E-05	8.0E-05	2.2E-05	6.5E-04	2.7E-04	3.3E-05	7.2E-05	4.7E-06	2.3E-06	BDL
FC B	0-8	5.0E-05	6.7E-05	2.4E-05	6.6E-04	2.6E-04	2.2E-05	4.6E-05	5.1E-06	1.9E-06	BDL
FC B	0-8	4.8E-05	6.5E-05	2.2E-05	6.8E-04	2.7E-04	3.8E-05	6.2E-05	4.7E-06	2.0E-06	6.9E-07
FC B	16-24	4.7E-05	6.6E-05	1.8E-05	BDL	2.5E-04	4.5E-05	8.8E-05	5.4E-06	2.0E-06	BDL
FC B	16-24	5.0E-05	7.1E-05	1.8E-05	6.2E-04	2.5E-04	2.8E-05	4.9E-05	4.7E-06	2.2E-06	BDL
WC A	0-10	6.7E-05	1.3E-04	2.0E-05	5.6E-04	3.9E-04	7.6E-05	1.0E-04	1.5E-05	2.0E-06	1.3E-06
WC A	0-12	5.4E-05	9.7E-05	2.6E-05	6.7E-04	2.7E-04	2.5E-05	BDL	5.3E-06	1.7E-06	BDL
WC A	0-14	4.9E-05	8.9E-05	2.3E-05	6.9E-04	2.4E-04	2.6E-05	4.5E-05	4.5E-06	1.9E-06	BDL
WC B	0-8	4.9E-05	9.2E-05	1.9E-05	6.4E-04	2.7E-04	2.2E-05	4.5E-05	5.3E-06	1.8E-06	BDL
WC B	0-8	5.6E-05	1.0E-04	2.4E-05	6.9E-04	2.8E-04	3.9E-05	5.1E-05	5.1E-06	2.3E-06	1.0E-06

Table S3B (continued): Elemental abundances (molar ratios, normalized to silicon) in sediment samples.

sample description		*element*									
location[a]	depth (cm)	Rb	Sr	Y	Zr	Ba	La	Ce	Pb	Th	U
WC C	0-8	1.3E-04	2.8E-04	2.8E-05	BDL	3.5E-04	3.9E-05	7.3E-05	1.4E-05	5.6E-06	3.0E-06
WC C	0-10	1.2E-04	2.5E-04	3.2E-05	BDL	3.3E-04	2.9E-05	7.8E-05	1.2E-05	5.2E-06	3.0E-06
WC C	4-6	1.7E-04	3.2E-04	3.4E-05	BDL	4.1E-04	7.0E-05	8.2E-05	1.7E-05	7.1E-06	3.3E-06
WC C	10-12	1.9E-04	3.7E-04	3.4E-05	BDL	4.7E-04	5.2E-05	1.3E-04	1.9E-05	7.5E-06	3.2E-06
WC C	20-22	5.7E-05	1.1E-04	1.2E-05	7.4E-04	3.3E-04	7.1E-05	6.6E-05	5.3E-06	1.3E-06	BDL
WC D	0-10	3.9E-05	7.6E-05	2.4E-05	8.4E-04	2.3E-04	4.8E-05	7.0E-05	5.2E-06	2.2E-06	BDL
WC D	0-11	3.5E-05	7.2E-05	2.4E-05	5.5E-04	2.0E-04	BDL	3.7E-05	3.1E-06	1.9E-06	BDL
WC D	30-44	2.1E-05	6.6E-05	1.7E-05	6.0E-04	2.3E-04	4.6E-05	6.9E-05	3.2E-06	8.1E-07	BDL
WC E	0-4	3.3E-05	5.9E-05	1.2E-05	4.5E-04	2.1E-04	3.5E-05	5.1E-05	2.5E-06	1.1E-06	BDL
WC E	0-8	2.9E-05	5.6E-05	8.2E-06	4.6E-04	1.8E-04	1.9E-05	4.0E-05	2.9E-06	6.7E-07	BDL
WC E	0-8	3.1E-05	6.0E-05	9.6E-06	4.8E-04	1.8E-04	2.2E-05	3.5E-05	3.5E-06	1.2E-06	BDL
WC E	16-24	4.1E-05	7.3E-05	1.8E-05	6.5E-04	2.5E-04	3.6E-05	4.8E-05	4.4E-06	1.3E-06	BDL
WC E	16-24	4.2E-05	7.0E-05	1.4E-05	4.7E-04	2.4E-04	4.1E-05	6.0E-05	3.7E-06	1.7E-06	BDL
TC A[c]	10-20	1.0E-04	3.0E-04	2.3E-05	BDL	4.9E-04	4.0E-05	7.4E-05	1.2E-05	4.2E-06	2.2E-06
TC A	35-45	1.2E-04	4.3E-04	4.0E-05	BDL	6.1E-04	6.1E-05	1.1E-04	1.8E-05	5.3E-06	3.2E-06
TC A	80-90	5.2E-05	1.3E-04	7.7E-06	BDL	2.9E-04	3.2E-05	6.3E-05	4.9E-06	6.4E-07	8.5E-07
TC A	123-133	1.1E-04	3.2E-04	2.9E-05	BDL	5.3E-04	2.6E-05	8.8E-05	1.6E-05	5.2E-06	3.1E-06
TC A	165-175	6.0E-05	1.3E-04	8.5E-06	5.8E-04	3.5E-04	3.6E-05	4.9E-05	5.5E-06	1.3E-06	BDL
TC A	187.5-197.5	6.7E-05	2.2E-04	1.0E-05	BDL	4.6E-04	5.6E-05	8.0E-05	6.0E-06	1.7E-06	1.7E-06
TC B[c]	7.5-17.5	7.7E-05	1.7E-04	1.2E-05	BDL	4.2E-04	4.6E-05	7.4E-05	6.6E-06	1.5E-06	1.3E-06
TC B	33-43	2.7E-05	9.8E-05	1.0E-05	4.6E-04	2.1E-04	2.6E-05	3.3E-05	2.7E-06	5.6E-07	BDL
TC B	50-58	1.2E-04	4.6E-04	3.8E-05	BDL	6.1E-04	7.9E-05	1.1E-04	2.0E-05	6.2E-06	4.1E-06
MC	0-8	4.5E-05	5.0E-05	6.0E-06	BDL	2.1E-04	2.6E-05	3.5E-05	3.9E-06	1.0E-06	BDL

Table S3B (continued): Elemental abundances (molar ratios, normalized to silicon) in sediment samples.

sample description		*element*									
location[a]	depth (cm)	Rb	Sr	Y	Zr	Ba	La	Ce	Pb	Th	U
SJ	0-5	7.3E-05	1.9E-04	1.9E-05	4.6E-04	3.8E-04	4.2E-05	7.3E-05	8.6E-06	3.2E-06	8.5E-07
SJ	0-6	6.3E-05	1.5E-04	1.7E-05	5.4E-04	3.6E-04	3.1E-05	4.4E-05	7.8E-06	2.6E-06	BDL
SJ	0-8	5.6E-05	1.3E-04	1.4E-05	5.9E-04	3.8E-04	4.0E-05	6.7E-05	4.8E-06	1.9E-06	8.2E-07
SJ	10-15	7.0E-05	1.8E-04	1.8E-05	5.8E-04	3.9E-04	2.7E-05	6.9E-05	6.1E-06	3.1E-06	9.0E-07
SJ	20-25	6.0E-05	1.3E-04	1.3E-05	4.5E-04	3.5E-04	3.3E-05	5.8E-05	5.3E-06	2.0E-06	BDL
SJ	30-35	5.7E-05	1.2E-04	1.5E-05	6.8E-04	4.0E-04	4.4E-05	7.2E-05	5.2E-06	2.2E-06	BDL
NC A	0-12	3.7E-05	3.2E-05	1.8E-05	5.4E-04	1.8E-04	2.3E-05	4.6E-05	2.9E-06	3.8E-07	BDL
NC B	0-8	5.2E-05	5.3E-05	1.1E-05	4.7E-04	2.4E-04	2.6E-05	3.4E-05	4.5E-06	1.4E-06	BDL
NC B	0-12	6.3E-05	7.2E-05	1.8E-05	5.2E-04	2.9E-04	3.3E-05	4.3E-05	4.8E-06	1.6E-06	BDL
median crustal abundance[b]		1.0E-04	4.2E-04	3.7E-05	1.8E-04	1.0E-07	2.2E-06	3.0E-04	6.7E-06	4.1E-06	1.1E-06

[a] "Location" refers to distance from Glen Canyon Dam (in river km) for delta samples and to side canyon location.

[b] Median crustal abundance data from Lide (2007).

[c] For DD and TC side canyon samples only, depth refers to depth below the tops of sets of cores collected above the water line. the water line

Table S4A: Bulk mineral composition (%) of select sediment core sections.

sample description		*non-clay minerals*					
location[a]	depth (cm)	ordered Microcline feldspar	intermediate Microcline feldspar	Sanidine feldspar	Orthoclase feldspar	Albite feldspar (Cleavelandite)	Oligoclase feldspar
Lakebed Samples, March 2006							
245.0	0-16	0.5	2.9	0.5	1.7	1.2	1.2
245.0	60-75	0.0	3.8	0.9	2.1	1.5	1.4
241.2	0-5	0.0	2.9	0.3	2.3	1.5	0.7
238.7	0-12.5	0.4	2.2	0.7	1.6	0.0	1.7
238.7	40-50	0.4	4.9	1.4	2.8	2.8	1.2
235.4	0-15	0.4	1.2	0.9	2.3	1.1	0.8
235.4	25-40	0.0	3.9	0.2	2.8	1.5	1.7
168.0	5-15	0.6	2.7	0.5	0.8	0.8	0.2
Delta Shoreline Samples							
249.5	-132 to -122	2.0	4.2	2.4	1.6	2.4	1.5
249.5	-102 to -94	3.7	4.7	1.1	1.6	1.9	2.0
249.5	-94 to -87	5.6	6.3	1.0	3.1	2.4	3.0
249.5	-77 to -67	3.7	7.4	0.2	2.6	1.6	3.5
249.5	-57 to -47	3.8	6.1	1.0	1.7	2.0	2.7
249.5	-47 to -37	0.1	4.8	0.3	1.8	1.9	1.0
249.5	-12 to -2	0.0	4.9	0.6	1.4	1.8	0.9
249.5	14 to 20	0.0	4.6	0.4	1.8	1.5	0.9
Side Canyon Samples							
FC	0-8	3.7	4.6	2.8	0.6	0.0	0.0
FC	16-24	4.0	4.4	2.4	0.0	0.0	0.0
WC	0-8	2.6	4.0	1.8	0.2	0.0	0.0
WC	16-24	3.6	4.4	2.3	0.6	0.0	0.0
MC	0-8	5.1	7.2	1.4	1.0	0.0	0.0
NC	0-18	4.4	7.4	0.7	2.4	0.2	0.0

Table S4A (continued): Bulk mineral composition (%) of select sediment core sections.

sample description		*non-clay minerals*					
location[a]	depth (cm)	Labradorite feldspar	Calcite	Dolomite	Hematite	Goethite	Maghemite
Lakebed Samples, March 2006							
245.0	0-16	0.0	9.7	5.0	0.3	0.2	1.6
245.0	60-75	0.0	9.5	5.3	0.3	0.3	1.2
241.2	0-5	0.1	9.0	3.9	0.3	0.0	1.5
238.7	0-12.5	0.5	7.5	3.6	0.4	0.3	0.5
238.7	40-50	0.8	9.5	5.9	0.2	0.3	1.3
235.4	0-15	0.0	8.4	3.4	0.1	0.2	1.8
235.4	25-40	0.0	8.7	3.8	0.2	0.1	1.5
168.0	5-15	0.0	10.0	3.8	0.0	0.5	0.0
Delta Shoreline Samples							
249.5	-132 to -122	1.1	9.1	5.6	0.0	0.6	1.5
249.5	-102 to -94	2.8	3.0	1.7	0.2	0.3	0.4
249.5	-94 to -87	3.2	5.5	2.1	0.0	1.0	1.1
249.5	-77 to -67	2.2	5.4	2.1	0.0	0.6	0.0
249.5	-57 to -47	2.4	3.3	1.3	0.0	0.7	0.2
249.5	-47 to -37	1.2	8.3	4.3	0.4	0.2	0.0
249.5	-12 to -2	0.6	8.6	4.1	0.3	0.2	0.0
249.5	14 to 20	0.2	8.6	4.1	0.1	0.2	1.5
Side Canyon Samples							
FC	0-8	0.0	3.0	6.5	0.6	0.3	0.2
FC	16-24	0.0	4.1	7.4	0.6	0.2	0.0
WC	0-8	0.0	2.5	5.1	0.2	0.4	0.0
WC	16-24	0.0	2.8	6.5	0.2	0.3	0.3
MC	0-8	0.0	1.6	0.3	0.2	0.4	0.0
NC	0-18	0.0	0.8	1.0	0.0	0.4	0.0

Table S4A (continued): Bulk mineral composition (%) of select sediment core sections.

sample description		*non-clay minerals*		*clay minerals*			
location[a]	depth (cm)	Apatite	Quartz	disordered Kaolinite	Na-Smectite	Ca-smectite	Ferruginous smectite
Lakebed Samples, March 2006							
245.0	0-16	0.9	19.1	4.3	5.6	0.0	5.7
245.0	60-75	0.8	22.8	4.8	0.1	1.1	7.2
241.2	0-5	0.6	19.0	5.9	0.1	6.5	9.4
238.7	0-12.5	0.6	16.0	6.0	0.1	4.4	8.5
238.7	40-50	0.7	29.0	2.3	0.5	2.6	4.6
235.4	0-15	0.9	18.9	6.8	2.6	0.0	7.4
235.4	25-40	0.4	22.1	3.9	2.1	1.8	5.4
168.0	5-15	0.7	22.0	7.1	2.0	7.3	7.1
Delta Shoreline Samples							
249.5	-132 to -122	0.9	36.5	3.1	0.6	0.0	3.8
249.5	-102 to -94	0.5	73.1	0.5	2.6	0.0	0.0
249.5	-94 to -87	0.4	67.5	0.0	1.5	0.0	0.0
249.5	-77 to -67	0.7	59.4	1.3	2.7	0.0	0.9
249.5	-57 to -47	0.4	70.4	0.1	3.4	0.0	0.0
249.5	-47 to -37	0.2	23.9	3.8	1.4	2.4	6.0
249.5	-12 to -2	0.3	22.6	4.0	1.4	2.3	6.1
249.5	14 to 20	0.8	24.2	4.2	5.7	0.0	4.3
Side Canyon Samples							
FC	0-8	0.6	72.1	1.3	0.0	0.0	0.0
FC	16-24	0.2	72.3	1.5	0.0	0.0	0.0
WC	0-8	0.4	79.7	0.5	1.9	0.0	0.0
WC	16-24	0.4	71.7	1.1	1.8	0.0	0.0
MC	0-8	0.2	75.8	0.5	3.6	0.0	0.5
NC	0-18	0.3	75.9	0.1	1.2	0.0	0.7

Table S4A (continued): Bulk mineral composition (%) of select sediment core sections.

sample description		*clay minerals*					
location[a]	depth (cm)	Illite (1Md) + Dioct. Mica + Smectite)	Illite (1M)	Biotite (1M)	Phlogopite (2M1)	Fe-Chlorite (Tusc)	Mg-Chlorite (Clinochlore)
Lakebed Samples, March 2006							
245.0	0-16	16.1	7.7	0.0	1.5	2.3	2.1
245.0	60-75	13.4	11.2	0.7	0.0	1.5	2.8
241.2	0-5	17.2	7.6	0.9	0.1	2.3	2.9
238.7	0-12.5	9.5	12.3	0.8	0.9	2.3	0.9
238.7	40-50	7.0	9.9	1.2	0.0	3.1	3.3
235.4	0-15	22.7	5.5	0.0	1.5	1.8	0.6
235.4	25-40	19.7	8.1	0.3	0.0	4.1	2.2
168.0	5-15	10.5	9.6	0.0	1.4	2.1	0.0
Delta Shoreline Samples							
249.5	-132 to -122	13.9	7.0	0.7	0.6	2.7	1.1
249.5	-102 to -94	0.0	4.4	0.0	1.2	0.9	0.4
249.5	-94 to -87	0.0	8.1	1.6	0.0	2.8	1.3
249.5	-77 to -67	0.0	5.1	1.4	0.7	0.9	0.3
249.5	-57 to -47	0.0	5.0	1.2	0.0	0.9	1.9
249.5	-47 to -37	10.2	12.6	1.0	0.0	2.3	2.1
249.5	-12 to -2	10.5	12.8	0.9	0.0	2.4	2.4
249.5	14 to 20	16.1	8.9	0.2	0.4	2.3	4.3
Side Canyon Samples							
FC	0-8	1.2	7.4	0.0	0.3	1.0	1.6
FC	16-24	1.5	4.2	0.0	0.8	0.0	0.0
WC	0-8	0.0	3.9	0.0	1.3	0.7	0.3
WC	16-24	0.7	4.8	0.0	0.3	0.7	1.1
MC	0-8	0.0	3.2	0.0	1.2	1.0	0.0
NC	0-18	1.1	4.4	0.6	0.3	0.7	2.3

Table S4A (continued): Bulk mineral composition (%) of select sediment core sections.

sample description		*clay mineral*	*totals*		
location[a]	depth (cm)	Muscovite (2M1)	Total non-clays	Total clays	Total
Lakebed Samples, March 2006					
245.0	0-16	5.7	44.7	51.0	95.7
245.0	60-75	6.9	49.9	49.6	99.5
241.2	0-5	6.9	42.1	59.6	101.7
238.7	0-12.5	7.1	36.1	52.7	88.8
238.7	40-50	3.6	61.2	38.1	99.3
235.4	0-15	7.8	40.3	56.7	97.0
235.4	25-40	5.3	46.8	52.9	99.8
168.0	5-15	5.7	42.5	52.7	95.2
Delta Shoreline Samples					
249.5	-132 to -122	4.5	69.4	38.1	107.5
249.5	-102 to -94	0.0	96.8	10.0	106.9
249.5	-94 to -87	0.0	102.2	15.2	117.4
249.5	-77 to -67	0.0	89.4	13.3	102.6
249.5	-57 to -47	0.0	95.9	12.6	108.5
249.5	-47 to -37	4.1	48.5	45.9	94.4
249.5	-12 to -2	4.3	46.4	47.2	93.5
249.5	14 to 20	5.6	48.7	51.9	100.6
Side Canyon Samples					
FC	0-8	0.5	94.9	13.1	108.0
FC	16-24	1.4	95.5	9.3	104.9
WC	0-8	0.0	96.9	8.7	105.6
WC	16-24	1.0	93.2	11.6	104.8
MC	0-8	0.0	93.3	10.1	103.4
NC	0-18	0.0	93.4	11.4	104.8

[a] "Location" refers to distance from Glen Canyon Dam (in river km) for delta samples and to side canyon location (see Table 1).

Table S4B: Bulk mineral composition (molar ratios, normalized to silica) of select sediment core sections.

sample description		*non-clay minerals*					
location[a]	depth (cm)	ordered Microcline feldspar	intermediate Microcline feldspar	Sanidine feldspar	Orthoclase feldspar	Albite feldspar (Cleavelandite)	Oligoclase feldspar
Lakebed Samples, March 2006							
245.0	0-16	0.006	0.032	0.006	0.019	0.014	0.014
245.0	60-75	0.000	0.036	0.009	0.020	0.015	0.014
241.2	0-5	0.000	0.033	0.003	0.026	0.018	0.008
238.7	0-12.5	0.006	0.030	0.010	0.021	0.000	0.024
238.7	40-50	0.003	0.036	0.011	0.021	0.022	0.010
235.4	0-15	0.004	0.014	0.011	0.026	0.014	0.010
235.4	25-40	0.000	0.038	0.002	0.028	0.015	0.017
168.0	5-15	0.006	0.026	0.005	0.008	0.008	0.002
Delta Shoreline Samples							
249.5	-132 to -122	0.012	0.025	0.014	0.009	0.015	0.010
249.5	-102 to -94	0.011	0.014	0.003	0.005	0.006	0.006
249.5	-94 to -87	0.018	0.020	0.003	0.010	0.008	0.010
249.5	-77 to -67	0.013	0.027	0.001	0.009	0.006	0.013
249.5	-57 to -47	0.012	0.019	0.003	0.005	0.006	0.009
249.5	-47 to -37	0.000	0.043	0.003	0.016	0.018	0.010
249.5	-12 to -2	0.000	0.046	0.006	0.014	0.018	0.009
249.5	14 to -20	0.000	0.041	0.003	0.016	0.015	0.008
Side Canyon Samples							
FC	0-8	0.011	0.014	0.009	0.002	0.000	0.000
FC	16-24	0.012	0.013	0.007	0.000	0.000	0.000
WC	0-8	0.007	0.011	0.005	0.001	0.000	0.000
WC	16-24	0.011	0.013	0.007	0.002	0.000	0.000
MC	0-8	0.015	0.021	0.004	0.003	0.000	0.000
NC	0-18	0.013	0.021	0.002	0.007	0.001	0.000

Table S4B (continued): Bulk mineral composition (molar ratio, normalized to silica) of select sediment core sections.

sample description		*non-clay minerals*					
location[a]	depth (cm)	Labradorite feldspar	Calcite	Dolomite	Hematite	Goethite	Maghemite
Lakebed Samples, March 2006							
245.0	0-16	0.0000	0.305	0.086	0.0054	0.0072	0.032
245.0	60-75	0.0000	0.250	0.076	0.0041	0.0086	0.021
241.2	0-5	0.0011	0.285	0.067	0.0059	0.0013	0.031
238.7	0-12.5	0.0070	0.283	0.073	0.0091	0.0126	0.012
238.7	40-50	0.0059	0.198	0.067	0.0022	0.0076	0.018
235.4	0-15	0.0000	0.266	0.058	0.0023	0.0073	0.035
235.4	25-40	0.0000	0.237	0.056	0.0028	0.0028	0.025
168.0	5-15	0.0000	0.272	0.056	0.0000	0.0160	0.000
Delta Shoreline Samples							
249.5	-132 to -122	0.0065	0.149	0.050	0.0001	0.0109	0.016
249.5	-102 to -94	0.0086	0.024	0.008	0.0008	0.0032	0.002
249.5	-94 to -87	0.0105	0.049	0.010	0.0000	0.0100	0.006
249.5	-77 to -67	0.0083	0.055	0.011	0.0001	0.0071	0.000
249.5	-57 to -47	0.0076	0.028	0.006	0.0000	0.0067	0.001
249.5	-47 to -37	0.0108	0.209	0.059	0.0066	0.0054	0.000
249.5	-12 to -2	0.0062	0.229	0.059	0.0048	0.0055	0.000
249.5	14 to -20	0.0017	0.214	0.055	0.0015	0.0056	0.023
Side Canyon Samples							
FC	0-8	0.0000	0.025	0.029	0.0030	0.0027	0.001
FC	16-24	0.0000	0.034	0.033	0.0032	0.0020	0.000
WC	0-8	0.0000	0.019	0.021	0.0008	0.0030	0.000
WC	16-24	0.0001	0.024	0.030	0.0012	0.0029	0.002
MC	0-8	0.0000	0.013	0.001	0.0011	0.0039	0.000
NC	0-18	0.0000	0.006	0.004	0.0000	0.0032	0.000

Table S4B (continued): Bulk mineral composition (molar ratio, normalized to silica) of select sediment core sections.

sample description		*non-clay minerals*		*clay minerals*			
location[a]	depth (cm)	Apatite	Quartz	disordered Kaolinite	Na-Smectite	Ca-smectite	Ferruginous smectite
Lakebed Samples, March 2006							
245.0	0-16	0.0054	1	0.052	0.0479	0.000	0.046
245.0	60-75	0.0043	1	0.049	0.0007	0.008	0.049
241.2	0-5	0.0035	1	0.072	0.0010	0.055	0.076
238.7	0-12.5	0.0047	1	0.088	0.0009	0.045	0.083
238.7	40-50	0.0027	1	0.018	0.0026	0.014	0.025
235.4	0-15	0.0055	1	0.084	0.0230	0.000	0.061
235.4	25-40	0.0022	1	0.042	0.0155	0.013	0.038
168.0	5-15	0.0037	1	0.075	0.0150	0.054	0.050
Delta Shoreline Samples							
249.5	-132 to -122	0.0030	1	0.020	0.0027	0.000	0.016
249.5	-102 to -94	0.0007	1	0.002	0.0059	0.000	0.000
249.5	-94 to -87	0.0007	1	0.000	0.0036	0.000	0.000
249.5	-77 to -67	0.0013	1	0.005	0.0074	0.000	0.002
249.5	-57 to -47	0.0007	1	0.000	0.0079	0.000	0.000
249.5	-47 to -37	0.0012	1	0.037	0.0099	0.016	0.039
249.5	-12 to -2	0.0016	1	0.042	0.0098	0.016	0.042
249.5	14 to -20	0.0040	1	0.040	0.0385	0.000	0.028
Side Canyon Samples							
FC	0-8	0.0010	1	0.004	0.0000	0.000	0.000
FC	16-24	0.0003	1	0.005	0.0000	0.000	0.000
WC	0-8	0.0006	1	0.002	0.0040	0.000	0.000
WC	16-24	0.0006	1	0.004	0.0041	0.000	0.000
MC	0-8	0.0003	1	0.002	0.0079	0.000	0.001
NC	0-18	0.0005	1	0.000	0.0027	0.000	0.001

Table S4B (continued): Bulk mineral composition (molar ratio, normalized to silica) of select sediment core sections.

sample description		*clay minerals*					
location[a]	depth (cm)	1Md illite (+dioct mica & smectite)	1M illite (R>1, 70-80%I)	Biotite (1M)	Phlogopite (2M1)	Fe-Chlorite (Tusc)	Mg-Chlorite (Clinochlore)
Lakebed Samples, March 2006							
245.0	0-16	0.128	0.061	0.0000	0.011	0.010	0.012
245.0	60-75	0.089	0.074	0.0038	0.000	0.005	0.013
241.2	0-5	0.137	0.060	0.0061	0.001	0.010	0.016
238.7	0-12.5	0.089	0.116	0.0061	0.008	0.012	0.006
238.7	40-50	0.037	0.052	0.0054	0.000	0.009	0.012
235.4	0-15	0.181	0.044	0.0000	0.012	0.008	0.003
235.4	25-40	0.135	0.056	0.0019	0.000	0.015	0.011
168.0	5-15	0.072	0.066	0.0000	0.009	0.008	0.000
Delta Shoreline Samples							
249.5	-132 to -122	0.058	0.029	0.0025	0.002	0.006	0.003
249.5	-102 to -94	0.000	0.009	0.0000	0.002	0.001	0.001
249.5	-94 to -87	0.000	0.018	0.0030	0.000	0.003	0.002
249.5	-77 to -67	0.000	0.013	0.0030	0.002	0.001	0.001
249.5	-57 to -47	0.000	0.011	0.0023	0.000	0.001	0.003
249.5	-47 to -37	0.064	0.079	0.0052	0.000	0.008	0.010
249.5	-12 to -2	0.070	0.085	0.0054	0.000	0.008	0.012
249.5	14 to -20	0.100	0.055	0.0008	0.002	0.008	0.019
Side Canyon Samples							
FC	0-8	0.002	0.015	0.0000	0.001	0.001	0.002
FC	16-24	0.003	0.009	0.0000	0.002	0.000	0.000
WC	0-8	0.000	0.007	0.0000	0.002	0.001	0.000
WC	16-24	0.001	0.010	0.0000	0.001	0.001	0.002
MC	0-8	0.000	0.006	0.0000	0.002	0.001	0.000
NC	0-18	0.002	0.009	0.0010	0.001	0.001	0.003

Table S4B (continued): Bulk mineral composition (molar ratio, normalized to silica) of select sediment core sections.

sample description		*clay mineral*	*totals*	
location[a]	depth (cm)	Muscovite (2M1)	Total non-clays	Total clays
Lakebed Samples, March 2006				
245.0	0-16	0.045	1.532	0.413
245.0	60-75	0.045	1.457	0.337
241.2	0-5	0.055	1.483	0.489
238.7	0-12.5	0.067	1.494	0.521
238.7	40-50	0.019	1.402	0.193
235.4	0-15	0.062	1.454	0.477
235.4	25-40	0.036	1.427	0.362
168.0	5-15	0.039	1.404	0.388
Delta Shoreline Samples				
249.5	-132 to -122	0.019	1.321	0.158
249.5	-102 to -94	0.000	1.092	0.021
249.5	-94 to -87	0.000	1.156	0.030
249.5	-77 to -67	0.000	1.152	0.034
249.5	-57 to -47	0.000	1.103	0.025
249.5	-47 to -37	0.026	1.383	0.294
249.5	-12 to -2	0.029	1.400	0.320
249.5	14 to -20	0.035	1.387	0.328
Side Canyon Samples				
FC	0-8	0.001	1.097	0.027
FC	16-24	0.003	1.105	0.021
WC	0-8	0.000	1.068	0.016
WC	16-24	0.002	1.093	0.025
MC	0-8	0.000	1.061	0.020
NC	0-18	0.000	1.057	0.021

[a] "Location" refers to distance from Glen Canyon Dam (in river km) for delta samples and to side canyon location (see Table 1).

Table S5A: Correlation significance thresholds.

number of samples in each correlation analysis[a]

	size parameters	organic C	total C	elements	minerals
particle size parameters	52	48	45	50	22
organic carbon			73	55	19
total carbon				55	18
elements				71	22
minerals					22

significance thresholds ($2\sigma = 2/\sqrt{n}$)

	size parameters	organic C	total C	elements	minerals
particle size parameters	0.277	0.289	0.298	0.283	0.426
organic carbon			0.234	0.270	0.459
total carbon				0.270	0.471
elements				0.237	0.426
minerals					0.426

high significance thresholds ($4\sigma = 4/\sqrt{n}$)

	size parameters	organic C	total C	elements	minerals
particle size parameters	0.555	0.577	0.596	0.566	0.853
organic carbon			0.468	0.539	0.918
total carbon				0.539	0.943
elements				0.475	0.853
minerals					0.853

[a] This analysis does not include samples from WC C, TC A, or TC B, which contained visible plant debris.

Table S5B: Correlation coefficients derived from elemental concentrations expressed as mass percentages[a].

	median	log (median)	mean	log (mean)	mode	log (mode)	organic C	total C	Mg	Al
median	1	**0.845**	**0.996**	**0.843**	**0.965**	**0.771**	**-0.692**	**-0.531**	**-0.771**	**-0.780**
log (median)		1	**0.835**	**0.986**	**0.838**	**0.944**	**-0.900**	**-0.708**	**-0.834**	**-0.935**
mean			1	**0.846**	**0.979**	**0.782**	**-0.680**	**-0.519**	**-0.749**	**-0.759**
log (mean)				1	**0.872**	**0.981**	**-0.878**	**-0.697**	**-0.811**	**-0.905**
mode					1	**0.837**	**-0.689**	**-0.534**	**-0.736**	**-0.728**
log (mode)						1	**-0.832**	**-0.687**	**-0.745**	**-0.846**
organic C							1	**0.659**	**0.730**	**0.821**
total C								1	**0.458**	**0.523**
Mg									1	**0.785**
Al										1

[a] Significant correlations (≥ 2σ from 0) are in bold text; highly significant correlations (≥ 4σ from 0) are in bold and red text.

Table S5B: Correlation coefficients derived from elemental concentrations expressed as mass percentages (continued).

	Si	P	S	Cl	K	Ca	Ti	V	Cr	Mn	Fe	Ni
median	**0.687**	**-0.610**	**-0.450**	-0.167	**-0.764**	**-0.504**	**-0.841**	**-0.657**	**-0.322**	**-0.697**	**-0.724**	**-0.808**
log (median)	**0.871**	**-0.846**	**-0.489**	-0.037	**-0.635**	**-0.676**	**-0.936**	**-0.937**	**-0.336**	**-0.890**	**-0.962**	**-0.890**
mean	**0.668**	**-0.598**	**-0.430**	-0.142	**-0.745**	**-0.477**	**-0.820**	**-0.647**	**-0.329**	**-0.675**	**-0.706**	**-0.779**
log (mean)	**0.838**	**-0.822**	**-0.455**	-0.006	**-0.621**	**-0.636**	**-0.914**	**-0.918**	**-0.346**	**-0.859**	**-0.933**	**-0.850**
mode	**0.654**	**-0.608**	**-0.371**	-0.051	**-0.683**	**-0.472**	**-0.799**	**-0.660**	**-0.313**	**-0.669**	**-0.698**	**-0.741**
log (mode)	**0.772**	**-0.778**	**-0.386**	0.043	**-0.555**	**-0.571**	**-0.847**	**-0.891**	**-0.316**	**-0.793**	**-0.885**	**-0.781**
organic C	**-0.746**	**0.863**	**0.523**	0.083	**0.440**	**0.678**	**0.812**	**0.864**	0.257	**0.873**	**0.883**	**0.802**
total C	**-0.628**	**0.648**	**0.331**	-0.014	0.180	**0.503**	**0.537**	**0.600**	0.153	**0.710**	**0.611**	**0.556**
Mg	**-0.479**	**0.610**	**0.328**	0.122	**0.638**	**0.783**	**0.839**	**0.703**	0.031	**0.750**	**0.776**	**0.797**
Al	**-0.615**	**0.740**	**0.503**	0.082	**0.796**	**0.568**	**0.971**	**0.888**	0.127	**0.830**	**0.955**	**0.887**
Si	1	**-0.685**	**-0.673**	-0.224	**-0.281**	**-0.607**	**-0.633**	**-0.661**	**-0.499**	**-0.645**	**-0.708**	**-0.674**
P		1	**0.539**	0.109	**0.337**	**0.714**	**0.712**	**0.824**	0.162	**0.844**	**0.784**	**0.709**
S			1	**0.361**	**0.338**	**0.381**	**0.498**	**0.453**	**0.268**	**0.487**	**0.498**	**0.510**
Cl				1	0.104	0.235	0.120	0.017	**0.456**	0.057	0.081	0.106
K					1	0.231	**0.797**	**0.504**	0.042	**0.501**	**0.651**	**0.697**
Ca						1	**0.628**	**0.618**	0.123	**0.712**	**0.640**	**0.626**
Ti							1	**0.850**	0.162	**0.844**	**0.936**	**0.889**
V								1	0.145	**0.833**	**0.952**	**0.812**
Cr									1	0.042	0.165	0.223
Mn										1	**0.870**	**0.762**
Fe											1	**0.885**
Ni												1

Table S5B: Correlation coefficients derived from elemental concentrations expressed as mass percentages (continued).

	Cu	Zn	Ga	As	Se	Br	Rb	Sr	Y	Zr	Ba
median	-0.126	**-0.653**	**-0.715**	**-0.607**	**-0.492**	**-0.627**	**-0.774**	**-0.541**	**-0.674**	**0.604**	0.054
log (median)	**-0.498**	**-0.942**	**-0.953**	**-0.880**	**-0.678**	**-0.850**	**-0.975**	**-0.815**	**-0.778**	**0.829**	0.037
mean	-0.092	**-0.639**	**-0.699**	**-0.585**	**-0.482**	**-0.612**	**-0.764**	**-0.529**	**-0.660**	**0.584**	0.045
log (mean)	**-0.453**	**-0.917**	**-0.924**	**-0.840**	**-0.650**	**-0.828**	**-0.958**	**-0.783**	**-0.770**	**0.787**	0.027
mode	-0.111	**-0.652**	**-0.689**	**-0.569**	**-0.465**	**-0.612**	**-0.762**	**-0.520**	**-0.685**	**0.569**	0.048
log (mode)	**-0.431**	**-0.883**	**-0.883**	**-0.782**	**-0.623**	**-0.776**	**-0.920**	**-0.730**	**-0.743**	**0.734**	0.058
organic C	0.226	**0.893**	**0.855**	**0.840**	**0.612**	**0.867**	**0.881**	**0.842**	**0.596**	**-0.849**	0.119
total C	**0.277**	**0.629**	**0.548**	**0.602**	**0.435**	**0.627**	**0.553**	**0.587**	**0.451**	**-0.525**	0.080
Mg	**0.386**	**0.731**	**0.729**	**0.778**	**0.501**	**0.594**	**0.715**	**0.538**	**0.753**	**-0.491**	-0.216
Al	**0.299**	**0.877**	**0.954**	**0.890**	**0.604**	**0.719**	**0.950**	**0.781**	**0.711**	**-0.660**	0.096
Si	**-0.256**	**-0.613**	**-0.638**	**-0.652**	**-0.503**	**-0.580**	**-0.652**	**-0.665**	**-0.298**	**0.695**	0.008
P	**0.257**	**0.833**	**0.770**	**0.761**	**0.614**	**0.789**	**0.769**	**0.876**	**0.663**	**-0.671**	**0.240**
S	0.142	**0.410**	**0.462**	**0.432**	**0.397**	**0.484**	**0.480**	**0.501**	0.208	**-0.485**	0.082
Cl	-0.018	-0.012	0.086	0.109	0.087	0.140	0.050	0.082	-0.046	-0.059	0.025
K	0.156	**0.496**	**0.669**	**0.593**	**0.352**	**0.375**	**0.685**	**0.346**	**0.568**	**-0.315**	0.048
Ca	**0.364**	**0.645**	**0.570**	**0.675**	**0.427**	**0.517**	**0.546**	**0.694**	**0.573**	**-0.549**	0.007
Ti	**0.315**	**0.850**	**0.918**	**0.865**	**0.592**	**0.690**	**0.919**	**0.736**	**0.760**	**-0.620**	0.058
V	**0.343**	**0.957**	**0.936**	**0.901**	**0.655**	**0.774**	**0.943**	**0.867**	**0.654**	**-0.766**	0.069
Cr	-0.035	0.067	0.135	0.138	0.107	0.064	0.142	0.121	-0.110	-0.164	0.057
Mn	**0.377**	**0.871**	**0.829**	**0.852**	**0.589**	**0.856**	**0.805**	**0.829**	**0.721**	**-0.698**	0.138
Fe	**0.342**	**0.934**	**0.980**	**0.951**	**0.655**	**0.777**	**0.968**	**0.846**	**0.694**	**-0.759**	0.024
Ni	**0.286**	**0.799**	**0.858**	**0.839**	**0.547**	**0.673**	**0.856**	**0.679**	**0.681**	**-0.663**	-0.064
Cu	1	**0.493**	**0.284**	**0.393**	0.149	**0.363**	**0.264**	**0.239**	**0.324**	-0.188	-0.013
Zn		1	**0.917**	**0.904**	**0.632**	**0.814**	**0.920**	**0.859**	**0.706**	**-0.718**	0.118
Ga			1	**0.926**	**0.644**	**0.759**	**0.973**	**0.838**	**0.694**	**-0.728**	0.067

Table S5B: Correlation coefficients derived from elemental concentrations expressed as mass percentages (continued).

	La	Ce	Pb	Th	U	ordered Microcline feldspar	intermediate Microcline feldspar	Sanidine feldspar	Orthoclase feldspar
median	0.012	-0.147	**-0.614**	**-0.758**	**-0.612**	**0.812**	**0.658**	0.118	0.035
log (median)	0.004	-0.264	**-0.881**	**-0.964**	**-0.855**	**0.928**	**0.727**	0.411	-0.178
mean	0.007	-0.148	**-0.597**	**-0.744**	**-0.596**	**0.813**	**0.655**	0.125	0.037
log (mean)	-0.022	-0.281	**-0.849**	**-0.946**	**-0.832**	**0.898**	**0.743**	0.385	-0.164
mode	-0.021	-0.179	**-0.587**	**-0.749**	**-0.589**	**0.789**	**0.673**	0.114	0.034
log (mode)	-0.038	**-0.302**	**-0.806**	**-0.907**	**-0.806**	**0.829**	**0.743**	0.390	-0.128
organic C	-0.001	0.207	**0.800**	**0.882**	**0.771**	**-0.879**	**-0.600**	**-0.532**	0.300
total C	0.041	0.130	**0.606**	**0.637**	**0.607**	**-0.896**	**-0.764**	-0.181	0.178
Mg	0.020	0.174	**0.646**	**0.757**	**0.632**	**-0.858**	**-0.772**	-0.110	0.055
Al	0.072	**0.320**	**0.873**	**0.931**	**0.818**	**-0.896**	**-0.706**	**-0.447**	0.296
Si	-0.083	-0.212	**-0.574**	**-0.637**	**-0.721**	**0.917**	**0.674**	**0.431**	-0.261
P	0.106	**0.247**	**0.776**	**0.798**	**0.817**	**-0.835**	**-0.548**	**-0.481**	**0.470**
S	0.000	0.088	**0.452**	**0.435**	**0.594**	**-0.748**	-0.372	**-0.503**	0.370
Cl	0.095	0.143	-0.022	0.027	0.135	-0.135	-0.282	0.117	-0.212
K	0.103	**0.258**	**0.601**	**0.609**	**0.480**	**-0.648**	**-0.591**	-0.127	0.101
Ca	0.035	0.166	**0.556**	**0.631**	**0.633**	**-0.761**	**-0.607**	-0.113	0.172
Ti	0.075	**0.342**	**0.824**	**0.924**	**0.797**	**-0.909**	**-0.728**	-0.305	0.213
V	0.029	**0.312**	**0.879**	**0.944**	**0.890**	**-0.920**	**-0.663**	**-0.559**	0.379
Cr	0.156	**0.258**	0.009	0.116	0.185	**-0.655**	-0.293	**-0.569**	0.394
Mn	0.081	**0.258**	**0.853**	**0.873**	**0.821**	**-0.901**	**-0.644**	-0.343	0.328
Fe	0.035	**0.314**	**0.888**	**0.961**	**0.872**	**-0.934**	**-0.708**	**-0.508**	0.340
Ni	0.073	**0.290**	**0.761**	**0.853**	**0.756**	**-0.885**	**-0.697**	-0.313	0.121
Cu	**0.348**	**0.366**	**0.510**	**0.309**	**0.315**	**-0.949**	**-0.745**	**-0.428**	0.203
Zn	0.116	**0.347**	**0.926**	**0.939**	**0.834**	**-0.929**	**-0.656**	**-0.570**	0.379
Ga	0.010	**0.303**	**0.870**	**0.953**	**0.844**	**-0.911**	**-0.715**	**-0.550**	0.309

Table S5B: Correlation coefficients derived from elemental concentrations expressed as mass percentages (continued).

	Albite feldspar (Cleavelandite)	Oligoclase feldspar	Labradorite feldspar	Calcite	Dolomite	Hematite	Goethite
median	0.040	**0.475**	**0.717**	**-0.711**	**-0.504**	-0.355	**0.668**
log (median)	-0.161	0.184	**0.504**	**-0.869**	-0.311	-0.184	**0.572**
mean	0.054	**0.477**	**0.728**	**-0.705**	**-0.494**	-0.348	**0.669**
log (mean)	-0.127	0.198	**0.505**	**-0.840**	-0.302	-0.199	**0.570**
mode	0.053	**0.487**	**0.703**	**-0.688**	**-0.476**	-0.370	**0.662**
log (mode)	-0.072	0.210	**0.465**	**-0.771**	-0.237	-0.194	**0.526**
organic C	0.273	-0.083	-0.404	**0.878**	0.158	0.110	**-0.507**
total C	0.434	-0.063	-0.296	**0.932**	**0.586**	0.207	-0.425
Mg	0.175	-0.154	**-0.492**	**0.861**	**0.655**	0.312	**-0.517**
Al	0.339	0.062	-0.292	**0.942**	0.281	0.101	**-0.427**
Si	-0.417	-0.100	0.226	**-0.943**	-0.362	-0.152	**0.427**
P	**0.557**	0.241	-0.084	**0.955**	0.236	-0.047	-0.258
S	**0.469**	0.133	-0.172	**0.877**	0.075	-0.151	-0.196
Cl	-0.229	-0.323	**-0.485**	0.172	**0.466**	0.389	**-0.426**
K	0.026	-0.167	**-0.475**	**0.685**	0.361	0.412	**-0.511**
Ca	**0.518**	0.169	-0.101	**0.878**	**0.633**	0.171	-0.265
Ti	0.289	-0.066	-0.402	**0.927**	**0.454**	0.233	**-0.512**
V	0.373	0.084	-0.253	**0.920**	0.167	0.040	-0.420
Cr	0.327	0.349	-0.091	**0.738**	0.081	-0.079	-0.233
Mn	**0.438**	0.085	-0.264	**0.919**	**0.468**	0.233	**-0.493**
Fe	0.352	0.077	-0.287	**0.938**	0.263	0.128	**-0.478**
Ni	0.242	-0.152	**-0.432**	**0.907**	0.408	0.193	**-0.473**
Cu	0.249	0.027	-0.374	**0.851**	0.347	0.199	**-0.609**
Zn	0.373	0.084	-0.273	**0.936**	0.195	0.067	**-0.456**
Ga	0.298	0.051	-0.287	**0.898**	0.175	0.091	**-0.476**

Table S5B: Correlation coefficients derived from elemental concentrations expressed as mass percentages (continued).

	Maghemite	Apatite	Quartz	Total non-clays	disordered Kaolinite	Na-Smectite	Ca-smectite
median	**-0.439**	-0.341	**0.796**	**0.833**	**-0.792**	0.145	**-0.477**
log (median)	**-0.518**	**-0.447**	**0.958**	**0.978**	**-0.934**	0.047	**-0.604**
mean	-0.423	-0.335	**0.796**	**0.836**	**-0.795**	0.146	**-0.488**
log (mean)	**-0.484**	-0.407	**0.937**	**0.962**	**-0.925**	0.089	**-0.636**
mode	-0.409	-0.289	**0.784**	**0.826**	**-0.788**	0.188	**-0.518**
log (mode)	-0.370	-0.314	**0.879**	**0.917**	**-0.907**	0.133	**-0.703**
organic C	**0.592**	**0.481**	**-0.930**	**-0.932**	**0.831**	0.053	**0.613**
total C	**0.644**	**0.518**	**-0.897**	**-0.845**	**0.776**	-0.218	**0.515**
Mg	**0.590**	**0.528**	**-0.842**	**-0.820**	**0.794**	-0.161	**0.480**
Al	**0.591**	**0.527**	**-0.971**	**-0.948**	**0.915**	-0.044	**0.631**
Si	**-0.562**	**-0.506**	**0.955**	**0.920**	**-0.858**	0.003	**-0.493**
P	**0.603**	**0.561**	**-0.930**	**-0.864**	**0.793**	-0.043	**0.568**
S	**0.452**	**0.475**	**-0.847**	**-0.804**	**0.717**	0.102	**0.611**
Cl	0.178	0.076	-0.115	-0.130	0.177	-0.099	0.129
K	**0.484**	0.354	**-0.759**	**-0.759**	**0.752**	-0.175	**0.442**
Ca	**0.571**	**0.548**	**-0.750**	**-0.661**	**0.609**	-0.112	0.359
Ti	**0.597**	**0.514**	**-0.948**	**-0.926**	**0.880**	-0.118	**0.552**
V	**0.557**	**0.477**	**-0.983**	**-0.970**	**0.905**	-0.001	**0.617**
Cr	0.314	**0.544**	**-0.738**	**-0.694**	**0.666**	0.044	0.403
Mn	**0.648**	**0.496**	**-0.913**	**-0.862**	**0.748**	-0.044	0.400
Fe	**0.604**	**0.506**	**-0.991**	**-0.974**	**0.911**	-0.017	**0.579**
Ni	**0.478**	**0.493**	**-0.920**	**-0.914**	**0.899**	-0.108	**0.624**
Cu	**0.597**	**0.545**	**-0.922**	**-0.924**	**0.862**	0.052	**0.442**
Zn	**0.576**	**0.468**	**-0.990**	**-0.974**	**0.905**	-0.001	**0.603**
Ga	**0.552**	**0.476**	**-0.976**	**-0.975**	**0.940**	-0.016	**0.656**

Table S5B: Correlation coefficients derived from elemental concentrations expressed as mass percentages (continued).

	Ferruginous smectite	Illite (1Md) + Dioct. Mica + Smectite	Illite (1M)	Biotite (1M)	Phlogopite (2M1)	Fe-Chlorite (Tusc)	Mg-Chlorite (Clinochlore)
median	**-0.791**	**-0.786**	**-0.603**	0.272	-0.002	**-0.526**	-0.384
log (median)	**-0.946**	**-0.895**	**-0.721**	0.085	-0.010	**-0.660**	-0.402
mean	**-0.796**	**-0.783**	**-0.593**	0.267	-0.013	**-0.522**	-0.365
log (mean)	**-0.940**	**-0.872**	**-0.688**	0.087	-0.051	**-0.663**	-0.318
mode	**-0.795**	**-0.767**	**-0.596**	0.268	-0.018	**-0.537**	-0.328
log (mode)	**-0.908**	**-0.796**	**-0.649**	0.094	-0.110	**-0.622**	-0.181
organic C	**0.901**	**0.843**	**0.668**	-0.012	0.074	**0.699**	0.406
total C	**0.818**	**0.781**	**0.772**	-0.015	-0.055	**0.684**	0.422
Mg	**0.787**	**0.791**	**0.632**	-0.104	-0.034	**0.623**	0.359
Al	**0.921**	**0.879**	**0.730**	0.056	-0.041	**0.751**	0.381
Si	**-0.887**	**-0.850**	**-0.779**	-0.151	0.128	**-0.658**	**-0.474**
P	**0.831**	**0.793**	**0.770**	0.255	-0.193	**0.812**	**0.485**
S	**0.772**	**0.677**	**0.652**	0.194	-0.022	**0.763**	0.337
Cl	0.151	0.206	-0.174	-0.311	0.164	-0.111	-0.028
K	**0.730**	**0.733**	**0.569**	-0.141	-0.038	**0.557**	0.268
Ca	**0.619**	**0.642**	**0.645**	0.156	-0.189	**0.631**	0.412
Ti	**0.891**	**0.880**	**0.735**	-0.005	-0.081	**0.718**	**0.427**
V	**0.940**	**0.882**	**0.773**	0.119	-0.072	**0.771**	**0.431**
Cr	**0.677**	**0.610**	**0.514**	0.277	-0.010	**0.470**	0.197
Mn	**0.812**	**0.830**	**0.724**	0.126	-0.160	**0.740**	**0.519**
Fe	**0.948**	**0.902**	**0.758**	0.096	-0.064	**0.741**	**0.438**
Ni	**0.878**	**0.834**	**0.727**	-0.062	-0.003	**0.646**	0.368
Cu	**0.878**	**0.890**	**0.646**	-0.047	-0.027	**0.587**	**0.471**
Zn	**0.945**	**0.901**	**0.761**	0.113	-0.081	**0.767**	**0.441**
Ga	**0.963**	**0.893**	**0.726**	0.057	-0.030	**0.696**	0.394

Table S5B: Correlation coefficients derived from elemental concentrations expressed as mass percentages (continued).

	Muscovite (2M1)	Total clays	total
median	**-0.839**	**-0.815**	0.705
log (median)	**-0.959**	**-0.969**	0.789
mean	**-0.835**	**-0.813**	0.722
log (mean)	**-0.934**	**-0.946**	0.801
mode	**-0.822**	**-0.804**	0.711
log (mode)	**-0.870**	**-0.889**	0.801
organic C	**0.878**	**0.924**	**-0.776**
total C	**0.857**	**0.862**	**-0.584**
Mg	**0.860**	**0.830**	**-0.606**
Al	**0.940**	**0.963**	**-0.690**
Si	**-0.908**	**-0.933**	**0.676**
P	**0.836**	**0.896**	**-0.570**
S	**0.722**	**0.809**	**-0.610**
Cl	0.206	0.122	-0.125
K	**0.796**	**0.759**	**-0.590**
Ca	**0.687**	**0.698**	-0.398
Ti	**0.931**	**0.938**	**-0.681**
V	**0.927**	**0.978**	**-0.727**
Cr	**0.624**	**0.678**	**-0.591**
Mn	**0.848**	**0.875**	**-0.631**
Fe	**0.954**	**0.982**	**-0.729**
Ni	**0.903**	**0.917**	**-0.698**
Cu	**0.926**	**0.922**	**-0.723**
Zn	**0.937**	**0.984**	**-0.725**
Ga	**0.957**	**0.984**	**-0.731**

Table S5B: Correlation coefficients derived from elemental concentrations expressed as mass percentages (continued).

	As	Se	Br	Rb	Sr	Y	Zr	Ba
As	1	**0.628**	**0.786**	**0.897**	**0.817**	**0.664**	**-0.733**	0.031
Se		1	**0.574**	**0.638**	**0.560**	**0.516**	**-0.585**	-0.108
Br			1	**0.728**	**0.731**	**0.560**	**-0.666**	0.094
Rb				1	**0.837**	**0.670**	**-0.741**	0.104
Sr					1	**0.547**	**-0.756**	**0.362**
Y						1	**-0.300**	-0.005
Zr							1	-0.001
Ba								1

Table S5B: Correlation coefficients derived from elemental concentrations expressed as mass percentages (continued).

	La	Ce	Pb	Th	U	ordered Microcline feldspar	intermediate Microcline feldspar	Sanidine feldspar	Orthoclase feldspar
As	0.038	**0.307**	**0.847**	**0.908**	**0.810**	**-0.876**	**-0.659**	**-0.474**	0.411
Se	-0.078	0.126	**0.558**	**0.610**	**0.648**	**-0.715**	-0.332	**-0.433**	0.407
Br	-0.001	0.158	**0.783**	**0.762**	**0.713**	**-0.846**	**-0.675**	**-0.495**	0.296
Rb	0.038	**0.308**	**0.874**	**0.958**	**0.847**	**-0.901**	**-0.676**	**-0.538**	0.310
Sr	0.031	**0.263**	**0.832**	**0.849**	**0.839**	**-0.835**	**-0.514**	**-0.579**	**0.526**
Y	-0.009	0.211	**0.641**	**0.732**	**0.588**	**-0.780**	**-0.608**	-0.269	0.280
Zr	0.018	-0.182	**-0.674**	**-0.721**	**-0.762**	**0.793**	**0.471**	**0.500**	-0.300
Ba	**0.316**	**0.307**	**0.267**	0.086	0.106	0.003	0.170	-0.171	**0.587**
La	1	**0.651**	0.177	0.034	0.069	-0.300	-0.132	-0.035	0.284
Ce		1	**0.379**	**0.354**	**0.289**	**-0.599**	-0.334	-0.335	0.287
Pb			1	**0.867**	**0.829**	**-0.832**	**-0.512**	**-0.639**	**0.518**
Th				1	**0.842**	**-0.910**	**-0.724**	-0.424	0.259
U					1	**-0.825**	**-0.510**	**-0.465**	**0.440**
ordered Microcline feldspar						1	**0.689**	**0.476**	-0.203
intermediate Microcline feldspar							1	0.04	0.154
Sanidine feldspar								1	**-0.615**
Orthoclase feldspar									1

Table S5B: Correlation coefficients derived from elemental concentrations expressed as mass percentages (continued).

	Albite feldspar (Cleavelandite)	Oligoclase feldspar	Labradorite feldspar	Calcite	Dolomite	Hematite	Goethite
As	**0.427**	0.240	-0.175	**0.921**	0.278	0.148	**-0.429**
Se	0.218	0.006	-0.349	**0.687**	0.168	0.035	-0.382
Br	0.279	0.019	-0.361	**0.847**	0.243	0.142	**-0.551**
Rb	0.268	0.007	-0.342	**0.900**	0.169	0.099	**-0.468**
Sr	**0.661**	0.389	0.060	**0.938**	0.105	-0.089	-0.240
Y	0.241	-0.120	-0.361	**0.776**	**0.429**	0.219	**-0.493**
Zr	-0.349	-0.007	0.290	**-0.814**	-0.004	0.041	0.375
Ba	**0.790**	**0.767**	**0.763**	0.225	-0.195	-0.161	0.261
La	0.420	0.131	0.156	0.349	0.177	0.192	-0.252
Ce	0.281	0.149	-0.006	**0.489**	0.088	0.177	-0.362
Pb	**0.536**	0.316	-0.019	**0.899**	0.065	-0.010	-0.321
Th	0.332	0.013	-0.309	**0.931**	0.297	0.153	**-0.469**
U	**0.472**	0.151	-0.143	**0.899**	0.202	0.010	-0.286
ordered Microcline feldspar	-0.272	0.076	0.414	**-0.860**	-0.343	-0.163	**0.622**
intermediate Microcline feldspar	0.096	0.242	**0.438**	**-0.596**	**-0.483**	-0.296	**0.502**
Sanidine feldspar	-0.345	-0.404	-0.133	**-0.449**	**0.526**	0.331	0.146
Orthoclase feldspar	**0.674**	**0.641**	0.394	0.375	-0.420	**-0.460**	0.160
Albite feldspar (Cleavelandite)	1	**0.659**	**0.609**	**0.529**	-0.124	-0.397	0.246
Oligoclase feldspar		1	**0.814**	0.188	-0.395	-0.410	0.516

Table S5B: Correlation coefficients derived from elemental concentrations expressed as mass percentages (continued).

	Maghemite	Apatite	Quartz	Total non-clays	disordered Kaolinite	Na-Smectite	Ca-smectite
As	**0.660**	**0.577**	**-0.942**	**-0.896**	**0.832**	-0.069	**0.519**
Se	0.382	**0.544**	**-0.763**	**-0.750**	**0.681**	-0.109	0.413
Br	**0.676**	**0.508**	**-0.883**	**-0.875**	**0.804**	0.132	**0.553**
Rb	**0.530**	**0.455**	**-0.982**	**-0.984**	**0.933**	-0.006	**0.623**
Sr	**0.628**	**0.538**	**-0.923**	**-0.852**	**0.742**	0.092	**0.470**
Y	**0.475**	**0.451**	**-0.823**	**-0.805**	**0.773**	-0.286	**0.518**
Zr	**-0.519**	-0.395	**0.868**	**0.864**	**-0.765**	-0.148	**-0.494**
Ba	0.335	0.117	-0.134	0.006	-0.124	0.070	-0.156
La	0.133	0.045	-0.340	-0.281	0.225	**-0.429**	0.372
Ce	0.086	0.126	**-0.597**	-0.591	**0.505**	-0.328	**0.613**
Pb	**0.585**	**0.427**	**-0.937**	**-0.889**	**0.777**	0.130	**0.489**
Th	**0.561**	**0.491**	**-0.967**	**-0.952**	**0.904**	-0.065	**0.630**
U	**0.472**	0.417	**-0.913**	**-0.866**	**0.785**	-0.149	**0.590**
ordered Microcline feldspar	**-0.491**	**-0.458**	**0.931**	**0.943**	**-0.854**	-0.004	**-0.550**
intermediate Microcline feldspar	**-0.486**	**-0.507**	**0.649**	**0.692**	**-0.801**	0.112	**-0.446**
Sanidine feldspar	-0.190	-0.098	**0.558**	**0.566**	**-0.443**	-0.369	-0.411
Orthoclase feldspar	**0.548**	0.270	-0.374	-0.274	0.126	0.061	0.063
Albite feldspar (Cleavelandite)	**0.462**	0.294	-0.365	-0.214	0.071	0.081	0.053
Oligoclase feldspar	0.208	0.214	-0.087	0.044	-0.117	0.153	-0.123

Table S5B: Correlation coefficients derived from elemental concentrations expressed as mass percentages (continued).

	Ferruginous smectite	Illite (1Md) + Dioct. Mica + Smectite	Illite (1M)	Biotite (1M)	Phlogopite (2M1)	Fe-Chlorite (Tusc)	Mg-Chlorite (Clinochlore)
As	**0.893**	**0.848**	**0.690**	0.205	-0.112	**0.697**	**0.449**
Se	**0.723**	**0.684**	**0.616**	0.159	-0.146	**0.532**	**0.484**
Br	**0.858**	**0.855**	**0.540**	-0.025	0.020	**0.682**	**0.457**
Rb	**0.960**	**0.888**	**0.749**	0.041	-0.008	**0.713**	0.377
Sr	**0.824**	**0.786**	**0.739**	0.333	-0.161	**0.792**	**0.480**
Y	**0.788**	**0.751**	**0.714**	0.029	-0.202	**0.590**	**0.471**
Zr	**-0.841**	**-0.791**	**-0.601**	-0.050	-0.072	**-0.699**	-0.332
Ba	-0.014	0.063	0.206	**0.594**	-0.418	0.413	0.246
La	0.328	0.221	0.378	0.265	-0.335	0.418	0.121
Ce	**0.595**	0.380	**0.607**	0.316	-0.248	**0.501**	0.264
Pb	**0.838**	**0.805**	**0.767**	0.277	-0.167	**0.810**	**0.484**
Th	**0.926**	**0.862**	**0.746**	0.028	-0.012	**0.734**	0.372
U	**0.847**	**0.753**	**0.804**	0.298	-0.168	**0.819**	0.375
ordered Microcline feldspar	**-0.897**	**-0.850**	**-0.714**	0.015	0.070	**-0.616**	**-0.513**
intermediate Microcline feldspar	**-0.694**	**-0.699**	-0.344	0.396	-0.355	-0.313	-0.005
Sanidine feldspar	**-0.548**	-0.437	-0.398	-0.350	0.072	**-0.443**	-0.339
Orthoclase feldspar	0.308	0.342	0.263	**0.657**	-0.409	**0.601**	**0.471**
Albite feldspar (Cleavelandite)	0.217	0.275	0.359	**0.640**	-0.424	**0.586**	**0.437**
Oligoclase feldspar	-0.026	-0.040	0.134	**0.700**	-0.237	0.289	0.048

Table S5B: Correlation coefficients derived from elemental concentrations expressed as mass percentages (continued).

	Muscovite (2M1)	Total clays	total
As	**0.907**	**0.916**	**-0.634**
Se	**0.687**	**0.741**	**-0.611**
Br	**0.861**	**0.898**	**-0.607**
Rb	**0.953**	**0.981**	**-0.776**
Sr	**0.812**	**0.881**	**-0.570**
Y	**0.806**	**0.814**	**-0.597**
Zr	**-0.817**	-0.862	**0.679**
Ba	-0.026	0.063	0.223
La	0.225	0.285	-0.207
Ce	**0.474**	**0.543**	**-0.614**
Pb	**0.826**	**0.905**	**-0.640**
Th	**0.935**	**0.955**	**-0.730**
U	**0.796**	**0.872**	**-0.658**
ordered Microcline feldspar	**-0.897**	**-0.927**	**0.784**
intermediate Microcline feldspar	**-0.789**	**-0.694**	**0.530**
Sanidine feldspar	-0.418	**-0.553**	**0.483**
Orthoclase feldspar	0.241	0.346	0.013
Albite feldspar (Cleavelandite)	0.177	0.302	0.110
Oligoclase feldspar	-0.067	0.006	0.189

Table S5B: Correlation coefficients derived from elemental concentrations expressed as mass percentages (continued).

	Labradorite feldspar	Calcite	Dolomite	Hematite	Goethite
Labradorite feldspar	1	-0.155	**-0.454**	-0.387	**0.668**
Calcite		1	0.320	-0.009	-0.286
Dolomite			1	**0.579**	-0.38
Hematite				1	**-0.588**
Goethite					1

Table S5B: Correlation coefficients derived from elemental concentrations expressed as mass percentages (continued).

	Maghemite	Apatite	Quartz	Total non-clays	disordered Kaolinite	Na-Smectite	Ca-smectite
Labradorite feldspar	-0.101	-0.097	0.288	0.406	**-0.440**	0.081	-0.218
Calcite	**0.629**	**0.596**	**-0.943**	**-0.877**	**0.824**	0.000	**0.530**
Dolomite	0.178	0.224	-0.21	-0.185	0.230	-0.376	0.053
Hematite	-0.156	-0.241	-0.057	-0.104	0.108	-0.391	0.075
Goethite	-0.208	-0.032	**0.454**	**0.546**	**-0.486**	0.040	-0.269
Maghemite	1	**0.683**	**-0.585**	**-0.509**	**0.457**	0.167	0.016
Apatite		1	**-0.526**	**-0.467**	**0.531**	0.191	0.081
Quartz			1	**0.982**	**-0.910**	-0.024	**-0.581**
Total non-clays				1	**-0.941**	-0.040	**-0.617**
disordered Kaolinite					1	-0.045	**0.671**
Na-Smectite						1	-0.336
Ca-smectite							1

Table S5B: Correlation coefficients derived from elemental concentrations expressed as mass percentages (continued).

	Ferruginous smectite	Illite (1Md) + Dioct. Mica + Smectite	Illite (1M)	Biotite (1M)	Phlogopite (2M1)	Fe-Chlorite (Tusc)	Mg-Chlorite (Clinochlore)
Labradorite feldspar	-0.367	-0.414	-0.058	**0.616**	-0.203	0.022	-0.130
Calcite	**0.852**	**0.830**	**0.730**	0.201	-0.093	**0.758**	0.425
Dolomite	0.149	0.213	0.248	-0.270	-0.095	0.048	0.136
Hematite	0.107	0.007	0.242	-0.297	-0.057	-0.160	0.018
Goethite	**-0.499**	**-0.533**	-0.206	0.467	-0.048	-0.107	-0.325
Maghemite	**0.498**	**0.755**	0.185	0.041	-0.057	**0.637**	**0.486**
Apatite	**0.452**	**0.563**	0.177	-0.052	0.278	0.306	0.215
Quartz	**-0.954**	**-0.893**	**-0.761**	-0.127	0.062	**-0.731**	**-0.459**
Total non-clays	**-0.969**	**-0.892**	**-0.723**	-0.004	-0.020	**-0.655**	-0.415
disordered Kaolinite	**0.942**	**0.853**	**0.604**	-0.120	0.181	**0.500**	0.197
Na-Smectite	-0.121	0.122	-0.241	-0.253	0.376	0.022	0.104
Ca-smectite	**0.705**	0.359	**0.542**	0.138	-0.050	0.400	0.095
Ferruginous smectite	1	**0.850**	**0.709**	0.094	-0.012	**0.614**	0.367
Illite (1Md) + Dioct. Mica + Smectite		1	**0.475**	-0.110	0.030	**0.668**	0.430
Illite (1M)			1	0.377	-0.397	**0.635**	**0.493**
Biotite (1M)				1	**-0.636**	0.323	0.313
Phlogopite (2M1)					1	-0.301	**-0.648**
Fe-Chlorite (Tusc)						1	**0.475**
Mg-Chlorite (Clinochlore)							1

Table S5B: Correlation coefficients derived from elemental concentrations expressed as mass percentages (continued).

	Muscovite (2M1)	Total clays	total
Labradorite feldspar	**-0.440**	-0.355	**0.477**
Calcite	**0.868**	0.911	**-0.575**
Dolomite	0.281	0.185	-0.142
Hematite	0.122	0.045	-0.267
Goethite	**-0.520**	**-0.487**	**0.608**
Maghemite	**0.635**	**0.617**	-0.052
Apatite	**0.571**	**0.518**	-0.201
Quartz	**-0.949**	**-0.985**	**0.754**
Total non-clays	**-0.958**	**-0.984**	**0.828**
disordered Kaolinite	**0.954**	**0.932**	**-0.759**
Na-Smectite	-0.041	0.037	-0.042
Ca-smectite	0.547	**0.600**	**-0.535**
Ferruginous smectite	**0.954**	**0.964**	**-0.772**
Illite (1Md) + Dioct. Mica + Smectite	**0.926**	**0.931**	**-0.567**
Illite (1M)	**0.632**	**0.708**	**-0.611**
Biotite (1M)	-0.059	0.046	0.125
Phlogopite (2M1)	0.053	-0.038	-0.198
Fe-Chlorite (Tusc)	**0.594**	**0.719**	-0.309
Mg-Chlorite (Clinochlore)	**0.375**	**0.467**	-0.157

Table S5B: Correlation coefficients derived from elemental concentrations expressed as mass percentages (continued).

	Muscovite (2M1)	Total clays	total
Muscovite (2M1)	1	**0.968**	**-0.713**
Total clays		1	**-0.716**
Total			1

Table S5C: Correlation coefficients derived from elemental concentrations expressed as molar ratios[a].

	median	log (median)	mean	log (mean)	mode	log (mode)	organic C	total C	Mg	Al
median	1	**0.833**	**0.996**	**0.836**	**0.966**	**0.770**	**-0.683**	**-0.549**	**-0.786**	**-0.767**
log (median)		1	**0.823**	**0.988**	**0.830**	**0.956**	**-0.910**	**-0.743**	**-0.916**	**-0.947**
mean			1	**0.838**	**0.979**	**0.780**	**-0.672**	**-0.537**	**-0.763**	**-0.745**
log (mean)				1	**0.865**	**0.984**	**-0.887**	**-0.732**	**-0.883**	**-0.912**
mode					1	**0.832**	**-0.683**	**-0.548**	**-0.747**	**-0.717**
log (mode)						1	**-0.840**	**-0.716**	**-0.812**	**-0.851**
organic C							1	**0.727**	**0.852**	**0.858**
total C								1	**0.648**	**0.630**
Mg									1	**0.906**
Al										1

[a] Significant correlations (≥ 2σ from 0) are in bold text; highly significant correlations (≥ 4σ from 0) are in bold and red text.

Table S5C: Correlation coefficients derived from elemental concentrations expressed as molar ratios (continued).

	Si	P	S	Cl	K	Ca	Ti	V	Cr	Mn	Fe	Ni
median		**-0.665**	**-0.475**	**-0.350**	**-0.806**	**-0.641**	**-0.810**	**-0.665**	**-0.335**	**-0.726**	**-0.722**	**-0.772**
log (median)		**-0.902**	**-0.519**	**-0.295**	**-0.851**	**-0.835**	**-0.952**	**-0.947**	**-0.351**	**-0.921**	**-0.960**	**-0.962**
mean		**-0.652**	**-0.452**	**-0.315**	**-0.782**	**-0.615**	**-0.789**	**-0.655**	**-0.341**	**-0.705**	**-0.703**	**-0.750**
log (mean)		**-0.874**	**-0.482**	-0.245	**-0.819**	**-0.790**	**-0.922**	**-0.927**	**-0.361**	**-0.887**	**-0.928**	**-0.928**
mode		**-0.659**	**-0.395**	-0.214	**-0.734**	**-0.604**	**-0.769**	**-0.670**	**-0.329**	**-0.697**	**-0.694**	**-0.732**
log (mode)		**-0.823**	**-0.412**	-0.173	**-0.744**	**-0.715**	**-0.855**	**-0.899**	**-0.330**	**-0.817**	**-0.878**	**-0.871**
organic C		**0.916**	**0.531**	**0.275**	**0.701**	**0.824**	**0.867**	**0.890**	**0.293**	**0.918**	**0.907**	**0.908**
total C		**0.654**	**0.348**	0.166	**0.539**	**0.642**	**0.651**	**0.680**	**0.300**	**0.697**	**0.700**	**0.695**
Mg		**0.858**	**0.587**	0.302	**0.834**	**0.871**	**0.934**	**0.843**	0.190	**0.937**	**0.905**	**0.910**
Al		**0.844**	**0.604**	0.235	**0.928**	**0.729**	**0.984**	**0.911**	0.190	**0.926**	**0.974**	**0.971**
Si												
P		1	**0.554**	**0.288**	**0.674**	**0.872**	**0.846**	**0.889**	**0.242**	**0.888**	**0.866**	**0.848**
S			1	**0.509**	**0.648**	**0.621**	**0.627**	**0.477**	**0.308**	**0.559**	**0.573**	**0.586**
Cl				1	**0.295**	**0.425**	**0.273**	0.129	**0.525**	0.234	0.225	**0.241**
K					1	**0.624**	**0.931**	**0.734**	**0.260**	**0.810**	**0.875**	**0.890**
Ca						1	**0.781**	**0.727**	**0.291**	**0.856**	**0.769**	**0.755**
Ti							1	**0.889**	0.233	**0.944**	**0.968**	**0.966**
V								1	0.150	**0.907**	**0.952**	**0.924**
Cr									1	0.165	0.201	0.200
Mn										1	**0.953**	**0.940**
Fe											1	**0.983**
Ni												1

Table S5C: Correlation coefficients derived from elemental concentrations expressed as molar ratios (continued).

	Cu	Zn	Ga	As	Br	Rb	Sr	Y	Zr	Ba
median	**-0.316**	**-0.663**	**-0.716**	**-0.652**	**-0.645**	**-0.754**	**-0.617**	**-0.755**	**0.552**	**-0.486**
log (median)	**-0.668**	**-0.949**	**-0.961**	**-0.913**	**-0.881**	**-0.972**	**-0.884**	**-0.919**	**0.786**	**-0.634**
mean	**-0.278**	**-0.650**	**-0.699**	**-0.630**	**-0.630**	**-0.741**	**-0.602**	**-0.737**	**0.532**	**-0.478**
log (mean)	**-0.615**	**-0.924**	**-0.931**	**-0.871**	**-0.857**	**-0.947**	**-0.847**	**-0.896**	**0.741**	**-0.616**
mode	-0.281	**-0.662**	**-0.691**	**-0.612**	**-0.631**	**-0.736**	**-0.594**	**-0.747**	**0.518**	**-0.469**
log (mode)	**-0.575**	**-0.888**	**-0.887**	**-0.810**	**-0.807**	**-0.904**	**-0.790**	**-0.848**	**0.693**	**-0.546**
organic C	**0.575**	**0.929**	**0.896**	**0.885**	**0.886**	**0.908**	**0.898**	**0.834**	**-0.838**	**0.687**
total C	**0.444**	**0.677**	**0.651**	**0.705**	**0.608**	**0.695**	**0.666**	**0.602**	**-0.561**	**0.512**
Mg	**0.532**	**0.859**	**0.876**	**0.891**	**0.832**	**0.877**	**0.814**	**0.905**	**-0.630**	**0.489**
Al	**0.471**	**0.907**	**0.971**	**0.937**	**0.842**	**0.963**	**0.857**	**0.888**	**-0.674**	**0.584**
Si										
P	**0.387**	**0.894**	**0.861**	**0.849**	**0.822**	**0.878**	**0.929**	**0.858**	**-0.685**	**0.679**
S	**0.281**	**0.456**	**0.537**	**0.519**	**0.465**	**0.595**	**0.581**	**0.473**	**-0.374**	**0.557**
Cl	0.096	0.117	0.207	0.231	**0.248**	0.225	**0.270**	0.162	-0.085	**0.369**
K	**0.430**	**0.725**	**0.859**	**0.830**	**0.675**	**0.864**	**0.698**	**0.793**	**-0.527**	**0.542**
Ca	**0.459**	**0.748**	**0.722**	**0.760**	**0.694**	**0.756**	**0.871**	**0.770**	**-0.628**	**0.641**
Ti	**0.475**	**0.892**	**0.953**	**0.924**	**0.826**	**0.956**	**0.857**	**0.914**	**-0.657**	**0.603**
V	**0.465**	**0.976**	**0.950**	**0.927**	**0.881**	**0.953**	**0.899**	**0.855**	**-0.757**	**0.554**
Cr	0.021	0.094	0.159	0.171	0.142	0.227	0.219	0.091	-0.072	**0.459**
Mn	**0.513**	**0.928**	**0.927**	**0.939**	**0.875**	**0.925**	**0.912**	**0.897**	**-0.744**	**0.624**
Fe	**0.491**	**0.949**	**0.987**	**0.971**	**0.877**	**0.985**	**0.903**	**0.897**	**-0.742**	**0.591**
Ni	**0.496**	**0.925**	**0.970**	**0.958**	**0.872**	**0.964**	**0.864**	**0.892**	**-0.733**	**0.567**
Cu	1	**0.558**	**0.457**	**0.510**	**0.488**	**0.446**	**0.394**	**0.482**	**-0.306**	**0.281**
Zn		1	**0.945**	**0.932**	**0.895**	**0.944**	**0.900**	**0.874**	**-0.752**	**0.563**
Ga			1	**0.960**	**0.871**	**0.979**	**0.890**	**0.891**	**-0.740**	**0.572**

Table S5C: Correlation coefficients derived from elemental concentrations expressed as molar ratios (continued).

	La	Ce	Pb	Th	U	ordered Microcline feldspar	intermediate Microcline feldspar	Sanidine feldspar	Orthoclase feldspar
median	**-0.302**	**-0.452**	**-0.670**	**-0.749**	**-0.644**	**0.734**	**-0.556**	**-0.489**	**-0.598**
log (median)	**-0.380**	**-0.626**	**-0.924**	**-0.971**	**-0.885**	**0.819**	**-0.671**	-0.366	**-0.781**
mean	**-0.299**	**-0.446**	**-0.651**	**-0.734**	**-0.627**	**0.730**	**-0.551**	**-0.487**	**-0.598**
log (mean)	**-0.389**	**-0.627**	**-0.887**	**-0.948**	**-0.861**	**0.772**	**-0.616**	-0.386	**-0.772**
mode	**-0.315**	**-0.465**	**-0.639**	**-0.737**	**-0.620**	**0.704**	**-0.520**	**-0.492**	**-0.597**
log (mode)	**-0.375**	**-0.617**	**-0.834**	**-0.906**	**-0.829**	**0.698**	**-0.529**	-0.338	**-0.718**
organic C	**0.360**	**0.583**	**0.907**	**0.922**	**0.818**	**-0.868**	**0.761**	0.369	**0.755**
total C	0.265	**0.437**	**0.661**	**0.705**	**0.652**	**-0.847**	**0.729**	0.408	**0.715**
Mg	**0.374**	**0.543**	**0.854**	**0.888**	**0.829**	**-0.809**	**0.648**	**0.469**	**0.766**
Al	**0.385**	**0.612**	**0.936**	**0.950**	**0.879**	**-0.800**	**0.712**	0.321	**0.828**
Si									
P	**0.379**	**0.577**	**0.847**	**0.889**	**0.851**	**-0.765**	**0.774**	0.289	**0.817**
S	**0.291**	**0.414**	**0.539**	**0.513**	**0.619**	**-0.689**	**0.779**	0.215	**0.708**
Cl	**0.283**	**0.309**	0.165	0.159	**0.284**	**-0.521**	0.365	0.184	**0.560**
K	**0.419**	**0.587**	**0.831**	**0.811**	**0.771**	**-0.765**	**0.684**	0.412	**0.803**
Ca	**0.403**	**0.549**	**0.738**	**0.768**	**0.787**	**-0.768**	**0.700**	0.418	**0.704**
Ti	**0.402**	**0.639**	**0.918**	**0.949**	**0.883**	**-0.820**	**0.710**	0.397	**0.810**
V	**0.304**	**0.587**	**0.929**	**0.964**	**0.899**	**-0.812**	**0.722**	0.244	**0.849**
Cr	**0.360**	**0.431**	0.122	0.163	**0.243**	**-0.607**	**0.677**	0.101	**0.653**
Mn	**0.363**	**0.573**	**0.928**	**0.942**	**0.882**	**-0.833**	**0.784**	0.349	**0.811**
Fe	**0.374**	**0.636**	**0.955**	**0.976**	**0.905**	**-0.836**	**0.757**	0.280	**0.849**
Ni	**0.389**	**0.628**	**0.940**	**0.958**	**0.884**	**-0.845**	**0.751**	0.277	**0.810**
Cu	**0.410**	**0.444**	**0.607**	**0.442**	**0.459**	**-0.842**	**0.749**	0.303	**0.813**
Zn	**0.353**	**0.607**	**0.954**	**0.963**	**0.875**	**-0.835**	**0.780**	0.228	**0.844**
Ga	**0.333**	**0.601**	**0.941**	**0.972**	**0.893**	**-0.817**	**0.729**	0.230	**0.829**

Table S5C: Correlation coefficients derived from elemental concentrations expressed as molar ratios (continued).

	Albite feldspar (Cleavelandite)	Oligoclase feldspar	Labradorite feldspar	Calcite	Dolomite	Hematite	Goethite
median	**-0.519**	-0.250	0.392	**-0.791**	**-0.865**	**-0.591**	-0.174
log (median)	**-0.655**	**-0.501**	0.193	**-0.956**	**-0.924**	**-0.625**	-0.361
mean	**-0.509**	-0.251	0.397	**-0.790**	**-0.861**	**-0.594**	-0.174
log (mean)	**-0.616**	**-0.494**	0.185	**-0.941**	**-0.906**	**-0.644**	-0.355
mode	**-0.498**	-0.242	0.375	**-0.785**	**-0.850**	**-0.613**	-0.174
log (mode)	**-0.532**	**-0.443**	0.156	**-0.896**	**-0.830**	**-0.627**	-0.374
organic C	**0.723**	**0.471**	-0.195	**0.939**	**0.909**	**0.629**	0.310
total C	**0.883**	**0.539**	-0.064	**0.917**	**0.955**	**0.644**	0.302
Mg	**0.713**	**0.554**	-0.147	**0.935**	**0.984**	**0.622**	0.344
Al	**0.735**	**0.631**	-0.031	**0.981**	**0.921**	**0.595**	**0.444**
Si							
P	**0.828**	**0.652**	0.106	**0.939**	**0.878**	**0.480**	**0.499**
S	**0.778**	**0.537**	0.058	**0.883**	**0.800**	0.377	**0.548**
Cl	**0.504**	0.292	-0.396	**0.690**	**0.749**	**0.468**	0.031
K	**0.680**	**0.611**	-0.082	**0.945**	**0.929**	**0.681**	0.364
Ca	**0.819**	**0.578**	0.067	**0.869**	**0.924**	**0.511**	0.388
Ti	**0.755**	**0.585**	-0.072	**0.963**	**0.955**	**0.625**	0.374
V	**0.741**	**0.637**	0.019	**0.974**	**0.874**	**0.581**	**0.444**
Cr	**0.590**	**0.624**	0.032	**0.780**	**0.713**	**0.472**	0.341
Mn	**0.815**	**0.640**	0.024	**0.912**	**0.948**	**0.651**	0.279
Fe	**0.754**	**0.657**	-0.002	**0.982**	**0.933**	**0.667**	0.376
Ni	**0.760**	**0.559**	-0.057	**0.972**	**0.932**	**0.625**	0.361
Cu	**0.708**	**0.639**	-0.061	**0.968**	**0.944**	**0.673**	0.345
Zn	**0.777**	**0.647**	0.033	**0.976**	**0.903**	**0.621**	0.395
Ga	**0.705**	**0.638**	-0.007	**0.978**	**0.898**	**0.646**	0.409

Table S5C: Correlation coefficients derived from elemental concentrations expressed as molar ratios (continued).

	Maghemite	Apatite	Quartz	Total non-clays	disordered Kaolinite	Na-Smectite	Ca-smectite
median	**-0.553**	**-0.664**		**-0.722**	-0.288	**-0.455**	**-0.729**
log (median)	**-0.645**	**-0.812**		**-0.897**	-0.384	**-0.590**	**-0.899**
mean	**-0.546**	**-0.660**		**-0.727**	-0.282	**-0.465**	**-0.734**
log (mean)	**-0.622**	**-0.784**		**-0.900**	-0.344	**-0.623**	**-0.904**
mode	**-0.529**	**-0.636**		**-0.731**	-0.248	**-0.494**	**-0.742**
log (mode)	**-0.521**	**-0.712**		**-0.899**	-0.283	**-0.690**	**-0.892**
organic C	**0.583**	**0.738**		**0.791**	0.424	**0.561**	**0.841**
total C	**0.570**	**0.702**		**0.740**	0.309	**0.507**	**0.816**
Mg	**0.702**	**0.819**		**0.805**	0.365	**0.488**	**0.829**
Al	**0.678**	**0.838**		**0.892**	0.399	**0.597**	**0.901**
Si							
P	**0.634**	**0.782**		**0.784**	0.386	**0.534**	**0.806**
S	**0.522**	**0.707**		**0.712**	0.395	**0.570**	**0.730**
Cl	**0.673**	**0.621**		**0.557**	0.378	0.360	**0.602**
K	**0.683**	**0.823**		**0.863**	0.382	**0.506**	**0.880**
Ca	**0.622**	**0.727**		**0.665**	0.361	0.393	**0.702**
Ti	**0.686**	**0.819**		**0.849**	0.389	**0.524**	**0.868**
V	**0.648**	**0.815**		**0.903**	0.419	**0.586**	**0.910**
Cr	**0.482**	**0.658**		**0.677**	0.353	0.421	**0.685**
Mn	**0.676**	**0.742**		**0.715**	0.410	0.396	**0.777**
Fe	**0.678**	**0.819**		**0.878**	0.411	**0.566**	**0.909**
Ni	**0.641**	**0.785**		**0.861**	0.396	**0.596**	**0.883**
Cu	**0.683**	**0.830**		**0.866**	**0.427**	**0.544**	**0.900**
Zn	**0.644**	**0.788**		**0.863**	0.425	**0.570**	**0.891**
Ga	**0.643**	**0.812**		**0.911**	0.376	**0.651**	**0.932**

Table S5C: Correlation coefficients derived from elemental concentrations expressed as molar ratios (continued).

	Ferruginous smectite	Illite (1Md) + Dioct. Mica + Smectite	Illite (1M)	Biotite (1M)	Phlogopite (2M1)	Fe-Chlorite (Tusc)	Mg-Chlorite (Clinochlore)
median	**-0.734**	**-0.723**	-0.250	-0.318	**-0.736**	**-0.585**	**-0.754**
log (median)	**-0.878**	**-0.876**	-0.392	-0.425	**-0.883**	**-0.654**	**-0.913**
mean	**-0.734**	**-0.721**	-0.254	-0.331	**-0.739**	**-0.569**	**-0.754**
log (mean)	**-0.868**	**-0.859**	-0.395	**-0.469**	**-0.892**	**-0.577**	**-0.904**
mode	**-0.728**	**-0.722**	-0.260	-0.345	**-0.747**	**-0.530**	**-0.751**
log (mode)	**-0.817**	**-0.828**	-0.372	**-0.521**	**-0.860**	**-0.441**	**-0.867**
organic C	**0.788**	**0.862**	0.439	0.332	**0.853**	**0.761**	**0.820**
total C	**0.723**	**0.925**	**0.496**	0.185	**0.833**	**0.764**	**0.795**
Mg	**0.832**	**0.827**	0.422	0.351	**0.845**	**0.694**	**0.857**
Al	**0.881**	**0.888**	**0.472**	0.398	**0.907**	**0.685**	**0.914**
Si							
P	**0.795**	**0.850**	**0.525**	0.290	**0.885**	**0.707**	**0.814**
S	**0.689**	**0.782**	**0.469**	0.293	**0.827**	**0.621**	**0.717**
Cl	**0.660**	**0.444**	0.173	0.354	**0.543**	**0.526**	**0.611**
K	**0.871**	**0.877**	**0.451**	0.393	**0.865**	**0.682**	**0.905**
Ca	**0.716**	**0.772**	**0.485**	0.214	**0.777**	**0.712**	**0.723**
Ti	**0.869**	**0.871**	**0.462**	0.363	**0.885**	**0.707**	**0.887**
V	**0.888**	**0.898**	**0.486**	0.414	**0.907**	**0.668**	**0.916**
Cr	**0.680**	**0.684**	**0.432**	0.319	**0.663**	**0.518**	**0.683**
Mn	**0.795**	**0.844**	**0.530**	0.232	**0.869**	**0.791**	**0.792**
Fe	**0.882**	**0.914**	**0.524**	0.363	**0.907**	**0.739**	**0.914**
Ni	**0.862**	**0.888**	**0.477**	0.347	**0.899**	**0.717**	**0.882**
Cu	**0.871**	**0.908**	**0.498**	0.359	**0.887**	**0.763**	**0.914**
Zn	**0.870**	**0.908**	**0.521**	0.348	**0.917**	**0.726**	**0.889**
Ga	**0.878**	**0.915**	**0.510**	0.381	**0.905**	**0.695**	**0.927**

Table S5C: Correlation coefficients derived from elemental concentrations expressed as molar ratios (continued).

	Muscovite (2M1)	Total clays
median	**-0.781**	**-0.770**
log (median)	**-0.943**	**-0.941**
mean	**-0.779**	**-0.771**
log (mean)	**-0.925**	**-0.934**
mode	**-0.772**	**-0.771**
log (mode)	**-0.865**	**-0.904**
organic C	**0.935**	**0.878**
total C	**0.938**	**0.831**
Mg	**0.947**	**0.875**
Al	**0.979**	**0.947**
Si		
P	**0.952**	**0.863**
S	**0.882**	**0.783**
Cl	**0.688**	**0.626**
K	**0.953**	**0.922**
Ca	**0.898**	**0.760**
Ti	**0.970**	**0.917**
V	**0.967**	**0.954**
Cr	**0.782**	**0.723**
Mn	**0.941**	**0.833**
Fe	**0.985**	**0.950**
Ni	**0.967**	**0.929**
Cu	**0.971**	**0.941**
Zn	**0.975**	**0.938**
Ga	**0.970**	**0.964**

Table S5C: Correlation coefficients derived from elemental concentrations expressed as molar ratios (continued).

	As	Br	Rb	Sr	Y	Zr	Ba
As	1	**0.898**	**0.944**	**0.884**	**0.861**	**-0.755**	**0.573**
Br		1	**0.854**	**0.807**	**0.783**	**-0.705**	**0.497**
Rb			1	**0.913**	**0.879**	**-0.737**	**0.630**
Sr				1	**0.805**	**-0.768**	**0.752**
Y					1	**-0.577**	**0.473**
Zr						1	**-0.434**
Ba							1

Table S5C: Correlation coefficients derived from elemental concentrations expressed as molar ratios (continued).

	La	Ce	Pb	Th	U	ordered Microcline feldspar	intermediate Microcline feldspar	Sanidine feldspar	Orthoclase feldspar
As	**0.345**	**0.604**	**0.931**	**0.943**	**0.867**	**-0.797**	**0.755**	0.280	**0.861**
Br	0.210	**0.457**	**0.849**	**0.862**	**0.771**	**-0.762**	**0.674**	0.165	**0.841**
Rb	**0.385**	**0.648**	**0.944**	**0.977**	**0.907**	**-0.808**	**0.753**	0.270	**0.809**
Sr	**0.356**	**0.599**	**0.888**	**0.911**	**0.892**	**-0.780**	**0.819**	0.222	**0.827**
Y	**0.307**	**0.546**	**0.851**	**0.905**	**0.823**	**-0.786**	**0.700**	0.396	**0.759**
Zr	-0.165	**-0.397**	**-0.713**	**-0.751**	**-0.738**	**0.625**	**-0.617**	-0.296	**-0.618**
Ba	**0.529**	**0.625**	**0.646**	**0.576**	**0.637**	**-0.569**	**0.766**	0.135	**0.670**
La	1	**0.728**	**0.411**	**0.342**	**0.354**	**-0.616**	**0.584**	0.294	**0.640**
Ce		1	**0.632**	**0.635**	**0.610**	**-0.691**	**0.645**	0.255	**0.648**
Pb			1	**0.931**	**0.883**	**-0.809**	**0.802**	0.179	**0.856**
Th				1	**0.894**	**-0.800**	**0.725**	0.349	**0.809**
U					1	**-0.721**	**0.694**	0.330	**0.801**
ordered Microcline feldspar						1	**-0.730**	-0.083	**-0.729**
intermediate Microcline feldspar							1	-0.103	**0.650**
Sanidine feldspar								1	0.129
Orthoclase feldspar									1

Table S5C: Correlation coefficients derived from elemental concentrations expressed as molar ratios (continued).

	Albite feldspar (Cleavelandite)	Oligoclase feldspar	Labradorite feldspar	Calcite	Dolomite	Hematite	Goethite
As	**0.751**	**0.748**	0.040	**0.959**	**0.927**	**0.665**	0.384
Br	**0.709**	**0.589**	-0.170	**0.944**	**0.897**	**0.619**	0.242
Rb	**0.711**	**0.625**	-0.014	**0.981**	**0.913**	**0.651**	**0.440**
Sr	**0.854**	**0.722**	0.208	**0.928**	**0.865**	**0.560**	**0.434**
Y	**0.722**	**0.524**	-0.056	**0.905**	**0.920**	**0.623**	0.332
Zr	**-0.600**	-0.411	0.127	**-0.775**	**-0.732**	**-0.502**	-0.288
Ba	**0.825**	**0.719**	**0.548**	**0.652**	**0.621**	**0.482**	0.270
La	**0.724**	**0.470**	0.276	**0.685**	**0.690**	**0.558**	0.186
Ce	**0.575**	**0.567**	0.220	**0.756**	**0.739**	**0.700**	0.260
Pb	**0.797**	**0.700**	0.132	**0.937**	**0.860**	**0.614**	0.358
Th	**0.735**	**0.624**	-0.006	**0.977**	**0.934**	**0.631**	**0.448**
U	**0.787**	**0.584**	0.143	**0.886**	**0.793**	**0.483**	**0.447**
ordered Microcline feldspar	**-0.703**	-0.398	0.165	**-0.790**	**-0.795**	**-0.580**	0.015
intermediate Microcline feldspar	**0.755**	**0.561**	0.222	**0.690**	**0.636**	**0.493**	0.192
Sanidine feldspar	0.134	0.144	-0.119	0.265	**0.455**	0.204	0.352
Orthoclase feldspar	**0.737**	**0.741**	0.001	**0.850**	**0.747**	**0.543**	0.178
Albite feldspar (Cleavelandite)	1	**0.457**	0.215	**0.702**	**0.656**	0.256	0.162
Oligoclase feldspar		1	0.405	**0.639**	**0.558**	**0.533**	**0.431**

Table S5C: Correlation coefficients derived from elemental concentrations expressed as molar ratios (continued).

	Maghemite	Apatite	Quartz	Total non-clays	disordered Kaolinite	Na-Smectite	Ca-smectite
As	**0.717**	**0.836**		**0.828**	0.372	**0.543**	**0.886**
Br	**0.772**	**0.814**		**0.814**	**0.478**	**0.570**	**0.864**
Rb	**0.617**	**0.817**		**0.896**	0.421	**0.596**	**0.913**
Sr	**0.633**	**0.753**		**0.754**	0.410	**0.481**	**0.806**
Y	**0.601**	**0.751**		**0.796**	0.293	**0.513**	**0.824**
Zr	**-0.533**	**-0.622**		**-0.680**	-0.328	**-0.429**	**-0.696**
Ba	**0.458**	**0.444**		**0.429**	0.239	0.268	**0.527**
La	0.400	0.421		**0.570**	0.014	**0.471**	**0.642**
Ce	0.340	**0.497**		**0.704**	0.078	**0.623**	**0.762**
Pb	**0.653**	**0.760**		**0.807**	**0.480**	**0.467**	**0.836**
Th	**0.637**	**0.815**		**0.877**	0.373	**0.602**	**0.898**
U	**0.557**	**0.700**		**0.794**	0.306	**0.507**	**0.806**
ordered Microcline feldspar	**-0.536**	**-0.569**		**-0.675**	-0.314	**-0.449**	**-0.727**
intermediate Microcline feldspar	0.329	0.397		**0.452**	0.305	0.373	**0.556**
Sanidine feldspar	0.291	**0.432**		0.269	-0.149	0.004	0.253
Orthoclase feldspar	**0.825**	**0.742**		**0.755**	0.331	0.423	**0.820**
Albite feldspar (Cleavelandite)	**0.608**	**0.507**		**0.442**	0.334	0.221	**0.513**
Oligoclase feldspar	**0.518**	**0.594**		**0.546**	0.209	0.271	**0.621**

Table S5C: Correlation coefficients derived from elemental concentrations expressed as molar ratios (continued).

	Ferruginous smectite	Illite (1Md) + Dioct. Mica + Smectite	Illite (1M)	Biotite (1M)	Phlogopite (2M1)	Fe-Chlorite (Tusc)	Mg-Chlorite (Clinochlore)
As	**0.841**	**0.887**	**0.582**	0.310	**0.878**	**0.769**	**0.890**
Br	**0.867**	**0.779**	0.420	0.399	**0.872**	**0.742**	**0.862**
Rb	**0.861**	**0.930**	**0.492**	0.410	**0.891**	**0.690**	**0.913**
Sr	**0.785**	**0.867**	**0.602**	0.242	**0.863**	**0.763**	**0.804**
Y	**0.798**	**0.854**	**0.487**	0.288	**0.814**	**0.695**	**0.828**
Zr	**-0.697**	**-0.681**	-0.333	-0.319	**-0.707**	**-0.530**	**-0.713**
Ba	**0.519**	**0.664**	**0.702**	-0.083	**0.677**	**0.701**	**0.508**
La	**0.577**	**0.649**	**0.611**	0.085	**0.656**	**0.470**	**0.590**
Ce	**0.603**	**0.818**	**0.661**	0.199	**0.752**	**0.520**	**0.704**
Pb	**0.847**	**0.882**	**0.536**	0.304	**0.894**	**0.767**	**0.849**
Th	**0.850**	**0.910**	**0.499**	0.392	**0.904**	**0.674**	**0.900**
U	**0.792**	**0.814**	**0.548**	0.347	**0.847**	**0.563**	**0.796**
ordered Microcline feldspar	**-0.739**	**-0.755**	**-0.437**	-0.068	**-0.742**	**-0.805**	**-0.719**
intermediate Microcline feldspar	**0.502**	**0.761**	**0.666**	-0.155	**0.709**	**0.830**	**0.510**
Sanidine feldspar	0.217	0.233	0.085	0.300	0.162	-0.032	0.318
Orthoclase feldspar	**0.878**	**0.724**	**0.541**	0.256	**0.880**	**0.727**	**0.837**
Albite feldspar (Cleavelandite)	**0.638**	**0.543**	**0.526**	-0.047	**0.667**	**0.758**	**0.514**
Oligoclase feldspar	**0.552**	**0.689**	**0.604**	0.213	**0.695**	**0.468**	**0.633**

Table S5C: Correlation coefficients derived from elemental concentrations expressed as molar ratios (continued).

	Muscovite (2M1)	Total clays
As	**0.978**	**0.914**
Br	**0.943**	**0.902**
Rb	**0.974**	**0.952**
Sr	**0.950**	**0.854**
Y	**0.913**	**0.860**
Zr	**-0.771**	**-0.733**
Ba	**0.712**	**0.566**
La	**0.709**	**0.628**
Ce	**0.761**	**0.744**
Pb	**0.950**	**0.899**
Th	**0.977**	**0.935**
U	**0.891**	**0.843**
ordered Microcline feldspar	**-0.783**	**-0.770**
intermediate Microcline feldspar	**0.714**	**0.604**
Sanidine feldspar	0.304	0.225
Orthoclase feldspar	**0.878**	**0.852**
Albite feldspar (Cleavelandite)	**0.743**	**0.584**
Oligoclase feldspar	**0.693**	**0.624**

Table S5C: Correlation coefficients derived from elemental concentrations expressed as molar ratios (continued).

	Labradorite feldspar	Calcite	Dolomite	Hematite	Goethite
Labradorite feldspar	1	-0.088	-0.164	0.044	0.289
Calcite		1	**0.928**	**0.621**	**0.432**
Dolomite			1	**0.696**	0.321
Hematite				1	-0.007
Goethite					1

Table S5C: Correlation coefficients derived from elemental concentrations expressed as molar ratios (continued).

	Maghemite	Apatite	Quartz	Total non-clays	disordered Kaolinite	Na-Smectite	Ca-smectite
Labradorite feldspar	-0.286	-0.216		-0.176	-0.217	-0.011	-0.094
Calcite	**0.714**	**0.877**		**0.920**	**0.454**	**0.610**	**0.934**
Dolomite	**0.684**	**0.823**		**0.803**	0.372	**0.493**	**0.840**
Hematite	0.332	**0.443**		**0.616**	0.065	**0.486**	**0.729**
Goethite	0.065	**0.504**		**0.447**	0.114	0.375	**0.372**
Maghemite	1	**0.814**		**0.627**	**0.507**	0.156	**0.640**
Apatite		1		**0.864**	**0.538**	0.396	**0.825**
Quartz							
Total non-clays				1	0.346	**0.702**	**0.971**
disordered Kaolinite					1	-0.141	**0.253**
Na-Smectite						1	**0.737**
Ca-smectite							1

Table S5C: Correlation coefficients derived from elemental concentrations expressed as molar ratios (continued).

	Ferruginous smectite	Illite (1Md) + Dioct. Mica + Smectite	Illite (1M)	Biotite (1M)	Phlogopite (2M1)	Fe-Chlorite (Tusc)	Mg-Chlorite (Clinochlore)
Labradorite feldspar	-0.263	0.118	**0.539**	-0.280	-0.015	-0.033	-0.177
Calcite	**0.902**	**0.890**	**0.450**	**0.478**	**0.903**	**0.686**	**0.943**
Dolomite	**0.803**	**0.848**	**0.426**	0.385	**0.820**	**0.701**	**0.860**
Hematite	**0.510**	**0.776**	**0.570**	0.202	**0.584**	**0.519**	**0.667**
Goethite	0.192	**0.458**	0.204	**0.465**	0.312	-0.081	0.381
Maghemite	**0.862**	0.417	0.149	0.402	**0.680**	**0.633**	**0.743**
Apatite	**0.858**	**0.691**	0.191	**0.687**	**0.715**	**0.524**	**0.906**
Quartz							
Total non-clays	**0.879**	**0.834**	0.340	**0.634**	**0.795**	**0.465**	**0.976**
disordered Kaolinite	**0.535**	0.230	-0.322	**0.548**	**0.401**	0.411	0.374
Na-Smectite	0.411	**0.657**	**0.515**	0.229	**0.572**	0.269	**0.611**
Ca-smectite	**0.862**	**0.890**	**0.520**	**0.495**	**0.834**	**0.575**	**0.976**
Ferruginous smectite	1	**0.689**	0.232	**0.521**	**0.842**	**0.628**	**0.923**
Illite (1Md) + Dioct. Mica + Smectite		1	**0.640**	0.297	**0.830**	**0.642**	**0.849**
Illite (1M)			1	-0.302	**0.478**	**0.525**	0.390
Biotite (1M)				1	0.323	-0.126	**0.572**
Phlogopite (2M1)					1	**0.675**	**0.836**
Fe-Chlorite (Tusc)						1	**0.583**
Mg-Chlorite (Clinochlore)							1

Table S5C: Correlation coefficients derived from elemental concentrations expressed as molar ratios (continued).

	Muscovite (2M1)	Total clays
Labradorite feldspar	-0.033	-0.139
Calcite	**0.992**	**0.973**
Dolomite	**0.940**	**0.872**
Hematite	**0.632**	**0.667**
Goethite	0.422	0.370
Maghemite	**0.746**	**0.713**
Apatite	**0.877**	**0.873**
Quartz		
Total non-clays	**0.883**	**0.972**
disordered Kaolinite	**0.438**	0.424
Na-Smectite	**0.556**	**0.651**
Ca-smectite	**0.913**	**0.977**
Ferruginous smectite	**0.893**	**0.930**
Illite (1Md) + Dioct. Mica + Smectite	**0.886**	**0.880**
Illite (1M)	**0.499**	0.420
Biotite (1M)	**0.428**	**0.531**
Phlogopite (2M1)	**0.910**	**0.888**
Fe-Chlorite (Tusc)	**0.721**	**0.637**
Mg-Chlorite (Clinochlore)	**0.928**	**0.985**

Table S5C: Correlation coefficients derived from elemental concentrations expressed as molar ratios (continued).

	Muscovite (2M1)	Total clays
Muscovite (2M1)	1	**0.953**
Total clays		1
Total		

Figure S1

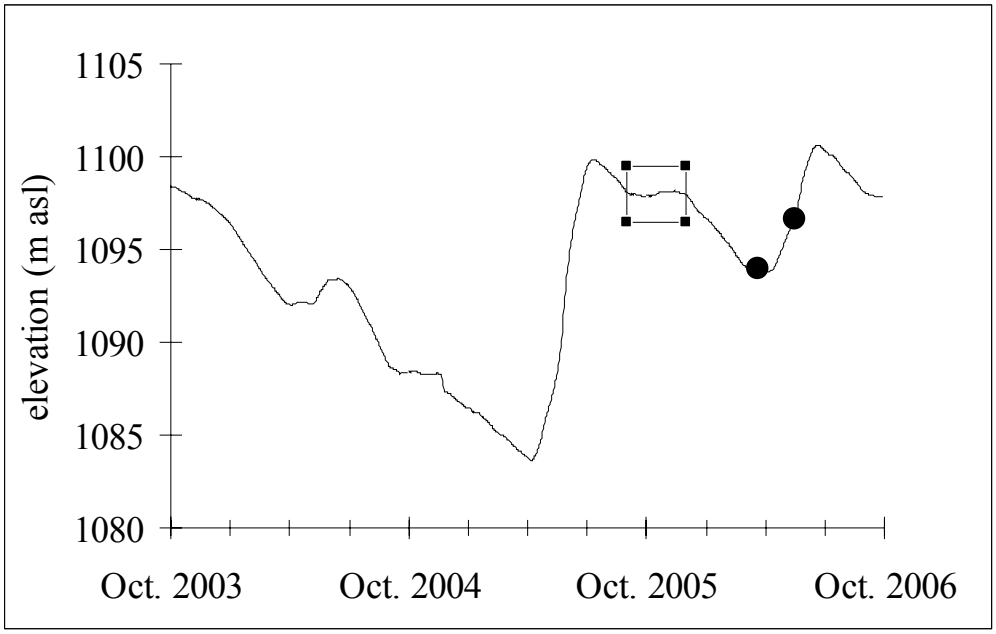

Figure S1: Water surface elevation of Lake Powell, hydrologic years 2004-2006. The square highlights three months of near-steady lake levels in advance of the lakebed sample collection, indicated by circles.

Figure S2

Figure S2: Layers of sediment at the 249.5 km delta shoreline location. The left panel shows sandy surface sediment underlain by a clay layer and another sandy layer. The right panel shows the same subsurface sandy layer as in the right panel underlain by another clay layer. Orange caps of core tubes are 5 cm in diameter.

Figure S3

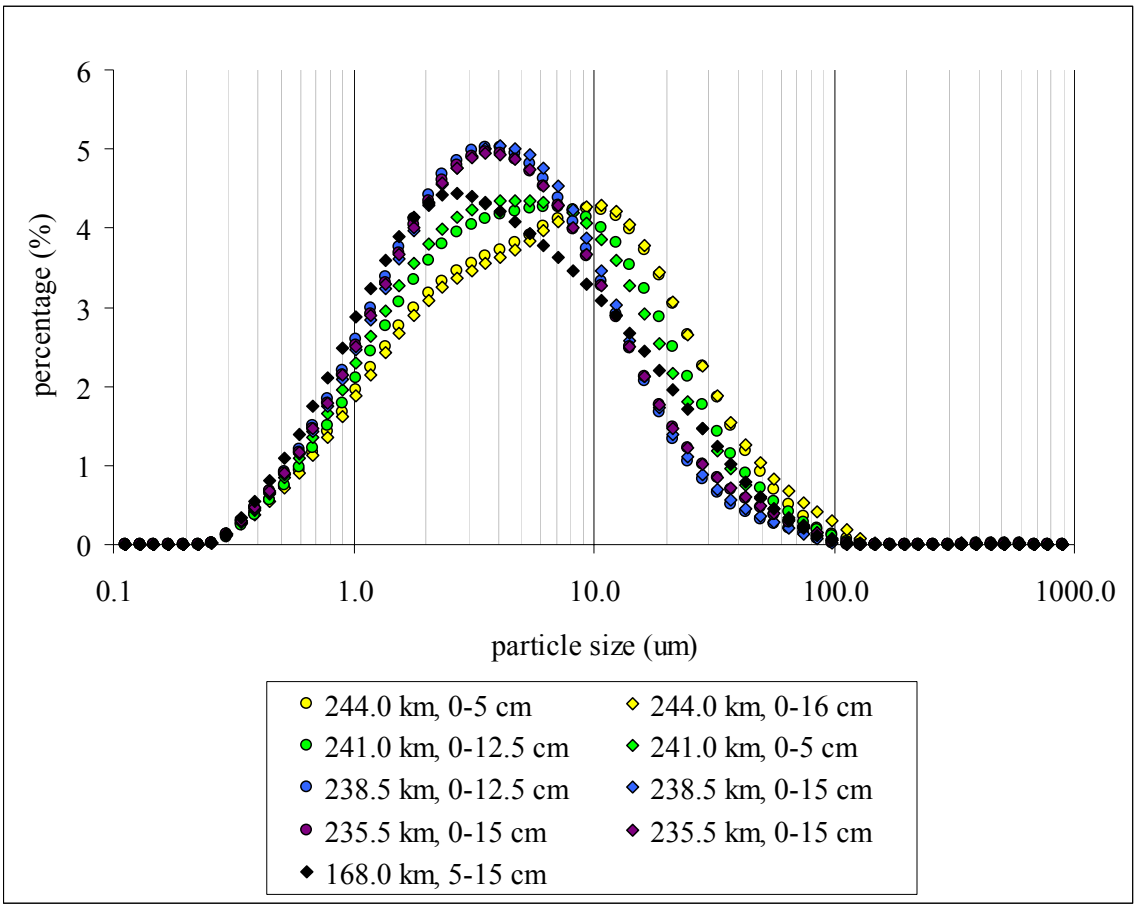

Figure S3: Particle size distributions of lakebed surface samples collected from delta sediment in March 2006.

Figure S4

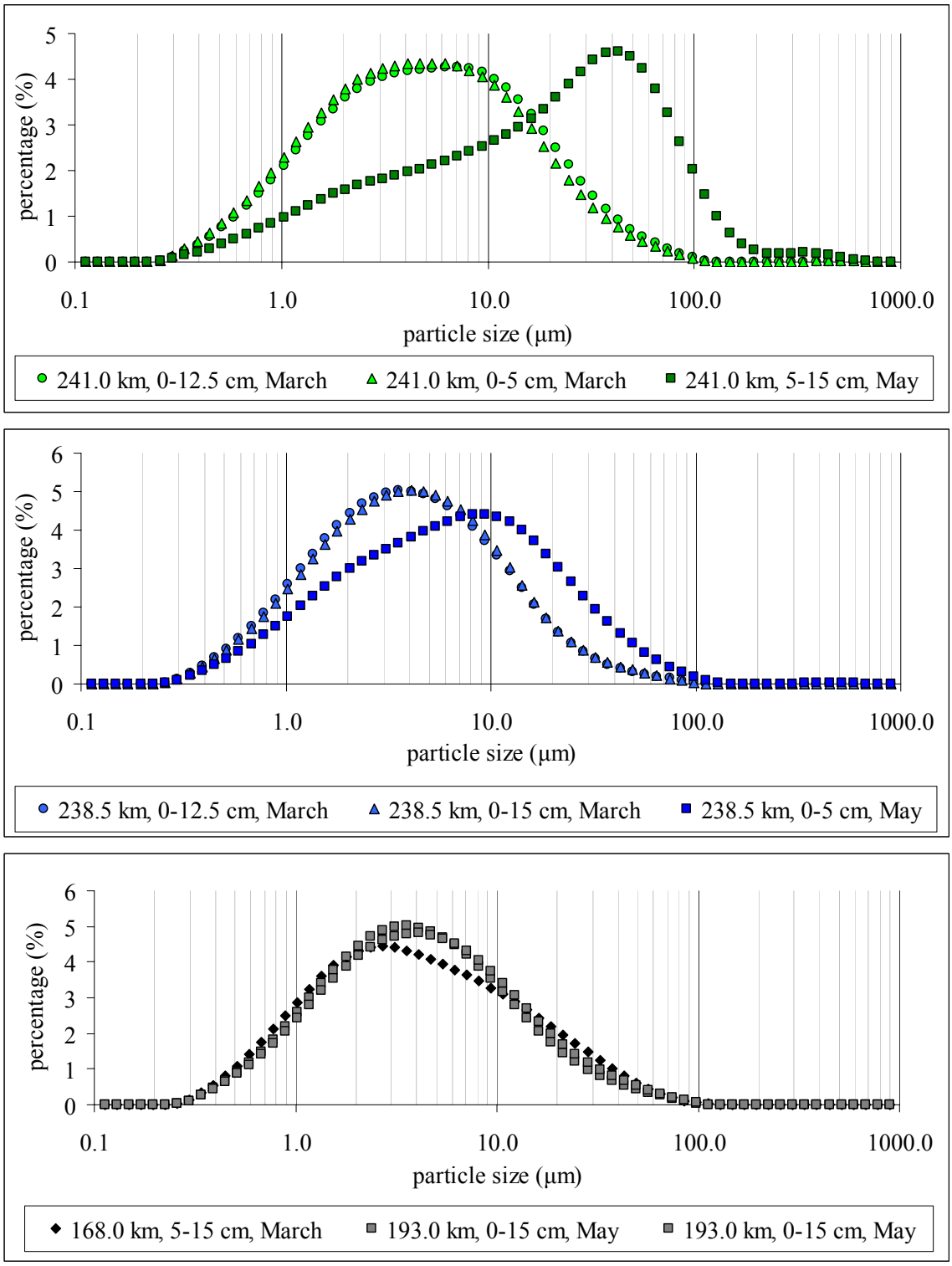

Figure S4: Particle size distributions of lakebed surface samples collected in March and May 2006. Upper panel: 241.0 km location; middle panel: 238.5 km location; lower panel: 168.0 and 178.0 km locations.

Figure S5

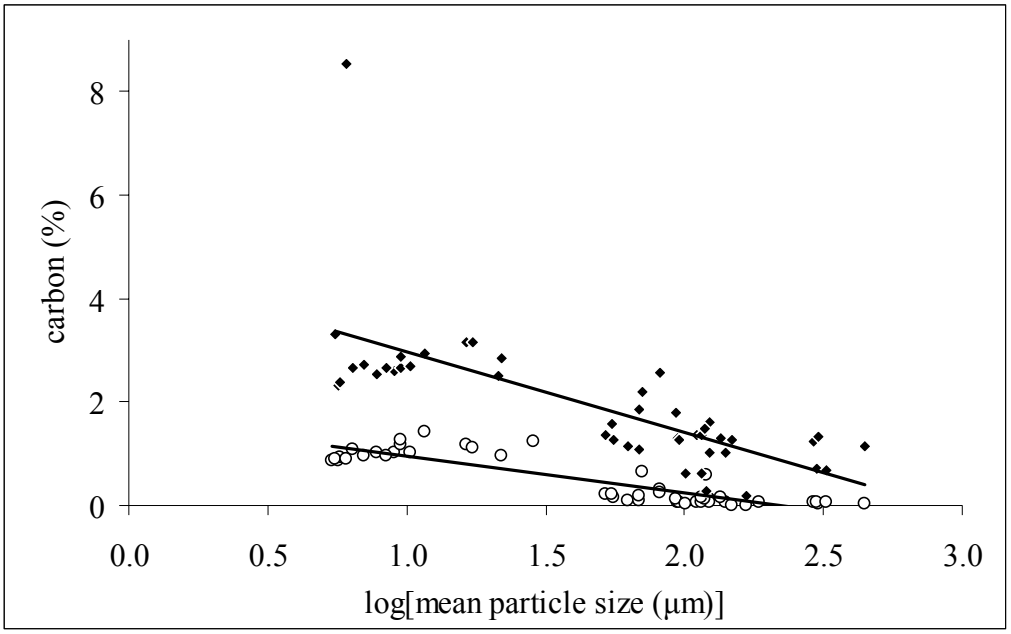

Figure S5: Total (♦) and organic (○) carbon in Lake Powell sediment. This graph does not include samples from cores TC A, TC B, or 247.5 C, in which plant debris were observed.

Figure S6

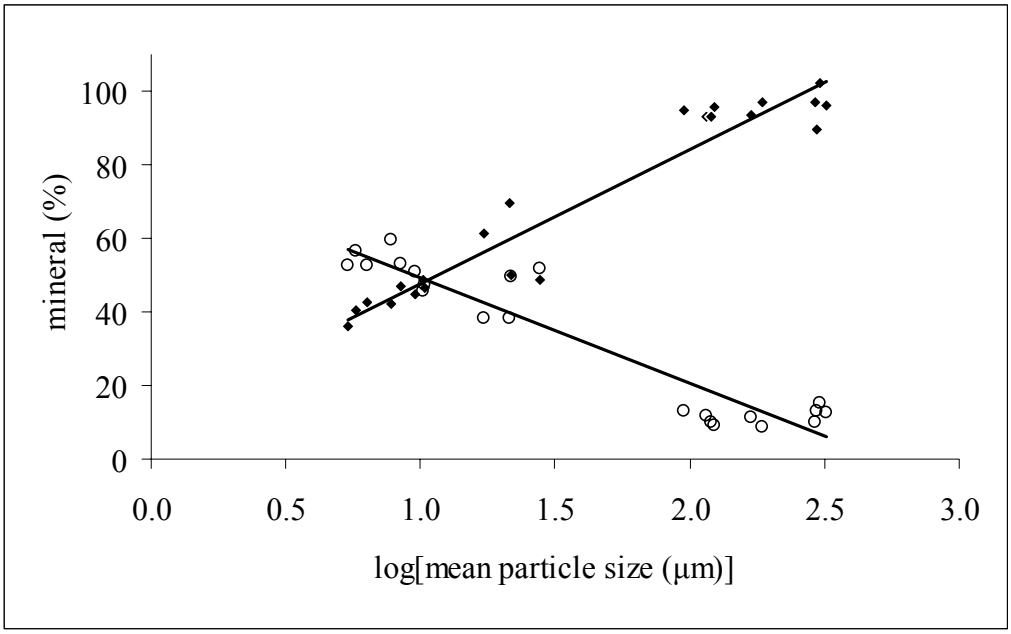

Figure S6: Concentrations of non-clay (♦) and clay (○) minerals in Lake Powell sediment.

Chapter 5

PHOSPHORUS RELEASE DURING SEDIMENT RESUSPENSION IN THE DELTA REGION OF A LARGE, OLIGOTROPHIC RESERVOIR (LAKE POWELL, UTAH, USA) DURING DECLINING WATER LEVEL

Richard A. Wildman, Jr. and Janet G. Hering

(in preparation for *Water Research*)

Abstract

At Lake Powell, a reservoir on the Colorado River, USA, low surface elevation may affect water quality. The exposed sediment delta is resuspended by the inflowing river, and this may release phosphorus into the water column. In the upper region of the reservoir, we measured dissolved phosphorus and trace elements during base and increased flow. We also performed phosphorus sorption experiments and sequential extractions on delta sediment. At base flow, resuspension of the exposed delta sediment increases the dissolved phosphorus concentration, whereas, at increased flow, sediment resuspension attenuates it. Seasonal advective currents appear to control solute transport in the lake. Phosphate is dominantly associated with calcite and apatite in sediment, and fine sediment sorbs much more phosphate than coarse sediment. Observed phytoplankton blooms during drawdown may result from a specific hydrologic condition in which

sediment resuspension during base flow releases phosphate and an overflow or interflow current transports it to the photic zone.

1. Introduction

Dissolved phosphorus (P) availability limits primary productivity in many freshwater ecosystems, and addition of dissolved P to a lake can cause dramatic increases in phytoplankton abundance (Schindler et al. 2008). Such phytoplankton blooms can be a serious water quality concern, as they have been associated with the presence of algal toxins (Naselli-Flores et al. 2007) and hypolimnetic anoxia (Nürnberg 1995). Oligotrophic lakes are especially sensitive to small changes in dissolved P (Müller et al. 2007), which indirectly affect fish populations (Wüest et al. 2007).

In unpolluted rivers, the vast majority of P is transported in particulate form (Meybeck 1982), so P is deposited to bottom sediments in lakes by settling. Subsequent release to the water column, a process dependent on P speciation in the solid phase, can be an important source of bioavailable P in lakes (Gächter and Müller 2003). In various environments, P has been shown to associate primarily with calcium (Ca)-bearing and apatite minerals (Blecker et al. 2006, Zhang et al. 2004), iron (Fe)-oxide minerals, or organic carbon (Jordan et al. 2008). Although the partitioning of P between the dissolved and these various solid phases is expected to reach equilibrium during transport over hundreds of km in a river, sedimentation leads to a new set of chemical conditions (e.g., due to the absence of oxygen below the sediment-water interface) that induce new chemical reactions that can change the speciation of P. Specifically, reductive dissolution of Mn- or Fe-oxide minerals or decomposition of organic matter can release P into

porewater or a labile sediment-associated phase. Once these reactions have occurred, diffusion (Ahlgren et al. 2006) or sediment resuspension (Zhang and Huang 2007, Niemistö et al. 2008) can be important sources of P to overlying water in quiescent or turbulent settings, respectively.

Sediment resuspension is common in reservoirs subject to drawdown. When water surface elevation has been maintained for several years and sediment deltas have accumulated near river inflows, a significant decrease of water level induces resuspension of erodible delta sediment by reservoir tributaries (Riggsbee et al. 2007, Cheng and Granata 2007, Snyder et al. 2006). Sediment resuspension induced by drawdown is important at Lake Powell, a large reservoir on the Colorado River in Utah and Arizona. There, decreased water levels have resulted in a doubling of suspended load of the inflowing river (Vernieu 1997) and transport of > 1 km^3 of sediment more than 100 km down the length of the reservoir (Pratson et al. 2008).

In Lake Powell, P limits primary productivity (Gloss et al. 1980), which is directly linked to fish populations (Vatland and Budy 2007). During a current drawdown, increases in surface water chlorophyll may be linked to resuspension of delta sediment (Chapter 4), suggesting that this process represents an important new source of P to the water column. Therefore, this study assesses the potential for resuspension of delta sediment to supply bioavailable P for primary productivity in Lake Powell. Phosphorus release is expected to depend on physical and mineralogical characteristics of the sediment as well as the speciation of P in the solid phase.

2. Sedimentation and Phosphorus in Lake Powell

Closed in 1963, Glen Canyon Dam (GCD) impounds the Colorado River in Lake Powell on the arid Colorado Plateau. This narrow, dendritic reservoir (Figure 1) can be up to 299 km long and up to 178 m deep. This reservoir is a major recreation destination as well as a crucial water storage component of the Colorado River, which supplies water to 25 million people and 6070 km^2 of farmland downstream. The Colorado River Basin has experienced a severe drought since 2000 (Woodhouse et al. 2006; Clayton 2008), yet GCD has maintained minimum releases as required by law, so the reservoir has been drawn down by as much as 42 m.

Sediment in the reservoir comes primarily from erodible sedimentary rocks of the Colorado Plateau and, to a lesser extent, from the Southern Rocky Mountains, which are formed by a variety of limestones, igneous, and metamorphic formations (Spahr et al. 2000; Anderson et al. 2003). In the lower portion of the reservoir, calcite precipitates (Reynolds 1978) and contributes ~0.08% of the sediment load to the entire reservoir (Condit et al. 1978). The sedimentation rate of the reservoir has been estimated at 21-52 Mt yr^{-1} (Ferrari 1988, Horowitz et al. 2001), implying a lifetime of 601-1488 years. Two large sediment deltas have aggraded in the inflow regions of the two main tributaries, the Colorado and San Juan Rivers, which contribute 80% and 15% of the water to the lake, respectively, yet equal amounts of sediment (Potter and Drake 1989, Ferrari 1988). Aeolian deposition contributes ~0.03% of the entire sediment load to the reservoir (Condit et al. 1978) and no information is available about how this might vary during period of sustained dry or wet weather in the Colorado Plateau.

This sedimentation is important for P transport into the reservoir, since 96-98% of P enters the lake in particulate form and is deposited in the lakebed (Horowitz et al. 2001, Gloss et al. 1981). When Lake Powell is not drawn down, annual loads of P are correlated with inflows and thus highly variable, approximately ranging from 4000-14000 t yr^{-1} total P and 240-390 t yr^{-1} total dissolved P (Gloss et al. 1981, Horowitz et al. 2001). The particulate P load is generally associated with clay minerals, which are deposited primarily in the lower portions of the river deltas (Gloss et al. 1980, Chapter 4). The source of this phosphorus in the basin has not been precisely determined, but it is likely to come from the limited agricultural and urban land use in the Upper Colorado River Basin (Spahr et al. 2000).

Yearly hydrologic patterns affect phosphorus mobility in Lake Powell. Seasonal overflow (approximately May-October) and underflow (approximately January-March) density currents transport dissolved P through the epilimnion and hypolimnion of the reservoir, respectively (Johnson and Merritt 1979, Potter and Drake 1989, Gloss et al. 1980). However, these currents are not equal in volume: the majority of P enters the reservoir in an overflow during spring snowmelt, which brings 60% of the yearly inflow to the reservoir during May-July (Potter and Drake 1989). Once in the epilimnion, dissolved P is expected to be transported to the sediment by settling of biomass and scavenging by calcite precipitation (Gloss et al. 1980). Lake Powell retains 74% of dissolved P that enters via all sources, with the underflow currents probably moving the rest below the photic zone and eventually through the dam (Gloss et al. 1981). Although the yearly pattern of density currents in Lake Powell varies, underflow currents are thought to transport sufficient dissolved oxygen (DO) to the sediment surface to prevent

the frequent sediment anoxia that would promote diffusion of P from lakebed sediment into the hypolimnion (Gloss et al. 1980).

Monitoring measurements showing a dissolved N:P ratio of 29:1 (i.e., far in excess of the Redfield ratio), laboratory algal assays, and *in situ* experiments have shown that P limits primary productivity in Lake Powell (Gloss 1977). More recent measurements have shown that agriculture in the valleys of the Colorado Plateau contributes notable amounts of nitrogen (N), P, and sediment to the Colorado River (Spahr et al. 2000). While we know of no subsequent studies examining the effects of agricultural development that has occurred since the earliest studies on Lake Powell, it seems reasonable that incoming Colorado River water would still be deficient in dissolved P relative to dissolved N because of sorption of P to suspended sediment.

3. Experimental

3.1. Hydrology

Lake level data for this study are taken from U.S. Bureau of Reclamation records (UBSR 2008), and flow on the Colorado River into Lake Powell is estimated by adding U.S. Geological Survey (USGS) stream gaging data from the Colorado River near Cisco, Utah and the Green River near Green River, Utah (USGS 2008).

3.2. Sample Collection and Processing

This study focuses on water and sediment chemistry of the Colorado River delta of Lake Powell, which is assumed to be generally representative of processes in the San Juan River delta. Water samples were collected on 21-23 March and 16-18 May 2006

from various depths along a longitudinal transect in the Colorado River inflow region of Lake Powell. Locations, identified by their distance from GCD (rounded to the nearest 0.5 km), were selected between the confluence of the Green and Colorado Rivers and the uppermost extent of Lake Powell (at 317.0 km above GCD), through the delta region (245.0 km, 241.0 km, 238.5 km, and 235.5 km), and below the delta (193.5 km and 178.0 km; Figure 1). Samples were collected from surface and bottom waters with a Van Dorn bottle. When the minimum DO (measured with a multiparameter instrument) did not occur in the surface or bottom water, a sample was collected at this depth as well. Not every location was sampled in both March and May. Water clarity was estimated with a secchi disk at 1-2 locations during each research cruise.

Shoreline effects were not considered in this study because shoreline runoff contributes < 1% of the total inflows to Lake Powell and because exchange of water between side canyons, where most of the shoreline perimeter is located, and the thalweg is minimal (Hart et al. 2004). Although the initial flooding of a reservoir is known to release nutrients from newly-submerged riparian biomass (Rydin et al. 2008), the region of Lake Powell studied is desert landscape with minimal vegetation and much of the thalweg is lined with vertical canyon walls. It is likely that nutrient release during initial reservoir flooding was minimal, and any such effects would have subsided well before the current study. More recently, riparian areas of the Colorado River, including those exposed by low water levels of Lake Powell, have been colonized by tamarisk (various species of the genus *Tamarix*). However, this plant is very tolerant of flooding (Potter and Drake 1989), so we do not expect the water level changes that occurred during the short time of this study to lead to nutrient enrichment due to decaying riparian biomass.

Samples were filtered through 0.2 μm polypropylene filters and stored in new, acid washed (1 M HCl), high-density polyethylene bottles. To preserve samples intended for trace element analysis, concentrated ultrapure HCl was added to a final concentration of 2%. Samples intended for P analysis were preserved with the magnesium-induced coprecipitation (MAGIC) method (Thompson-Bulldis and Karl 1998) as modified by Colman et al. (*in preparation*). Briefly, 1 mL of 2.25 M $MgCl_2$ was added to a ~100 mL water sample, followed by 1.25 mL of 1 M NaOH. This leads to precipitation of a MgOH flocculent mass that quantitatively scavenges phosphate and remains stable indefinitely. All samples were transported on ice to the laboratory, where they were stored at 5°C.

"Lakebed" sediment samples were collected concurrently with water samples at locations in (245.0, 241.0, 238.5, and 235.5 km above GCD) and below (168.0 km above GCD) the main portion of Colorado River delta of Lake Powell (Figure 1). Since these locations probably only sample the lower portion of the delta (Pratson et al. 2008), a 1.5-m series of stacked sediment cores was collected from a shoreline location near Hite Marina, 249.5 km above GCD (Figure 1). At this location, Colorado River sediment deposited when lake levels were higher was exposed above the water level and accessible from land. Distinct sediment layers of coarse (mean size > 400 μm) and fine (mean size < 20 μm) particles (Chapter 4) imply that this location has received sediment deposited at very different lake levels such that it coincided with the uppermost part of the delta at low lake levels and the far downstream end of the delta at high lake levels. This provides a useful contrast to the lakebed samples, which were collected from different locations at very similar lake levels.

All sediment samples were collected in plastic, 5 cm × 1 m core liners, transported on ice to the laboratory, and frozen ≤ 3 d after collection. Cores were sampled anoxically based on visual inspection, leading to "surface" (0-30 cm) samples from all lakebed cores and "deep" (25-80 cm) samples from several cores. Eight samples were collected from the shoreline cores from layers of fine particle size at depth ranges -132 to -109 cm (negative values indicate depths above the sediment-water interface), -47 to 14 cm and 14 to 20 cm and from layers of coarse particle size at -109 to -77 cm and -77 to -47 cm. For more information on the sampling and characterization of sediment used in this study, see Chapter 4.

3.3. Analysis of Dissolved Chemical Constituents

Water samples preserved for trace-element analysis were diluted as necessary and analyzed with an Agilent 4500 inductively-coupled plasma mass spectrometer (ICP-MS) for Li, Ti, Cr, Mn, Zn, As, Se, Br, Cd, Pb, and U. ICP-MS data were calibrated with multi-element calibration solutions prepared from ICP-grade single element standards for each element (EMD Chemicals). Analytical relative standard deviations were < 5%.

Water samples preserved by MAGIC were centrifuged and MgOH pellets were dissolved in 0.1 M trace-metal-grade HNO_3 following Colman et al. (*in preparation*). Samples were concentrated by re-precipitating MgOH through a second addition of 1 M NaOH. This new precipitate was again centrifuged and dissolved in acid. Samples were treated with a reducing agent to minimize arsenate interference (Johnson 1971) and analyzed for soluble reactive phosphorus (SRP) with the molybdate-blue method (Murphy and Riley 1962) on a UV-visible spectrophotometer at a wavelength of 883 nm.

This method involves treatment of a sample with a "mixed reagent" containing 24 mM ammonium paramolybdate ($(NH_4)_6Mo_7O_{24}\cdot 4H_2O$), 2.42 M sulfuric acid, 0.31 M ascorbic acid, and 4.2 mM potassium antimonyl tartrate in a ratio of 1:2.5:1:0.5. The sample, reducing agent, and mixed reagent were combined at a ratio of 10:1:1. All analyses took place 30-120 minutes after the addition of the mixed reagent, as recommended by previous researchers (Sjosten and Blomqvist 1997). Results were calibrated with potassium hydrogen phosphate (K_2HPO_4) solutions in distilled water that were carried through the MAGIC procedure along with the samples, and the detection limit was 0.030 μM.

Since this study focuses on the release of bioavailable P from sediment, only SRP was measured; this parameter can be taken to represent a minimum value for the bioavailable dissolved P in a system. Total dissolved P was not measured because it has been known to overpredict bioavailable P in the water column (Ellison and Brett 2006).

3.4. Sequential Extraction

Speciation of P in the solid phase was assessed by a sequential extraction, a sequence of reactions of sediment dispersed in successive solutions designed to target phosphorus bound in operationally-defined geochemical phases. Although limitations to sequential extractions, such as lack of specificity or sorption or precipitation of solubilized phosphorus onto the remaining mineral surface, have been noted (e.g., Peltier et al. 2006), this measurement technique provides valuable information about the geochemical phases in which phosphorus is present. The method of Ruttenberg (1992) as modified by Zhang et al. (2004) was selected because it differentiates between reactive

Fe-oxide solids and calcite (Table 1), both of which are expected to be present in Lake Powell sediment. Major steps were: 1) magnesium chloride ($MgCl_2$), targeting exchangeable P; 2) bicarbonate plus dithionite added in solid form (BD), targeting reactive Fe(III)-bound P; 3) sodium acetate buffered to pH 3.7 with acetic acid, targeting P bound to authigenic carbonate, fluoroapatite, calcite, or biogenic apatite; 4) hydrochloric acid (HCl), targeting P bound to detrital apatite; and 5) heating at 550°C followed by hydrochloric acid (ash+HCl), targeting organic P. To minimize error due to re-sorption or re-precipitation of extracted P, steps 1-3 were followed by at least one additional treatment of each of magnesium chloride and distilled water.

Samples were not dried before the extraction, which was performed in 50 mL polypropylene centrifuge tubes shaken end-over-end. After each treatment, tubes were centrifuged and the supernatant was filtered through a 0.45 μm filter and analyzed for SRP with the molybdate-blue method using separate sets of calibration standards that matched the respective extractant solutions. Since color development of the molybdate-blue reaction is dependent on pH (Zhang et al. 2004), before the addition of the reducing agent and the mixed reagent, it was necessary to add 1.20 mL of 1 M NaOH to 1.35 mL of sample in an HCl matrix or 0.4 mL of 178 mM HCl to 0.1 mL sample in a BD matrix. Before analysis, all BD solutions were left open to air for ≥ 3 d to allow excess dithionite to oxidize and leave the solution as SO_2 (Zhang et al. 2004). The SRP concentrations of multiple parts of each step (i.e., the chemical unique to that step and any subsequent washes with water or $MgCl_2$) were added together to give the SRP bound in a given geochemical phase.

3.5. Sorption Experiments

Sorption experiments were performed without drying sediment samples in order to avoid any geochemical changes (e.g., oxidation) to the sediment matrix and to retain the original porewater in the sediment samples. Frozen sediment was thawed and portioned into polypropylene centrifuge tubes such that wet masses ranged from 0.10-0.28 g (mean = 0.16 g, standard deviation (σ) = 0.04). Separate portions of the sediment samples were freeze-dried to determine water content; the wet masses used for the sorption experiments correspond to dry masses of 0.06-0.17 g (mean = 0.09 g, σ = 0.02 g). Although it has been shown that anoxic resuspension of sediment releases much more P than oxic resuspension (Mitchell and Baldwin 1998), no effort was made to maintain anoxic conditions once sediment samples were thawed because it was assumed that the turbulent Colorado River would be oxygenated as it resuspends sediment.

Sediment samples were resuspended in 44 mL artificial Lake Powell water (ALPW) made following Reynolds (1978). Sodium bicarbonate ($2.00 \cdot 10^{-3}$ M), calcium sulfate ($1.30 \cdot 10^{-3}$ M), magnesium chloride ($7.70 \cdot 10^{-4}$ M), magnesium sulfate ($3.00 \cdot 10^{-4}$ M), potassium bicarbonate ($7.00 \cdot 10^{-5}$ M), and sodium trisilicate ($3.50 \cdot 10^{-5}$ M) were combined in distilled water with vigorous stirring overnight. After all solids had dissolved, pH was adjusted to 8.05 with 1 M HCl, following Mayer and Gloss (1980). Eight subsamples of each sediment sample were shaken on an end-over-end shaker for $\geq$ 96 h in the dark (Zhang and Huang 2007, Müller et al. 2006). After this equilibration period, a total of 1 additional mL (final volume = 45 mL) of ALPW and K_2HPO_4 was added to give final concentrations of 0.00 µM, 0.05 µM, 0.10 µM, 0.25 µM, 0.50 µM, 0.75 µM, 1.00 µM, and 1.50 µM and shaken for 24 h in the dark. These phosphate

concentrations are generally representative of Lake Powell; monitoring data indicate that total P and SRP rarely exceeds 3.23 μM and 0.65 μM, respectively (Vernieu, *in preparation*). Samples were centrifuged, filtered through 0.22 μm polypropylene filters, and analyzed with the molybdate-blue method using calibration standards made with potassium phosphate in ALPW.

3.6. Sorption Isotherms

In these sorption experiments, SRP was added to sediment containing some amount of labile P, and thus the concentration of SRP in the system can be written as

$$SRP_{sorbed} + SRP_{final} = SRP_{added} + SRP_{labile} \quad (1)$$

where SRP_{sorbed} is the concentration of SRP sorbed to the sediment, SRP_{final} is the measured concentration in solution at the end of the experiment, SRP_{added} is the concentration added to solution at the beginning of the experiment, and SRP_{labile} is the concentration of sediment-associated SRP that is labile under the experimental conditions. The difference between the added and final concentrations of SRP was used to calculate the amount sorbed (positive values) or desorbed (negative values) such that

$$\Delta SRP_{sed} = (SRP_{added} - SRP_{final}) \cdot 0.045 / m_{sed}\,, \quad (2)$$

where ΔSRP_{sed} is the amount sorbed or desorbed (in μmol g^{-1} of dry sediment), SRP_{added} and SRP_{final} are expressed in μM, 45 is the volume of solution in each experiment (in mL), and m_{sed} is the mass of dry sediment (in g) calculated from the mass of wet sediment added. This value can be modeled from SRP_{final} with a modified Freundlich equation (see Limousin et al. 2007 for a review of sorption modeling),

$$\Delta SRP_{sed} = F \cdot SRP_{final}^{\ n} - A \ . \qquad (3)$$

The empirical parameters F (in L g^{-1} dry sediment), n (dimensionless), and A (in μmol g^{-1} dry sediment) were determined by using a computer program (written in the software package R 2.8.0; RDCT 2008) to find the values of each that minimized the residual sum of squares between the calculated and measured values of ΔSRP_{sed}. Ranges tested were 0.1-2.0, 0.1-1.0, and 0.1-1.5 for F, n, and A, respectively, and each parameter was incremented in steps of 0.1. The parameter A was introduced into the Freundlich equation to account for SRP desorbed from sediment at low SRP_{added}. When determining parameters, one obvious outlier was removed from each of: the lakebed sample collected at 238.5 km, 40-50 cm depth; a lakebed sample collected at 235.5 km, 0-15 cm depth; a shoreline sample representing -77 to -47 cm depth; and a shoreline sample representing -47 to 14 cm depth. The equilibrium phosphorus concentration (EPC, in μM), the value of SRP_{final} when $\Delta SRP_{sed} = 0$ and thus that at which no adsorption or desorption occurs, was calculated.

4. Results

4.1. Lake Level and River Flow

During the March 2006 sampling, the surface elevation of Lake Level decreased from 1094.0 to 1093.9 m above sea level (asl) and the mean Colorado River flow was 192.6 $m^3 s^{-1}$. In May, rapidly increasing springtime snowmelt increased the river flow from 619.4 to 716.5 $m^3 s^{-1}$ during the sampling trip, and the lake surface increased from 1096.5 to 1096.7 m asl. At the 245.0 km sampling location, there was substantial current from the inflowing river and an anchor was necessary to maintain a steady position of the sampling boat. By the 238.5 km location, the current was substantially less and no anchor was necessary, though periodic motoring was needed to offset drift.

In March, an obvious plungeline between the 241.0 km and 238.5 km sampling locations was observed, consistent with an underflow density current that occurs in winter and early spring (Johnson and Merritt 1979). Visual observations in May indicated that sediment-laden water remained on the surface of the lake many km below the inflow region, consistent with a summer overflow current (Johnson and Merritt 1979). In the delta region, the suspended sediment concentration was qualitatively substantially higher in May than in March. At the 168.0 km location, the secchi depth was estimated at 10 m in March; at the 178.0 km location, it was estimated at 1.5 m in May. In May, at the 178.0 km location, surface water appeared more green than brown, suggesting turbidity due more to phytoplankton (i.e., chlorophyll) than suspended sediment.

4.2. Dissolved Trace Elements

Consistent with previous research (Hart et al. 2004), Lake Powell water is very low in trace elements (Table 2), with no elements exceeding primary or secondary drinking water standards of the U.S. Environmental Protection Agency (US EPA 2008). Concentrations of Br measured by ICP-MS are assumed to correspond to bromide, a conservative environmental tracer (Harvey et al. 2005). In March, Br concentrations in deep samples are closer to that of the inflowing river (317.0 km) than those in shallow samples, supporting the visual observation of an underflow density current entering the reservoir in March. The river inflow has much lower Br concentrations in May than in March, consistent with the spring snowmelt being more dilute in most solutes (Johnson and Merritt 1979). In May, the inflow concentration of Br resembles that in surface water at the 193.5 km location, but not at the 178.0 km location, implying that the overflow density current had reached the former location, but not the latter.

Concentrations of P, Mn, and Se increase substantially in March from the 317.0 km location to the 245.0 km location. Below this location, deeper samples are consistently higher in P, Mn, Li, U, and, with the exception of the deep sample at the 241.0 km location, Se than shallower ones. In May, P is the only element with higher concentrations at the 317.0 km location than in March. The concentration of P is lower at the 245.0 km and 238.5 km locations than at the 317.0 km, which is also different from the other elements. Concentrations of Mn, Br, Se, Li, and U all increase from the 317.0 km location to the 245.0 km location in May. Concentrations of all elements, including P, are highest in the deep water at the 193.5 km location.

4.3. Phosphorus Speciation in Sediment Samples

Total concentrations of SRP estimated from sequential extraction of Lake Powell sediment are 55.4-99.9% (mean = 79.0%, σ = 12.0%) of total concentrations measured by X-ray fluorescence (Chapter 4). SRP is dominantly associated with fractions extracted by acetate (1.7-11.6 μmol P g^{-1}; mean = 7.7 μmol P g^{-1}, σ = 2.8 μmol P g^{-1}) and by HCl (2.4-5.1 μmol P g^{-1}; mean = 4.0 μmol P g^{-1}, σ = 0.8 μmol P g^{-1}; Figure 2, Table 3). A much smaller fraction of phosphorus was extracted by BD (0.5-2.1 μmol P g^{-1}; mean = 1.5 μmol P g^{-1}, σ = 0.6 μmol P g^{-1}), with approximately equal, still smaller amounts extracted by $MgCl_2$ (0.1-1.0 μmol g^{-1}; mean = 0.7 μmol P g^{-1}, σ = 0.3 μmol P g^{-1}) and ash+HCl (0.3-1.7 μmol P g^{-1}; mean = 1.0 μmol P g^{-1}, σ = 0.4 μmol P g^{-1}). While no sequential extraction is perfectly accurate, these results can be interpreted with confidence because general trends are clear and because Ruttenberg rigorously verified the specificity and efficiency of the extraction method (Ruttenberg 1992).

The specificity of Ruttenberg's extraction is most suspect with regard to organic P; however, potential artifacts were examined by conducting the full extraction procedure on freshly collected phytoplankton and zooplankton that were freeze-dried before extraction. In these samples, she observed that 80% of P was extracted in the first step ($MgCl_2$, targeting exchangeable P) and the remaining 20% was extracted in the fifth step (targeting organic P). It is likely that freeze-drying may have liberated P during cell lysis; this has little bearing on our study since the $MgCl_2$-extractable P was the smallest fraction. Ruttenberg observed no extraction of P in steps 2-4, indicating that the variation in pH during these steps does not hydrolyze non-exchangeable organic P from fresh organic

matter (which might also be present in surface sediment of the Lake Powell inflow region).

The rather large variability in the concentrations of SRP extracted from each geochemical phase results from the influence of particle size; coarse sediment contained significantly less (t-test, $p < 0.05$) SRP than fine sediment in every fraction. When coarse samples were removed from the data set, the ash+HCl-extractable fraction was the only geochemical phase with a significant difference (t-test, $p < 0.05$) between shoreline and lakebed samples, with higher concentrations in samples from the lakebed. Among lakebed samples, there was no significant difference (t-test, $p < 0.05$) between those collected in March or May 2006. Lakebed surface samples contained more acetic-acid-extractable SRP (t-test, $p < 0.1$) and less HCl-extractable SRP (t-test, $p < 0.05$) than deep samples. Fine and coarse sediment contained much more and slightly less acetate-extractable SRP than HCl-extractable SRP, respectively.

BD- and ash+HCl-extractable SRP increased slightly towards GCD in the 245.0-235.5 km lakebed samples (Figure 3). The other fractions showed no trends with distance, but, notably, the 168.0 km location contained slightly higher acetic-acid-extractable SRP than the other locations.

4.4. Phosphorus Sorption

In experiments with $SRP_{added} = 0$, values of ΔSRP_{sed} are < 0, which represents desorption of some SRP_{labile} during resuspension in oxic conditions at 25°C. Desorbed SRP ranged from 0.03-0.14 μmol g^{-1} dry sediment (mean = 0.07 μmol g^{-1}; $\sigma = 0.03$ μmol g^{-1}). Interestingly, shoreline samples of fine particle size were significantly (t-test, $p <$

0.05) higher in desorbed SRP than lakebed samples; no other pairings of sample groups are significant.

The modified Freundlich equation provided an adequate model to describe P sorption in Lake Powell sediment. Both F and n were significantly higher (t-test, $p < 0.01$) in fine samples than in coarse ones, indicating a much higher affinity for P in fine sediment (Figure 4, Table 4). This agrees with previous research at Lake Powell, which shows that bulk P is associated with sediments of small particle size and high clay content (Chapter 4). The isotherms from the lakebed cores overlap those of the fine shoreline sediment and show no significant trend with location (i.e., distance from the dam). Values of EPC ranged from 0.05-0.37 μM (mean = 0.19 μM, $\sigma = 0.07$ μM) and no significant differences existed between groups of samples. These EPC values are much lower than 1.3 ± 0.6 μM reported for Lake Powell delta sediment by Mayer and Gloss (1980), who used air-dried sediment. This is generally consistent with previous research showing that submerged lakebed sediment has a higher affinity for phosphate than air-dried sediment from the shoreline of the same lake (Baldwin 1996).

5. Discussion

5.1. Colorado River Inflow to Lake Powell during Drawdown

The two sampling events captured notably different hydrologic conditions. March sampling was conducted with the Colorado River at base flow, and both visual observations and Br data indicate that an underflow density current existed at this time and began between the 241.0 km and 238.5 km sampling locations. In May, sampling occurred during both an overflow current and increased flow caused by snowmelt runoff

in the Rocky Mountains. During this study, the surface elevation of the reservoir was > 31 m below its maximum; hence, the river entered the lake near the 245.0 km sampling location after passing through as much as 55 km of exposed sediment delta.

Although suspended sediment concentrations were not measured in this study, visual observations indicate that the inflow in May was substantially more turbid than that in March. This increase in suspended sediment is most probably due to a combination of increased river flow, which leads to increased suspended sediment load (Potter and Drake 1989), and flow through the exposed Colorado River delta of Lake Powell, a process observed to double the suspended sediment load during low surface elevations of this reservoir (Vernieu 1997).

Flow through the sediment delta appears to affect concentrations of solutes in the inflow region. In March, an increase in SRP from 0.065 μM at the 317.0 km location to 0.090 μM at the 245.0 km location suggests that resuspension of exposed delta sediment may represent a source of P to Lake Powell that did not exist when the lake was full. Other sources of P in this reach are unlikely, as the river flows through arid, sparsely vegetated land that is quite remote and subject to little direct human influence. This finding agrees with the study of a previous, less extreme drawdown at Lake Powell (Vernieu 1997).

Based on the measured SRP concentrations, a river flow of 192.6 $m^3 s^{-1}$ in March corresponds to loads of 1082 and 1498 mol SRP d^{-1} at the 317.0 km and 245.0 km locations, respectively. Based on an average desorption of 0.07 μmol SRP g^{-1} of dry sediment, this 38% increase in SRP load suggests resuspension of 5.9 kt d^{-1} of sediment. Horowitz et al. (2001) report an average yearly suspended sediment load of 16.8 ± 9.3 Mt

entering Lake Powell via the Colorado River. If we assume that 20% of the yearly sediment load enters Lake Powell with the 40% of the water that enters at base flow (August-April), then this implies a suspended sediment load of 12.5 ± 7 kt d^{-1} at base flow. The estimated amount of sediment required to be resuspended to produce the observed increase in SRP load is about half of the estimate of the suspended load at base flow.

The SRP values measured in the Lake Powell inflow region in March are near the minimum EPC values calculated from the sorption experiments, yet they are closer to values measured in the inflow region during a previous drawdown (< 0.1 – 0.2 μM, mean = 0.1 μM, σ = 0.05 μM; Vernieu 1997). This suggests that our laboratory experiments may not have accurately replicated sorption processes in the Colorado River. Variation of the solid:solution ratio has been observed to significantly affect sorption of P to river sediment (Müller et al. 2006) and sorption results show an significant influence of particle size, so the experiments in this study may not have matched the concentration or composition (i.e., coarse vs. fine sediment) of the suspended load entering Lake Powell. Furthermore, sorption of P to sediment has been observed to decrease as salinity increases from 0 to a range of 5-12 salinity units (Spiteri et al. 2008). The ALPW used for the sorption experiments was based on average reservoir composition and may not have matched the specific conditions in the inflow region during the sampling times. Lastly, the temperature conditions in the laboratory experiments are likely to have been higher than the ambient temperature of the river in the spring (not measured). Previous research using Mn-oxides as sorbents shows that higher temperatures lead to a relatively minor decrease in sorption of P (Mustafa et al. 2008), which suggests that our

experimental conditions may have led to lower sorption in the laboratory relative to the field. However, other studies of similar sorbates (i.e., arsenic) and sorbents (i.e., Fe-oxides) show the opposite effect (Banerjee et al. 2008), and thus we note that the response of sorption to temperature may vary between different study systems, yet is not a major influence at environmentally-relevant temperature ranges.

In May, higher river flows dilute the incoming load of most trace solutes, yet SRP increases, an observation consistent with previous results (Gloss et al. 1980). In contrast to March, SRP decreases between the 317.0 km location and the 245.0 km location, despite an apparent increase in suspended sediment between these locations. The similarity of the March (0.090 μM) and May (0.077 μM) SRP concentrations at the 245.0 km location suggest that these values may represent a true EPC value at this site. Since sorption results indicate that fine sediment has a significantly greater affinity for phosphate than coarse sediment, the low EPC measured at the 245.0 km site may be driven by abundant fine particles in suspension.

5.2. Mechanisms of Phosphorus Release and Sorption

Resuspension of sediment in Colorado River water is most similar to step 1 of the sequential extraction; loosely-sorbed, exchangeable SRP is the most likely geochemical phase to partition into the water column. The SRP desorbed from sediment without P added (mean = 0.07 μmol g^{-1}) is much lower than the total exchangeable SRP of fine sediment (mean = 0.80 μmol g^{-1}) and about half that of coarse sediment (mean = 0.16 μmol g^{-1}). Total exchangeable SRP accounts for only ~10% of the total extractable SRP; thus, only a small fraction of the total P appears to desorb from sediment in ALPW with

no P added. The higher affinity of fine sediment for SRP suggests that its low desorption of exchangeable SRP might be explained by resorption to other geochemical phases.

The large increase of dissolved Mn between the 317.0 km and 245.0 km locations in March may help explain the low desorption of SRP. At circumneutral pH, only Mn^{2+}, the environmentally-relevant, reduced form of Mn, is soluble, so the presence of dissolved Mn indicates low reduction potential. However, microbially-mediated reactions oxidize dissolved Mn^{2+} to solid Mn(III/IV)-oxide minerals in the presence of dissolved oxygen on a time scale of hours (Bargar et al. 2000). The observed increase in dissolved Mn probably comes from resuspension of exposed delta sediment with reducing porewater, and, upon resuspension, oxidative precipitation of Mn-oxides is likely. A similar process is likely for Fe, based on its geochemical similarity to Mn (Stumm and Morgan 1996). Newly precipitated Fe- and Mn-oxide minerals in suspension are likely to sorb SRP; thus, sediment resuspension may decrease SRP through sorption processes while also increasing it through the release of exchangeable SRP. That the apparent EPC of the Colorado River is lower than the EPC calculated in sorption experiments may suggest that sorption of exchangeable SRP to freshly precipitated Fe- and Mn-oxides is more prevalent in the Colorado River than in the laboratory experiments of this study.

Although sorption to Fe- and Mn-oxides may be an important sink for desorbed SRP upon resuspension, calcite and apatite minerals appear to be the dominant sink for P in Lake Powell. Organic compounds were found to inhibit calcite precipitation in the inflow region of Lake Powell (Reynolds 1978), so association of P with calcite is expected to be even greater in areas of the lake below those at which we collected samples, a hypothesis consistent with the highest calcite-associated SRP concentration

occurring at the 168.0 km location. Minor trends of increasing association of SRP with easily reducible or organic geochemical phases in the delta sediment may be related to weak trends in particle size in the region studied (Chapter 4).

5.3. Phosphorus in Lake Powell

Downstream of the 245.0 km location, higher concentrations of SRP and Br suggest that P transport is controlled by the seasonal underflow density current in March. This implies that P is transported below the photic zone, which is shallow due to turbidity in the upper 30-60 km of the reservoir (Gloss et al. 1980) and the depth of wind-driven circulation (~20 m, Johnson and Merritt 1979). This phenomenon has been cited as a mechanism for oligotrophication at Arrow Lakes Reservoir, British Columbia, Canada (Matzinger et al. 2007). Thus, when base flow and an underflow current occur together, most SRP released from sediment resuspension may not be available to support primary productivity. If this occurs, then the additional P load may be removed by summertime calcite precipitation in the lower portion of Lake Powell, or it may be eventually exported through GCD.

In May, the incoming SRP load appears to be decreased by sorption to resuspended sediment. The upstream location with two depths measured for SRP (238.5 km) shows a higher concentration in surface water, consistent with the overflow current indicated by Br. Decreased surface water SRP at the 193.5 km location could be the results of uptake by biomass, which is consistent with qualitative observations of green-colored surface water at this location.

These observations suggest that resuspension of the exposed sediment delta should not contribute additional SRP to the surface water of Lake Powell, where it would lead to an increase in primary productivity. However, monitoring data indicate that, during drawdown, summertime chlorophyll has increased by about an order of magnitude in the surface water of the upper part of the reservoir (Chapter 4). The most likely explanation for this discrepancy is the synoptic nature of our sampling. We did not observe base flow entering the reservoir as an overflow or interflow current, which would contribute SRP added from delta sediment resuspension to the photic zone. These conditions would be expected in April, when the river has warmed enough to end the underflow current, yet the high-elevation snowpack in the headwaters of the Colorado River Basin has not increased flow substantially.

Thus, increased concentrations of chlorophyll during drawdown may result from a pulsed addition of P to surface water that results from specific hydrologic conditions in this reservoir. This mechanism differs substantially from the mechanism of increased chlorophyll concentration during reservoir drawdown in Lake Hume, New South Wales, Australia. There, the very shallow depth of the nearly-empty reservoir allowed wind-driven circulation to bring anoxic, nutrient-rich bottom water to the photic zone (Baldwin et al. 2008). In this setting, nutrients are supplied to bottom water by diffusion from sediment, a situation of apparently minor importance in Lake Powell. The mechanism for increased primary productivity during reservoir drawdown therefore depends on both the chemical speciation of nutrients in sediment and the hydrology of river inflows, which may lead to significant variability in water quality during times of low water levels in different reservoirs.

6. Conclusions

1. During drawdown of Lake Powell and subsequent exposure of several km of delta sediment, sediment resuspension appears to increase SRP concentration at baseflow through desorption of P yet decrease SRP concentration at increased flow through sorption of P.
2. Sediment resuspension appears to involve opposing effects of desorption and re-sorption of P. The desorbed fraction is probably loosely-sorbed, exchangeable SRP and subsequent sorption could be to newly precipitated Mn- and Fe-oxide minerals.
3. The amount of SRP desorbed from sediment samples in laboratory experiments is small compared to the measured exchangeable SRP, which is about 10% of the total extractable SRP. The majority of SRP is released by extractions targeting calcite, biogenic apatite, and hydroxyapatite phases.
4. The EPC estimated through sorption experiments conducted at 25°C in ALPW is higher than the apparent EPC measured in the Lake Powell inflow region.
5. Fine sediment sorbs significantly more SRP than coarse sediment, although there is no significant difference between the two in the amount of SRP desorbed by sediment resuspension in ALPW.
6. Seasonal density currents transport inflowing solutes, including SRP, to bottom waters in March and surface waters in May. Increased primary productivity during drawdown may result from a specific hydrologic scenario in which baseflow enters Lake Powell as an overflow or interflow current in the late spring.

Acknowledgements

The authors are very grateful to Jerry Miller (U.S. Bureau of Reclamation) and Mike Easler (Caltech), without whom this study would not have been possible. Robert Radkte, Nick Williams, Rafael Lopez (each USBR), and Jesse Granet (Glen Canyon National Recreation Area) assisted with sample collection; Kate Campbell, Nathan Dalleska (Caltech), Thomas Rüttimann, and Caroline Stengel (Eawag) were indispensable during sample analysis; Claire Farnsworth (Caltech), René Gächter, and Alfred Wüest (Eawag) were very helpful during data analysis and interpretation. This work was funded by NSF SGER grant EAR-0621371, the Alice Tyler Foundation, USBR grant 06PG400222, and a Summer Undergraduate Research Fellowship awarded to Mike Easler at Caltech. The U.S. Bureau of Reclamation, Upper Colorado Region provided sampling assistance.

References

Ahlgren, J., K. Reitzel, L. Tranvik, A. Gogll, and E. Rydin. (2006) Degradation of organic phosphorus compounds in anoxic Baltic Sea sediments: A ^{31}P nuclear magnetic resonance study. *Limnology and Oceanography* 51(5): 2341-2348.

Anderson, P. B., T. C. Chidsey, D. A. Sprinkel, and G. C. Willis. (2003) Geology of Glen Canyon National Recreation Area, Utah-Arizona. In *Geology of Utah's Parks and Monuments, second edition* (Sprinkel, D.A., T. C. Chidsey, and P. B. Anderson, eds.), Utah Geological Association Publication 28: Salt Lake City, 2003.

Baldwin, D. S. (1996). Effects of exposure to air and subsequent drying on the phosphate sorption characteristics of sediments from a eutrophic reservoir. *Limnology and Oceanography* 41(8): 1725-1732.

Baldwin, D. S., H. Gigney, J. S. Wilson, G. Watson, and A. N. Boulding. (2008) Drivers of water quality in a large water storage reservoir during a period of extreme drawdown. *Water Research* 42: 4711-4724.

Banerjee, K., G. L. Amy, M. Prevost, S. Nour, M. Jekel, P. M. Gallagher, and C. D. Blumenschein. (2008) Kinetic and thermodynamic aspects of adsorption of arsenic onto granular ferric hydroxide (GFH). *Water Research* 42(13): 3371-3378.

Bargar, J. R., B. M. Tebo, and J. E. Villinski. (2000) In situ characterization of Mn(II) oxidation by spores of the marine *Bacillus* sp. strain SG-1. *Geochim. Cosmochim. Acta* 64: 2775-2778.

Blecker, S. W., J. A. Ippolito, J. E. Barrett, D. H. Wall, R. A. Virginia, and K. L. Norvell. (2006) Phosphorus fractions in soils of Taylor Valley, Antarctica. *Soil Science Society of America Journal* 70: 806-815.

Cheng, F. and T. Granata. (2007) Sediment transport and channel adjustments associated with dam removal: Field observations. *Water Resources Research* 43: W03444, doi: 10.1029/2005WR004271.

Clayton, R. (2008) Upper Colorado Region Water Operations: Current Status: Lake Powell. Website updated on 14 December 2008 and viewed at http://www.usbr.gov/uc/water/crsp/cs/gcd.html on 7 January 2009.

Colman, A. S., R. E. Blake, D. M. Karl, R. A. Wildman, B. P. Colman, and M. L. Fogel. Method for measuring the oxygen isotope composition of phosphate in seawater, fresh water, and waste water treatment plant effluent. In preparation for *Analytical Chemistry*.

Condit, W., C. L. Drake, L. Mayer, and R. Spydell. *Lake Powell Research Project Bulletin 64: Sedimentation in Lake Powell* (Varady, J. M. and O. L. Anderson, eds.). Los Angeles: University of California, 1978.

Ellison, M. E. and M. T. Brett. (2006) Particulate phosphorus bioavailability as a function of stream flow and land cover. *Water Research* 40: 1258-1268.

Ferrari, R. (1988) *1986 Lake Powell Survey*. U.S. Bureau of Reclamation Technical Report REC-ERC-88-6: Denver, CO, 67 pp.

Gächter, R. and B. Müller. (2003) Why the phosphorus retention of lakes does not necessarily depend on the oxygen supply to their sediment surface. *Limnology and Oceanography* 48(2): 929-933.

Gloss, S. P., L. M. Mayer, and D. E. Kidd. (1980) Advective control of nutrient dynamics in the epilimnion of a large reservoir. *Limnology and Oceanography* 15(4): 873-884.

Gloss, S. P., R. C. Reynolds, L. M. Mayer, and D. E. Kidd. (1981) "Reservoir influences on salinity and nutrient fluxes in the arid Colorado River Basin", p. 1618-1629. *In:* H.G. Stefan (ed.), Proceedings of the Symposium on Surface Water Impoundments. American Society of Civil Engineers, New York.

Hart, R. J., H. E. Taylor, R. C. Antweiler, G. G. Fisk, G. M. Anderson, D. A. Roth, M. E. Flynn, D. B. Pearl, M. Truini, and L. B. Barber. (2004) Physical and chemical characteristics of Knowles, Forgotten, and Moqui Canyons, and effects of recreational use on Water Quality, Lake Powell, Arizona and Utah. *United States Geological Survey Scientific Investigations Report* 2004-5120.

Harvey, J. W., J. E. Saiers, and J. T. Newlin. (2005) Solute transport and storage mechanisms in wetlands of the Everglades, south Florida. *Water Resources Research* 41: W05009, doi:10.1029/2004WR003507.

Horowitz, A.J., K. A. Elrick, and J. J. Smith. (2001) Annual suspended sediment and trace element fluxes in the Mississippi, Columbia, Colorado, and Rio Grande drainage basins. *Hydrological Processes* 15: 1169-1207.

Johnson, D. L. (1971) Simultaneous determination of arsenate and phosphate in natural waters. *Environmental Science and Technology* 5(5): 411-414.

Johnson, N. M. and D. H. Merritt. (1979) Convective and advective circulation of Lake Powell, Utah-Arizona, during 1972-1975. *Water Resources Research* 15: 873-884.

Jordan, T. E., J. C. Cornwell, W. R. Boynton, and J. T. Anderson. (2008) Changes in phosphorus biogeochemistry along an estuarine salinity gradient: The iron conveyor belt. *Limnology and Oceanography* 53(1): 172-184.

Limousin, G., J.-P. Gaudet, L. Charlet, S. Szenknect, V. Barthès, and M. Krimissa. (2007) Sorption isotherms: A review on physical bases, modeling and measurement. *Applied Geochemistry* 22: 249-275.

Matzinger, A., R. Pieters, K. I. Ashley, G. A. Lawrence, A. Wüest. (2007) Effects of impoundment on nutrient availability and productivity in lakes. *Limnology and Oceanography* 52(6): 2629-2640.

Mayer, L. M. and S. P. Gloss. (1980) Buffering of silica and phosphate in a turbid river. *Limnology and Oceanography* 25(1): 12-22.

Meybeck, M. (1982) Carbon, nitrogen, and phosphorus transport by world rivers. *American Journal of Science* 282: 401-450.

Mitchell, A. M. and D. S. Baldwin. (1998) Effect of desiccation/oxidation on the potential for bacterially mediated P release from sediments. *Limnology and Oceanography* 43(3): 481-487.

Müller, B., R. Stierli, and A. Wüest. (2006) Phosphate adsorption by mineral weathering particles in oligotrophic waters of high particle content. *Water Resources Research* 42: W10414, doi: 10.1029/2005WR004778.

Müller, R., M. Breitenstein, M. M. Bia, C. Rellstab, and A. Kirchhofer. (2007) Bottom-up control of whitefish populations in ultra-oligotrophic Lake Brienz. *Aquatic Science* 69: 271-288.

Murphy, J. and J. P. Riley. (1962) A modified single solution method for the determination of phosphate in natural waters. *Analytica Chimica Acta* 27: 31-36.

Mustafa, S., M. I. Zaman, and S. Khan. (2008) Temperature effect on the mechanism of phosphate anions sorption by beta-MnO2. *Chemical Engineering Journal* 141(1-3): 51-57.

Naselli-Flores, L., R. Barone, I. Chorus, and R. Kurmayer. (2007) Toxic cyanobacterial blooms in reservoirs under a semiarid Mediterranean climate: The magnification of a problem. *Environmental Toxicology* doi 10.1002/tox.20268.

Niemistö, J., H. Holmroos, Z. Pekcan-Hekim, and J. Horppila. (2008) Interactions between sediment resuspension and sediment quality decrease the TN : TP ratio in a shallow lake. *Limnology and Oceanography* 53(6): 2407-2415.

Nürnberg, G. (1995) Quantifying anoxia in lakes. *Limnology and Oceanography* 40(6): 1100-1111.

Peltier, E., A. L. Dahl, and J.-F. Gaillard. (2006) Metal speciation in anoxic sediments: when sulfides can be construed as oxides. *Environmental Science and Technology* 39(1): 311-316.

Potter, L. D. and C. L. Drake. *Lake Powell: Virgin Flow to Dynamo.* University of New Mexico Press, Albuquerque, 1989.

Pratson, L., J. Hughes-Clarke, M. Anderson, T. Gerber, D. Twichell, R. Ferrari, C. Nittrouer, J. Beaudoin, J. Granet, and J. Crockett. (2008) Timing and patterns of basin infilling as documented in Lake Powell during a drought. *Geology* 36(11): 843-846.

R Development Core Team. 2008. R: A language and environment for statistical computing. R Foundation for Statistical Computing, Vienna, Austria. ISBN 3-900051-07-0, URL http://www.R-project.org.

Reynolds, Jr., R. C. (1978) Polyphenol inhibition of calcite precipitation in Lake Powell. *Limnology and Oceanography* 23(4): 585-597.

Riggsbee, J. A., J. P. Julian, M. W. Doyle, and R. G. Wetzel. (2007) Suspended sediment, dissolved organic carbon, and dissolved nitrogen export during the dam removal process. *Water Resources Research* 43: W09414, doi:10.1029/2006WR005318.

Ruttenberg, K. C. (1992). Development of a sequential extraction method for different forms of phosphorus in marine sediments. *Limnology and Oceanography* 37(7): 1460-1482.

Rydin, E., Vrede, T., Persson, J., Holmgren, S., Jansson, M., Tranvik, L., and Milbrink, G. (2008) Compensatory nutrient enrichment in an oligotrophicated mountain reservoir – effects and fate of added nutrients. *Aquatic Science* 70: 323-336.

Schindler, D. W., R. E. Hecky, D. L. Findlay, M. P. Stainton, B. R. Parker, M. J. Paterson, K. G. Beaty, M. Lyng, and S. E. M. Kasian. (2008) Eutrophication of lakes cannot be controlled by reducing nitrogen input: Results of a 37-year whole-ecosystem experiment. *Proceedings of the National Academy of Sciences of the USA* 105(32): 11254-11258.

Sjosten, A. and S. Blomqvist. (1997) Influence of phosphate concentration and reaction temperature when using the molybdenum blue method for determination of phosphate in water. *Water Research* 31(7): 1818-1823.

Snyder, N. P., S. A. Wright, C. N. Alpers, L. E. Flint, C. W. Holmes, and D. M. Rubin. (2006) Reconstructing depositional processes and history from reservoir stratigraphy: Englebright Lake, Yuba River, northern California. *Journal of Geophysical Research* 111: F04003, doi:10.1029/2005JF000451.

Spahr, N. E., L. E. Apodaca, J. R. Deacon, J. B. Bails, N. J. Bauch, C. M. Smith, and N. E. Driver. (2000) Water quality in the Upper Colorado River Basin, Colorado, 1996-98. *U.S. Geological Survey* Circular 1214.

Spiteri, C., P. van Cappellen, and P. Regnier. (2008) Surface complexation effects on phosphate adsorption to ferric iron oxyhydroxides along pH and salinity gradients in estuaries and coastal aquifers. *Geochimica et Cosmochimica Acta* 72: 3431-3445.

Stumm, W. and J. J. Morgan. *Aquatic Chemistry, 3rd Edition.* John Wiley and Sons, Inc.: New York, 1996.

Thomson-Bulldis, A. and D. M. Karl. (1998) Application of a novel method for phosphorus determinations in the oligotrophic North Pacific Ocean. *Limnology and Oceanography* 43(7): 1565-1577.

United States Bureau of Reclamation. (2008) *Bureau of Reclamation: Upper Colorado Region Historic Data*. Webpage viewed at http://www.usbr.gov/uc/crsp/GetSiteInfo on 21 December 2008.

United States Environmental Protection Agency. (2008) *Drinking Water Contaminants.* Webpage viewed at http://www.epa.gov/safewater/contaminants/index.html on 21 December 2008.

United States Geological Survey. (2008) *USGS Real-Time Data for Utah – Streamflow*. Webpage viewed at http://waterdata.usgs.gov/ut/nwis/current/?type=flow on 21 December 2008.

Vatland, S. and P. Budy. (2007) Predicting the invasion success of an introduced omnivore in a large, heterogeneous reservoir. *Canadian Journal of Fisheries and Aquatic Sciences* 64: 1329-1345.

Vernieu, W. S. (1997) Effects of reservoir drawdown on resuspension of deltaic sediments in Lake Powell *Journal of Lake and Reservoir Management* 13(1): 67-78.

Woodhouse, C. A., S. T. Gray, and D. M. Meko. (2006) Updated streamflow reconstructions for the Upper Colorado River Basin. *Water Resources Research* 42: W05415, doi:10.1029/2005WR004455.

Wüest, A., M. Zeh, and J. D. Ackerman. (2007) Lake Brienz Project: An interdisciplinary catchment-to-lake study. *Aquatic Science* 69: 173-178.

Zhang, J.-Z., C. J. Fischer, and P. B. Ortner. (2004) Potential availability of sedimentary phosphorus to sediment resuspension in Florida Bay. *Global Biogeochemical Cycles* 18: GB4008, doi:10.1029/2004GB002255.

Zhang, J.-Z. and X.-L. Huang. (2007) Relative importance of solid-phase phosphorus and iron on the sorption behavior of sediments. *Environmental Science and Technology* 41: 2789-2795.

Tables

Table 1. Sequential extraction conditions[a] used to determine operational speciation of sedimentary SRP

step	extractant(s)	time	target
1A	1 M $MgCl_2$	2 h	exchangeable or
1B	1 M $MgCl_2$	2 h	loosely-sorbed P
1C	dH_2O	2 h	
1D	dH_2O	2 h	
2A	1 M $NaHCO_3$ + 1.125 g $Na_2S_2O_4$	8 h	easily reducible or reactive Fe(III)-bound P
2B	1 M $MgCl_2$	2 h	
2C	dH_2O	2 h	
3A	1 M $NaH_2C_3O_2$ buffered to pH 3.7 with $H_3C_3O_2$	6 h	P bound to authigenic carbonate, fluoroapatite, calcite, or biogenic apatite
3B	1 M $MgCl_2$	2 h	
3C	1 M $MgCl_2$	2 h	
3D	dH_2O	2 h	
3E	dH_2O	2 h	
4	1 M HCl	16 h	P bound to detrial apatite
5	heating at 550°C for 2 h, followed by 1 M HCl	16 h	organic P

[a] Extractions were performed with an initial dry mass of ~ 0.5 g, at a temperature of 25°C, and in solution volumes of 50 mL, except for step 2A, which was 45 mL, following Ruttenberg (1992) as modified by Zhang et al. (2004).

Table 2. Dissolved inorganic elemental concentrations[a] (μM) in the inflow region of Lake Powell

location		*element*						
distance[b]	depth[c]	Li	P	Mn	Zn	Br	Se	U
				March, 2006				
317.0	0.5	3.5	0.065	0.053	0.092	0.63	0.031	0.019
245.0	0.5	3.7	0.090	0.677	0.039	0.64	0.050	0.020
241.0	1.3	3.9	0.045	0.230	BDL	0.57	0.033	0.019
241.0	6.3	4.6	0.058	0.282	BDL	0.62	0.030	0.020
238.5	0.5	3.5	BDL	0.115	0.332	0.48	0.027	0.018
238.5	19	4.1	0.052	0.377	BDL	0.57	0.042	0.019
235.5	0.5	3.4	0.032	0.109	0.056	0.47	0.030	0.018
235.5	27	3.8	0.055	0.230	BDL	0.56	0.035	0.019
				May, 2006				
317.0	0.5	1.5	0.130	BDL	BDL	0.27	0.029	BDL
245.0	0.2	1.6	0.077	0.152	BDL	0.32	0.036	0.010
238.5	0.6	2.7	0.087	0.038	BDL	0.40	0.035	0.014
238.5	19.1		0.058					
193.5	1.5	1.9	BDL	BDL	BDL	0.29	BDL	0.010
193.5	19.5	2.3	0.045	0.042	0.044	0.36	0.042	0.012
193.5	54.5	3.7	0.058	0.624	0.173	0.52	0.030	0.018
178.0	6	2.3		BDL	0.032	0.77	BDL	0.010
178.0	12	1.9	0.032	0.117	0.188	0.57	BDL	0.010
178.0	66.5	3.6	0.081	0.554	0.051	0.53	0.045	0.018
				statistics and elemental information				
	mean	3.1	0.064	0.257	0.112	0.50	0.035	0.016
	σ	1.0	0.026	0.219	0.101	0.14	0.007	0.004
	EPA limit[d]			0.910	76.4		0.633	0.126
	detection limit	0.29	0.030	0.036	0.031	0.025	0.025	0.008

[a] Concentrations of Ti, Cr, As, Cd, and Pb were below detection limits for all samples.

[b] Distance is measured in kilometers from Glen Canyon Dam.

[c] Depth is measured in meters below the lake surface.

[d] EPA limit is a primary maximum contaminant level for Se and U and a secondary standard for Mn and Zn (US EPA 2008).

Table 3. Amount of phosphorus[a] extracted in sequential fractions

location (km)[b]	depth (cm)[c]	$MgCl_2$	BD	acetate	HCl	ash+HCl
lakebed samples						
245.0	15-30	0.83	1.53	8.20	4.58	1.29
245.0	60-75	0.77	1.39	8.08	4.86	0.95
241.0	0- 5	0.95	1.87	11.25	3.35	1.26
241.0	0-12.5	0.86	1.64	9.63	3.34	1.48
241.0[d]	5-15	0.51	1.09	6.66	3.92	0.82
238.5	0-15	0.83	1.87	10.15	3.20	1.12
238.5	25-40	0.73	1.91	7.90	5.14	1.17
238.5	0-12.5	0.77	1.89	9.68	3.45	0.95
238.5	40-50	0.78	1.78	9.30	4.47	1.26
238.5[d]	0- 5	1.03	2.13	9.88	3.89	1.35
235.5	0-15	0.88	2.01	8.57	4.19	1.35
235.5	0-15	0.87	2.01	8.21	4.45	1.63
235.5	25-40	0.81	2.04	7.63	4.19	1.68
168.0	5-15	0.83	2.11	11.56	4.43	1.12
lakebed mean		0.82	1.81	9.05	4.10	1.24
lakebed σ		0.12	0.30	1.40	0.60	0.25
shoreline samples						
249.5	-132 to -109	0.52	0.85	7.26	4.79	0.67
249.5	-132 to -109	0.53	0.88	8.77	4.69	0.58
249.5	-109 to -77	0.13	0.46	1.74	2.43	0.33
249.5	-109 to -77	0.15	0.61	2.44	3.05	0.32
249.5	-77 to -47	0.17	0.70	2.12	2.80	0.36
249.5	-77 to -47	0.19	0.47	2.66	2.86	0.26
249.5	-47 to 14	0.97	1.84	8.20	4.88	0.80
249.5	-47 to 14	0.74	1.89	7.39	4.54	1.33
249.5	14 to 20	0.93	1.71	9.91	3.60	0.69
shoreline mean		0.48	1.05	5.61	3.74	0.59
shoreline σ		0.34	0.59	3.30	0.99	0.34

[a] Phosphorus was measured as SRP and is expressed in μmol g^{-1} of dry sediment.

[b] Distances are upstream from Glen Canyon Dam.

[c] Depth is positive below the sediment-water interface; negative depths denote sediment exposed to air.

[d] These samples are from May 2006; all other samples are from March 2006.

Table 4. Sorption isotherm parameters and results

location (km)[a]	depth (cm)[b]	ΔSRP_{sed} ($\mu mol\ g^{-1}$) when $SRP_{init} = 0$	F[c]	n[c]	A[c]	EPC (μM)[d]
lakebed samples						
245.0	15-30	0.05	0.9	0.9	0.2	0.188
245.0	60-75	0.06	1.4	0.5	0.6	0.184
241.0	0- 5	0.05	1.0	1.0	0.2	0.200
241.0	0-12.5	0.04	1.3	0.8	0.3	0.160
241.0[e]	5-15	0.05	0.8	0.7	0.1	0.051
238.5	0-15	0.09	1.8	0.5	0.9	0.250
238.5	25-40	0.03	1.8	1.0	0.2	0.111
238.5	0-12.5	0.09	1.6	0.8	0.5	0.234
238.5	40-50	0.07	1.9	0.4	0.8	0.115
238.5[e]	0- 5	0.09	1.4	0.6	0.6	0.244
235.5	0-15	0.07	1.7	0.4	0.9	0.204
235.5	0-15	0.07	1.4	0.8	0.4	0.209
235.5	25-40	0.05	1.8	0.5	0.7	0.151
168.0	5-15	0.03	1.8	1.0	0.2	0.111
shoreline samples						
249.5	-132 to -109	0.06	1.3	0.3	0.7	0.127
249.5	-132 to -109	0.07	0.9	0.6	0.3	0.160
249.5	-109 to -77	0.03	0.5	0.1	0.4	0.107
249.5	-109 to -77	0.09	1.5	0.1	1.3	0.239
249.5	-77 to -47	0.04	0.3	0.2	0.2	0.132
249.5	-77 to -47	0.07	1.0	0.1	0.9	0.349
249.5	-47 to 14	0.09	2.0	0.7	0.6	0.179
249.5	-47 to 14	0.13	1.9	1.0	0.7	0.368
249.5	14 to 20	0.14	2.0	0.5	0.9	0.203

[a] Distances are upstream from Glen Canyon Dam.

[b] Depth is positive below the sediment-water interface; negative depths denote sediment exposed to air.

[c] Freundlich isotherm parameters determined according to equation (3) (see text).

[d] The equilibrium phosphorus concentration.

[e] These samples are from May 2006; all other samples are from March 2006.

Figure 1

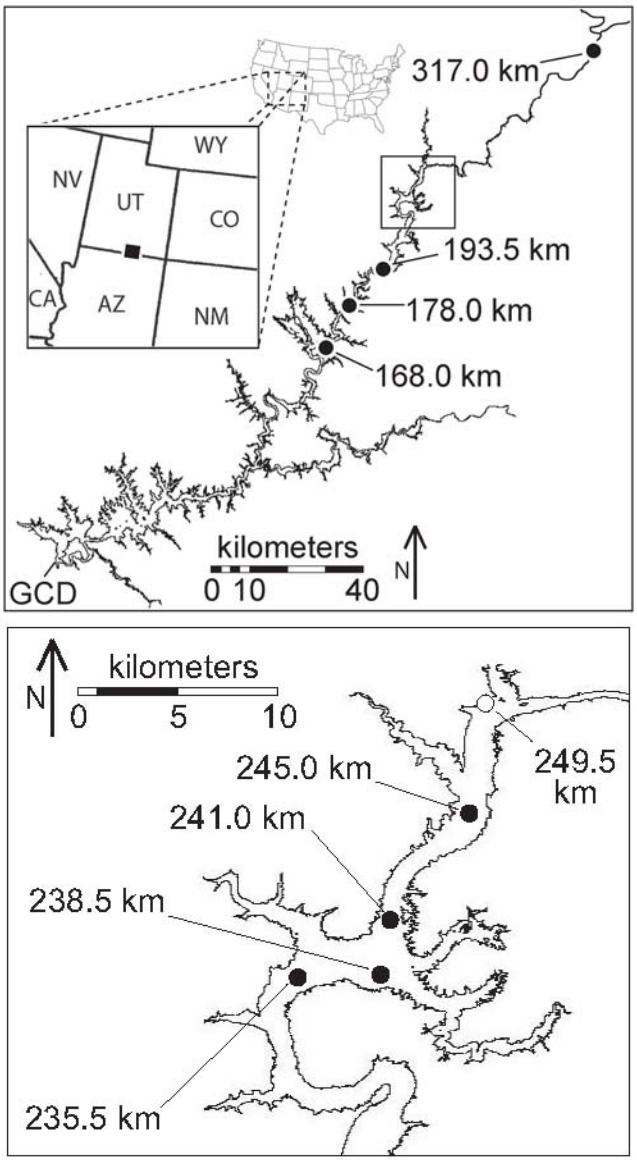

Figure 1. Sampling locations at Lake Powell. White and black circles represent shoreline and lakebed sampling sites, respectively. Dissolved and lakebed sampling sites denoted by river km from Glen Canyon Dam (GCD). The black box on the border of Arizona (AZ) and Utah (UT) denotes the approximate location of the upper panel, and the box in the upper panel denotes the location of the lower panel.

Figure 2

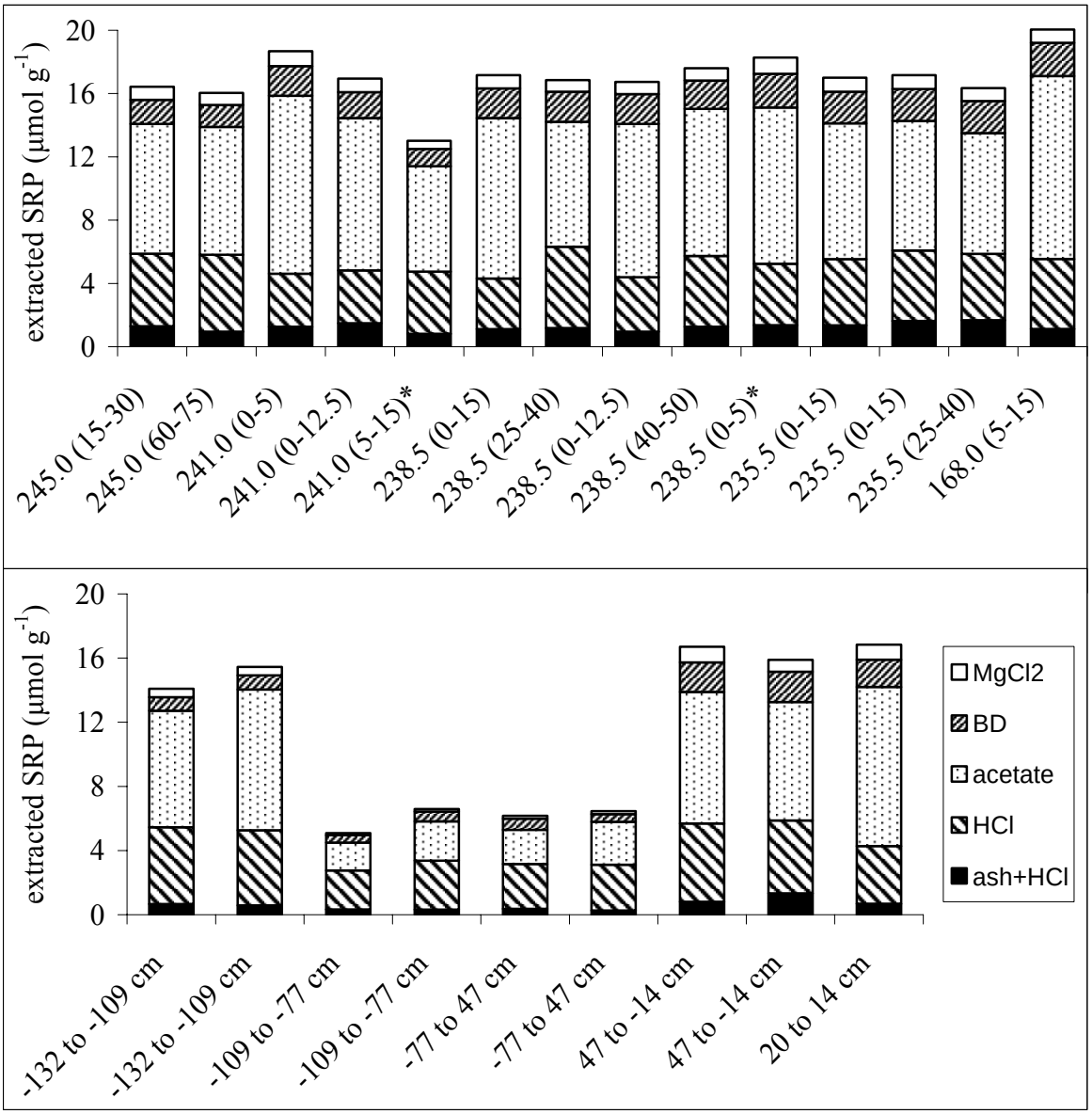

Figure 2. Results from phosphorus sequential extractions. Fractions displayed are magnesium chloride ($MgCl_2$), bicarbonate + dithionite (BD), sodium acetate buffered to pH 3.7 with acetic acid (acetate), hydrochloric acid (HCl), and heating at 550°C followed by hydrochloric acid (ash+HCl). *Upper panel*: Lakebed sediment samples denoted by distance from Glen Canyon Dam, with depth (in cm) below the sediment water interface in parentheses. Asterisks denote samples from May 2006; all others were collected in March 2006. *Lower panel*: Shoreline sediment samples denoted by depth above (negative values) and below (positive values) the sediment water interface (in cm).

Figure 3

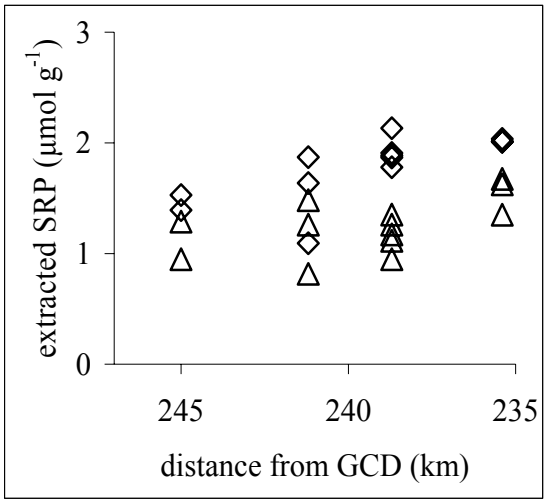

Figure 3. Phosphorus extracted by bicarbonate + dithionite (◇) and heating at 550°C followed by hydrochloric acid (△) plotted against distance from Glen Canyon Dam.

Figure 4

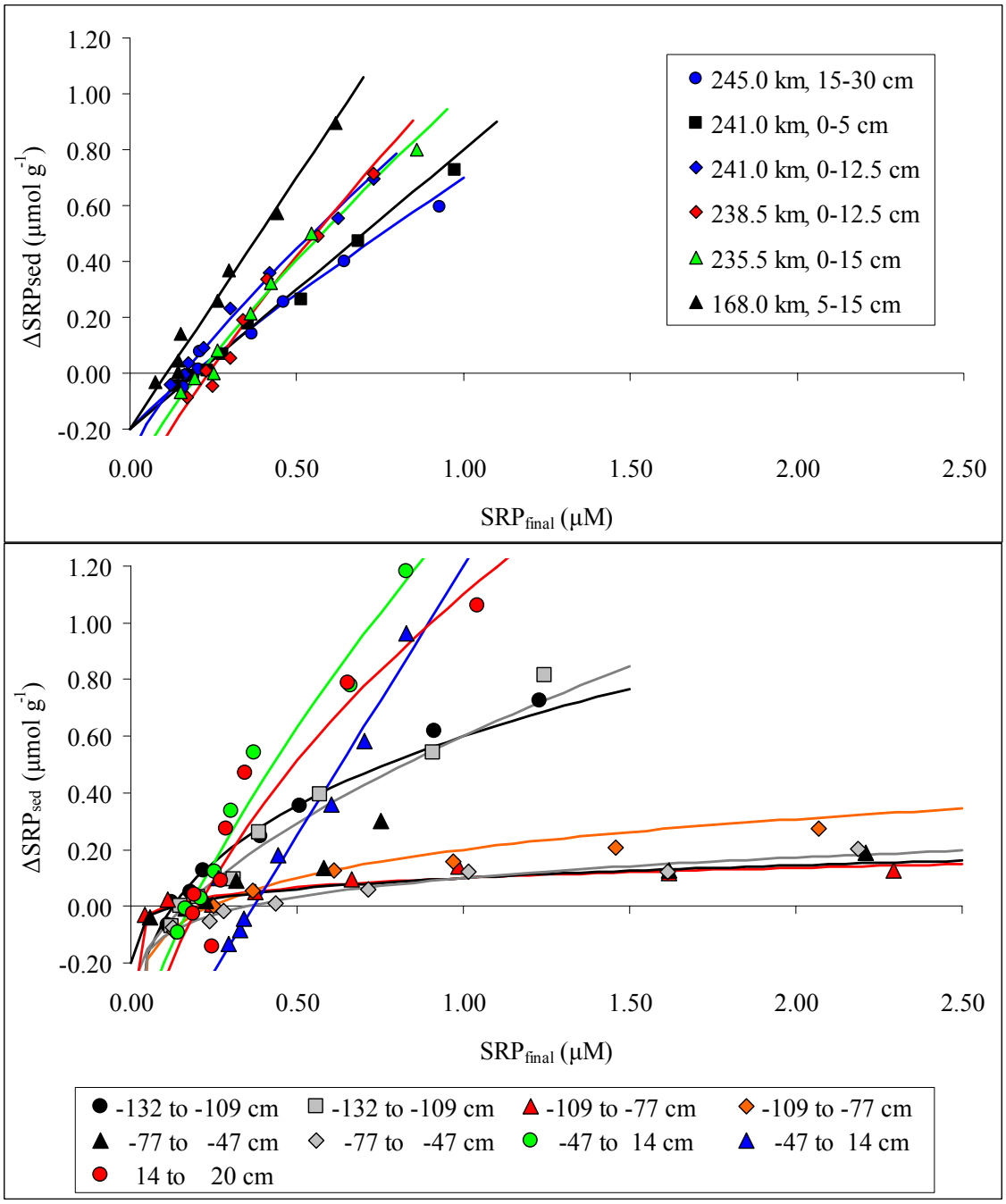

Figure 4. Results from phosphorus sorption experiments on lakebed samples (*upper panel*) and shoreline samples (*lower panel*). Only lakebed samples from surface sediment collected in March are shown. For clarity, only replicates from the 241.0 km location are shown; other replicates are identical. These results generally bracket the variability of the other lakebed samples.

Chapter 6

HYDROLOGIC AND BIOGEOCHEMICAL CONTROLS OF RIVER SUBSURFACE SOLUTES UNDER AGRICULTURALLY-ENHANCED GROUNDWATER FLOW

Richard A. Wildman, Jr., Joseph L. Domagalski, and Janet G. Hering

(accepted by *Journal of Environmental Quality*)

ABSTRACT

The relative influences of hydrologic processes and biogeochemistry on minor solutes were compared using groundwater samples collected beneath and adjacent to a reach of the Merced River (California, USA) that receives subsurface discharge enhanced by seasonal agricultural irrigation. Filtered groundwater samples were collected beneath the riverbed from 30 wells at different depths and riverbed locations in March, June, and October 2004. Hydrologic processes were inferred from specific conductance (SC) and bromine (Br) concentrations; manganese (Mn) was used as an indicator of redox conditions. The separate responses of the minor solutes strontium (Sr), barium (Ba), uranium (U), and phosphorus (P) to these influences were examined. Correlation and principal component analyses (PCA) indicate that hydrologic processes dominate the distribution of trace elements in the groundwater. Redox conditions appear to be independent of hydrologic processes and account for most of the remaining data

variability. With some variability, major processes are consistent in two well transects separated by 100 m.

INTRODUCTION

Agricultural practices can degrade groundwater and surface water quality. Common impacts on aquifers include introduction of pesticides and herbicides (e.g., Puckett and Hughes, 2005) and nutrient enrichment (e.g., Harned et al., 2004). Surface water quality can be degraded by overland flow of agricultural runoff (e.g., McKergow et al., 2006) or by the increase of suspended and dissolved solids due to increased erosion (e.g., Montgomery, 2007). As demands on water in agricultural areas of the United States increase due to climate change, population growth (Anderson and Woosley, 2006), and protection of endangered species habitat (via increase of residual stream flows at the expense of agricultural diversions, Franssen et al., 2007), mitigation of agricultural impacts is an active area of both research and watershed management.

Surface- and groundwater quality are linked through exchange in the riverbed. Hydraulic connection in the shallow river subsurface provides an additional pathway for surface water degradation. This region of active mixing between riverbed groundwater and surface water, known as the hyporheic zone, is characterized by short length scales of exchange with overlying water and oxygenation of surface sediment (Findlay, 1995; Packman and Bencala, 2000). Hyporheic subsurface advection transports minor solutes, while biogeochemical reactions can sequester or mobilize them, making the hyporheic zone important for the fate and transport of aqueous contaminants.

Both abiotic (Kennedy et al., 1984) and biogeochemical (e.g., Harvey and Fuller, 1998) processes can retard or enhance subsurface solute transport. Many studies detail the sorption of trace elements to solid iron (Fe), Mn, and aluminum oxides (e.g., Beauchemin and Kwong, 2006; Han et al., 2006; Tonkin et al., 2004). Both Fe and Mn oxides dissolve under reducing conditions, potentially mobilizing elements sorbed onto the surfaces of these solids (e.g., van Griethuysen et al., 2005). Such reactions are especially likely at interfaces between parcels of water with different geochemical characteristics (Kneeshaw et al., 2007; McGuire et al., 2002). Microbial redox reactions are important in the hyporheic zone, where dissimilatory microbial reduction of Fe and Mn oxides is likely (Harvey and Fuller, 1998). The river subsurface provides an environment for enhanced abiotic and biogeochemical reactions that may influence porewater redox chemistry and stream transport of nutrients (Haggard et al., 2005; Valett et al., 1996) and other inorganic solutes (Salehin et al., 2004; Bencala, 2000; Packman and Bencala, 2000).

Agricultural irrigation can substantially alter hydrologic regimes in aquifers and influence the behavior of subsurface solutes. Previous research has examined hyporheic systems where surface water is the dominant source of riverbed groundwater and hydrology is relatively unperturbed (e.g., Choi et al., 2000; Harvey et al., 2005). In areas with extensive irrigation, local groundwater advection may compress or eliminate the hyporheic zone by inducing a dominant flow from the subsurface into the river. Groundwater flow from impacted aquifers can be the major source of contaminants to surface water (Brown et al., 2007). Furthermore, groundwater from the local aquifer may differ from the river subsurface in redox potential. So, in addition to influencing mixing

of groundwater and surface water, an irrigation-driven flow regime may also affect subsurface redox chemistry.

We examined such an agriculturally-influenced system, a reach of the lower Merced River in the Central Valley of California. The Merced flows into the San Joaquin River, which feeds the Sacramento-San Joaquin Delta, a major drinking water source for Southern California and the western San Joaquin valley (Gronberg and Kratzer, 2007). The Delta is ecologically sensitive and home to the threatened delta smelt (Hypomesus transpacificus) and other declining fish species (Feyrer et al., 2007). The San Joaquin River, once habitat for a thriving Chinook salmon (Oncorhynchus tshawytscha) population, is a target for ecological restoration (Lucas et al., 2002).

This field site is a focus of the U.S. Geological Survey National Water Quality Assessment (NAWQA) program, Cycle II. Cycle I of this program was designed to assess national water quality and understand trends and influential factors (Gilliom et al., 1995). Cycle II of NAWQA emphasizes processes and trends controlling water quality and features an Agricultural Chemicals Transport (ACT) study that has been carried out in five different river basins (Capel et al., 2008).

The goals of this study were to evaluate chemical tracers for hydrologic processes and redox conditions in the Merced River riverbed and to use these tracers to assess the dominant influences on the distribution of four specific solutes (Sr, Ba, U, and P) in the subsurface. These “response elements” were chosen to represent a range of chemical behaviors from elements observed to have measurable concentrations by an initial survey. Each solute is expected to be influenced by hydrologic processes to some extent. In addition, U is redox active and its solubility is dependent on its oxidation state. Changes

in oxidation state are not expected for Ba and P, but their dissolved concentrations are likely to be influenced by the precipitation or dissolution of other redox-active species, particularly Fe and Mn. Specifically, these elements are expected to sorb to solid Fe- and Mn-oxides and enter the dissolved phase when these oxide minerals dissolve. The transport of Sr is expected to be conservative and independent of redox processes, in contrast to that of U, Ba, and P.

FIELD SITE: THE MERCED RIVER

The geography of the Merced River is typical of the eastern San Joaquin Valley, California. Below two water-storage reservoirs, the lower Merced River flows west through productive agricultural land (Gronberg and Kratzer, 2007). The field site was a reach approximately 20 km above the confluence with the San Joaquin River (Figure 1). In this area, the land surface slopes westward from the Sierra Nevada with a slope of about 1-4 m km^{-1} (Phillips et al., 2007). The semi-arid Mediterranean climate delivers 31 cm yr^{-1} of rainfall, mostly during winter, and necessitates summertime crop irrigation (Capel et al., 2008; Gronberg and Kratzer, 2007). The yearly average flow is 19.4 m^3 s^{-1} at the confluence of the Merced and San Joaquin Rivers (Capel et al., 2008).

Agricultural practices have substantially altered the hydrology of the lower Merced River. Water is retained upstream of the field site in multiple reservoirs, diverted for agricultural use, and returned via five irrigation canals to the lower section of the river (Gronberg and Kratzer, 2007). Additional water is transported into the basin and applied to fields and orchards. Crops cover 55% of the lower Merced Basin (Capel et al., 2008);

our field site is surrounded by an almond orchard, a field of feed corn, native vegetation, and a vineyard (Figure 1).

Groundwater near the Merced River lies in a < 43 m thick surface aquifer that is composed of highly permeable, low organic carbon, medium- to coarse-grained sand (Capel et al., 2008). The water table is approximately 6.5 m below ground surface (Domagalski et al., 2008b). After entering the water table, irrigation water applied 1 km from the river has been observed to flow towards the Merced River with a travel time of about 30 years (Domagalski et al., 2008b). A groundwater flow model for the lower Merced River region in the year 2000 (which was based on groundwater elevation measurements) indicates that surface recharge, mostly from irrigation, accounts for 76% of the total aquifer recharge and that 65% of the groundwater is discharged to the river. Thus, local groundwater experiences a net gain that is discharged to the Merced River and then transported out of the basin (Phillips et al., 2007). In other settings, altered hydrologic patterns affect solute transport and trace element mobility (e.g., Harvey et al., 2006; Kneeshaw et al., 2007), and the same may be true at the Merced River.

The streambed sediment is sandy and subject to vigorous bedload transport (Zamora, 2008). Flux across the streambed between groundwater and the Merced River ranges from $-1.1 \cdot 10^{-7}$ to $5.9 \cdot 10^{-7}$ m^3 m^{-2} s^{-1}, where positive values indicate flow from the riverbed into the river. Groundwater generally flows to the Merced River (mean $1.8 \cdot 10^{-7}$ m^3 m^{-2} s^{-1}) except during increased river flow (Essaid et al., 2008). Hydraulic conductivity was calculated to be $1.2 \cdot 10^{-5}$ m^3 m^{-2} s^{-1} (Essaid et al., 2008). Hyporheic exchange is not consistent spatially or temporally (Domagalski et al., 2008b).

In the groundwater beneath the Merced River, reduction of O_2, denitrification, and reduction of Mn^{4+} and Fe^{3+} have been characterized (Puckett et al., 2008). The riverbed is much more reducing than the surrounding aquifer; denitrification has been observed as groundwater flows from the local aquifer into the riverbed (Domagalski et al., 2008b). Reduction of electron acceptors occurs because the residence time in the subsurface is long (Puckett et al., 2008). There are no robust spatial patterns in the reduction of Mn- and Fe-oxide minerals (Domagalski et al., 2008b), possibly due to pockets of high organic carbon in the aquifer material (Puckett et al., 2008), but reducing conditions appear stronger in the summertime (Domagalski et al., 2008b).

METHODS

Field and Laboratory Procedures

Wells in "upstream" and "downstream" transects were installed 100 m apart at this field site (Figure 1). Each transect consists of five well locations (Figure 2), three of which, "northwest river", "center", and "southeast river", are evenly spaced across the river. Two additional well locations, "northwest riparian" and "southeast riparian", are about 5 m from the riverbank. At these locations, stainless steel drive point tips with 2 cm screened openings were installed 0.3 m, 0.5 m, and 3 m below the riverbed. These drive point tips were connected to Nylon tubing that was routed to the river bank (Capel et al., 2008).

Groundwater samples were collected by attaching a peristaltic pump to the Nylon tubes that led to each screened well opening. Approximately 1 L of water was pumped before any samples were collected. Specific conductance, pH, and temperature were

measured with a YSI probe (Geotech Environmental Equipment). When these parameters had stabilized, approximately 2-L samples were collected for various analyses. For collection of filtered samples, 0.45 μm cartridge filters (Supor model, Pall) were pre-rinsed with 1 L of distilled, deionized water and connected in-line with the peristaltic pump tubing. Samples were collected in high-density polyethylene bottles that had been washed with 3% HCl and rinsed with distilled, deionized water prior to use. Within 2 h of collection, samples were acidified with concentrated HNO_3 to a final concentration of 2%. Samples were open to the atmosphere during sample collection. Routine field and equipment blanks were collected and showed no evidence of carryover or cross-contamination. Sampling was performed on March 29-31, June 28-30, and October 5-7, 2004 to assess the effects of seasonal groundwater and river flow conditions on groundwater solute transport.

Samples were returned to the laboratory and analyzed using inductively-coupled plasma mass spectrometry (ICP-MS; Agilent 4500). Concentrations of Br, Mn, Sr, Ba, U, and P were quantified based on multi-element calibration solutions prepared from ICP-grade single element standards for Mn, Sr, Ba, U, P and an ion chromatography standard for Br (EMD Chemicals). Analytical detection limits (μM) were: 0.008 for U, 0.02 for Ba and Sr, 0.03 for Br, and 0.07 for P.

Dissolved organic carbon (DOC) measurements were made with a persulfate wet oxidation method that used a reaction in a gas-tight vessel and analysis by an Oceanography International (OI) Model 700 carbon analyzer (Aiken, 1992). Samples were introduced into the reaction vessel by means of a fixed-volume sample loop. Linear instrument response was maintained by limiting sample mass to 50 μg C. A 0.5 mL

aliquot of 5% v/v H_3PO_4 was added to the sample, which was then purged with N_2 for 2.0 min and treated with 0.5 mL of 0.42 M sodium persulfate solution for 5 min.

Statistical Analyses

Three statistical methods were used to evaluate the data collected. A matrix of correlation estimates ("correlations") for the six measured elements was constructed using the software package R (The R Project for Statistical Computing). Errors of correlation estimates are assumed to have a normal distribution, which implies that the standard deviation (σ) of these errors is $1/\sqrt{n}$, where n is the number of samples. Correlations were deemed significant when they differed from zero by at least 2σ, creating thresholds of ± 0.324 and ± 0.316 for the upstream and downstream transects, respectively. For simplicity, only values exceeding these thresholds are reported. Values differing from zero by 4σ or more are interpreted as strong correlations.

The parameters included in the correlation analysis were fit to a linear regression model (created with R) in which Br was the single predictor variable and Mn, Sr, Ba, U, and P were the response variables. Regressions were not forced to pass through the origin. The set of model residuals, which constitutes the variability not associated with Br, was added to the correlation analysis.

Principal component analysis quantifies the extent to which different parameters explain the variability of a data set (e.g., Báez-Cazull et al., 2008). More general than analysis of residuals, PCA does not require the initial assignment of a predictor variable. Instead, principal component vectors, linear combinations of parameters that are orthogonal to one another, describe the variance of the data set. Correlations of principal

component scores are interpreted on the basis of scientific background knowledge. Before PCA (using R), the data for the six measured elements were centered around zero by subtracting the mean of a parameter from every value of that parameter. They were then divided by the standard deviation for that parameter, a step that compensates for varying parameter ranges.

RESULTS AND DISCUSSION

Extensive agricultural irrigation in the Merced River basin has altered its hydrologic regime. The variability of the measured parameters in Merced River groundwater is illustrated by the summary of results shown in Table 1. Statistical analyses help explain the effect of local hydrology on groundwater mixing, redox chemistry, and trace solutes in the riverbed subsurface. Groundwater mixing patterns and redox chemistry are inferred from SC, Br, and Mn data; these relationships will be explained here as a conceptual framework for the data that are presented and discussed in the following subsections.

Although synoptic sampling provides information only at fixed time points, comparison of groundwater chemistry at three sampling times and multiple locations within the study reach provides insight into separate groundwater sources and their mixing patterns. Specific conductance data can be used to characterize the major element composition of groundwater during each sampling event. Bromine measured by ICP-MS is assumed to correspond to bromide, a common conservative and non-reactive tracer (e.g., Green et al., 2005; Harvey et al., 2005). Taken together, these data can be used to infer hydrologic processes beneath the Merced River.

Manganese is used as an indicator of redox state, which results from biogeochemical processes in the riverbed. In natural soils and sediments, Mn occurs nearly exclusively as solid Mn(III, IV) oxide minerals or as dissolved Mn(II) species. Generally, Mn data from acidified samples analyzed by ICP-MS can be assumed to correspond to Mn^{2+} concentrations. The kinetics of aqueous and surface-bound oxidation of Mn(II) by O_2(aq) are very slow compared to the time required for groundwater sampling (Morgan, 2005; Davies and Morgan, 1989). Hence, exposure to the atmosphere should not lead to artifacts in the Mn data.

In the aquatic environment, oxidized Mn exists as solid oxide minerals. These species dissolve upon accepting electrons from reduced chemical species, generally DOC. On the basis of thermodynamics, microbes should reduce Mn oxides after dissolved oxygen and nitrate are depleted, though this sequence of electron-accepting processes is not always distinct (McGuire et al., 2002). This redox chemistry controls dissolved Mn concentrations across oxic-anoxic gradients, which often correspond to depth gradients and are well-understood in the general case. Based on free-energy calculations and field measurements in marine and lake sediments, dissolved Mn is generally expected to be low in surficial (oxygenated) sediment and then to increase with depth as dissolved oxygen decreases.

Decreases in dissolved Mn at greater depths may result from precipitation of Mn minerals, such as rhodocrocite, $MnCO_3$, and albandite, MnS (e.g., Trefry and Presley, 1982; Canfield et al., 1993). However, precipitation reactions are not expected to influence observed Mn concentrations in this study. Groundwater samples were determined to be undersaturated by several orders of magnitude with respect to

rhodocrocite ($K_s = 7.94x10^{-5}$; Foulliac and Criaud, 1984) based on carbonate concentrations calculated from measured pH and alkalinity (Table A1). Sediment samples have very low concentrations of acid-volatile sulfide (Puckett et al. 2008), and thus we expect that minimal precipitation of albandite, which is usually undersaturated even in sulfidic porewaters (e.g., Naylor et al., 2006), has occurred.

Specific Conductance, Bromine, and Advective Patterns

Specific conductance values in Merced River groundwater ranged from 72 to 907 μS cm^{-1} at 298 K, and Br concentrations ranged from below the detection limit to 23.5 μM (Table 1). Values of SC in the river (i.e., surface water) were 136 μS cm^{-1} in March, 222 μS cm^{-1} in June, and 72 μS cm^{-1} in October; Br was not measured in surface water (Table 2). The deepest wells range in SC from 96 to 611 μS cm^{-1} (mean = 374 μS cm^{-1}) upstream and from 80 to 812 μS cm^{-1} (mean = 443 μS cm^{-1}) downstream. Upstream, northwest riparian wells ranged in Br from 2.6 to 4.4 μM (mean = 3.2 μM), whereas southeast riparian Br values ranged from 18.3 to 23.5 μM (mean = 20.5 μM). Similarly, downstream, northwest riparian wells range in Br from 0.7 to 2.8 μM (mean = 2.1 μM) and in SC from 220 to 420 μS cm^{-1} (mean 333 μS cm^{-1}), whereas southeast riparian wells range in Br from 9.1 to 15.4 μM (mean = 11.9 μM) and in SC from 700 to 907 μS cm^{-1} (mean = 796 μS cm^{-1}).

Spatial patterns in SC and Br data indicate significant differences between water sources. Values of SC in surface water are significantly lower (t-test, $p < 0.05$) than the deepest groundwater samples in each transect, an observation consistent with previous work showing that the Merced River generally gains water from local groundwater

(Essaid et al., 2008; Phillips et al., 2007). Furthermore, comparisons of riparian Br in each transect and of riparian SC in the downstream transect indicate that groundwater entering the riverbed from the northwest is significantly different (t-test, $p < 0.01$) from that entering from the southeast. While it is possible that surface water infiltration may dilute conservative tracers in the riparian wells, this process does not blur the differences between surface water and local aquifer groundwater. Thus, three separate sources appear to contribute water to the Merced River subsurface: surface water, the local aquifer to the northwest, and that to the southeast. During these comparisons, it is assumed that SC signature of groundwater entering the riverbed from the local aquifer does not change significantly in time during the sampling period, which is supported by measurements in the local aquifer northwest of the river (Domagalski et al. 2008b; Table A2).

Concentrations of Br are significantly higher (t-test, $p < 0.01$) in both sets of upstream riparian wells relative to those downstream. This implies that, while each transect has three distinct groundwater sources, riverbed mixing patterns will be clearer upstream because of larger differences in Br between surface water and aquifer-derived groundwater. Furthermore, regional groundwater models confirm differences in flow between these two transects. At the upstream transect, water contributions are equal from both sides of the river; however, 70% of the riverbed groundwater comes from the southeast side at the downstream transect (Domagalski et al., 2008b). Hence, riverbed groundwater mixing will be discussed separately for each transect here.

At all sampling times in the upstream transect, the center, shallow well has an SC value that is far closer to that of surface water than to that of any riparian well. Thus, water in this well must come from surface water, and surface water can be assumed to

have Br values of < 2 μM. Bromine correlates strongly with SC (r = 0.715), allowing these two variables to be used as conservative tracers interchangeably. In the upstream transect, SC was not measured at several locations, so Br will be used to describe riverbed mixing here.

Surface water infiltration to the hyporheic zone at this site has been observed to be spatially variable (Domagalski et al., 2008b; Essaid et al., 2008), yet some trends can be isolated. Several well depths at the center and southeastern riverbed locations show Br values < 2 μM, which are significantly lower (t-test, $p < 0.01$) than those in riparian wells. This trend is notably more prevalent in March than in October, where only the shallow well in the center of the river has SC and Br values nearer to those of surface water than to riparian wells. The opposite trend is true in the northwest river location, where Br concentrations are < 2 μM only in October. Thus, surface water infiltration occurs in the center and southeast river locations in March, only in the center location in June, and in the center and northwest river locations in October.

In the downstream transect, SC and Br again correlate strongly (r = 0.914). Here, lower concentrations of Br in the riparian wells complicate differentiation between surface water and local aquifer groundwater from the northwest. However, riparian SC data are more plentiful in this transect, so SC will be used to evaluate riverbed mixing. Only a few SC measurements in the riverbed wells are much closer to the surface water than to either riparian location (Table 2). Otherwise, SC values in the northwest and southeast river locations are generally between those of the surface water and the corresponding riparian locations, indicating significant contributions of local aquifer water to these locations. This indicates that riverbed groundwater is derived roughly

equally from three sources in this transect, with none prevailing consistently in many well locations.

Seasonal hydraulic patterns of the local aquifer groundwater are overlain on these spatial variations. In the 2004 growing season, irrigation in the almond orchard and the corn field to the northwest of the river (Figure 1) raised the local groundwater table by approximately 0.7-0.8 m and as much as 1.5 m, respectively, beginning in early May and persisting throughout the study period (Phillips et al., 2007). The observations of SC show that the signature of surface water in the shallow riverbed wells is present before the irrigation season (March) but not after it (October), consistent with data reported elsewhere (Domagalski et al., 2008b). Irrigation patterns and groundwater composition of the vineyard to the southeast of the river are not known, but data from the southeast river and riparian wells indicate no clear seasonality.

This pattern is perturbed by varying river flows. During calendar year 2004, flow averaged 7.76 $m^3 s^{-1}$ with a depth of 1.0-1.5 m at the center of the river (Essaid et al., 2008). Stream stage increased for about four weeks between mid-April and mid-May, with depth reaching a maximum of 3.0-3.5 m for about 1 week. While the Merced River generally experiences a net gain from the surrounding aquifers, this increase in surface water hydraulic head led to surface water infiltration into the subsurface during this 4-week period (Essaid et al., 2008). Riverbed groundwater has a long residence time due to low head differences with surface water (Puckett et al., 2008, Essaid et al., 2008). Thus, specific conductance in the subsurface did not recover for nearly two months after the spring high flow event. Furthermore, the decrease in SC at the 3 m depth due to surface water infiltration lags that at the 0.3 m depth by two months (Puckett et al., 2008).

This slow groundwater response to variations in flux across the sediment-water interface can explain seemingly anomalous riverbed SC values. In the upstream transect, the SC value at the upstream center well location in June is closer to the surface water SC value in March than to that measured in June. In addition, the June SC measurement in the deep, downstream, center well resembles the March surface water SC value more than the June SC value. These low riverbed SC values probably indicate signatures of remnant surface water that infiltrated into the subsurface some time before the sampling event. Consistent surface water flows after May 2004 (Essaid et al., 2008) imply a midsummer return of steady groundwater flux from the riverbed to the river during the late summer; the October sampling is not expected to be affected by the late-spring flow reversal. While they do not directly imply directions of groundwater flow, conclusions drawn from our SC and Br data match those drawn by studies based on thermal and chemical tracers, groundwater flow modeling, and hydraulic head measurements at this site (Essaid et al., 2008; Domagalski et al., 2008b; Phillips et al., 2007).

Manganese and Redox Conditions

In filtered samples, Mn ranges from below detection limit to 206.7 μM with high standard deviations and coefficients of variation in both transects (Table 1), suggesting substantial heterogeneity in redox conditions. Its spatial and temporal patterns do not resemble those of the conservative tracers, but are generally similar to DOC, which ranges from 0.06 to 0.54 mM C (Table 4). Subsurface dissolved oxygen is expected to be supplied by diffusion and infiltration from surface water. Manganese concentrations in filtered groundwater samples (Tables 1, 4) are generally greater than 1 μM, implying

consumption of dissolved oxygen and reductive dissolution of Mn-oxide minerals. This is consistent with data showing total consumption of oxygen, denitrification, and reduction of Mn- and Fe-oxides (Puckett et al., 2008). Denitrification appears to remove the vast majority of nitrate entering the river subsurface from the northwest (Domagalski et al., 2008b), implying that Mn and Fe reduction may be the dominant terminal electron accepting processes in much of the riverbed.

Maximum Mn frequently occurs in shallow wells, even though their proximity to the river bottom should allow for the maximal introduction of dissolved oxygen via diffusion or infiltration of surface water. Lower Mn concentrations in deeper wells are more likely to reflect decreased microbial activity since precipitation of reduced Mn solids is not expected (discussed above). However, DOC (Table 4) is usually highest in the shallow wells, suggesting that infiltration of surface water is important for supply of DOC to the subsurface. DOC may be supplied as a dissolved component of surface water, or it may originate from degradation of particulate organic carbon deposited to the river bottom. DOC in shallow wells may provide a substrate for microbial respiration and reductive dissolution of Mn-oxides. However, DOC and Mn do not correlate significantly and linear models based on DOC predict Mn poorly, indicating that the enhancement of Mn oxide dissolution by DOC may be a localized phenomenon.

Concentrations of Mn are strikingly high in the center shallow well of both transects in June and in the center and southeast river wells of the upstream transect in October. These extreme cases of Mn oxide reduction probably result from enhanced microbial activity due to high ambient temperatures coupled with ample DOC supply.

This finding is consistent with previous research that shows the hyporheic zone as an area of increased microbial activity (e.g., Harvey and Fuller, 1998).

In March, the lowest Mn concentrations were observed in the wells at 1 m depth, except in the center of the river in the upstream transect. Data are not available for this depth in June, but in October, this trend is observed only in the center of the river. At all other wells, the lowest observed Mn concentrations are in the deepest (3 m) wells.

The northwest wells of the downstream transect contradict observed Mn depth trends. At the downstream northwest riparian location, the maximum observed Mn concentration occurs at 0.5 m in March and at 3 m in June and October. At the northwest river location, anomalously low Mn concentrations were observed at all depths and sampling times.

Relative Influence of Hydrologic and Biogeochemical Processes

Since Mn is expected to reflect *in situ* biogeochemical processes, it is reasonable that its concentration in filtered samples does not correlate with that of Br, which represents hydrologic processes (e.g., conservative groundwater advection and mixing). The variability in the data set due to hydrologic processes was removed by assigning Br as the predictor variable in a linear regression model. Model residuals correlate positively and very strongly with Mn (Table 3).

Principal component analysis (Table 5) shows that Br and Mn correspond to distinct contributions to the data variability. In the upstream well transect, principal component (PC) 1 accounts for about 56% of the variability and shows a high score for Br and a score near 0 for Mn. In PC 2, the magnitude of these scores is reversed, though

this PC accounts for ~24% of the variability. This trend is similar, but weaker, in the downstream transect. There, Br scores highly on PC 1 and Mn on PC 2. However, Mn and Br are not as close to 0 in PC 1 and PC 2, respectively, as in the upstream transect. PC 1 accounts for ~50% of the variability and PC 2 for ~29% of the data variability, a slightly diminished difference from upstream. In the upstream and downstream transects, PC 3 accounts for ~11% and ~14% of the variability, respectively, and the magnitude of the Mn score is much greater than that of the Br score in each case.

Thus, hydrologic processes do not predict reducing conditions in this system. Reducing conditions correlate very strongly with the data variability for which a linear model based on hydrologic processes do not account. Correlation analyses indicate that these two factors describe separate and exclusive portions of the data set. Furthermore, PCA suggests that hydrologic processes drive 50-56% of the variability and redox conditions influence 35-42% of the variability. Together, these two factors explain > 90% of the variability in the data set. Hydrologic processes appear to be slightly more important in the upstream transect, where conservative tracers indicate more surface water infiltration and less riverbed mixing than in the downstream transect.

Responses of Sr, Ba, U, and P

The response elements (Sr, Ba, U, P; Tables 6, 7) show considerable variation across sampling locations and times, with very large coefficients of variation (Table 1). Generally, a gradient across the well transects, with highest concentrations in the southeast, especially upstream, is consistent with the contribution of different groundwater sources to the riverbed.

Bromine correlates with Sr, Ba, and U in both transects and also with P in the downstream transect (Table 3). Principal component analyses (Table 5) also show the association of response elements with Br. In both transects, PC 1 shows moderately high scores of matching sign for Br, Sr, Ba, and U. Downstream, P also matches Br in PC 1. Since PC 1 accounts for the majority of the data variance and shows Mn scores of lower magnitude than those of Br, these statistical analyses indicate a principal influence of hydrologic processes on these response elements.

The residuals from the Br-based linear regression model correlate positively with P in both transects and with Ba in the downstream transect (Table 3), indicating that variability in P (in both transects) and Ba (downstream) is not completely explained by hydrologic processes. Similar correlations of P and Ba with Mn further suggest that these two elements respond to changes in redox biogeochemistry. In the PCA from both transects (Table 5), PC 2 has high scores of matching sign for Mn and P, indicating that this PC accounts for variability due to redox conditions and that P responds to this variability. Upstream, P in PC 3 shows a notably high score with opposite sign from that of Mn. Downstream, U scores highly and Sr scores moderately on PC 2, and their signs are opposite from that of Mn. These last two observations suggest responses to redox conditions that are relevant, yet opposite, to that of Mn.

Strontium transport appears to be dominated by hydrologic processes with a slight influence of redox chemistry downstream. This contrasts a previous study in a cobble-bed stream, where retention of Sr relative to a conservative tracer was described (Kennedy et al., 1984). Nevertheless, no association between Sr and redox chemistry was expected, and none was observed. The discrepancy between these two studies may be explained by

greater amounts of clay minerals in the riverbed sediment or by incorporation of Sr into calcite ($CaCO_3$, e.g., Tesoriero and Pankow, 1996) in the study of Kennedy et al. (1984). This latter mechanism is not addressed in either of these studies, yet the strong association of Sr with hydrologic processes in our study may suggest that calcite precipitation does not control trace element mobility at the Merced River.

Barium and uranium are controlled by hydrologic processes in both transects, and also by biogeochemical processes downstream. Redox influence on Ba can be explained in part by sorption to Mn oxides (Tonkin et al., 2004). Anti-correlation between U and Mn scores in downstream PC 2 are consistent with the opposite effects of redox conditions on the stability of Mn- and U-containing solids (Lovley and Phillips, 1992). Well location is an important predictor variable for both elements: the aquifer groundwater entering the riverbed from the southeast contains high concentrations of each. Occasionally, U exceeds 0.126 μM (30 μg L^{-1}), the maximum drinking water contaminant level set by the United States Environmental Protection Agency (California Department of Health Services: http://www.dhs.ca.gov/ps/ddwem/chemicals/MCL/EPAandDHS.pdf).

Phosphorus variability is not explained well by hydrologic processes in either transect, though they do appear to have some effect downstream, where concentrations significantly exceed those of the upstream transect (t-test, $p < 0.05$; Tables 1, 7). Phosphorus is expected to enter the river subsurface by decomposition of dissolved organic matter (e.g., Krom and Berner, 1981) and by the transport and breakdown of fertilizer from the local aquifers. When P loads to a river are high, sediment P sorption capacity can be saturated (Haggard et al., 2005). Thus, higher concentrations may lead to

hydrologic control of P transport in the downstream transect, whereas lower concentrations upstream are governed by redox processes.

The effect of redox conditions on P appears to be relevant, yet inconsistent. Principal component analysis scores of P and Mn are high in PCs 2 and 3 in the analysis corresponding to each transect. However, the signs of the scores are the same in PC 2 and the opposite in PC 3. This indicates that reductive dissolution of Mn-oxide minerals may also release sorbed P, but also that dissolved P may increase during oxidizing conditions that lead to Mn precipitation. Taken together, these contrasting signals lead to overall weakly significant correlations between P and Mn. Many dissolved forms of P, including most phosphate species, sorb to Fe and Mn oxides (Arias et al., 2006), which can control dissolved P concentrations through their response to redox conditions (e.g., Gächter and Wehrli, 1998). Oxic conditions may stimulate microbial breakdown of particulate organic matter, a process that mobilizes P (Qiu and McComb, 1994). Based on the relative importance of PC 2 and PC 3, sorption to metal oxides appears to be about twice as important for P mobility than organic matter decomposition in this river reach.

CONCLUSIONS

Results presented in this study show that hydrological processes, which are probably closely related to regional irrigation patterns (Phillips et al., 2007), dominate subsurface distribution of Sr, Ba, and U beneath a reach of the lower Merced River. Their influence is strongest on Sr, which shows a minor response to biogeochemical redox conditions. Upstream, hydrological processes also control Ba and U, but, downstream, redox trends are also relevant. Phosphorus transport is controlled by hydrological

processes at high concentrations and redox conditions otherwise. Comparison among these elements is useful because they have different sorption and redox properties in addition to different probable sources in this system.

Overall, hydrological processes account for a little more than 50% of the variance in data collected from Merced River groundwater samples. The influence of redox conditions is less important, accounting for 35-42% of the variability. Trends are not consistent between two transects separated by 100 m; redox chemistry influences minor solutes more in the downstream transect. This is a curious finding that is worthy of future research.

These results complement prior reports on the behavior of nutrients and pesticides at this field site (Gronberg et al., 2004; Domagalski et al., 2008a, 2008b; Puckett et al. 2008) by suggesting that changes in groundwater flow derived from agricultural irrigation control inorganic solute transport in river subsurface. Differences in the controls of Ba, U, and P in the two proximal transects suggest a complex connection between aquifer flowpaths and the riverine subsurface.

Previous research on transport and biogeochemical processes in the hyporheic zone has focused on streams with unperturbed hydrology. This study suggests that nearby agricultural irrigation influences the distribution of solutes in the subsurface. With riverbed hydraulic characteristics established by previous work, statistical analyses of natural tracer concentrations and groundwater redox indicators provide insight into subsurface systems subject to a combination of lateral advection, hyporheic exchange, and mixing of surface water and ground water.

ACKNOWLEDGEMENTS

The authors gratefully acknowledge Steven Phillips and Celia Zamora (USGS) for field assistance. Laboratory analysis would have been impossible without Nathan Dalleska, Megan Ferguson, Kate Campbell, and Giehyeon Lee (Caltech). Tapio Schneider and Drew Keppel (Caltech) gave advice at key points during statistical analysis. The manuscript was improved with the help of Claire Farnsworth (Caltech), Peter Reichert (Eawag), Laura Sigg (Eawag), and 2 anonymous reviewers. This work was partially supported by the U.S. Geological Survey National Water Quality Assessment Program (ACT study). NSF SGER grant EAR-0408329 funded sample analysis and Rich Wildman's graduate study.

Use of trade names is for identification purposes only and does not imply endorsement by the U.S.G.S.

REFERENCES

Aiken, G.R. 1992. Chloride interference in the analysis of dissolved organic carbon by the wet oxidation method. Environ. Sci. Technol. 26:2435-2439.

Anderson, M.T. and L.H. Woosley, Jr. 2006. Water availability for the Western United States – Key scientific challenges. U.S. Geological Survey Circular 1261, Reston, VA.

Arias, M., J. Da Silva-Carballal, L. Garcia-Rio, J. Mejuto, and A. Nunez. 2006. Retention of phosphorus by iron and aluminum-oxides-coated quartz particles. J. Coll. Int. Sci. 295:65-70.

Báez-Cazull, S.E., J.T. McGuire, I.M. Cozzarelli, M.A. Voytek. 2008. Determination of dominant biogeochemical processes in a contaminated aquifer-wetland system using multivariate statistical analysis. J. Environ. Qual. 37:30-46.

Beauchemin, S. and Y.T.J. Kwong. 2006. Impact of redox conditions on arsenic mobilization from tailings in a wetland with neutral drainage. Environ. Sci. Technol. 40:6297-6303.

Bencala, K.E. 2000. Hyporheic zone hydrological processes. Hydrol. Processes 14:2797-2798.

Brown, B.V., H.M. Valett, and M.E. Schreiber. 2007. Arsenic transport in groundwater, surface water, and the hyporheic zone of a mine-influenced stream-aquifer system. Wat. Resour. Res. 43: W11404, doi:10.1029/2006WR005687.

Canfield, D.E., B. Thamdrup, and J.W. Hansen. 1993. The anaerobic degradation of organic matter in Danish coastal sediments: Iron reduction, manganese reduction, and sulfate reduction. Geochim. Cosmochim. Acta 57:3867-3883.

Capel, P.D., K.A. McCarthy, and J.E. Barbash. 2008. National, holistic, watershed-scale approach to understand the sources, transport, and fate of agricultural chemicals. J. Environ. Qual. 37:983-993.

Choi, J., J.W. Harvey, and M.H. Conklin. 2000. Characterizing multiple timescales of stream and storage zone interaction that affect solute fate and transport in streams. Wat. Resour. Res. 36(6):1511-1518.

Davies, S.H.R. and J.J. Morgan. 1989. Manganese(II) oxidation kinetics on metal oxide surfaces. J. Col. Int. Sci. 129(1):63-77.

Domagalski, J.L., S. Ator, R. Coupe, K. McCarthy, D. Lampe, M. Sandstrom, and N. Baker. 2008a. Comparative study of transport processes of nitrogen, phosphorus, and herbicides to streams in five agricultural basins, USA. J. Environ. Qual. 37:1158-1169.

Domagalski, J. L., S. P. Phillips, R. E. Bayless, C. Zamora, C. Kendall, R. A. Wildman, and J. G. Hering. (2008b). Influences of the unsaturated, saturated, and riparian zones on the transport of nitrate near the Merced River, California. Hydrogeol. J. 16(4):675-690.

Essaid, H.I., C.M. Zamora, K.A. McCarthy, J.R. Vogel, and J.T. Wilson. 2008. Using heat to characterize streambed water flux variability in four stream reaches. J. Environ. Qual. 37:1010-1023.

Feyrer, F., M.L. Nobriga, and T.R. Sommer. 2007. Multidecadal trends for three declining fish species: habitat patterns and mechanisms in the San Francisco Estuary, California, USA. Can. J. Fish. Aquat. Sci. 64:723-734.

Findlay, S. 1995. Importance of surface-subsurface exchange in stream ecosystems: The hyporheic zone. Limnol. Oceanogr. 40(1):159-164.

Foulliac, C. and A. Criaud. 1984. Carbonate and bicarbonate trace metal complexes: Critical reevaluation of stability constants. Geochem. J. 18:297-303.

Franssen, N.R., K.B. Gido, and D.L. Propst. 2007. Flow regime affects availability of native and nonnative prey of an endangered predator. Biol. Conserv. 138:330-340.

Gächter, R. and B. Wehrli. 1998. Ten years of artificial mixing and oxygenation: No effect on the internal phosphorus loading of two eutrophic lakes. Environ. Sci. Technol. 32:3659-3665.

Gilliom, R.J., W.M. Alley, M.E. Gurtz. 1995. Design of the National Water-Quality Assessment Program: Occurrence and distribution of water-quality conditions. U.S. Geological Survey Circular 1112, Sacramento, CA.

Green, C.T., D.A. Stonestrom, B.A. Bekins, K.C. Akstin, and M.S. Schulz. 2005. Percolation and transport in a sandy soil under a natural hydraulic gradient. Wat. Resour. Res. 41:W10414, doi: 10.1029/2005WR004061.

Gronberg, J.M. and C.R. Kratzer. 2007. Environmental setting of the lower Merced River Basin, California. U.S. Geological Survey Scientific Investigations Report 2006-5152, Sacramento, CA.

Gronberg, J.M., C.R. Kratzer, K.R. Burow, J.L. Domagalski, and S.P. Phillips. 2004. Water-quality assessment of the San Joaquin-Tulare Basins: Entering a new decade. U.S. Geological Survey Fact Sheet 2004-3012, Sacramento, CA.

Haggard, B.E., E.H. Stanley, and D.E. Storm. 2005. Nutrient retention in a point-source enriched stream, J. Nor. Amer. Benthol. Soc. 24(1): 29-47.

Han, R., W. Zou, Z. Zhang, J. Shi, and J. Yang. 2006. Removal of copper(II) and lead(II) from aqueous solution by manganese oxide coated sand I. Characterization and kinetic study. J. Haz. Mat. B137: 384-395.

Harned, D.A., J. B. Atkins, and J.S. Harvill. 2004. Nutrient mass balance and trends, Mobile River Basin, Alabama, Georgia, and Mississippi. J. Amer. Wat. Resour. Assoc. June 2004:765-793.

Harvey, C.F., K.N. Ashfaque, W. Yu, A.B.M. Badruzzaman, M.A. Ali, P.M. Oates, H.A. Michael, R.B. Neumann, R. Beckie, S. Islam, and M.F. Ahmed. (2006). Groundwater dynamics and arsenic contaminations in Bangladesh. Chem. Geol. 228(1-3):112-136.

Harvey, J.W. and C.C. Fuller. 1998. Effect of enhanced manganese oxidation in the hyporheic zone on basin-scale geochemical mass balance. Wat. Resour. Res. 34(4):623-636.

Harvey, J.W., J.E. Saiers, and J.T. Newlin. 2005. Solute transport and storage mechanisms in wetlands of the Everglades, south Florida. Wat. Resour. Res. 41: W05009, doi:10.1029/2004WR003507.

Kennedy, V.C., A.P. Jackman, S.M. Zand, G.W. Zellweger, and R.J. Avanzino. 1984. Transport and concentration controls for chloride, strontium, potassium and lead in Uvas Creek, a small cobble-bed stream in Santa Clara County, California, U.S.A. J. Hydrol. 75:67-110.

Kneeshaw, T.A., J.T. McGuire, E.W. Smith, and I.M. Cozzarelli. 2007. Evaluation of sulfate reduction at experimentally induced mixing interfaces using small-scale push-pull tests in an aquifer-wetland system. Appl. Geochem. 22:2618-2629.

Krom, M. D. and R.A. Berner. 1981. The diagenesis of phosphorus in a nearshore marine sediment. Geochim. Cosmochim. Acta 45:207-216.

Lovley, D. R. and E.P. Phillips. 1992. Reduction of uranium by Desulfovibrio desulfuricans. App. Env. Microbiol. 58(3):850-856.

Lucas, L.V., J.E. Cloern, J.K. Thompson, and N.E. Monsen. 2002. Functional variability of habitats within the Sacramento-San Joaquin Delta: Restoration implications. Ecol. App. 12(5):1528-1547.

McGuire, J.T., D.T. Long, M.J. Klug, S.K. Haack, and D.W. Hyndman. 2002. Evaluating behavior of oxygen, nitrate, and sulfate during recharge and quantifying reduction rates in a contaminated aquifer. Environ. Sci. Technol. 36:2693-2700.

McKergow, L.A., I.P. Prosser, D.M. Weaver, R.B. Grayson, and E.G. Reed. 2006. Performance of grass and eucalyptus riparian buffers in a pasture catchment, Western Australia, part 2: water quality. Hydrol. Processes 20:2327-2346.

Montgomery, D.R. 2007. Soil erosion and agricultural sustainability. Proc. Nat. Acad. Sci. USA 104(33):13268-13272.

Morgan, J.J. 2005. Kinetics of reaction between O_2 and Mn(II) species in aqueous solutions. Geochim. Cosmochim. Acta 69(1):35-48.

Naylor, C., W. Davison, M. Motelica-Heino, G.A. Van Den Berg, L.M. Van Der Heijdt. 2006, Potential kinetic availability of metals in sulphidic freshwater sediments. Sci. Tot. Environ. 357:208-220.

Packman, A.I. and K.E. Bencala. 2000. Modeling Surface-Subsurface Hydrological Interactions. p. 45-80. In J.A. Jones and P.J. Mulholland (ed.) Streams and Ground Waters. Academic Press: San Diego.

Phillips, S.P., C.T. Green, K.R. Burow, J.L. Shelton, and D.L. Rewis. 2007. Simulation of multiscale ground-water flow in part of the Northeastern San Joaquin Valley, California. U.S. Geological Survey Scientific Investigations Report 2007-5009, Sacramento, CA.

Puckett, L.J. and W.B. Hughes. 2005. Transport and fate of nitrate and pesticides: Hydrogeology and riparian zone processes. J. Environ. Qual. 34:2278-2292.

Puckett, L.J., C. Zamora, H. Essaid, J.T. Wilson, H.M. Johnson, M.J. Brayton, and J.R. Vogel. 2008. Transport and fate of nitrate at the ground-water/surface-water interface. J. Environ. Qual. 37:1034-1050.

Qiu, S. and A.J. McComb. 1994. Effects of oxygen concentration on phosphorus release from reflooded air-dried wetland sediments. Australian J. Mar. Freshwat. Res. 45:1319-1328.

Salehin, M., A.I. Packman, and M. Paradis. 2004. Hyporheic exchange with heterogeneous streambeds: Laboratory experiments and modeling. Wat. Resour. Res. 40: W11504, doi: 10.1029/2003WR002567.

Tesoriero, A.J. and J.F. Pankow. 1996. Solid solution portioning of Sr^{2+}, Ba^{2+}, and Cd^{2+} to calcite. Geochim. Cosmochim. Acta 60(6):1053-1063.

Tonkin, J.W., L.S. Balistrieri, and J.W. Murray. 2004. Modeling sorption of divalent metal cations on hydrous manganese oxide using the diffuse double layer model. Appl. Geochem. 19:29-53.

Trefry, J.H. and B.J. Presley. 1982. Manganese fluxes from Mississippi Delta sediments. Geochim. Cosmochim. Acta 46:1715-1726.

Valett, H.M., J.A. Morrice, C.N. Dahm, and M.E. Campana. 1996. Parent lithology, surface-groundwater exchange, and nitrate retention in headwater streams. Limnol. Oceanogr. 41(2):333-345.

van Griethuysen, C., M. Luitwieler, J. Joziasse, and A.A. Koelmans. 2005. Temporal variation of trace metal geochemistry in floodplain lake sediment subject to dynamic hydrological conditions. Environ. Pollut. 137:281-294.

Zamora, C. 2008. Estimating water fluxes across the sediment-water interface in the lower Merced River, California. U.S. Geological Survey Scientific Investigations Report 2007-5216, Sacramento, CA.

FIGURE CAPTIONS

Figure 1: Regional and detailed setting and near-river land uses of the Merced River field site. In the inset, (A) represents almond orchards, (B) feed corn, (C) native vegetation, and (D) a vineyard (after Phillips et al., 2007). The river flows from right to left in the inset.

Figure 2: Schematic of well locations beneath the Merced River, looking upstream. Circles indicate locations where samples for analysis of specific conductance, manganese, strontium, barium, uranium, phosphorus, bromine, and dissolved organic carbon were collected in each transect. Dimensions are not to scale.

TABLES

Table 1: Descriptive statistics for full data set (SC in µS/cm at 298 K, all elemental concentrations in µM).

statistic	*element*						
	SC	Br	Mn	Sr	Ba	U	P
	upstream transect						
number[†]	25	38	38	38	38	38	38
max	732	23.5	206.7	11.4	2.0	0.15	16.6
min	72	<0.03	<0.04	<0.02	0.1	<0.008	<0.07
median	441	2.9	5.8	2.7	1.0	0.01	0.6
mean	343	6.1	17.8	3.6	1.0	0.03	2.0
σ[‡]	212	7.1	39.9	3.0	0.6	0.04	3.8
CV[§]	62	116.4	224.2	83.3	60.0	133.3	190.0
	downstream transect						
number[†]	33	40	40	40	40	40	40
max	907	15.4	168.8	6.4	1.9	0.16	40.8
min	72	<0.03	<0.04	0.1	<0.02	<0.008	<0.07
median	343	2.3	3.7	2.3	0.6	0.01	2.4
mean	400	4.2	10.5	2.8	0.7	0.02	8.0
σ[‡]	230	4.3	26.8	1.6	0.5	0.04	10.6
CV[§]	57	102.4	255.2	57.1	71.4	200.0	132.5

[†] The number of samples analyzed from each transect.

[‡] σ is the population standard deviation.

[§] CV is the coefficient of variation. CV = σ/mean * 100%.

Table 2: Specific conductance (μS/cm at 298 K) and Br (μM) in surface water and groundwater.

depth	*upstream transect*									
	northwest riparian		northwest river		center		southeast river		southeast riparian	
	SC	Br	SC	Br	SC	Br	SC	Br	SC	Br
					March 2004					
river					136					
0.3 m		3.3	704	10.8	161	0.5	103	0.2		20.4
0.5 m		2.9		2.2		0.2		0.1		18.3
3.0 m		3.3	467	11.5	96	0.2	97	0.2		21.9
					June 2004					
river					222					
0.3 m	490	4.4	441	3.1	117	1.5	171	2.8		
0.5 m										
3.0 m	483	3.1	450	2.7	123	1.8	262	4.4		
					October 2004					
river					72					
0.3 m	530	2.9	445	1.5	127	<0.03	732	10.1		18.5
0.5 m		2.6		1.7		1.0		7.6		20.5
3.0 m	511	2.7	496	1.2	516	8.5	611	10.7		23.5

	downstream transect									
	northwest riparian		northwest river		center		southeast river		southeast riparian	
	SC	Br	SC	Br	SC	Br	SC	Br	SC	Br
					March 2004					
river					136					
0.3 m	307	2.2	99	0.2	292	1.6	457	5.0	806	13.0
0.5 m		2.2		1.0		4.7		4.9		9.3
3.0 m	355	0.7	312	0.2	402	1.9	529	5.8	756	13.7
					June 2004					
river					222					
0.3 m	297	2.6	340	1.4	326	2.6	175	0.9	793	15.4
0.5 m										
3.0 m	398	2.8	343	1.5	80	0.1	458	6.2	700	12.2
					October 2004					
river					72					
0.3 m	220	1.6	103	<0.03	342	1.6	664	5.7	907	12.0
0.5 m		2.1		0.1		1.7		4.5		10.4
3.0 m	420	2.4	364	1.1	381	2.7	335	1.1	812	9.1

Table 3: Correlation matrices[†] for trace elements and residuals from a linear model with Br as a predictor variable.

upstream transect

	Br	Mn	Sr	Ba	U	P	residuals[‡]
Br			0.941	0.703	0.905		
Mn						0.353	0.996
Sr				0.733	0.828		
Ba					0.512		
U							
P							0.424
residuals							

downstream transect

	Br	Mn	Sr	Ba	U	P	residuals[‡]
Br			0.673	0.747	0.441	0.599	
Mn				0.515		0.365	0.974
Sr				0.546	0.697		
Ba						0.726	0.534
U							
P							0.514
residuals							

[†] Only correlations exceeding significance thresholds of ±0.324 (upstream) and ±0.316 (downstream) are shown.

[‡] The parameter "residuals" is the set of residuals from the linear regression model using bromine as the predictor variable.

Table 4: Manganese (μM) and DOC (mM C) in filtered Merced River groundwater.

depth	*upstream transect*									
	northwest riparian		northwest river		center		southeast river		southeast riparian	
	Mn	DOC	Mn	DOC	Mn	DOC	Mn	DOC	Mn	DOC
					March 2004					
0.3 m	10.2		17.7	0.12	24.1	0.54	8.2	0.14	14.2	
0.5 m	3.2		4.2		0.7		0.2		7.1	
3.0 m	5.8		14.1	0.13	0.2	0.07	4.6	0.11	12.7	
					June 2004					
0.3 m	7.3		9.8	0.10	135.8	0.22	13.0	0.11		
0.5 m										
3.0 m	3.3		2.7	0.07	<0.04	0.12	<0.04			
					October 2004					
0.3 m	5.9		5.3		74.5		206.7		7.0	
0.5 m	5.9		4.6		0.5		43.4		11.6	
3.0 m	1.7		1.8		3.3		1.3		5.2	

	downstream transect									
	northwest riparian		northwest river		center		southeast river		southeast riparian	
	Mn	DOC	Mn	DOC	Mn	DOC	Mn	DOC	Mn	DOC
					March 2004					
0.3 m	1.9	0.10	<0.04	0.12	12.3	0.15	9.4	0.17	9.6	0.22
0.5 m	21.0		0.1		0.2		0.2		1.8	
3.0 m	4.0	0.10	<0.04	0.08	9.2	0.07	15.2	0.10	13.8	0.11
					June 2004					
0.3 m	3.5		<0.04		168.8	0.13	4.2	0.28	11.4	0.16
0.5 m										
3.0 m	34.7	0.07	<0.04	0.06		0.08	0.1	0.06	2.9	0.12
					October 2004					
0.3 m	2.7		<0.04		13.1		10.1		9.2	
0.5 m	3.9		<0.04		8.7		11.1		12.3	
3.0 m	23.6		<0.04		<0.04		<0.04		2.5	

Table 5: Principal component analysis of measured parameters and spatial variables in Merced River groundwater.

upstream transect				
principal component scores:				
	PC1	PC2	PC3	PC4
Br	-0.535	0.022	0.108	-0.133
Mn	-0.039	-0.704	-0.587	-0.381
Sr	-0.528	0.097	0.026	0.067
Ba	-0.437	-0.206	-0.275	0.728
U	-0.491	0.056	0.206	-0.533
P	0.040	-0.670	0.725	0.137
importance of components:				
proportion of variance	0.556	0.235	0.112	0.074
cumulative proportion	0.556	0.791	0.903	0.977

downstream transect				
principal component scores:				
	PC1	PC2	PC3	PC4
Br	-0.519	0.125	-0.346	0.198
Mn	-0.196	-0.475	0.775	0.129
Sr	-0.442	0.398	0.137	-0.572
Ba	-0.523	-0.244	0.044	-0.345
U	-0.253	0.597	0.354	0.584
P	-0.399	-0.429	-0.365	0.395
importance of components:				
proportion of variance	0.501	0.287	0.135	0.043
cumulative proportion	0.501	0.788	0.923	0.965

Table 6: Sr and Ba (μM) in filtered Merced River groundwater.

depth	*upstream transect*									
	northwest riparian		northwest river		center		southeast river		southeast riparian	
	Sr	Ba	Sr	Ba	Sr	Ba	Sr	Ba	Sr	Ba
					March 2004					
0.3 m	2.3	1.1	6.1	1.4	1.2	0.7	1.0	0.2	10.1	2.0
0.5 m	3.7	1.7	3.5	0.6	0.8	0.2	1.0	0.1	11.4	1.5
3.0 m	2.8	1.3	6.6	1.5	0.8	0.5	1.0	0.2	10.7	2.0
					June 2004					
0.3 m	2.9	1.5	3.7	1.0	1.1	1.0	1.3	0.5		
0.5 m										
3.0 m	3.4	1.7	3.3	0.6	<0.02	0.1	2.6	0.3		
					October 2004					
0.3 m	2.1	0.8	1.7	0.5	0.6	1.2	4.1	1.6	6.3	1.6
0.5 m	2.1	0.8	1.9	0.6	0.8	0.4	4.2	1.3	7.5	1.5
3.0 m	2.1	1.1	2.4	0.4	3.6	1.4	5.5	0.9	9.4	1.4

	downstream transect									
	northwest riparian		northwest river		center		southeast river		southeast riparian	
	Sr	Ba	Sr	Ba	Sr	Ba	Sr	Ba	Sr	Ba
					March 2004					
0.3 m	2.1	0.5	1.1	0.2	3.0	0.5	4.8	0.9	4.1	1.5
0.5 m	1.9	0.7	1.6	0.2	2.7	0.3	4.7	0.5	6.1	0.9
3.0 m	2.0	0.6	1.3	0.2	3.4	<0.02	6.4	1.3	3.7	1.7
					June 2004					
0.3 m	2.0	0.6	1.8	0.3	2.4	1.9	1.5	0.3	3.5	1.6
0.5 m										
3.0 m	2.3	1.0	2.2	0.2	0.2	<0.02	3.8	0.5	5.9	0.9
					October 2004					
0.3 m	1.5	0.5	1.0	0.2	2.8	0.6	5.6	1.2	3.8	1.6
0.5 m	1.8	0.7	1.3	0.2	2.9	0.6	4.7	1.2	3.0	1.4
3.0 m	2.0	0.8	1.8	0.2	2.3	0.3	2.1	0.3	5.4	0.8

Table 7: U and P (μM) in filtered Merced River groundwater.

depth	*upstream transect*									
	northwest riparian		northwest river		center		southeast river		southeast riparian	
	U	P	U	P	U	P	U	P	U	P
					March 2004					
0.3 m	0.01	<0.07	0.02	0.2	0.02	8.9	0.02	<0.07	0.11	4.1
0.5 m	0.01	<0.07	0.02	<0.07	0.02	0.1	0.02	<0.07	0.10	<0.07
3.0 m	0.01	<0.07	0.02	<0.07	0.02	<0.07	0.02	0.4	0.13	<0.07
					June 2004					
0.3 m	<0.008	0.4	<0.008	2.6	<0.008	16.6	0.01	0.7		
0.5 m										
3.0 m	<0.008	1.2	0.01	1.5	<0.008	3.8	0.01	0.5		
					October 2004					
0.3 m	<0.008	0.2	<0.008	0.4	<0.008	3.5	0.05	1.4	0.11	7.8
0.5 m	<0.008	1.6	<0.008	2.8	<0.008	2.4	0.02	3.9	0.15	3.4
3.0 m	<0.008	4.1	0.01	9.4	<0.008	8.1	0.06	<0.07	0.11	<0.07

	downstream transect									
	northwest riparian		northwest river		center		southeast river		southeast riparian	
	U	P	U	P	U	P	U	P	U	P
					March 2004					
0.3 m	<0.008	0.1	<0.008	0.1	<0.008	6.1	0.05	3.6	0.01	27.5
0.5 m	<0.008	3.5	0.01	0.6	0.02	0.7	0.07	0.2	0.12	3.0
3.0 m	<0.008	1.1	<0.008	0.1	<0.008	7.7	0.03	1.8	0.01	24.4
					June 2004					
0.3 m	0.01	0.7	0.02	1.2	0.01	24.1	0.02	13.0	0.01	31.3
0.5 m										
3.0 m	0.01	9.5	0.02	1.3	0.01	7.7	0.06	1.7	0.16	4.8
					October 2004					
0.3 m	<0.008	<0.07	<0.008	0.8	<0.008	12.5	0.05	18.5	<0.008	25.5
0.5 m	<0.008	1.5	<0.008	<0.07	<0.008	22.1	0.01	6.7	<0.008	40.8
3.0 m	<0.008	14.4	<0.008	<0.07	0.01	<0.07	0.02	<0.07	0.12	0.7

FIGURE 1

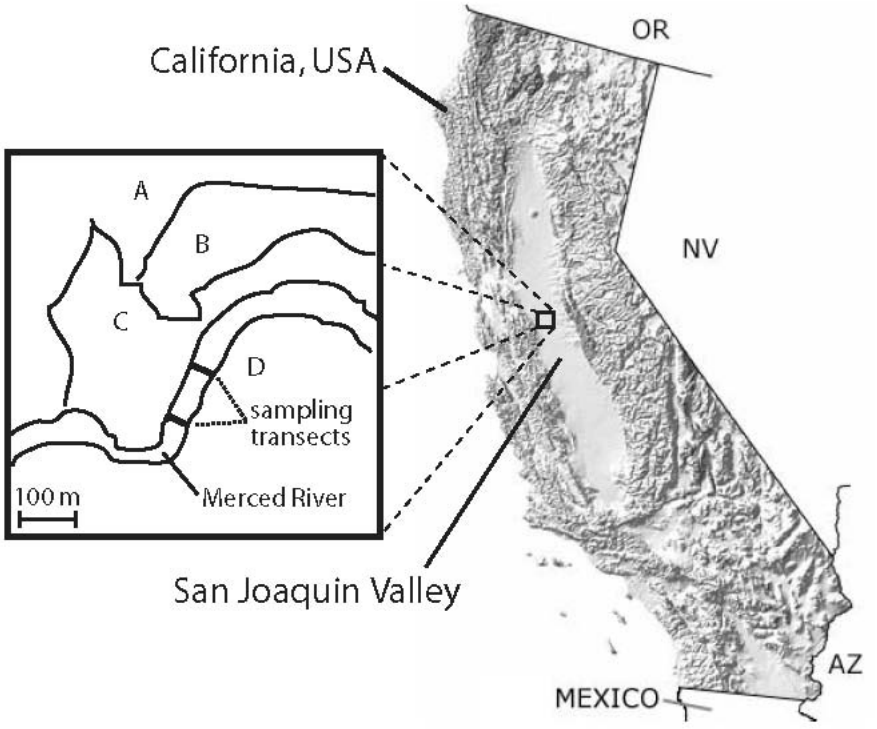
California, USA
OR
NV
AZ
MEXICO
San Joaquin Valley
A
B
C
D
sampling
transects
100 m
Merced River

FIGURE 2

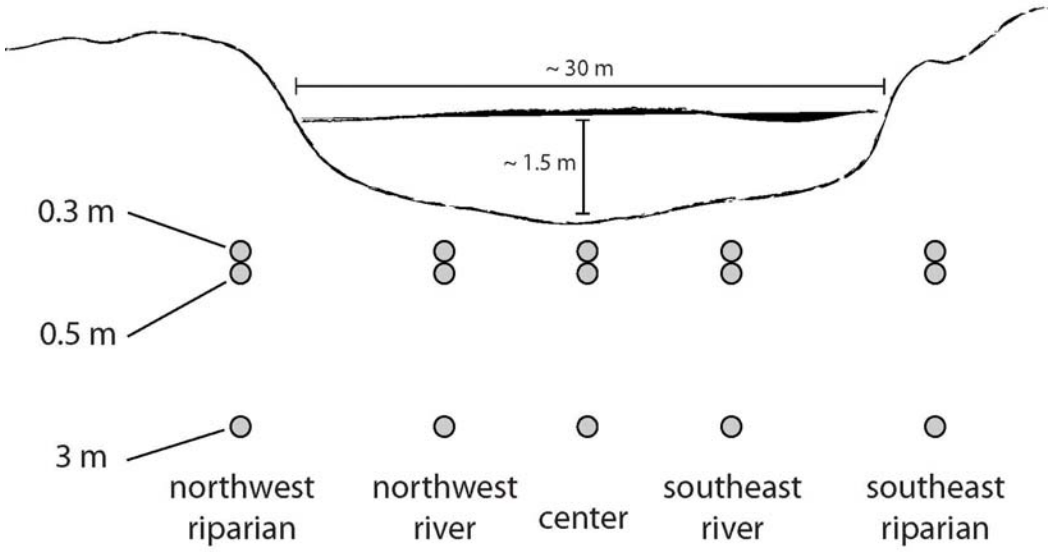
~ 30 m
~ 1.5 m
0.3 m
0.5 m
3 m
northwest riparian
northwest river
center
southeast river
southeast riparian

APPENDIX

Table A1. pH and alkalinity[a] in the Merced River subsurface[b].

upstream transect

depth	northwest riparian		northwest river		center		southeast river		southeast riparian	
	pH	alk	pH	alk	pH	alk	pH	alk	pH	alk
					March 2004					
0.3 m			6.49	150.2	6.70	58.8	6.87	34.3		
3.0 m			6.94	88.3	7.20	28.3	6.89	33.3		
					June 2004					
0.3 m	6.30	72.6	6.70	71.7	6.30	33.7	6.60	40.0		
3.0 m	6.60	59.5	6.90	74.1	6.80	16.6	6.60	50.2		
					Ocobter 2004					
0.3 m	6.87		6.78		6.90		6.79			
3.0 m	6.93		6.77		6.69		6.53			

downstream transect

depth	northwest riparian		northwest river		center		southeast river		southeast riparian	
	pH	alk	pH	alk	pH	alk	pH	alk	pH	alk
					March 2004					
0.3 m	6.69	99.7	7.00	58.8	7.17	121.1	7.30	171.0	7.20	270.7
3.0 m	7.19	76.3	7.17	84.3	7.20	109.0	7.28	143.6	7.20	196.3
					June 2004					
0.3 m	6.50	72.5	7.20	74.1	6.70	147.6	7.10	66.8	6.90	235.8
3.0 m	6.70	69.6	7.00	79.2	7.20	20.4	7.10	124.7	6.90	173.3
					October 2004					
0.3 m	6.78		7.04		7.13		7.23		6.96	907.0
3.0 m	7.16		7.40		7.46		7.37		7.02	

[a] All data collected by the United States Geological Survey and shared by Joseph L. Domagalski.

[b] Alkalinity is reported as mg L^{-1} $CaCO_3$. It was measured in the field by a gran titration.

Table A-2. Specific conductance (in μS cm-1) and trace elements (in μM) in the local aquifer to the northwest of the Merced River[a].

well location[b] and depth		sampling month	specific conductance	Br	Mn	Sr	Ba	U	P
1 km	8.8 m	April	600	6.9	BDL	5.30	0.31	0.050	30.35
		June	571	5.4	BDL	5.25	0.34	0.046	11.49
		October	609	5.0	BDL	5.02	0.36	0.055	20.15
	13.9 m	April	597	3.1	1.09	8.40	0.08	0.034	132.35
		June	633	2.7	1.42	8.24	0.22	0.067	27.19
		October	648	1.9	BDL	7.64	0.15	0.059	32.39
	19.5 m	April	568	3.1	0.93	7.08	0.55	0.029	17.89
		June	550	3.4	0.69	6.62	0.60	0.034	11.85
		October	582	2.1	BDL	6.56	0.63	0.029	9.43
	25.9 m	April	585	2.7	0.24	6.90	0.92	0.042	6.59
		June	602	3.3	0.18	6.93	0.99	0.050	2.97
		October	596	2.8	BDL	6.63	0.93	0.042	5.23
0.5 km	13.9 m	April	308	1.5	BDL	3.24	0.21	BDL	26.28
		June	304	1.7	0.05	3.24	0.28	BDL	12.04
		October	293	0.8	BDL	2.93	0.31	BDL	10.82
	19.5 m	April	871	9.8	0.05	11.81	0.83	0.046	48.60
		June	878	11.2	0.07	12.12	1.10	0.055	15.63
		October	843	8.0	BDL	10.27	0.98	0.042	16.95
	25.9 m	April	365	1.9	BDL	2.93	0.23	BDL	31.09
		June	379	2.1	0.05	2.82	0.28	BDL	9.88
		October	385	1.7	BDL	2.98	0.31	BDL	15.63
0.1 km	8.8 m	April	552	2.5	1.22	3.97	0.66	0.017	3.13
		June	549	2.7	1.07	4.28	0.75	0.021	1.16
		October	573	2.2	BDL	4.35	0.69	0.017	2.68
	13.9 m	April	499	1.9	0.76	4.01	0.51	0.013	2.36
		June	506	2.1	0.76	4.17	0.55	0.013	0.90
		October	481	1.4	BDL	3.73	0.49	BDL	1.52
	25.9 m	April	290	1.2	0.07	1.27	0.17	BDL	2.58
		June	282	1.2	0.07	1.31	0.17	BDL	1.07
		October	286	0.8	BDL	1.28	0.16	BDL	1.13
	29.0 m	April	288	1.3	0.31	0.96	0.18	BDL	3.45
		June	284	1.3	0.25	0.96	0.19	BDL	0.61
		October	288	1.0	BDL	0.82	0.17	BDL	2.87
	53.3 m	April	463	3.6	1.49	1.29	0.17	BDL	10.40
		October	452	2.3	BDL	1.31	0.17	BDL	4.52
detection limit				0.025	0.04	0.02	0.01	0.008	0.06

[a] Specific conductance and trace elements were measured on unfiltered and filtered (0.2 μm) samples, respectively.

[b] Details of well installations described by Phillips et al. (2007).

Chapter 7

CONCLUSIONS

7.1. Summary of Research Findings

This Ph.D. thesis explored the effects of two hydrologic consequences of irrigation, changing reservoir surface elevation and perturbed groundwater-surface water exchange, on biogeochemical processes in sediment, surface water, and groundwater. Reducing conditions in porewater of submerged sediment located at the shoreline of Lake Powell were assessed before and after changing water level exposed that sediment to air and then resubmerged it. The sedimentation of chemicals in the Colorado River delta of Lake Powell was described quantitatively and its implications for primary productivity in the reservoir were discussed. In combination with required minimum dam releases, the ongoing drought in the Colorado River Basin has lowered the surface elevation of Lake Powell substantially, and this process has induced the erosion and resuspension of the Colorado River delta. The possibility of release of phosphorus, the limiting nutrient in Lake Powell, from resuspended sediment was assessed in a combined field and laboratory study. At the Merced River, a chemical analysis of groundwater samples collected from the riverbed was used to compare the relative influence of hydrologic processes and biogeochemistry on the transport and sequestration of trace solutes. The findings from each of these projects will be summarized in the following subsections, and their implications and significance will be discussed in the second section of this chapter.

7.1.1. Water Level Fluctuations at the Shoreline of Lake Powell

Lake Powell is long and narrow, and many fingers, known as “side canyons”, extend away from the mainstem of the reservoir and receive sediment from small creeks. Porewater sampled from shoreline sediment deposited at the edge of two side canyons, Farley Canyon and White Canyon, was analyzed for the dissolved concentrations of several chemical constituents including manganese (Mn) and uranium (U). These elements provide information about the redox state of the system. In both sampling locations, reduction and mobilization of solid-phase Mn occurs < 10 cm below the sediment-water interface, suggesting that the intermittently rapid sedimentation in these locations deposits sufficient organic carbon to consume dissolved oxygen a very short distance into the sediment. This is notably different than previous studies at the bottom of lakes or marine basins, because, where oxygenated bottom waters have been observed, dissolved oxygen diffuses into the sediment and dissolved Mn is not generally produced at such shallow depths.

Decreasing water level at Lake Powell exposes shoreline sediment to air. Three weeks of exposure appeared to be sufficient to create oxidizing conditions in the exposed sediment, as indicated by higher concentrations of porewater U after resubmergence. Samples collected 3.5 days after the sediment-water interface had been resubmerged show that reducing conditions returned quickly in Farley Canyon, with the shape of the dissolved Mn profile resembling that collected before the water level fluctuation. However, U does not appear to respond to reducing conditions nearly as quickly as Mn: whereas the 3.5 days appears to be enough to remobilize Mn, the U curve did not resemble its previous shape even after a deeper portion of the sediment column had been

resubmerged for ~12 days. This *in situ* relationship between Mn and U has not been previously observed at high resolution in sediment porewater or groundwater, and these temporal constraints for the reestablishment of metal reduction in groundwater are new.

In White Canyon, the subsurface gradients of Mn measured after the lake level fluctuation do not resemble those measured before it. Rather, dissolved Mn increases at a much greater depth, and regions of increase or steady concentrations with depth are not distinct from one other. This suggests that, 3.5 days after resubmergence of the sediment-water interface, sediment porewater at this site is not as reducing as it was before the lake-level fluctuation. The difference between White Canyon and Farley Canyon may be related to the local topography around the sampling sites; an ~8 m hill near the Farley Canyon sampling location may have supplied groundwater discharge to the sediment above the reservoir water level, preventing air from infiltrating and oxidizing reduced Mn. Conversely, the sediment bank adjacent to the White Canyon sampling location was only ~1 m high and appeared dry when samples were collected, suggesting that air may have infiltrated and delayed the onset of reducing conditions relative to Farley Canyon. Thus, physical characteristics of sediment may play an important role in the rate of reestablishment of Mn reduction in sediment on the shoreline of Lake Powell.

In White Canyon, U concentrations are much higher than in Farley Canyon, possibly because of the mining history of this watershed. There is not a clear relationship between Mn and U as in Farley Canyon, suggesting that different geochemical processes or microbial communities are present in the two canyons. Still, exposure to air greatly increases dissolved U concentrations after resubmergence, suggesting that reservoir level fluctuations may significantly affect the cycling of this contaminant.

7.1.2. Sedimentation of Inorganic Chemicals in Lake Powell

As the Colorado River enters Lake Powell, coarse particles are deposited first, followed by fine particles. High-resolution particle size measurements of sediment samples collected from the lakebed in the inflow region show a trend of decreasing particle size away from the river inflow, but the trend is not strong due to a small range of particle sizes measured. This implies that these samples were collected too close together to represent the full range of sediment deposition in the delta. Since visual observations of these samples during collection indicated that they were of small particle size, yet sampling further upstream was not possible due to the low level of Lake Powell, a series of stacked sediment cores was collected from a shoreline location. This sediment included coarse, sandy layers that must have been deposited when this location was at the upper edge of the reservoir as well as fine, clayey layers that must have been deposited when the reservoir was higher and this location was far from the river inflow. Trace element, mineral, and carbon data from these sample sets indicates that particle size is a strong predictor of chemical parameters. Small particles are higher in carbon, trace elements, and clay minerals, whereas coarse particles are higher in quartz and zirconium.

These findings contribute to a conceptual understanding of the broad spatial distributions of chemicals in the Colorado River delta of Lake Powell. While trends over ~10 km are slight, major trends exist over the > 100 km delta, with sediment further from the dam lower in inorganic chemicals than sediment closer to the dam. This is significant because it may help explain an increase in summertime surface water chlorophyll measured in the upper region of the reservoir during a recent period of low water level. Monitoring data collected by the U.S. Geological Survey show that chlorophyll did not

increase in the first three years of reservoir drawdown, and then it increased dramatically. This may suggest that, during the initial decrease of the reservoir level, resuspension of the sediment delta by the Colorado River only disturbed coarse sediment with low chemical concentrations. However, there may be a water level threshold that led to resuspension of fine sediment rich in phosphorus (P), the limiting nutrient for primary productivity in the reservoir. The initiation of resuspension of fine sediment may have caused the increase in surface water chlorophyll. This is significant because it suggests that manipulation of reservoir level can change the quality of the water stored.

Sediment collected from shoreline locations is derived from the sedimentary rock formations surrounding Lake Powell. This sediment was sandy and low in most trace elements. If the type of rock formation surrounding a shoreline region (i.e., sandstone or shale) influences particle size of the shoreline, too few samples were collected to demonstrate a significant trend.

7.1.3. The Effect of Sediment Resuspension on Dissolved Phosphorus in Lake Powell

During low water levels, the Colorado River has been observed to resuspend the portion of its delta in Lake Powell that is exposed above water. Field measurements indicate that sediment resuspension buffers the concentration of dissolved P in the river as it flows through the exposed sediment delta. Consequently, low dissolved P concentration at base flow is increased during sediment resuspension, whereas high dissolved P concentration during the spring flood is decreased. Once in the reservoir, seasonal advective density currents determine whether P enters the photic zone or passes beneath it. Spring sampling captured base flow and an underflow density current, a

scenario that implies release of P by sediment resuspension and subsequent transport to the bottom waters of the reservoir. Conversely, sampling in the early summer during snowmelt runoff and an overflow density current captured a scenario of P uptake by sediment resuspension and transport to the photic zone by an overflow current. Neither of these scenarios would seem to add P to the photic zone, yet primary productivity has increased during low reservoir levels (see section 7.1.2 and Chapter 4). This suggests that a specific hydrologic scenario of low river flow and an overflow or interflow current may occur in the late spring, and this scenario adds P to the reservoir at a depth where it can stimulate primary productivity.

These field measurements were supported by sequential extractions and sorption experiments conducted in the laboratory. Sequential extractions indicated that most of the sediment-associated P in the Lake Powell delta is extracted by a chemical treatment targeting P bound to calcite and biogenic hydroxyapatite. This implies that, despite observed inhibition of calcite precipitation in the upper region of Lake Powell by organic carbon compounds, the calcite precipitation that does occur effectively scavenges P from the water column. The step targeting easily exchangeable P, the most likely P to desorb during sediment resuspension, extracted ~10% of the total extractable P. Sorption experiments indicate that P has a much higher affinity for fine sediment than for coarse sediment. Equilibrium phosphorus concentrations calculated from Freundlich isotherms fit to the laboratory data are higher than the concentration of P entering Lake Powell, suggesting that experimental conditions did not adequately match those in the field. The amount of P desorbed from sediment resuspensions with no P added was much lower than the putative exchangeable P measured during the sequential extraction.

7.1.4. Hydrological Processes and Biogeochemistry in Groundwater beneath the Merced River

During the growing season, irrigation of agricultural fields surrounding the study reach of the Merced River raises the water table and induces groundwater discharge to the river. However, increases in river stage can reverse this exchange, pushing surface water back into the riverbed. Concentrations of bromine (Br) and Mn in groundwater samples collected from the riverbed reflect this complicated hydrology. Correlation analysis and analysis of the residuals from a linear model using Br as the predictor variable show that there is no statistical relationship between Br and Mn. Thus, Br, which can be interpreted as a conservative tracer of hydrologic processes, and Mn, which reflects the redox state of groundwater, can be used to represent these two separate influences on the transport of trace solutes.

Principal component analysis performed on a data set that included Mn, Br, strontium (Sr), barium (Ba), U, and P in groundwater suggest that hydrological processes accounted for > 50% of the variability, whereas 35-42% of the variability can be explained by trends in redox chemistry. Transport of Sr appears to be mainly by hydrological processes. Trends of Ba and U vary in two transects located ~100 m apart, but hydrological processes are generally more important for these two elements. Where P concentrations are high, P appears to follow hydrologic trends, whereas, where concentrations are lower, it appears to be controlled by redox chemistry.

7.2. Wider Implications and Significance

7.2.1. Interdisciplinary Significance of Research Topics

The broad aim of this Ph.D. thesis has been to connect variations in physical hydrology with biogeochemical processes that control the partitioning of inorganic chemicals between the solid and dissolved phases. The four research topics have attempted to extend areas of scientific understanding outside their traditional disciplines. In Chapter 3, the sampling methods and theory of early diagenesis, a process that has been studied nearly exclusively in deep lacustrine and marine basins with a steady sedimentation rate, were applied to the shoreline of a reservoir, an area with rapid, intermittent sedimentation. The results obtained there provide important knowledge about how subsurface redox gradients recover after a hydrological disturbance. Additionally, the application of high-resolution porewater sampling to the shoreline of a reservoir can also pertain to other environments that experience unsaturated conditions, such as floodplains and soils. Perhaps the most useful way to follow this research would be to study chemical transformations during unsaturation explicitly. This would give a clearer picture of trace metal mobility *during* a fluctuation in water level, since the current project sampled only *before* and *after* water level fluctuation.

The results of Chapter 4 bring basic concepts of sedimentation to bear on reservoir water quality and management. The sharp increase of primary productivity observed after three years of decreasing water level of Lake Powell suggests that a certain lake surface elevation was reached below which resuspension of the sediment delta may have supplied nutrients to the water column. This implies that, if reservoir managers wish to avoid major perturbations to the reservoir ecosystem, then reservoir drawdown should be halted

before significant quantities of fine sediment are resuspended. However, such a management decision carries significant political implications. Additionally, the results of this project were made possible by several precise analytical measurements that have rarely (if ever) been applied to the study of a reservoir delta. The trends described in Chapter 4 would not have been clear without high-resolution measurements of particle size, trace element composition, and mineralogical composition.

The discussion of Chapter 5 describes a tight connection between sediment geochemistry and physical limnology, with both contributing to influence the amount of P released from Colorado River delta sediment and transported to the photic zone of Lake Powell. This implies that both natural factors, such as the volume of river flow, the timing of spring runoff, and the temperature difference between a river and a reservoir, and management decisions, such as the timing and extent of reservoir drawdown and the physical features (i.e., width and depth) of a valley flooded when a dam is built, contribute to perturbations in nutrient cycling during low water levels. This study of nutrient release in a reservoir where small changes in P cycling can be measured is important for the study of nutrient enrichment in both oligotrophic and eutrophic systems. The conclusions of this research could be enhanced by detailed field monitoring during a greater variety of lake levels and hydrologic conditions. Furthermore, a wider range of laboratory conditions are needed if sorption experiments are to adequately represent field processes.

Taken together, Chapters 4 and 5 show the significance of dam releases that do not correspond to natural river flows. This has already been clearly described for river reaches below dams, but it has been studied infrequently for the water quality of

reservoirs. Engineers who operate dams are asked to optimize a variety of parameters, such as the generation of electricity, ecological health of downstream rivers, water supply to downstream communities, flood control, the water quality of rivers, the aesthetic value of a water body, and the water quality of reservoirs. The last of these is not usually a high priority, and this research gives an indication of how it can be affected when dam release schedules are designed to prioritize other factors.

Whereas many studies have examined groundwater flow patterns beneath rivers, and others have addressed the release or sequestration of trace solutes by redox processes in the subsurface, the study reported in Chapter 6 quantitatively compares these processes in the same setting. Its results indicate that increased groundwater flow induced by summertime irrigation and subsequent groundwater infiltration may be more important for trace element mobility than redox processes. These results, which may be applicable to a wide range of agricultural areas, contribute to scientific understanding of how trace chemicals respond to major hydrologic and chemical trends. An ideal complement to this study would be a similar measurement campaign in a reach of the Merced River that is not characterized by irrigation-induced groundwater flow.

Taken together, the four projects in this thesis make a contribution to understanding the effects of water infrastructure on the quality of the water being managed. The extensive construction of new water infrastructure is frequently cited as a means towards economic revival in developed countries and economic development in primitive ones. Furthermore, as water stress increases across the American West due to rising population and climate change, the effective management of water infrastructure is sure to grow in importance during the 21st century. In each of these cases, a detailed scientific

understanding of the coupling between natural and engineered systems is crucial to supply clean water and protect environmental health.

7.2.2. Broader Impacts of this Research

In addition to producing the results discussed in previous chapters, this Ph.D. thesis has supported the education of two undergraduate students and a high school student. Caltech Summer Undergraduate Research Fellows Nathan Chan and Michael Easler both provided important field and laboratory help, and they will be included as co-authors on publications resulting from this research. Nathan also did his senior research project under the supervision of Dr. Hering and myself. Each has found direction in his young career, with Nathan completing a master's program in public policy and Mike transferring to the University of Minnesota to pursue an avid interest in Landscape Architecture.

In addition to these in-depth research experiences, research at Lake Powell introduced a Caltech undergraduate, Andrew Kositsky, and a junior graduate student, Claire Farnsworth, to field-based research.

This research also served as the basis for an outreach effort at the Environmental Charter High School. Located in Lawndale, California, this school serves low-income, low-ambition students from ethnicities rarely found in academia. The outreach program began as a series of guest lectures by other Caltech graduate students and me, and it evolved into a year-long elective class called Science and Society. During my frequent visits to the school while co-teaching this class, I identified a student, Fabian Ponciano, with an interest in a research career in the fields of geology and natural hazards. Fabian

spent a summer working with me on a literature survey about Lake Powell, and later graduated with honors and now attends the University of California, Santa Cruz.

Finally, this work has also developed my understanding of a diverse set of fields outside of my immediate areas of specialization. My projects are tangentially related to river restoration, soil science, climate change, and water resource management. I have had an initial exposure to complicated social issues surrounding the flooding of a productive river valley and the development of a natural resource in a region populated by disadvantaged people (the Navajo and Hopi Indian tribes) who do not benefit from that development.

I first learned of Glen Canyon and Lake Powell from Edward Abbey's book *Desert Solitaire*, in which he campaigns for an appreciation of the wild places of the American West and vilifies the U.S. Bureau of Reclamation for building Glen Canyon Dam. However, after working with scientists from many different government agencies, reading the work of a few non-governmental organizations, and working at Lake Powell myself, I have come to understand that the use of natural resources in the American West is not easily described in absolute terms. Should my career involve an opportunity to manage natural resources, I will approach such a responsibility with both a healthy respect for the many various demands placed on a river system and a conviction that optimal use and appreciation is crucially reliant upon sound scientific knowledge.